https://ntrs.nasa.gov/search.jsp?R=19920005045 2020-03-17T14:37:22+00:00Z

Ames Rem
N-30-CR
vol. 2
57139
P-193

THE OHIO STATE UNIVERSITY

SATCOM Antenna Siting Study on P-3C Aircraft

D.A. Bensman and R.J. Marhefka

The Ohio State University

ElectroScience Laboratory

Department of Electrical Engineering
Columbus, Ohio 43212

Final Report 721711-4, Volume II
Grant No. NAG 2-542
September 1991

Naval Air Test Center
Patuxent River, MD 20670
and
NASA — Ames Research Center
Moffett Field, CA 94035

(NASA-CR-189515) SATCOM ANTENNA SITING STUDY ON P-3C AIRCRAFT, VOLUME 2 Final Report (Ohio State Univ.) 193 p CSCL 20N

N92-14263

Unclas
G3/32 0057139

A. Approved for public release; Distribution is unlimited

NOTICES

When Government drawings, specifications, or other data are used for any purpose other than in connection with a definitely related Government procurement operation, the United States Government thereby incurs no responsibility nor any obligation whatsoever, and the fact that the Government may have formulated, furnished, or in any way supplied the said drawings, specifications, or other data, is not to be regarded by implication or otherwise as in any manner licensing the holder or any other person or corporation, or conveying any rights or permission to manufacture, use, or sell any patented invention that may in any way be related thereto.

50272-101

REPORT DOCUMENTATION PAGE	1. REPOBT NO.	2.	3. Recipient's Accession No.

4. Title and Subtitle

SATCOM Antenna Siting Study on P-3C Aircraft

5. Report Date
September 1991

6.

7. Author(s)
D.A. Bensman and R.J. Marhefka

8. Performing Org. Rept. No.
721711-4, Volume II

9. Performing Organization Name and Address
The Ohio State University
ElectroScience Laboratory
1320 Kinnear Road
Columbus, OH 43212

10. Project/Task/Work Unit No.

11. Contract(C) or Grant(G) No.
(C)
(G) NAG 2-542

12. Sponsoring Organization Name and Address
University Affairs Branch
NASA — Ames Research Center 241-25
Moffett Field, CA 94035

13. Report Type/Period Covered
Final Report

14.

15. Supplementary Notes

16. Abstract (Limit: 200 words)

The purpose of this effort is to use the NEC-BSC to study the performance of a SATCOM antenna on a P-3C aircraft. After plate - cylinder fields are added to Version 3.1 of the NEC-BSC, it is shown that the NEC-BSC can be used to accurately predict the performance of a SATCOM antenna system on a P-3C aircraft. The study illustrates that the NEC-BSC gives good results when compared with scale model measurements provided by Boeing and Lockheed.

17. Document Analysis a. Descriptors

AIRCRAFT
DIFFRACTION
UTD
ANALYSIS
MODELLING

b. Identifiers/Open-Ended Terms

c. COSATI Field/Group

18. Availability Statement
A. Approved for public release;
Distribution is unlimited.

19. Security Class (This Report)
Unclassified

21. No. of Pages
192

20. Security Class (This Page)
Unclassified

22. Price

(See ANSI-Z39.18)

See Instructions on Reverse

OPTIONAL FORM 272 (4-77)
Department of Commerce

List of Figures

1 Geometry of the cylindrical model of the P-3C aircraft used in the NEC-BSC showing the antenna location. (Test Location 1) 3

2 NEC-BSC calculated roll plane pattern for antenna location on top center-line of the fuselage between the wing and vertical stabilizer for right hand circular polarization at 300 MHz. (Test Location 1) 4

3 NEC-BSC calculated elevation plane pattern for antenna location on top center-line of the fuselage between the wing and vertical stabilizer for right hand circular polarization at 300 MHz. (Test Location 1) 5

4 NEC-BSC calculated azimuth plane pattern for antenna location on top center-line of the fuselage between the wing and vertical stabilizer for right hand circular polarization at 300 MHz. (Test Location 1) 6

5 NEC-BSC calculated conical plane pattern 10° above the horizon for antenna location on top center-line of the fuselage between the wing and vertical stabilzer for right hand circular polarization at 300 MHz. (Test Location 1) 7

6 NEC-BSC calculated conical plane pattern 20° above the horizon for antenna location on top center-line of the fuselage between the wing and vertical stabilzer for right hand circular polarization at 300 MHz. (Test Location 1) 8

7 NEC-BSC calculated conical plane pattern 30° above the horizon for antenna location on top center-line of the fuselage between the wing and vertical stabilzer for right hand circular polarization at 300 MHz. (Test Location 1) 9

8 NEC-BSC calculated roll plane pattern for antenna location on top center-line of the fuselage between the wing and vertical stabilizer for left hand circular polarization at 300 MHz. (Test Location 1) 10

9 NEC-BSC calculated elevation plane pattern for antenna location on top center-line of the fuselage between the wing and vertical stabilizer for left hand circular polarization at 300 MHz. (Test Location 1) 11

10 NEC-BSC calculated azimuth plane pattern for antenna location on top center-line of the fuselage between the wing and vertical stabilizer for left hand circular polarization at 300 MHz. (Test Location 1) 12
11 NEC-BSC calculated conical plane pattern 10° above the horizon for antenna location on top center-line of the fuselage between the wing and vertical stabilzer for left hand circular polarization at 300 MHz. (Test Location 1) 13
12 NEC-BSC calculated conical plane pattern 20° above the horizon for antenna location on top center-line of the fuselage between the wing and vertical stabilzer for left hand circular polarization at 300 MHz. (Test Location 1) 14
13 NEC-BSC calculated conical plane pattern 30° above the horizon for antenna location on top center-line of the fuselage between the wing and vertical stabilzer for left hand circular polarization at 300 MHz. (Test Location 1) 15
14 Geometry of the cylindrical model of the P-3C aircraft used in the NEC-BSC showing the antenna location. (Test Location 2) 17
15 NEC-BSC calculated roll plane pattern for antenna location on top center-line of the fuselage forward of the aircraft wing for right hand circular polarization at 300 MHz. (Test Location 2) 18
16 NEC-BSC calculated elevation plane pattern for antenna location on top center-line of the fuselage forward of the aircraft wing for right hand circular polarization at 300 MHz. (Test Location 2) . . 19
17 NEC-BSC calculated azimuth plane pattern for antenna location on top center-line of the fuselage forward of the aircraft wing for right hand circular polarization at 300 MHz. (Test Location 2) 20
18 NEC-BSC calculated conical plane pattern 10° above the horizon for antenna location on top center-line of the fuselage forward of the aircraft wing for right hand circular polarization at 300 MHz. (Test Location 2) 21
19 NEC-BSC calculated conical plane pattern 20° above the horizon for antenna location on top center-line of the fuselage forward of the aircraft wing for right hand circular polarization at 300 MHz. (Test Location 2) 22
20 NEC-BSC calculated conical plane pattern 30° above the horizon for antenna location on top center-line of the fuselage forward of the aircraft wing for right hand circular polarization at 300 MHz. (Test Location 2) 23

21 NEC-BSC calculated roll plane pattern for antenna location on top center-line of the fuselage forward of the aircraft wing for left hand circular polarization at 300 MHz. (Test Location 2) 24
22 NEC-BSC calculated elevation plane pattern for antenna location on top center-line of the fuselage forward of the aircraft wing for left hand circular polarization at 300 MHz. (Test Location 2) 25
23 NEC-BSC calculated azimuth plane pattern for antenna location on top center-line of the fuselage forward of the aircraft wing for left hand circular polarization at 300 MHz. (Test Location 2) 26
24 NEC-BSC calculated conical plane pattern 10° above the horizon for antenna location on top center-line of the fuselage forward of the aircraft wing for left hand circular polarization at 300 MHz. (Test Location 2) 27
25 NEC-BSC calculated conical plane pattern 20° above the horizon for antenna location on top center-line of the fuselage forward of the aircraft wing for left hand circular polarization at 300 MHz. (Test Location 2) 28
26 NEC-BSC calculated conical plane pattern 30° above the horizon for antenna location on top center-line of the fuselage forward of the aircraft wing for left hand circular polarization at 300 MHz. (Test Location 2) 29
27 Geometry of the cylindrical model of the P-3C aircraft used in the NEC-BSC showing the antenna location. (Test Location 3) 31
28 NEC-BSC calculated roll plane pattern for antenna location on top center-line of the fuselage between the nose and wing for right hand circular polarization at 300 MHz. (Test Location 3) 32
29 NEC-BSC calculated elevation plane pattern for antenna location on top center-line of the fuselage between the nose and wing for right hand circular polarization at 300 MHz. (Test Location 3) . . 33
30 NEC-BSC calculated azimuth plane pattern for antenna location on top center-line of the fuselage between the nose and wing for right hand circular polarization at 300 MHz. (Test Location 3) 34
31 NEC-BSC calculated conical plane pattern 10° above the horizon for antenna location on top center-line of the fuselage between the nose and wing for right hand circular polarization at 300 MHz. (Test Location 3) 35
32 NEC-BSC calculated conical plane pattern 20° above the horizon for antenna location on top center-line of the fuselage between the nose and wing for right hand circular polarization at 300 MHz. (Test Location 3) 36

33 NEC-BSC calculated conical plane pattern 30° above the horizon for antenna location on top center-line of the fuselage between the nose and wing for right hand circular polarization at 300 MHz. (Test Location 3) 37
34 NEC-BSC calculated roll plane pattern for antenna location on top center-line of the fuselage between the nose and wing for left hand circular polarization at 300 MHz. (Test Location 3) 38
35 NEC-BSC calculated elevation plane pattern for antenna location on top center-line of the fuselage between the nose and wing for left hand circular polarization at 300 MHz. (Test Location 3) 39
36 NEC-BSC calculated azimuth plane pattern for antenna location on top center-line of the fuselage between the nose and wing for left hand circular polarization at 300 MHz. (Test Location 3) 40
37 NEC-BSC calculated conical plane pattern 10° above the horizon for antenna location on top center-line of the fuselage between the nose and wing for left hand circular polarization at 300 MHz. (Test Location 3) 41
38 NEC-BSC calculated conical plane pattern 20° above the horizon for antenna location on top center-line of the fuselage between the nose and wing for left hand circular polarization at 300 MHz. (Test Location 3) 42
39 NEC-BSC calculated conical plane pattern 30° above the horizon for antenna location on top center-line of the fuselage between the nose and wing for left hand circular polarization at 300 MHz. (Test Location 3) 43
40 Geometry of the composite ellipsoid model of the P-3C aircraft used in the NEC-BSC showing the antenna location. (Test Location 4) 45
41 NEC-BSC calculated roll plane pattern for antenna location on center-line of the fuselage near the aircraft nose for right hand circular polarization at 300 MHz. (Test Location 4) 46
42 NEC-BSC calculated elevation plane pattern for antenna location on center-line of the fuselage near the aircraft nose for right hand circular polarization at 300 MHz. (Test Location 4) 47
43 NEC-BSC calculated azimuth plane pattern for antenna location on center-line of the fuselage near the aircraft nose for right hand circular polarization at 300 MHz. (Test Location 4) 48
44 NEC-BSC calculated conical plane pattern 10° above the horizon for antenna location on center-line of the fuselage near the aircraft nose for right hand circular polarization at 300 MHz. (Test Location 4) 49

45 NEC-BSC calculated conical plane pattern 20° above the horizon for antenna location on center-line of the fuselage near the aircraft nose for right hand circular polarization at 300 MHz. (Test Location 4) 50
46 NEC-BSC calculated conical plane pattern 30° above the horizon for antenna location on center-line of the fuselage near the aircraft nose for right hand circular polarization at 300 MHz. (Test Location 4) 51
47 NEC-BSC calculated roll plane pattern for antenna location on center-line of the fuselage near the aircraft nose for left hand circular polarization at 300 MHz. (Test Location 4) 52
48 NEC-BSC calculated elevation plane pattern for antenna location on center-line of the fuselage near the aircraft nose for left hand circular polarization at 300 MHz. (Test Location 4) 53
49 NEC-BSC calculated azimuth plane pattern for antenna location on center-line of the fuselage near the aircraft nose for left hand circular polarization at 300 MHz. (Test Location 4) 54
50 NEC-BSC calculated conical plane pattern 10° above the horizon for antenna location on center-line of the fuselage near the aircraft nose for left hand circular polarization at 300 MHz. (Test Location 4) 55
51 NEC-BSC calculated conical plane pattern 20° above the horizon for antenna location on center-line of the fuselage near the aircraft nose for left hand circular polarization at 300 MHz. (Test Location 4) 56
52 NEC-BSC calculated conical plane pattern 30° above the horizon for antenna location on center-line of the fuselage near the aircraft nose for left hand circular polarization at 300 MHz. (Test Location 4) 57
53 Geometry of the composite ellipsoid model of the P-3C aircraft used in the NEC-BSC showing the antenna location. (Test Location 5) 59
54 NEC-BSC calculated roll plane pattern for antenna location on center-line of the fuselage near the aircraft nose for right hand circular polarization at 300 MHz. (Test Location 5) 60
55 NEC-BSC calculated elevation plane pattern for antenna location on center-line of the fuselage near the aircraft nose for right hand circular polarization at 300 MHz. (Test Location 5) 61
56 NEC-BSC calculated azimuth plane pattern for antenna location on center-line of the fuselage near the aircraft nose for right hand circular polarization at 300 MHz. (Test Location 5) 62

57 NEC-BSC calculated conical plane pattern 10° above the horizon for antenna location on center-line of the fuselage near the aircraft nose for right hand circular polarization at 300 MHz. (Test Location 5) 63
58 NEC-BSC calculated conical plane pattern 20° above the horizon for antenna location on center-line of the fuselage near the aircraft nose for right hand circular polarization at 300 MHz. (Test Location 5) 64
59 NEC-BSC calculated conical plane pattern 30° above the horizon for antenna location on center-line of the fuselage near the aircraft nose for right hand circular polarization at 300 MHz. (Test Location 5) 65
60 NEC-BSC calculated roll plane pattern for antenna location on center-line of the fuselage near the aircraft nose for left hand circular polarization at 300 MHz. (Test Location 5) 66
61 NEC-BSC calculated elevation plane pattern for antenna location on center-line of the fuselage near the aircraft nose for left hand circular polarization at 300 MHz. (Test Location 5) 67
62 NEC-BSC calculated azimuth plane pattern for antenna location on center-line of the fuselage near the aircraft nose for left hand circular polarization at 300 MHz. (Test Location 5) 68
63 NEC-BSC calculated conical plane pattern 10° above the horizon for antenna location on center-line of the fuselage near the aircraft nose for left hand circular polarization at 300 MHz. (Test Location 5) 69
64 NEC-BSC calculated conical plane pattern 20° above the horizon for antenna location on center-line of the fuselage near the aircraft nose for left hand circular polarization at 300 MHz. (Test Location 5) 70
65 NEC-BSC calculated conical plane pattern 30° above the horizon for antenna location on center-line of the fuselage near the aircraft nose for left hand circular polarization at 300 MHz. (Test Location 5) 71
66 Geometry of the cylindrical model of the P-3C aircraft used in the NEC-BSC showing the antenna location. (Test Location 6) 73
67 NEC-BSC calculated roll plane pattern for antenna location on the port side of the fuselage above the wing and 38.7° down from the top center-line for right hand circular polarization at 300 MHz. (Test Location 6) 74

68 NEC-BSC calculated elevation plane pattern for antenna location on the port side of the fuselage above the wing and 38.7° down from the top center-line for right hand circular polarization at 300 MHz. (Test Location 6) 75
69 NEC-BSC calculated azimuth plane pattern for antenna location on the port side of the fuselage above the wing and 38.7° down from the top center-line for right hand circular polarization at 300 MHz. (Test Location 6) 76
70 NEC-BSC calculated conical plane pattern 10° above the horizon for antenna location on the port side of the fuselage above the wing and 38.7° down from the top center-line for right hand circular polarization at 300 MHz. (Test Location 6) 77
71 NEC-BSC calculated conical plane pattern 20° above the horizon for antenna location on the port side of the fuselage above the wing and 38.7° down from the top center-line for right hand circular polarization at 300 MHz. (Test Location 6) 78
72 NEC-BSC calculated conical plane pattern 30° above the horizon for antenna location on the port side of the fuselage above the wing and 38.7° down from the top center-line for right hand circular polarization at 300 MHz. (Test Location 6) 79
73 NEC-BSC calculated roll plane pattern for antenna location on the port side of the fuselage above the wing and 38.7° down from the top center-line for left hand circular polarization at 300 MHz. (Test Location 6) 80
74 NEC-BSC calculated elevation plane pattern for antenna location on the port side of the fuselage above the wing and 38.7° down from the top center-line for left hand circular polarization at 300 MHz. (Test Location 6) 81
75 NEC-BSC calculated azimuth plane pattern for antenna location on the port side of the fuselage above the wing and 38.7° down from the top center-line for left hand circular polarization at 300 MHz. (Test Location 6) 82
76 NEC-BSC calculated conical plane pattern 10° above the horizon for antenna location on the port side of the fuselage above the wing and 38.7° down from the top center-line for left hand circular polarization at 300 MHz. (Test Location 6) 83
77 NEC-BSC calculated conical plane pattern 20° above the horizon for antenna location on the port side of the fuselage above the wing and 38.7° down from the top center-line for left hand circular polarization at 300 MHz. (Test Location 6) 84

78 NEC-BSC calculated conical plane pattern 30° above the horizon for antenna location on the port side of the fuselage above the wing and 38.7° down from the top center-line for left hand circular polarization at 300 MHz. (Test Location 6) 85
79 Geometry of the cylindrical model of the P-3C aircraft used in the NEC-BSC showing the antenna location. (Test Location 7) 87
80 NEC-BSC calculated roll plane pattern for antenna location on the port side of the fuselage between the nose and the wing 38.7° down from the top center-line for right hand circular polarization at 300 MHz. (Test Location 7) 88
81 NEC-BSC calculated elevation plane pattern for antenna location on the port side of the fuselage between the nose and the wing 38.7° down from the top center-line for right hand circular polarization at 300 MHz. (Test Location 7) 89
82 NEC-BSC calculated azimuth plane pattern for antenna location on the port side of the fuselage between the nose and the wing 38.7° down from the top center-line for right hand circular polarization at 300 MHz. (Test Location 7) 90
83 NEC-BSC calculated conical plane pattern 10° above the horizon for antenna location on the port side of the fuselage between the nose and the wing 38.7° down from the top center-line for right hand circular polarization at 300 MHz. (Test Location 7) 91
84 NEC-BSC calculated conical plane pattern 20° above the horizon for antenna location on the port side of the fuselage between the nose and the wing 38.7° down from the top center-line for right hand circular polarization at 300 MHz. (Test Location 7) 92
85 NEC-BSC calculated conical plane pattern 30° above the horizon for antenna location on the port side of the fuselage between the nose and the wing 38.7° down from the top center-line for right hand circular polarization at 300 MHz. (Test Location 7) 93
86 NEC-BSC calculated roll plane pattern for antenna location on the port side of the fuselage between the nose and the wing 38.7° down from the top center-line for left hand circular polarization at 300 MHz. (Test Location 7) 94
87 NEC-BSC calculated elevation plane pattern for antenna location on the port side of the fuselage between the nose and the wing 38.7° down from the top center-line for left hand circular polarization at 300 MHz. (Test Location 7) 95

88 NEC-BSC calculated azimuth plane pattern for antenna location on the port side of the fuselage between the nose and the wing 38.7° down from the top center-line for left hand circular polarization at 300 MHz. (Test Location 7) 96
89 NEC-BSC calculated conical plane pattern 10° above the horizon for antenna location on the port side of the fuselage between the nose and the wing 38.7° down from the top center-line for left hand circular polarization at 300 MHz. (Test Location 7) 97
90 NEC-BSC calculated conical plane pattern 20° above the horizon for antenna location on the port side of the fuselage between the nose and the wing 38.7° down from the top center-line for left hand circular polarization at 300 MHz. (Test Location 7) 98
91 NEC-BSC calculated conical plane pattern 30° above the horizon for antenna location on the port side of the fuselage between the nose and the wing 38.7° down from the top center-line for left hand circular polarization at 300 MHz. (Test Location 7) 99
92 Geometry of the cylindrical model of the P-3C aircraft used in the NEC-BSC showing the antenna location. (Test Location 8) 101
93 NEC-BSC calculated roll plane pattern for antenna location on the port side of the vertical stabilizer for right hand circular polarization at 300 MHz. (Test Location 8) 102
94 NEC-BSC calculated elevation plane pattern for antenna location on the port side of the vertical stabilizer for right hand circular polarization at 300 MHz. (Test Location 8) 103
95 NEC-BSC calculated azimuth plane pattern for antenna location on the port side of the vertical stabilizer for right hand circular polarization at 300 MHz. (Test Location 8) 104
96 NEC-BSC calculated conical plane pattern 10° above the horizon for antenna location on the port side of the vertical stabilizer for right hand circular polarization at 300 MHz. (Test Location 8) . . 105
97 NEC-BSC calculated conical plane pattern 20° above the horizon for antenna location on the port side of the vertical stabilizer for right hand circular polarization at 300 MHz. (Test Location 8) . . 106
98 NEC-BSC calculated conical plane pattern 30° above the horizon for antenna location on the port side of the vertical stabilizer for right hand circular polarization at 300 MHz. (Test Location 8) . . 107
99 NEC-BSC calculated roll plane pattern for antenna location on the port side of the vertical stabilizer for left hand circular polarization at 300 MHz. (Test Location 8) 108

100 NEC-BSC calculated elevation plane pattern for antenna location on the port side of the vertical stabilizer for left hand circular polarization at 300 MHz. (Test Location 8) 109
101 NEC-BSC calculated azimuth plane pattern for antenna location on the port side of the vertical stabilizer for left hand circular polarization at 300 MHz. (Test Location 8) 110
102 NEC-BSC calculated conical plane pattern 10° above the horizon for antenna location on the port side of the vertical stabilizer for left hand circular polarization at 300 MHz. (Test Location 8) . . 111
103 NEC-BSC calculated conical plane pattern 20° above the horizon for antenna location on the port side of the vertical stabilizer for left hand circular polarization at 300 MHz. (Test Location 8) . . 112
104 NEC-BSC calculated conical plane pattern 30° above the horizon for antenna location on the port side of the vertical stabilizer for left hand circular polarization at 300 MHz. (Test Location 8) . . 113
105 Geometry of the cylindrical model of the P-3C aircraft used in the NEC-BSC showing the antenna location. (Test Location 9) 115
106 NEC-BSC calculated roll plane pattern for antenna location on top of the vertical stabilizer for right hand circular polarization at 300 MHz. (Test Location 9) 116
107 NEC-BSC calculated elevation plane pattern for antenna location on top of the vertical stabilizer for right hand circular polarization at 300 MHz. (Test Location 9) 117
108 NEC-BSC calculated azimuth plane pattern for antenna location on top of the vertical stabilizer for right hand circular polarization at 300 MHz. (Test Location 9) 118
109 NEC-BSC calculated conical plane pattern 10° above the horizon for antenna location on top of the vertical stabilizer for right hand circular polarization at 300 MHz. (Test Location 9) 119
110 NEC-BSC calculated conical plane pattern 20° above the horizon for antenna location on top of the vertical stabilizer for right hand circular polarization at 300 MHz. (Test Location 9) 120
111 NEC-BSC calculated conical plane pattern 30° above the horizon for antenna location on top of the vertical stabilizer for right hand circular polarization at 300 MHz. (Test Location 9) 121
112 NEC-BSC calculated roll plane pattern for antenna location on top of the vertical stabilizer for left hand circular polarization at 300 MHz. (Test Location 9) 122
113 NEC-BSC calculated elevation plane pattern for antenna location on top of the vertical stabilizer for left hand circular polarization at 300 MHz. (Test Location 9) 123

114 NEC-BSC calculated azimuth plane pattern for antenna location on top of the vertical stabilizer for left hand circular polarization at 300 MHz. (Test Location 9) 124
115 NEC-BSC calculated conical plane pattern 10° above the horizon for antenna location on top of the vertical stabilizer for left hand circular polarization at 300 MHz. (Test Location 9) 125
116 NEC-BSC calculated conical plane pattern 20° above the horizon for antenna location on top of the vertical stabilizer for left hand circular polarization at 300 MHz. (Test Location 9) 126
117 NEC-BSC calculated conical plane pattern 30° above the horizon for antenna location on top of the vertical stabilizer for left hand circular polarization at 300 MHz. (Test Location 9) 127
118 Geometry of the cylindrical model of the P-3C aircraft used in the NEC-BSC showing the antenna location. (Test Location 10) . . . 129
119 NEC-BSC calculated roll plane pattern for antenna location on the port side horizontal stabilizer for right hand circular polarization at 300 MHz. (Test Location 10) 130
120 NEC-BSC calculated elevation plane pattern for antenna location on the port side horizontal stabilizer for right hand circular polarization at 300 MHz. (Test Location 10) 131
121 NEC-BSC calculated azimuth plane pattern for antenna location on the port side horizontal stabilizer for right hand circular polarization at 300 MHz. (Test Location 10) 132
122 NEC-BSC calculated conical plane pattern 10° above the horizon for antenna location on the port side horizontal stabilizer for right hand circular polarization at 300 MHz. (Test Location 10) 133
123 NEC-BSC calculated conical plane pattern 20° above the horizon for antenna location on the port side horizontal stabilizer for right hand circular polarization at 300 MHz. (Test Location 10) 134
124 NEC-BSC calculated conical plane pattern 30° above the horizon for antenna location on the port side horizontal stabilizer for right hand circular polarization at 300 MHz. (Test Location 10) 135
125 NEC-BSC calculated roll plane pattern for antenna location on the port side horizontal stabilizer for left hand circular polarization at 300 MHz. (Test Location 10) 136
126 NEC-BSC calculated elevation plane pattern for antenna location on the port side horizontal stabilizer for left hand circular polarization at 300 MHz. (Test Location 10) 137
127 NEC-BSC calculated azimuth plane pattern for antenna location on the port side horizontal stabilizer for left hand circular polarization at 300 MHz. (Test Location 10) 138

128 NEC-BSC calculated conical plane pattern 10° above the horizon for antenna location on the port side horizontal stabilizer for left hand circular polarization at 300 MHz. (Test Location 10) 139
129 NEC-BSC calculated conical plane pattern 20° above the horizon for antenna location on the port side horizontal stabilizer for left hand circular polarization at 300 MHz. (Test Location 10) 140
130 NEC-BSC calculated conical plane pattern 30° above the horizon for antenna location on the port side horizontal stabilizer for left hand circular polarization at 300 MHz. (Test Location 10) 141

131 DM C99-2 airborne UHF satellite communication antenna of Dorne & Margolin. 151
132 E_θ antenna pattern at 244 MHz for DM C99-2 antenna in free space. 152
133 E_ϕ antenna pattern at 244 MHz for DM C99-2 antenna in free space. 153
134 Right hand circular polarized antenna pattern at 244 MHz for DM C99-2 antenna in free space. 154
135 E_θ antenna pattern at 318 MHz for DM C99-2 antenna in free space. 155
136 E_ϕ antenna pattern at 318 MHz for DM C99-2 antenna in free space. 156
137 Right hand circular polarized antenna pattern at 318 MHz for DM C99-2 antenna in free space. 157
138 Geometry of the forward section of the actual P-3C aircraft which includes a model for the DM C99-2 antenna. 159
139 Geometry of twelve-sided flat plate used to model the fuselage surface which includes a model for the DM C99-2 antenna. 160
140 Roll plane pattern for DM C99-2 antenna placed in radome located in the nose of the P-3C aircraft for right hand circular polarization at 244 MHz. 162
141 Elevation plane pattern for DM C99-2 antenna placed in radome located in the nose of the P-3C aircraft for right hand circular polarization at 244 MHz. 163
142 Azimuth plane pattern for DM C99-2 antenna placed in radome located in the nose of the P-3C aircraft for right hand circular polarization at 244 MHz. 164
143 Conical plane pattern 10° above the horizon for DM C99-2 antenna placed in radome located in the nose of the P-3C aircraft for right hand circular polarization at 244 MHz. 165
144 Conical plane pattern 20° above the horizon for DM C99-2 antenna placed in radome located in the nose of the P-3C aircraft for right hand circular polarization at 244 MHz. 166

145 Conical plane pattern 30° above the horizon for DM C99-2 antenna placed in radome located in the nose of the P-3C aircraft for right hand circular polarization at 244 MHz. 167
146 Roll plane pattern for DM C99-2 antenna placed in radome located in the nose of the P-3C aircraft for left hand circular polarization at 244 MHz. 168
147 Elevation plane pattern for DM C99-2 antenna placed in radome located in the nose of the P-3C aircraft for left hand circular polarization at 244 MHz. 169
148 Azimuth plane pattern for DM C99-2 antenna placed in radome located in the nose of the P-3C aircraft for left hand circular polarization at 244 MHz. 170
149 Conical plane pattern 10° above the horizon for DM C99-2 antenna placed in radome located in the nose of the P-3C aircraft for left hand circular polarization at 244 MHz. 171
150 Conical plane pattern 20° above the horizon for DM C99-2 antenna placed in radome located in the nose of the P-3C aircraft for left hand circular polarization at 244 MHz. 172
151 Conical plane pattern 30° above the horizon for DM C99-2 antenna placed in radome located in the nose of the P-3C aircraft for left hand circular polarization at 244 MHz. 173

Chapter 1

Location Study

1.1 Introduction

This study is a continuation of the work presented in Volume I of this report [1]. This volume contains an antenna location study for the P-3C aircraft. From this location study, a determination can be made of the complete antenna system required to achieve the desired pattern and polarization coverage. The antenna used in this location study is the same Dorne & Margolin DM 1501341 (Batwing) airborne UHF satellite communications antenna which has been defined and validated in Chapter 2 of Volume I. The aircraft model used in the majority of the locations studied is the simple cylindrical aircraft model defined and validated in Chapters 3 and 5 of the previous volume. However, the simple cylindrical model is not used when the antenna location is near the nose of the aircraft and the aircraft's elliptical nose is critical to the radiation patterns. In these cases, the composite ellipsoid aircraft model defined in Chapter 3 of Volume I is used.

Sections 1.2 through 1.11 contain information for the ten antenna locations which are investigated. Each of these sections contains an illustration of the aircraft model which shows the location of the antenna and the radiation patterns for both right hand and left hand circular polarizations in the roll plane, the elevation plane, the azimuth plane and conical cuts from 10° to 30° above the horizon. These

radiation patterns are calculated using the improved version of the NEC-BSC. Note that many of the antenna locations investigated in this report are identical to the ones previously investigated in Reference [2]. Any differences between the radiation patterns presented here and the ones presented in [2] for the respective antenna locations are due to the fact that the improved version of the NEC-BSC is used in this report and Version 3.1 of the NEC-BSC is used in [2]. Section 1.12 summarizes the antenna locations investigated in this chapter and Section 1.13 draws some conclusions on the final antenna system configuration.

1.2 Test Location 1

In this section, the antenna is located on the top center-line of the fuselage between the wing and the vertical stabilizer. The cylindrical aircraft model used in the NEC-BSC is illustrated in Figure 1, which also shows the location of the antenna on the fuselage. The calculated results obtained using the improved version of the NEC-BSC at 300 MHz for the right hand circular polarized or co-polarized fields are shown for the roll plane in Figure 2, for the elevation plane in Figure 3, for the azimuth plane in Figure 4 and for the conical planes 10°, 20° and 30° above the horizon in Figures 5, 6 and 7, respectively. For completeness, the left hand circular polarized or cross-polarized results are also included. These cross-polarized results are shown for the roll plane in Figure 8, for the elevation plane in Figure 9, for the azimuth plane in Figure 10 and for the conical planes 10°, 20° and 30° above the horizon in Figures 11, 12 and 13, respectively.

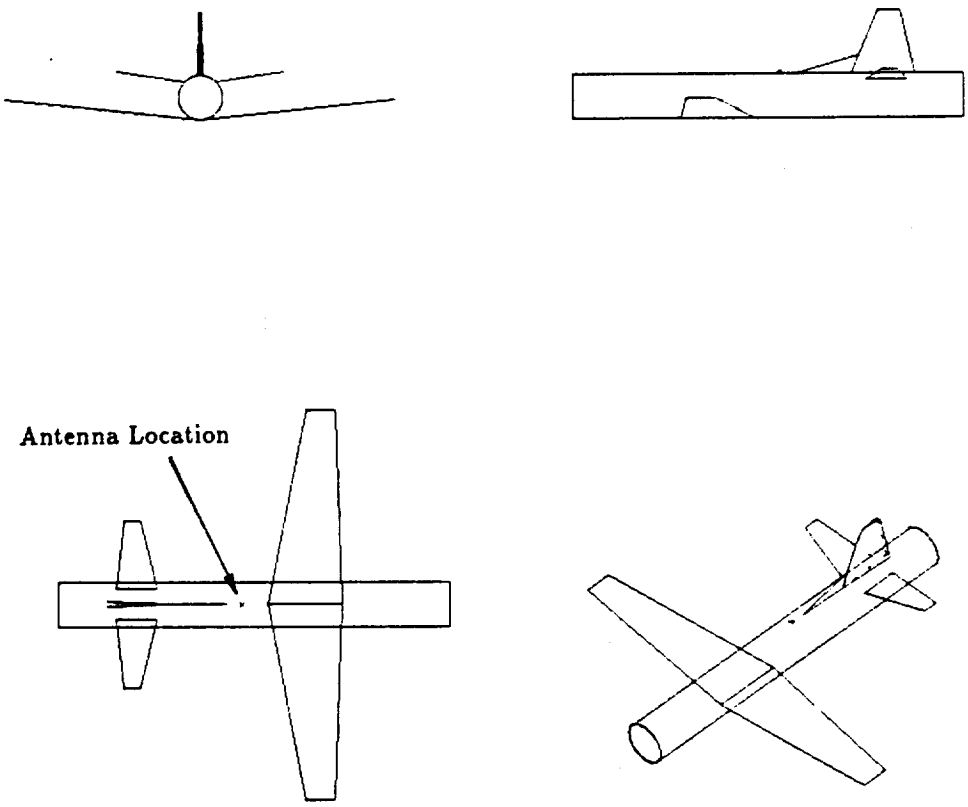

Figure 1: Geometry of the cylindrical model of the P-3C aircraft used in the NEC-BSC showing the antenna location. (Test Location 1)

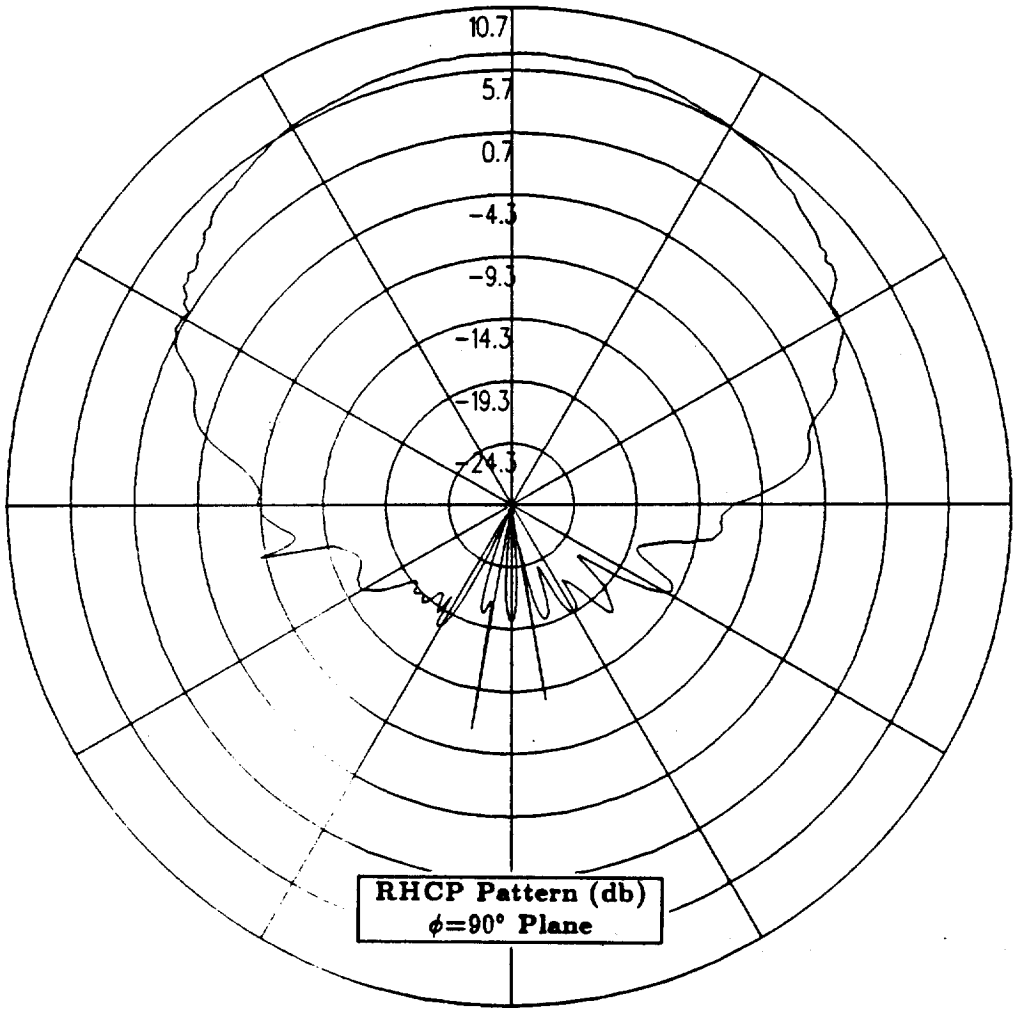

Figure 2: NEC-BSC calculated roll plane pattern for antenna location on top center-line of the fuselage between the wing and vertical stabilizer for right hand circular polarization at 300 MHz. (Test Location 1)

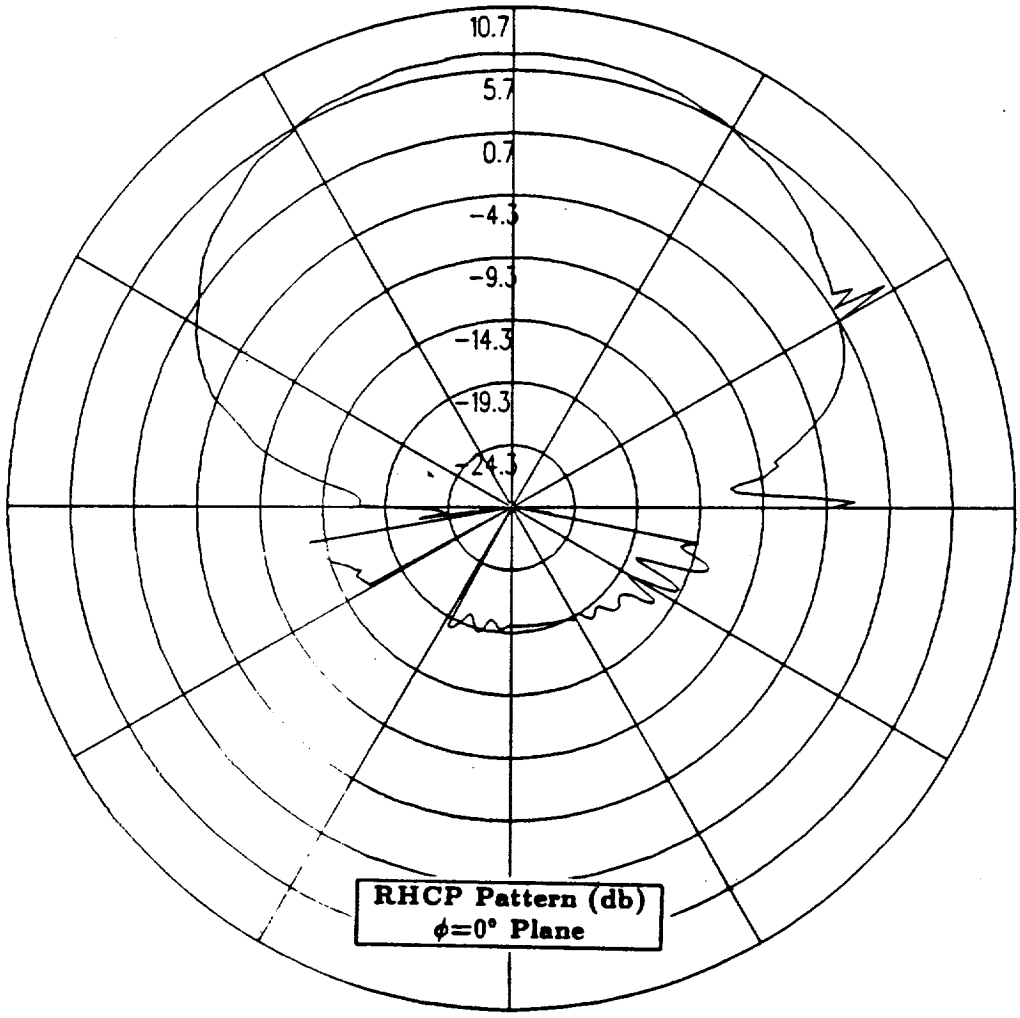

Figure 3: NEC-BSC calculated elevation plane pattern for antenna location on top center-line of the fuselage between the wing and vertical stabilizer for right hand circular polarization at 300 MHz. (Test Location 1)

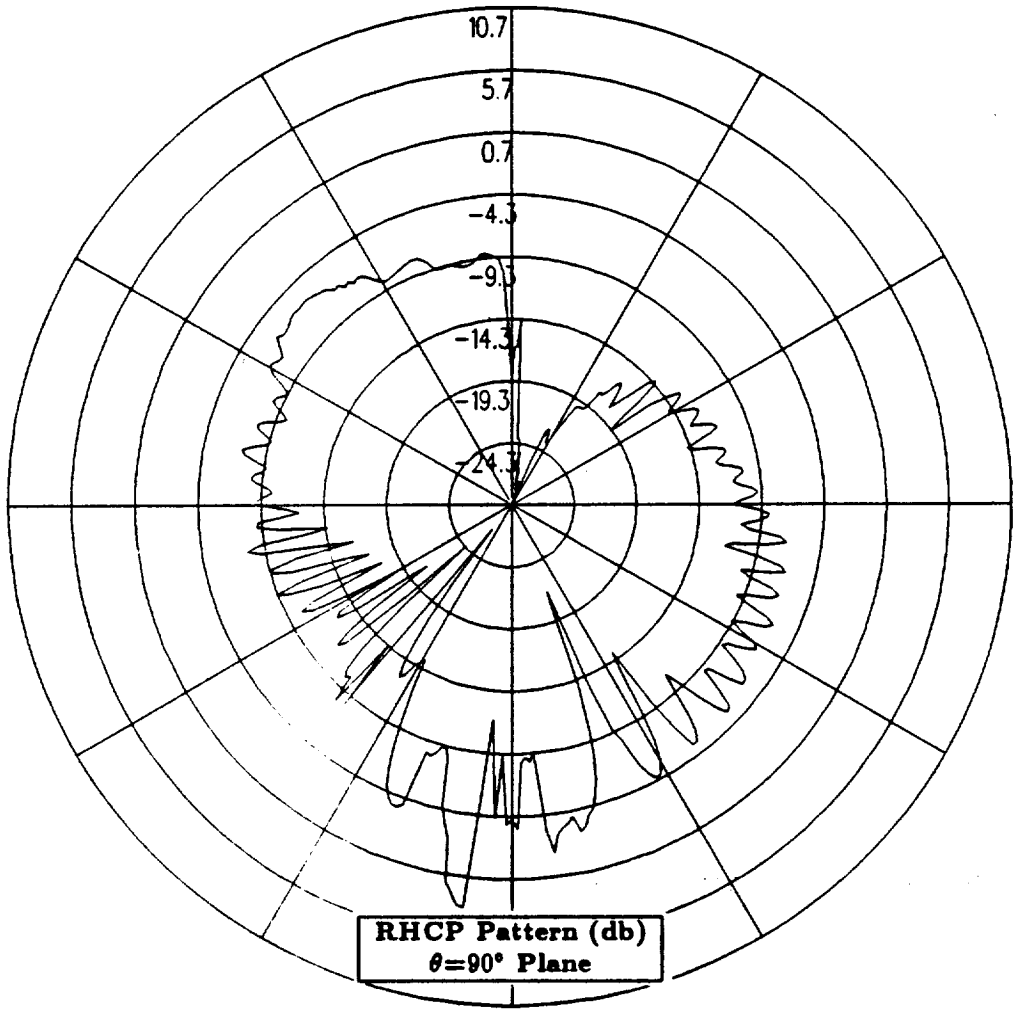

Figure 4: NEC-BSC calculated azimuth plane pattern for antenna location on top center-line of the fuselage between the wing and vertical stabilizer for right hand circular polarization at 300 MHz. (Test Location 1)

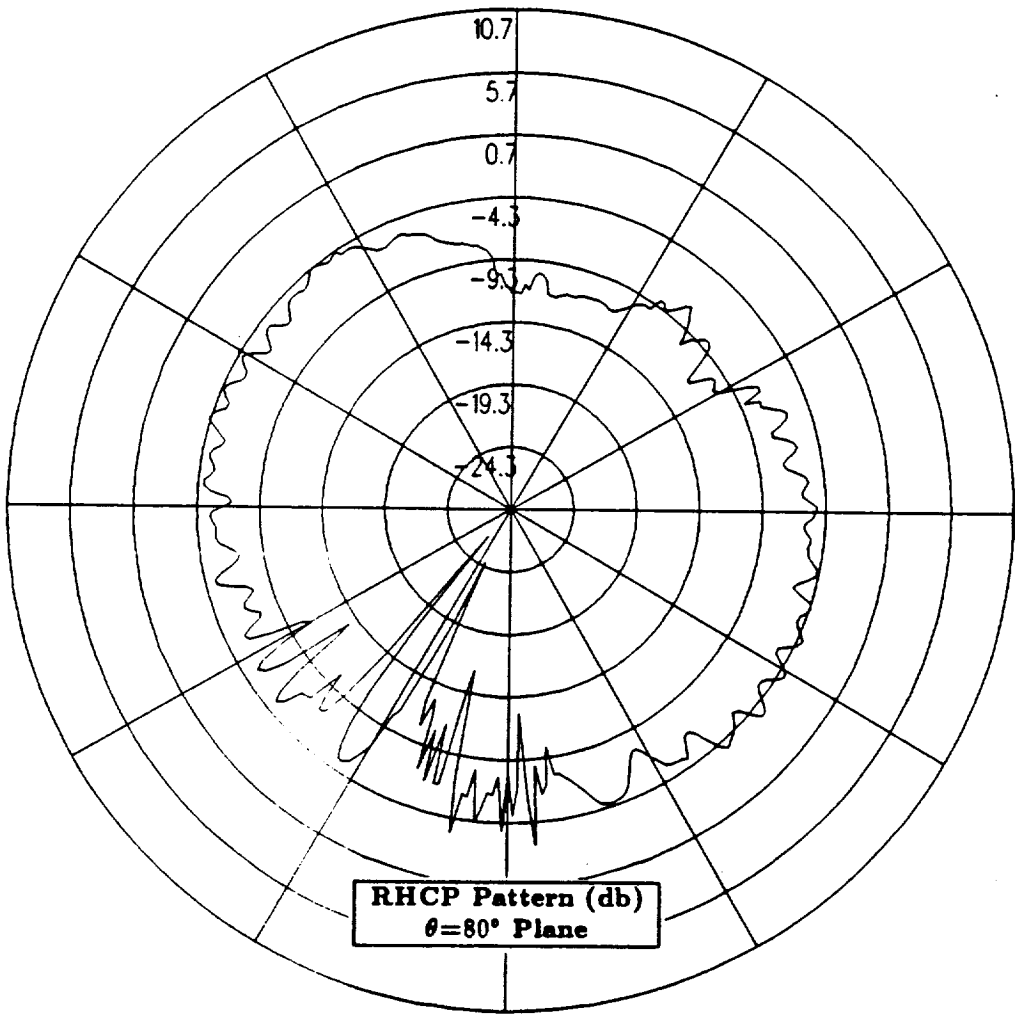

Figure 5: NEC-BSC calculated conical plane pattern 10° above the horizon for antenna location on top center-line of the fuselage between the wing and vertical stabilzer for right hand circular polarization at 300 MHz. (Test Location 1)

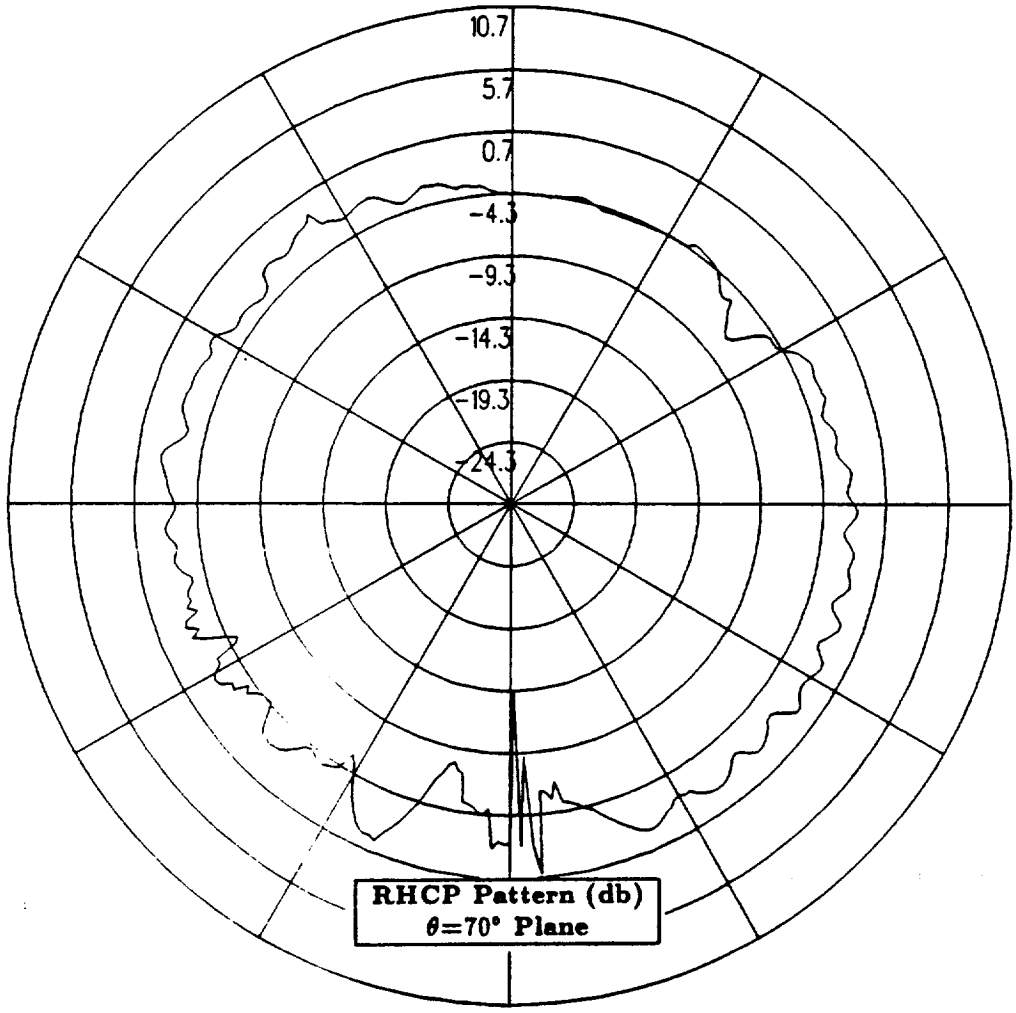

Figure 6: NEC-BSC calculated conical plane pattern 20° above the horizon for antenna location on top center-line of the fuselage between the wing and vertical stabilzer for right hand circular polarization at 300 MHz. (Test Location 1)

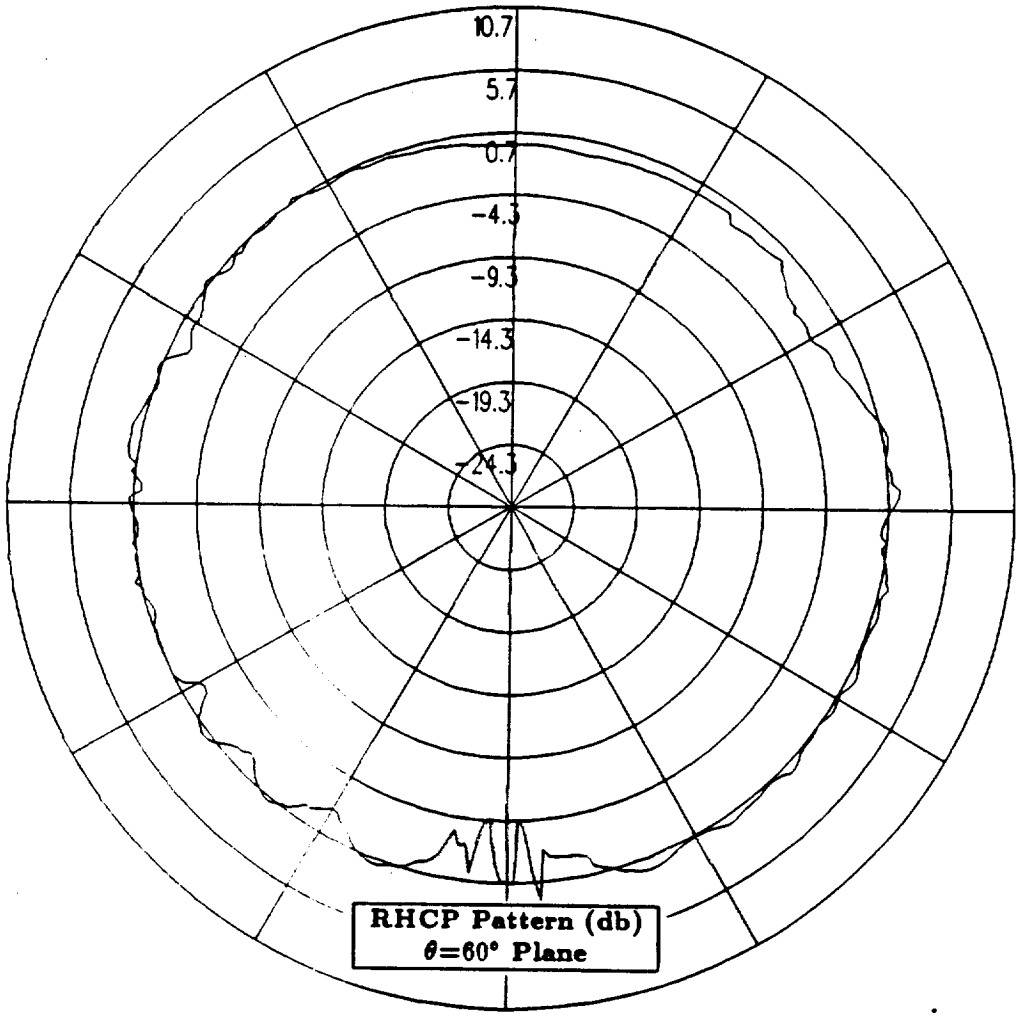

Figure 7: NEC-BSC calculated conical plane pattern 30° above the horizon for antenna location on top center-line of the fuselage between the wing and vertical stabilzer for right hand circular polarization at 300 MHz. (Test Location 1)

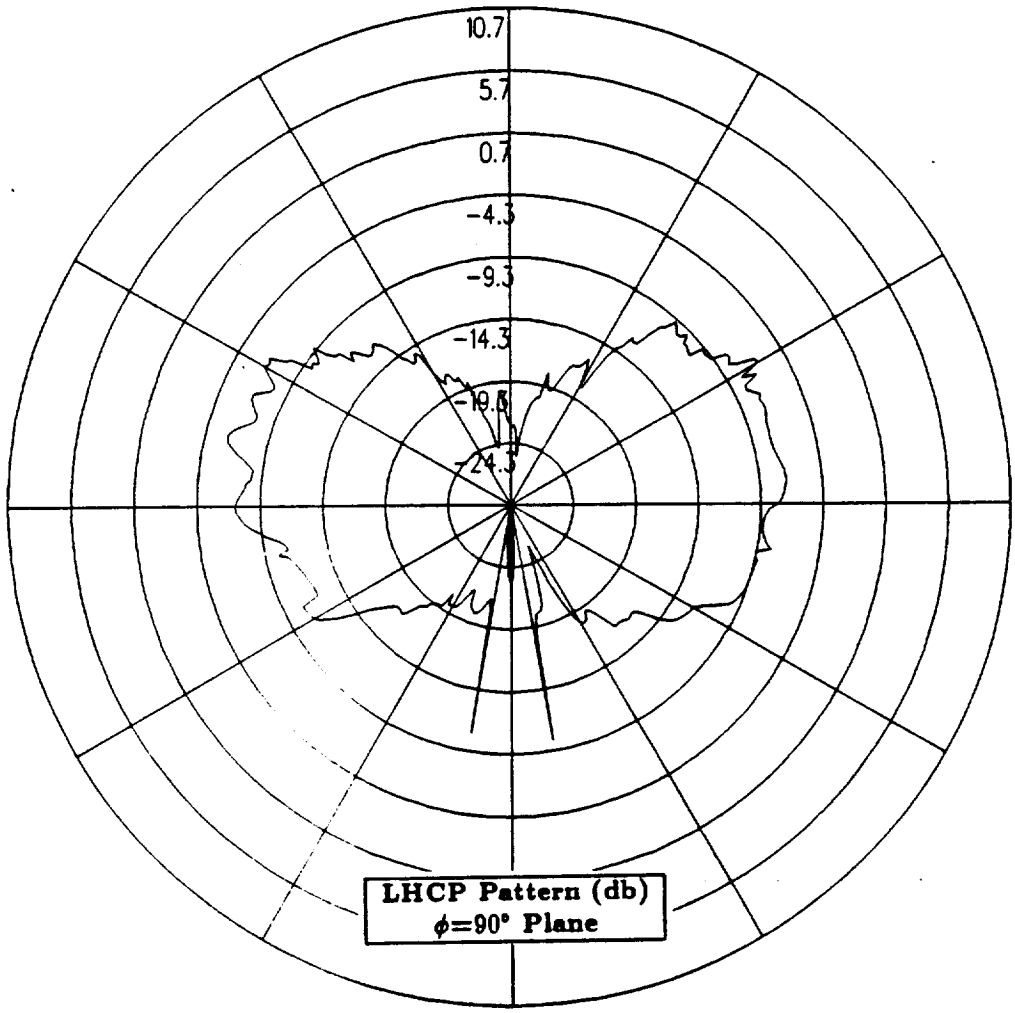

Figure 8: NEC-BSC calculated roll plane pattern for antenna location on top center-line of the fuselage between the wing and vertical stabilizer for left hand circular polarization at 300 MHz. (Test Location 1)

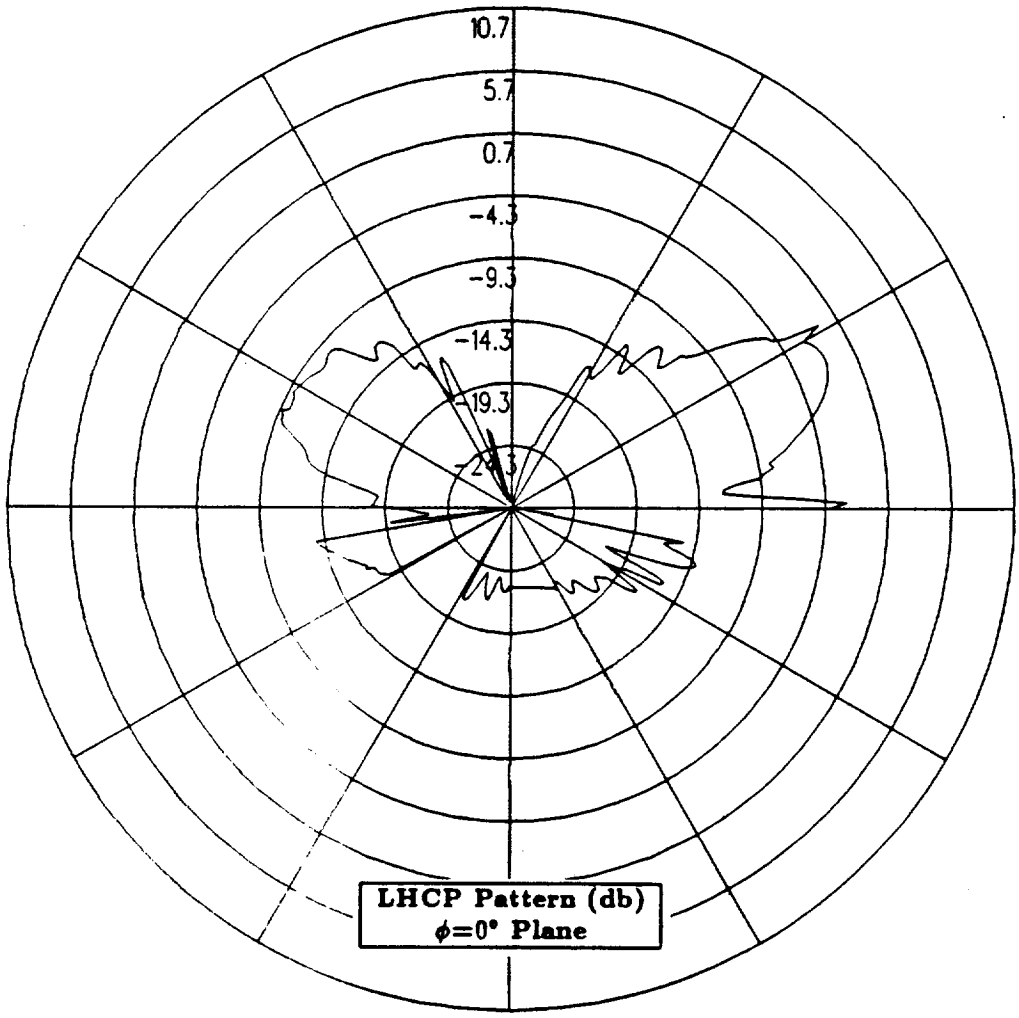

Figure 9: NEC-BSC calculated elevation plane pattern for antenna location on top center-line of the fuselage between the wing and vertical stabilizer for left hand circular polarization at 300 MHz. (Test Location 1)

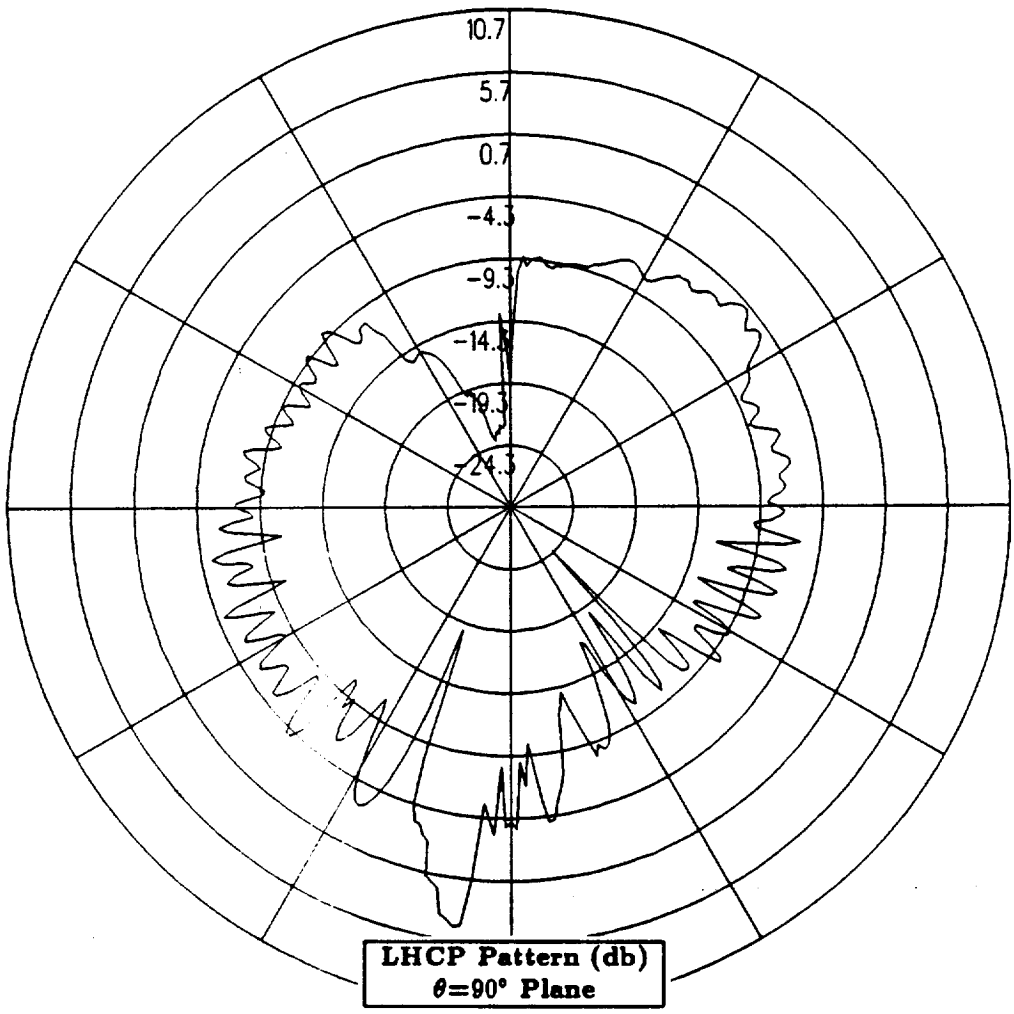

Figure 10: NEC-BSC calculated azimuth plane pattern for antenna location on top center-line of the fuselage between the wing and vertical stabilizer for left hand circular polarization at 300 MHz. (Test Location 1)

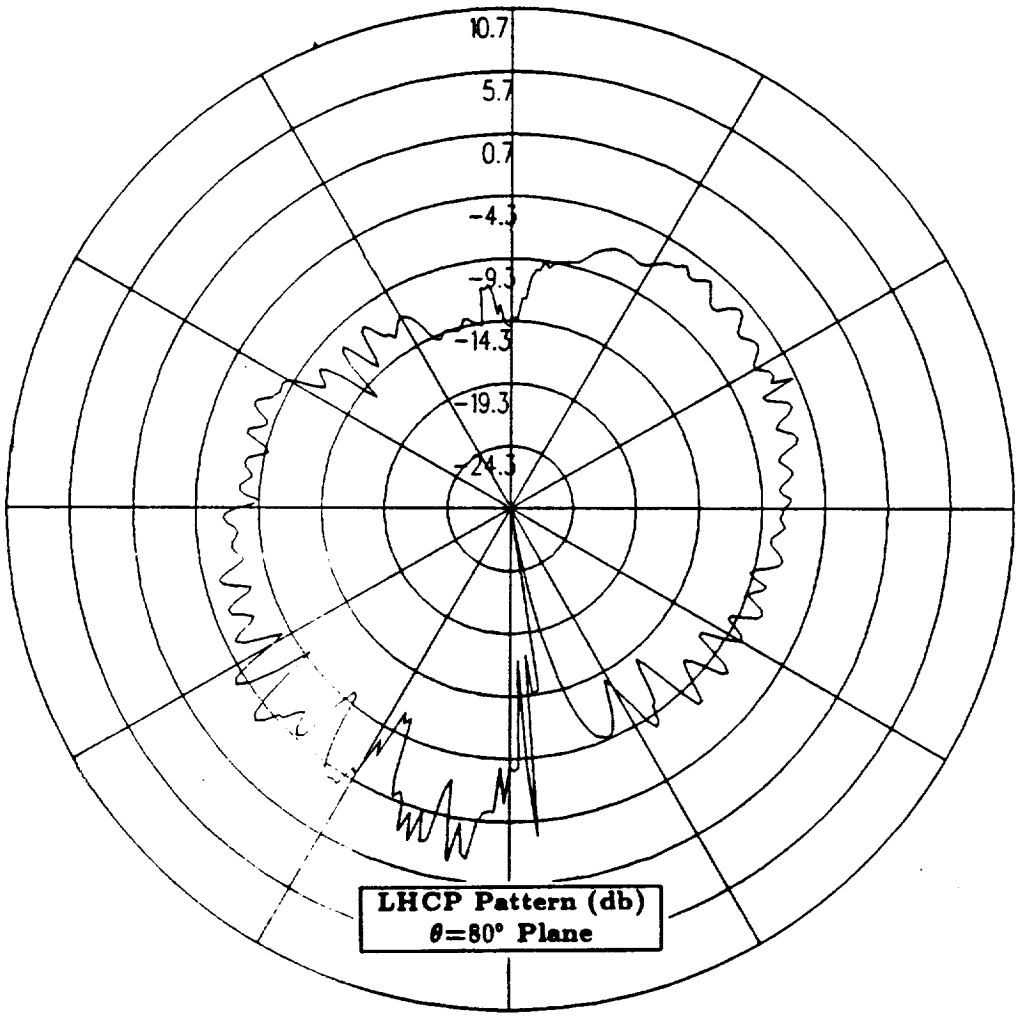

Figure 11: NEC-BSC calculated conical plane pattern 10° above the horizon for antenna location on top center-line of the fuselage between the wing and vertical stabilzer for left hand circular polarization at 300 MHz. (Test Location 1)

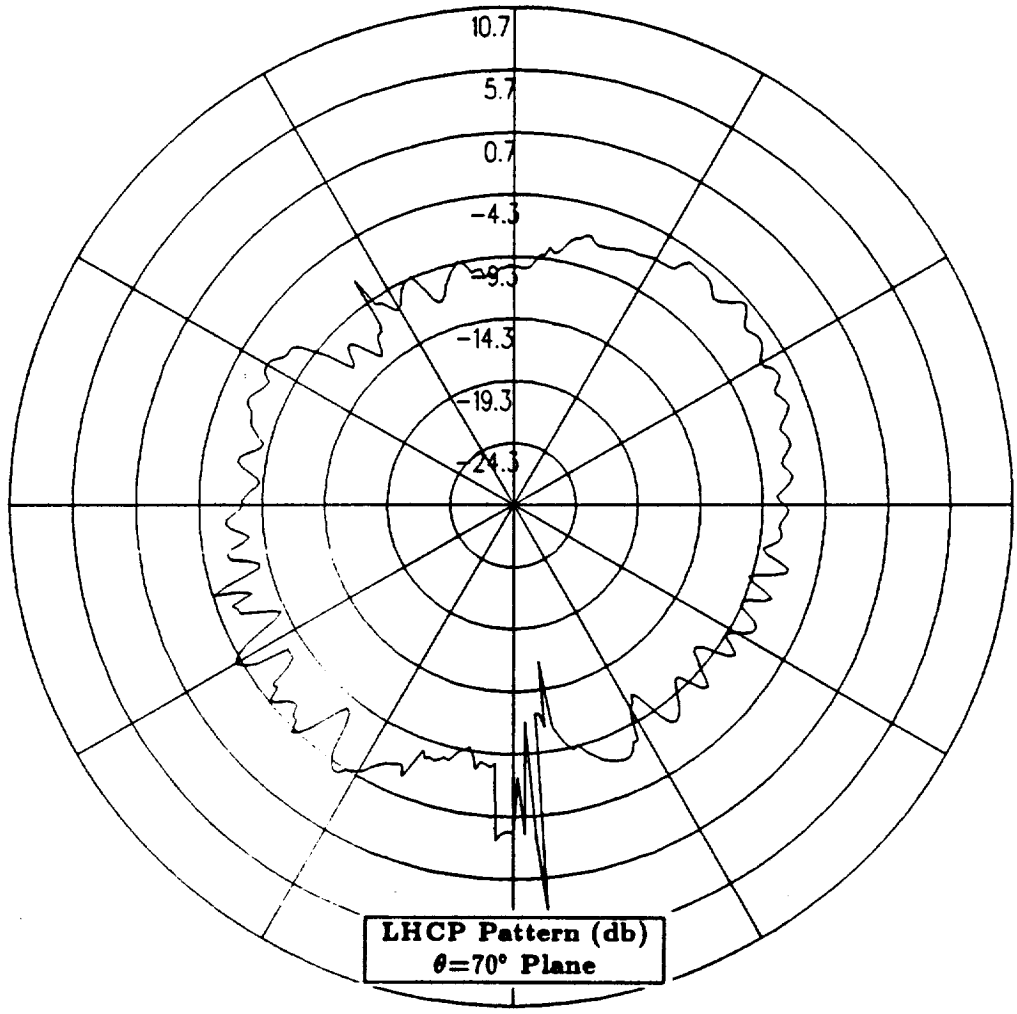

Figure 12: NEC-BSC calculated conical plane pattern 20° above the horizon for antenna location on top center-line of the fuselage between the wing and vertical stabilzer for left hand circular polarization at 300 MHz. (Test Location 1)

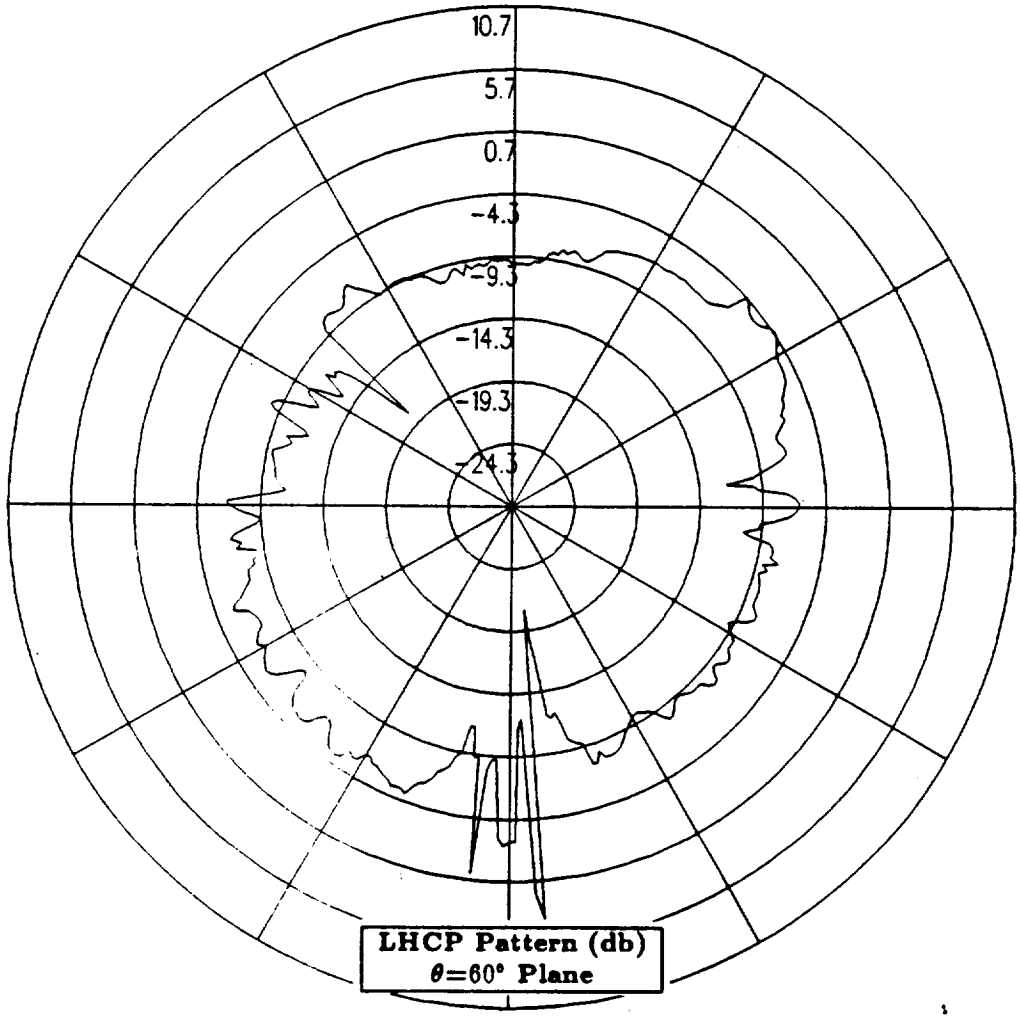

Figure 13: NEC-BSC calculated conical plane pattern 30° above the horizon for antenna location on top center-line of the fuselage between the wing and vertical stabilzer for left hand circular polarization at 300 MHz. (Test Location 1)

1.3 Test Location 2

In this section, the antenna is located on the top center-line of the fuselage forward of the aircraft wing. The cylindrical aircraft model used in the NEC-BSC is illustrated in Figure 14, which also shows the location of the antenna on the fuselage. The calculated results obtained using the improved version of the NEC-BSC at 300 MHz for the right hand circular polarized or co-polarized fields are shown for the roll plane in Figure 15, for the elevation plane in Figure 16, for the azimuth plane in Figure 17 and for the conical planes 10°, 20° and 30° above the horizon in Figures 18, 19 and 20, respectively. For completeness, the left hand circular polarized or cross-polarized results are also included. These cross-polarized results are shown for the roll plane in Figure 21, for the elevation plane in Figure 22, for the azimuth plane in Figure 23 and for the conical planes 10°, 20° and 30° above the horizon in Figures 24, 25 and 26, respectively.

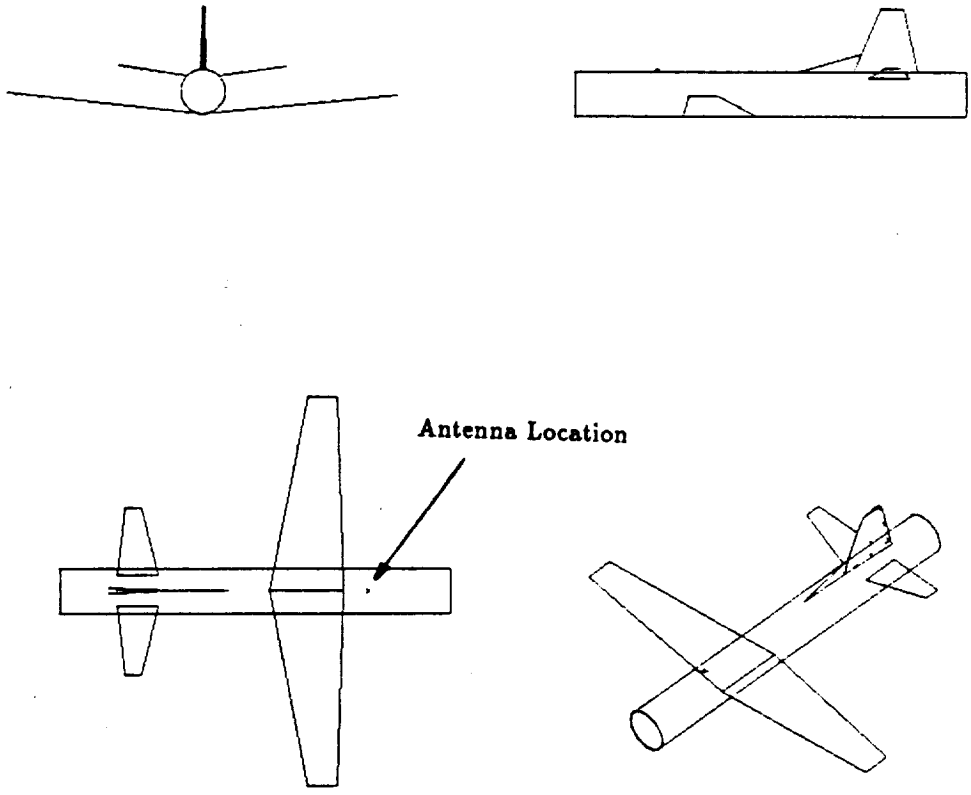

Figure 14: Geometry of the cylindrical model of the P-3C aircraft used in the NEC-BSC showing the antenna location. (Test Location 2)

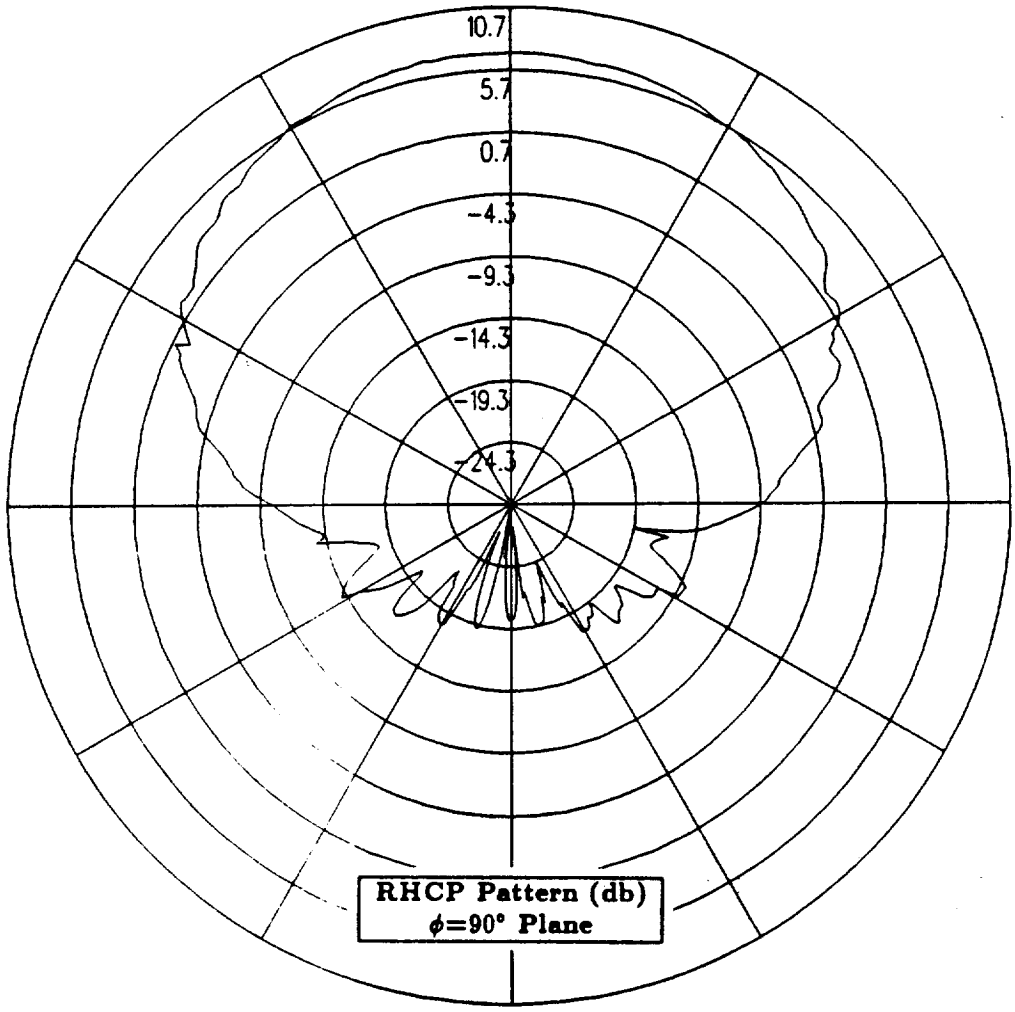

Figure 15: NEC-BSC calculated roll plane pattern for antenna location on top center-line of the fuselage forward of the aircraft wing for right hand circular polarization at 300 MHz. (Test Location 2)

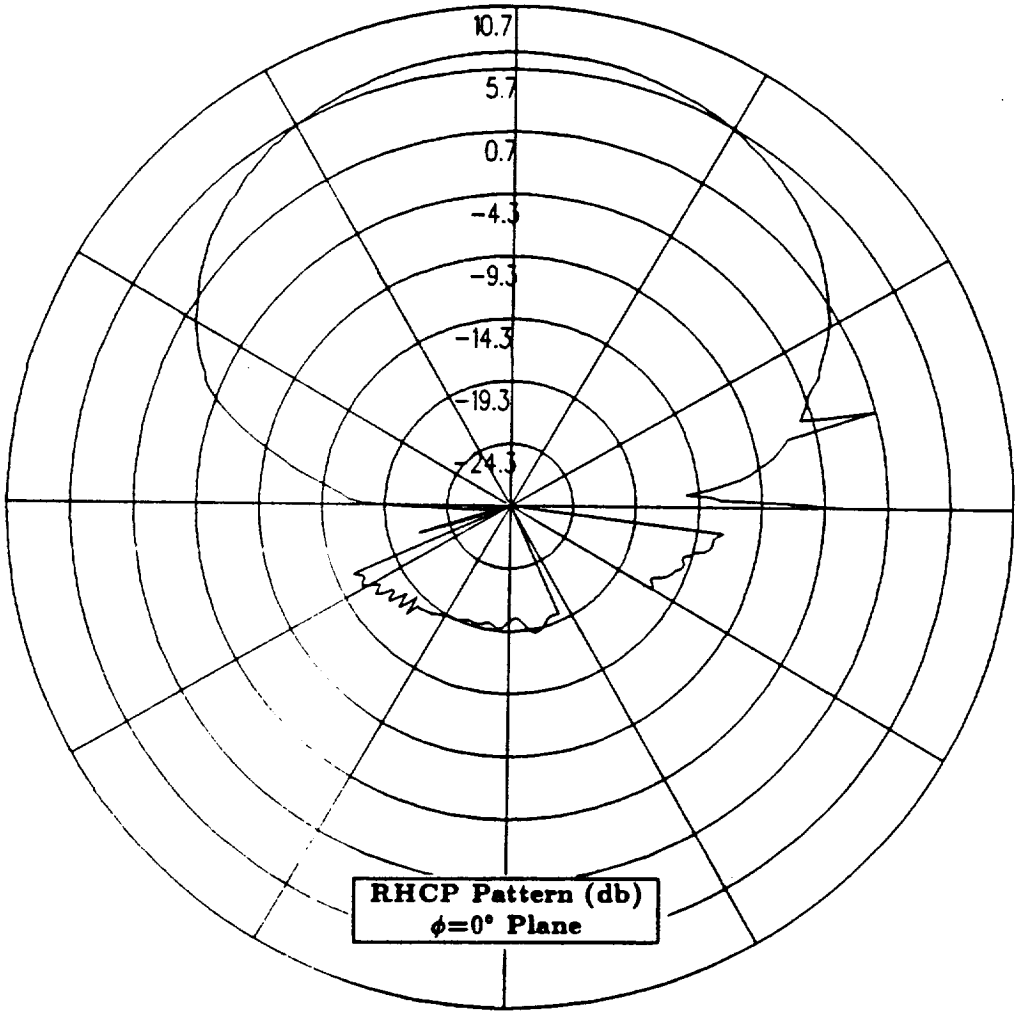

Figure 16: NEC-BSC calculated elevation plane pattern for antenna location on top center-line of the fuselage forward of the aircraft wing for right hand circular polarization at 300 MHz. (Test Location 2)

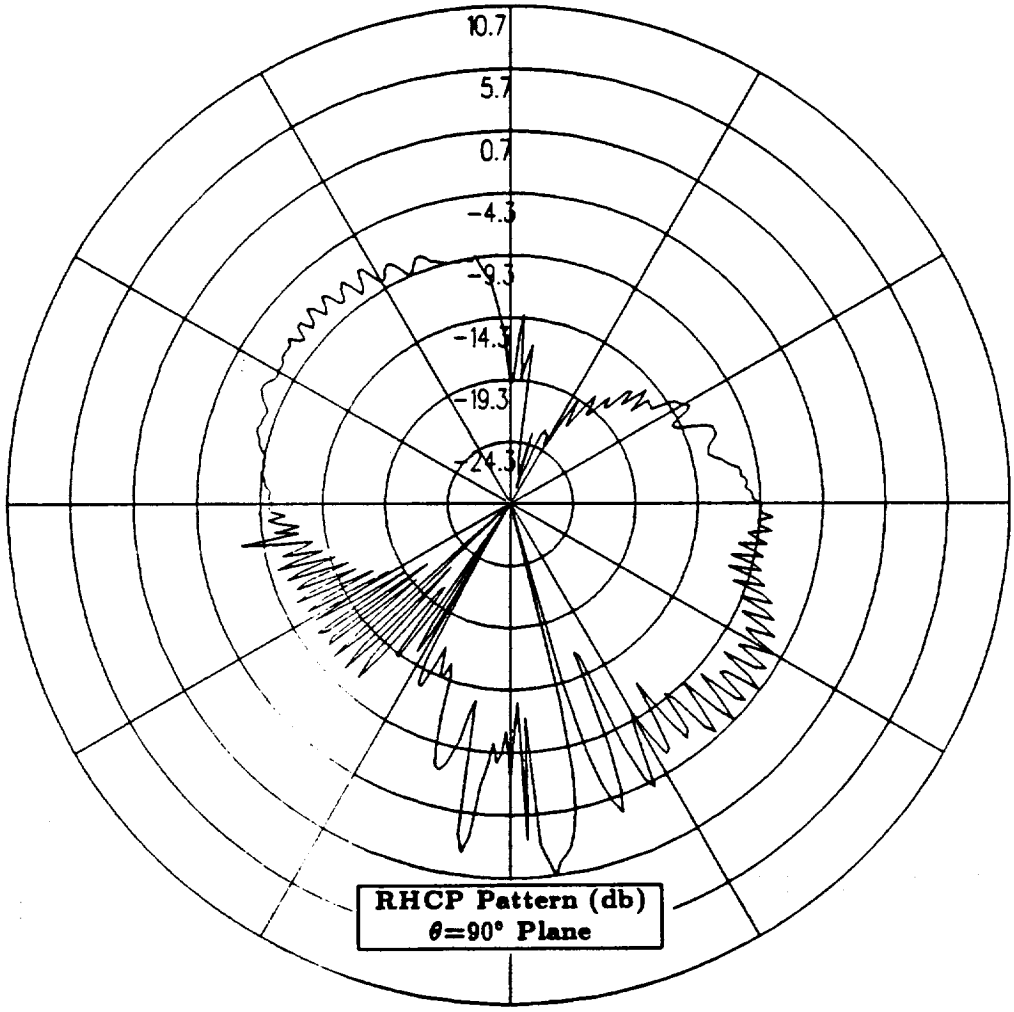

Figure 17: NEC-BSC calculated azimuth plane pattern for antenna location on top center-line of the fuselage forward of the aircraft wing for right hand circular polarization at 300 MHz. (Test Location 2)

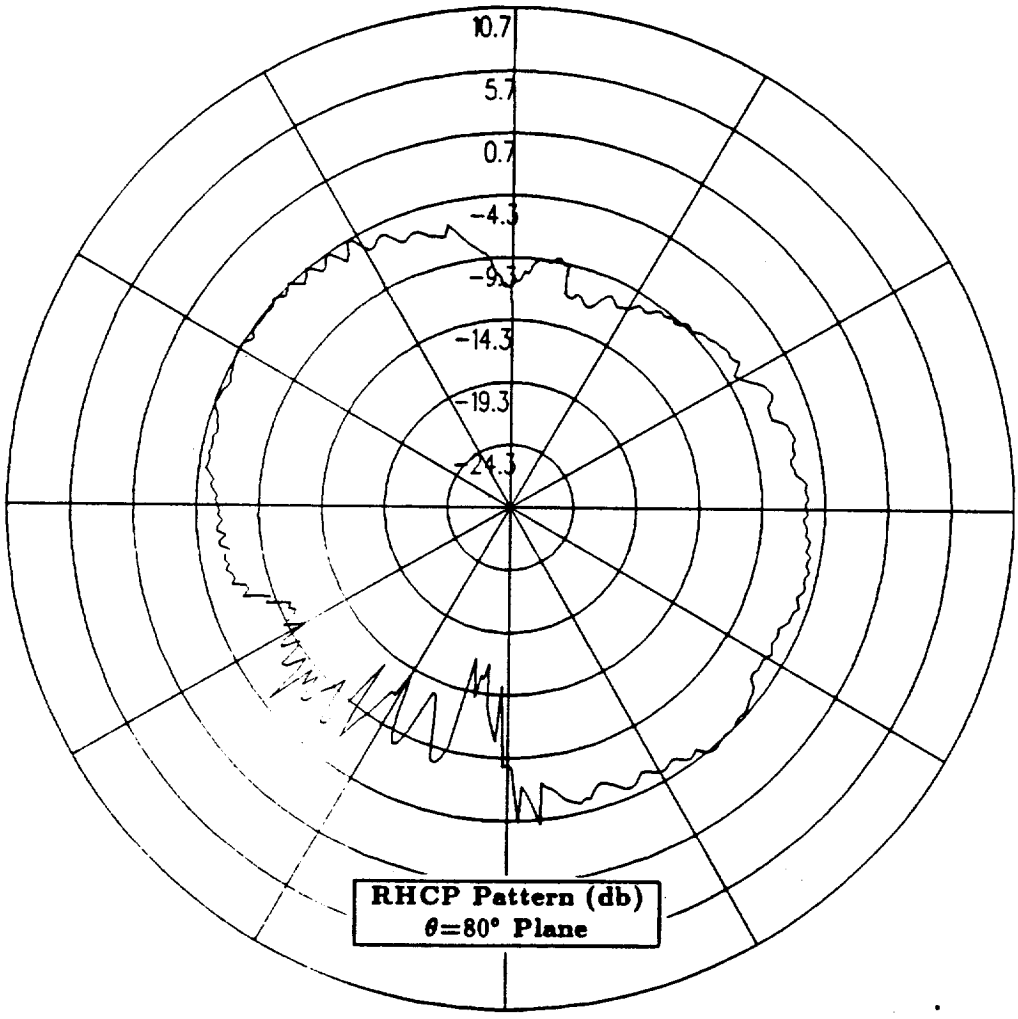

Figure 18: NEC-BSC calculated conical plane pattern 10° above the horizon for antenna location on top center-line of the fuselage forward of the aircraft wing for right hand circular polarization at 300 MHz. (Test Location 2)

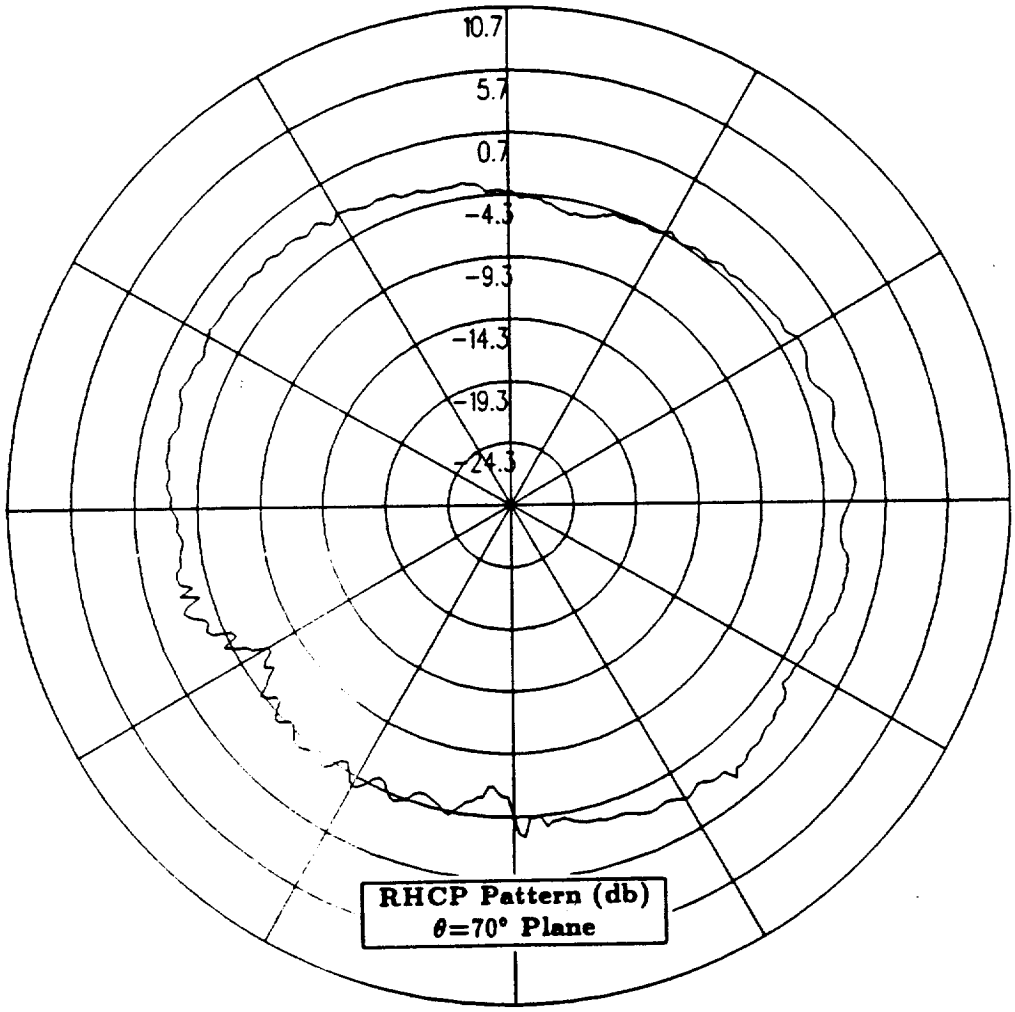

Figure 19: NEC-BSC calculated conical plane pattern 20° above the horizon for antenna location on top center-line of the fuselage forward of the aircraft wing for right hand circular polarization at 300 MHz. (Test Location 2)

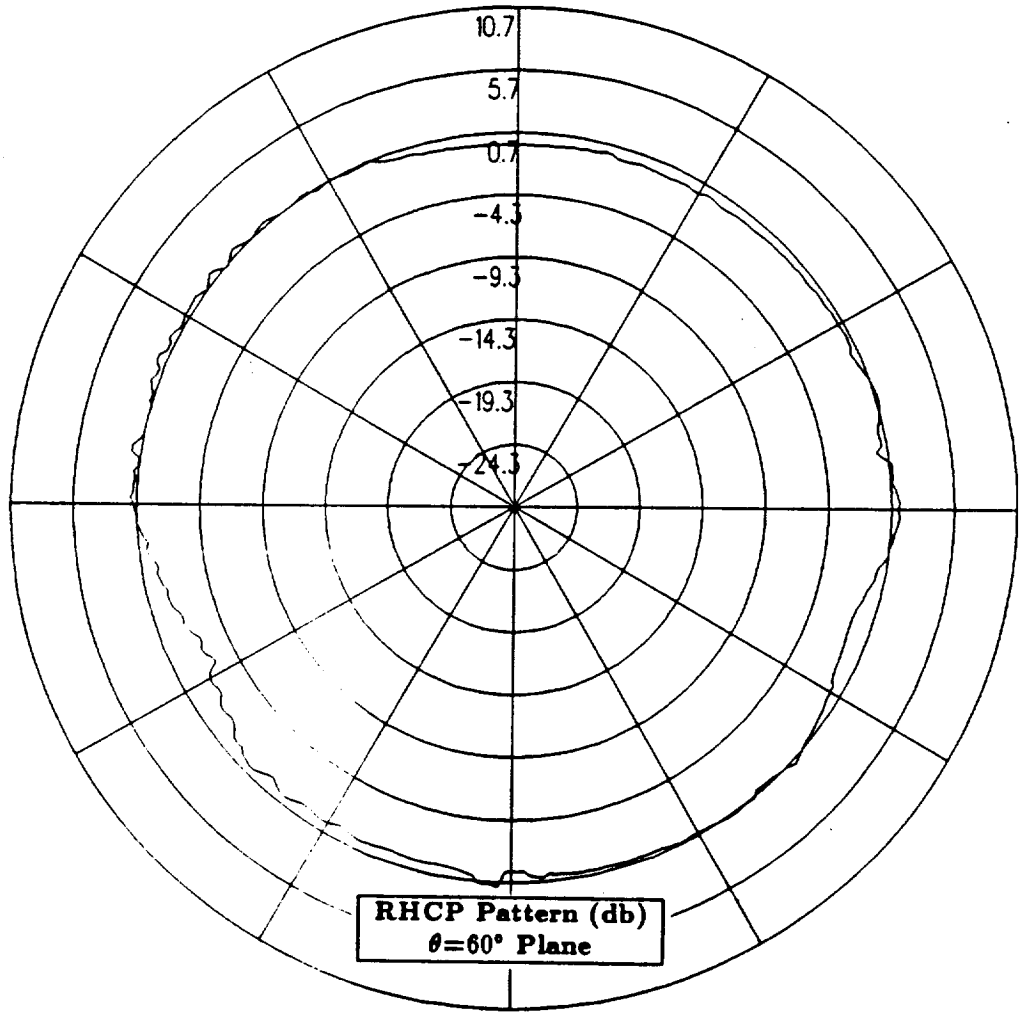

Figure 20: NEC-BSC calculated conical plane pattern 30° above the horizon for antenna location on top center-line of the fuselage forward of the aircraft wing for right hand circular polarization at 300 MHz. (Test Location 2)

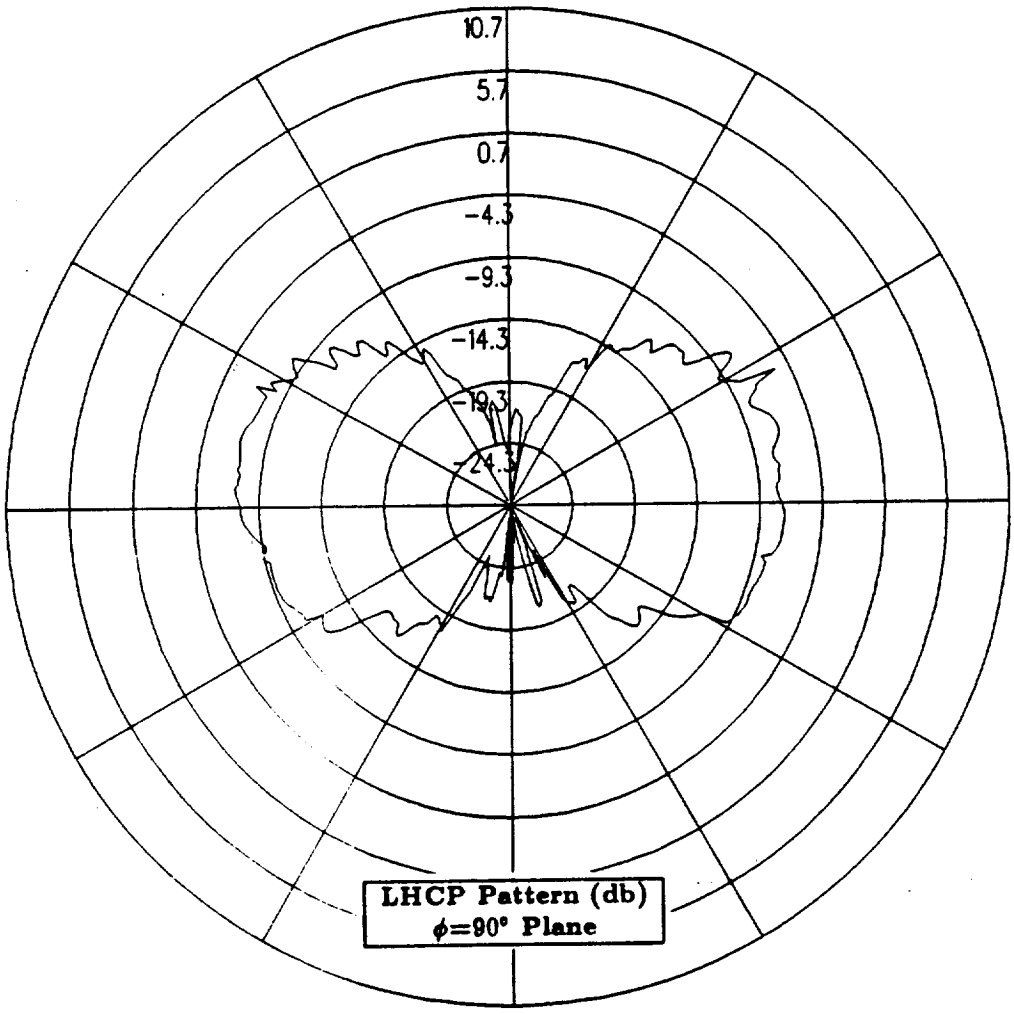

Figure 21: NEC-BSC calculated roll plane pattern for antenna location on top center-line of the fuselage forward of the aircraft wing for left hand circular polarization at 300 MHz. (Test Location 2)

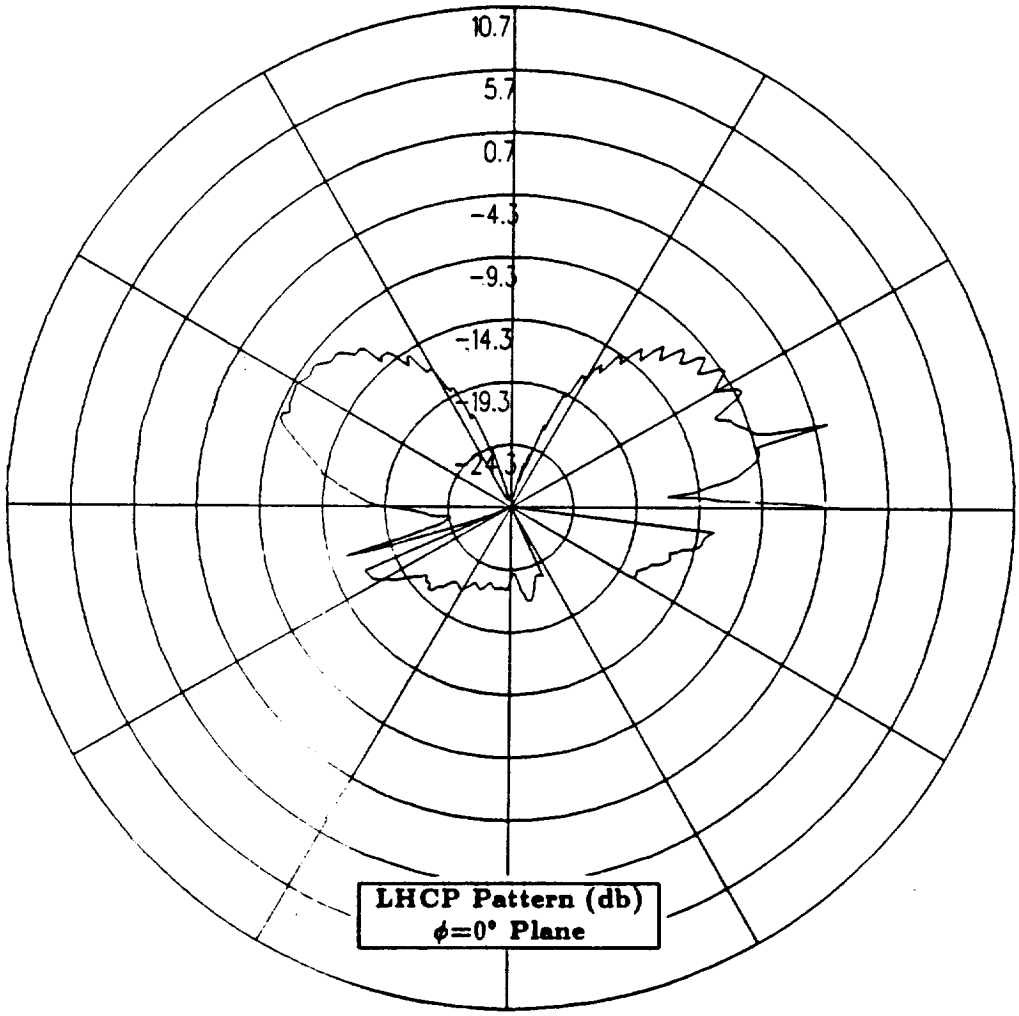

Figure 22: NEC-BSC calculated elevation plane pattern for antenna location on top center-line of the fuselage forward of the aircraft wing for left hand circular polarization at 300 MHz. (Test Location 2)

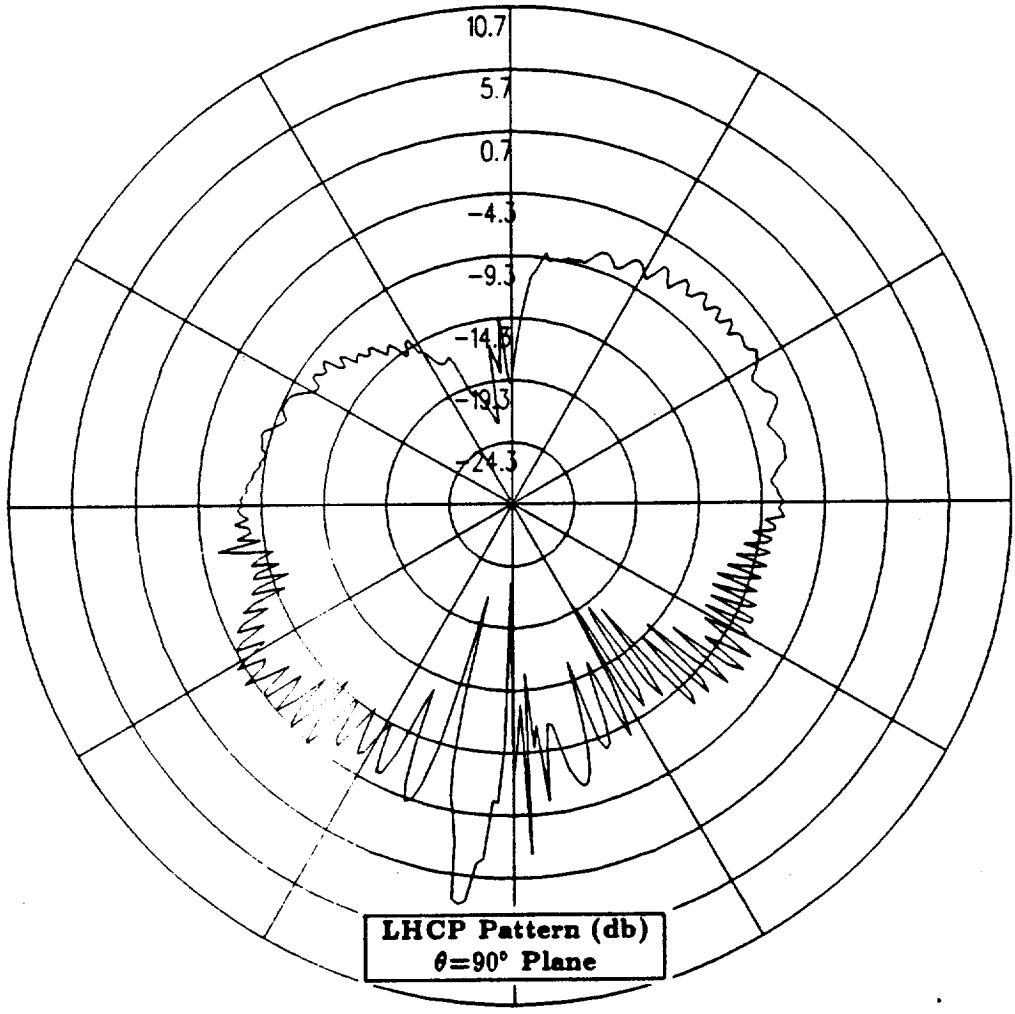

Figure 23: NEC-BSC calculated azimuth plane pattern for antenna location on top center-line of the fuselage forward of the aircraft wing for left hand circular polarization at 300 MHz. (Test Location 2)

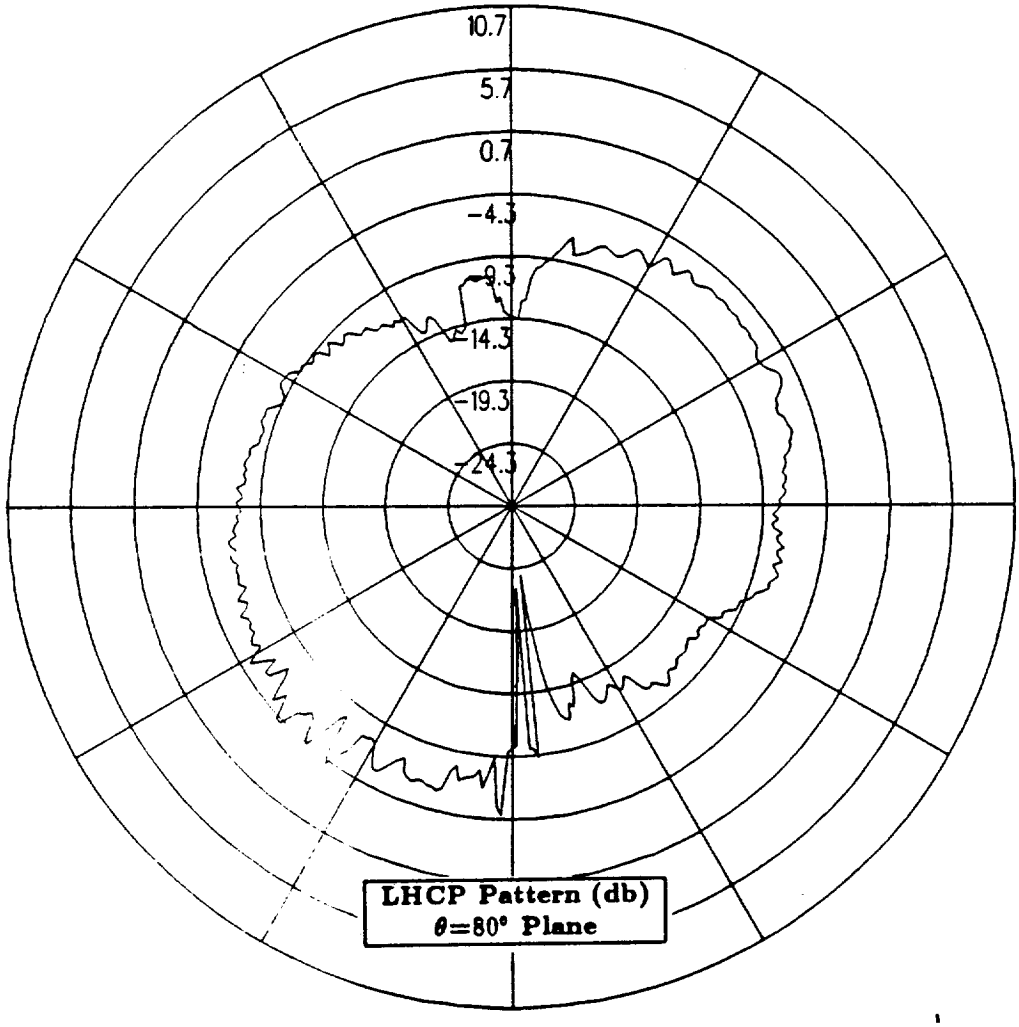

Figure 24: NEC-BSC calculated conical plane pattern 10° above the horizon for antenna location on top center-line of the fuselage forward of the aircraft wing for left hand circular polarization at 300 MHz. (Test Location 2)

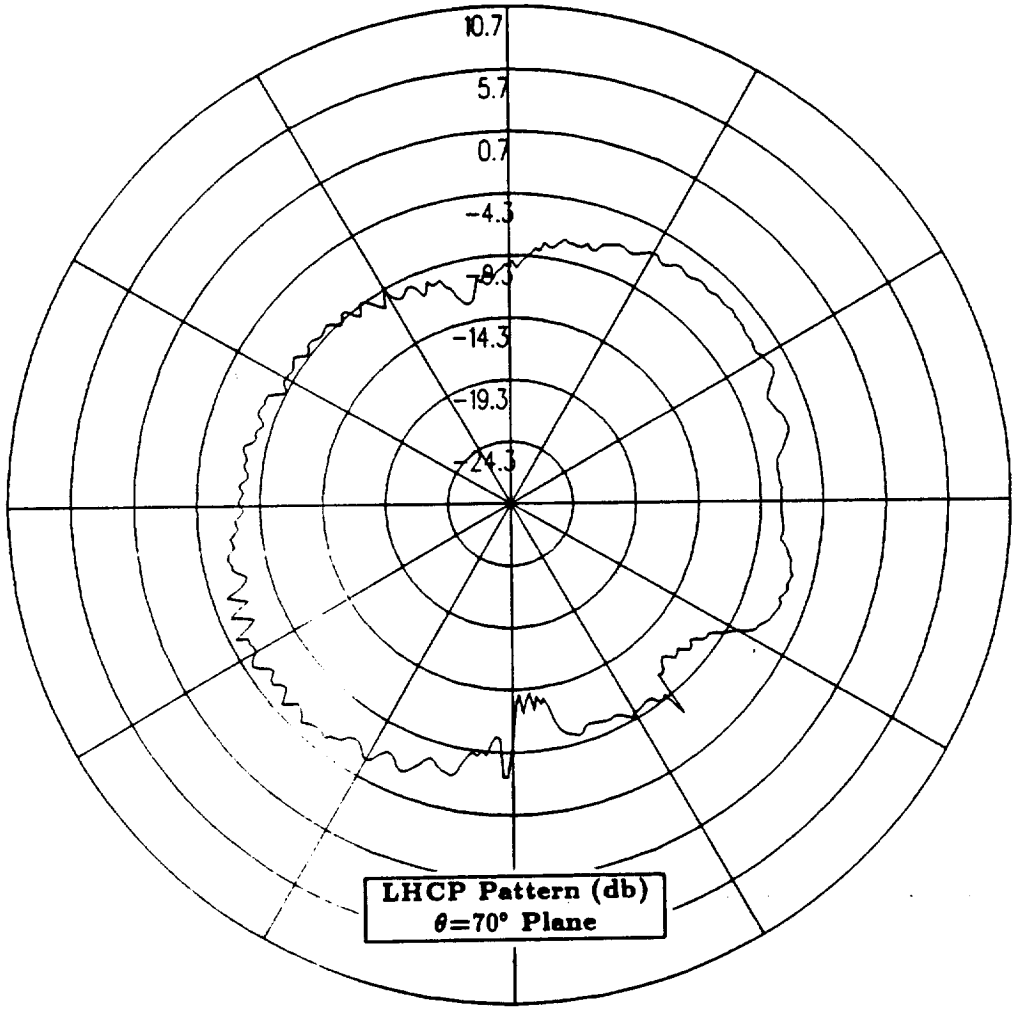

Figure 25: NEC-BSC calculated conical plane pattern 20° above the horizon for antenna location on top center-line of the fuselage forward of the aircraft wing for left hand circular polarization at 300 MHz. (Test Location 2)

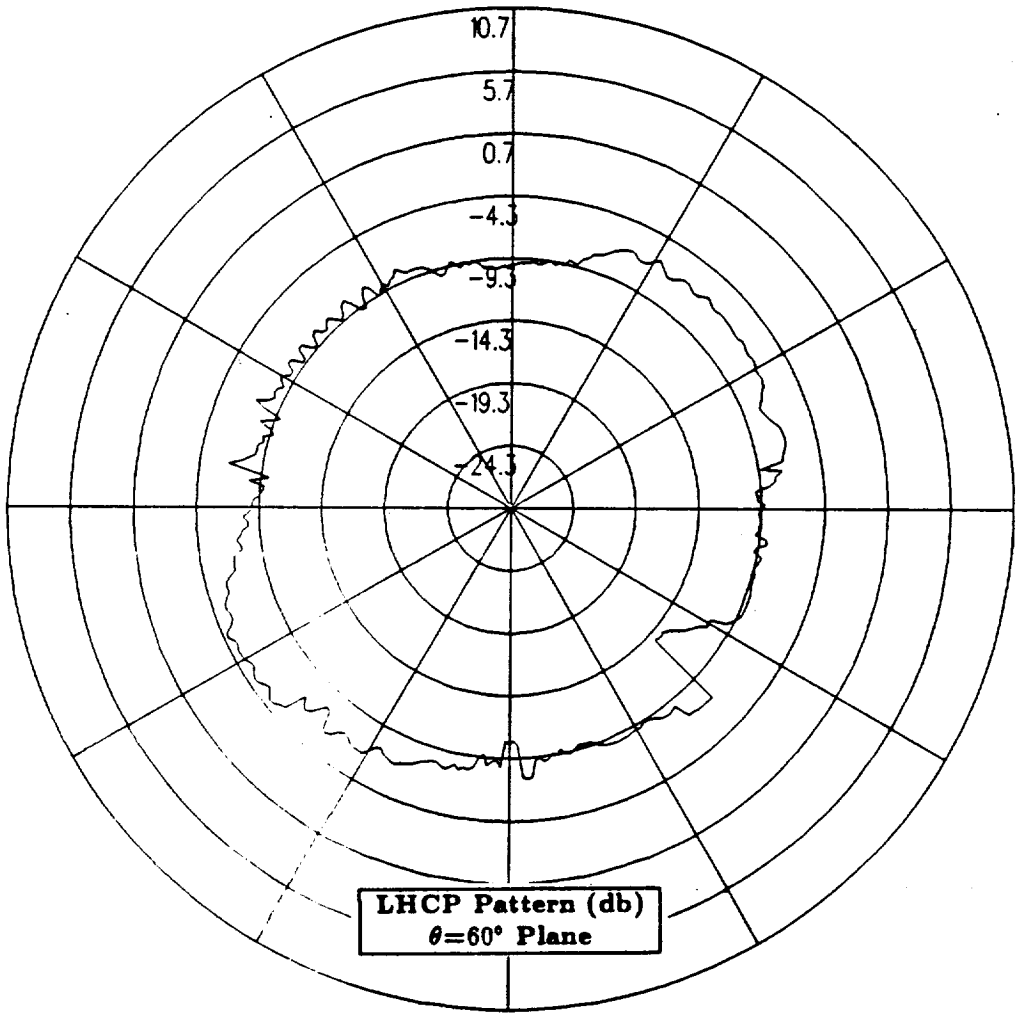

Figure 26: NEC-BSC calculated conical plane pattern 30° above the horizon for antenna location on top center-line of the fuselage forward of the aircraft wing for left hand circular polarization at 300 MHz. (Test Location 2)

1.4 Test Location 3

In this section, the antenna is located on the top center-line of the fuselage between the nose and the wing of the aircraft. The cylindrical aircraft model used in the NEC-BSC is illustrated in Figure 27, which also shows the location of the antenna on the fuselage. The calculated results obtained using the improved version of the NEC-BSC at 300 MHz for the right hand circular polarized or co-polarized fields are shown for the roll plane in Figure 28, for the elevation plane in Figure 29, for the azimuth plane in Figure 30 and for the conical planes 10°, 20° and 30° above the horizon in Figures 31, 32 and 33, respectively. For completeness, the left hand circular polarized or cross-polarized results are also included. These cross-polarized results are shown for the roll plane in Figure 34, for the elevation plane in Figure 35, for the azimuth plane in Figure 36 and for the conical planes 10°, 20° and 30° above the horizon in Figures 37, 38 and 39, respectively.

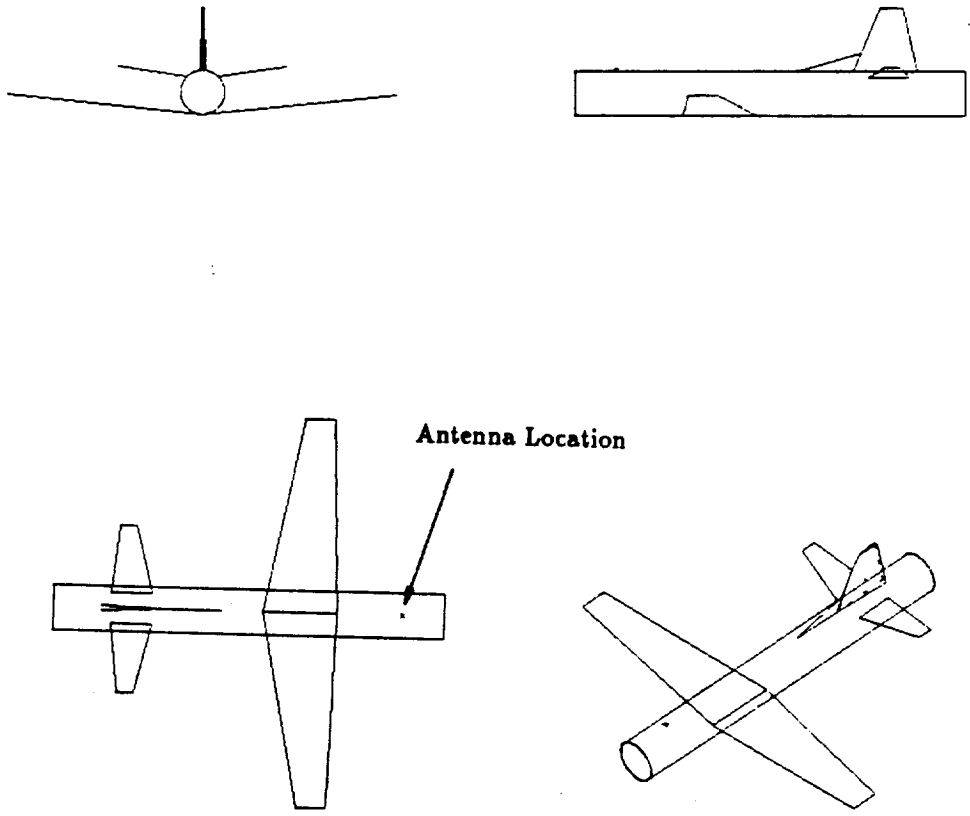

Figure 27: Geometry of the cylindrical model of the P-3C aircraft used in the NEC-BSC showing the antenna location. (Test Location 3)

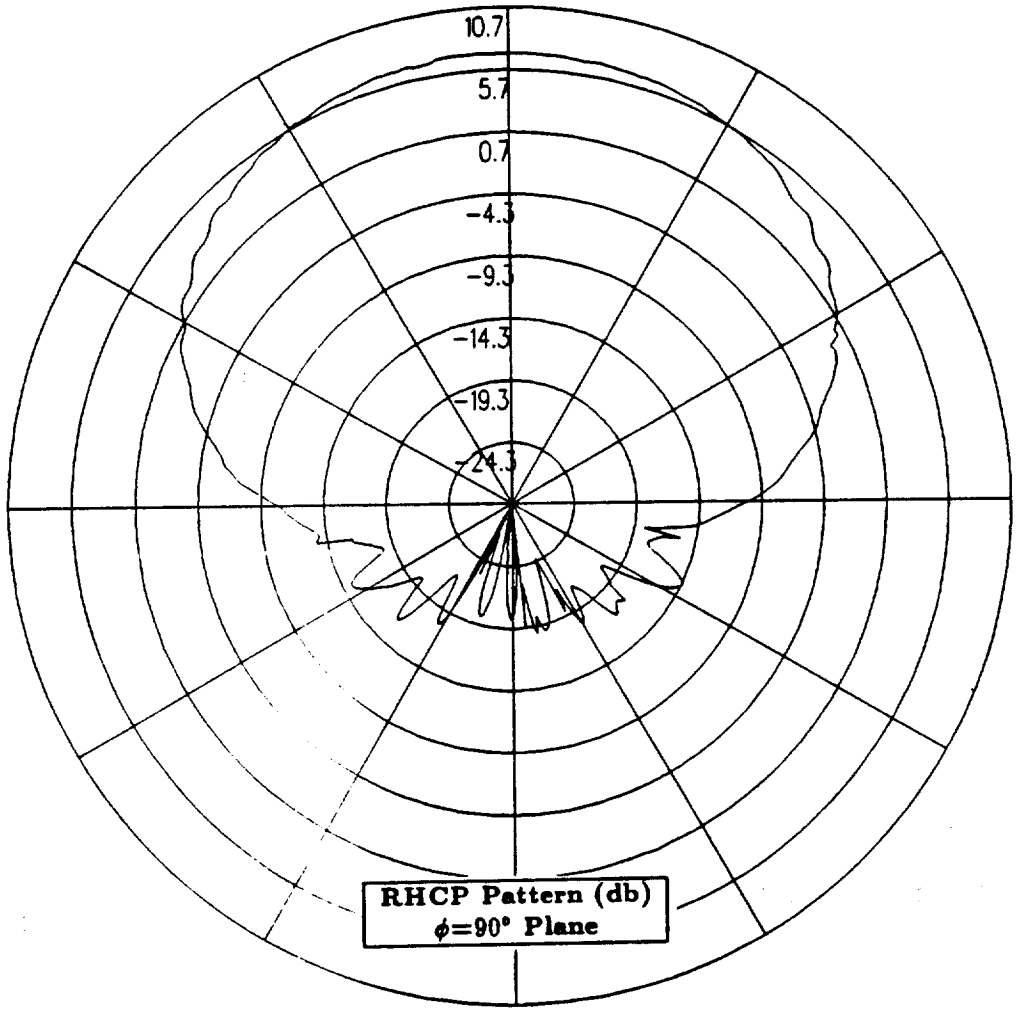

Figure 28: NEC-BSC calculated roll plane pattern for antenna location on top center-line of the fuselage between the nose and wing for right hand circular polarization at 300 MHz. (Test Location 3)

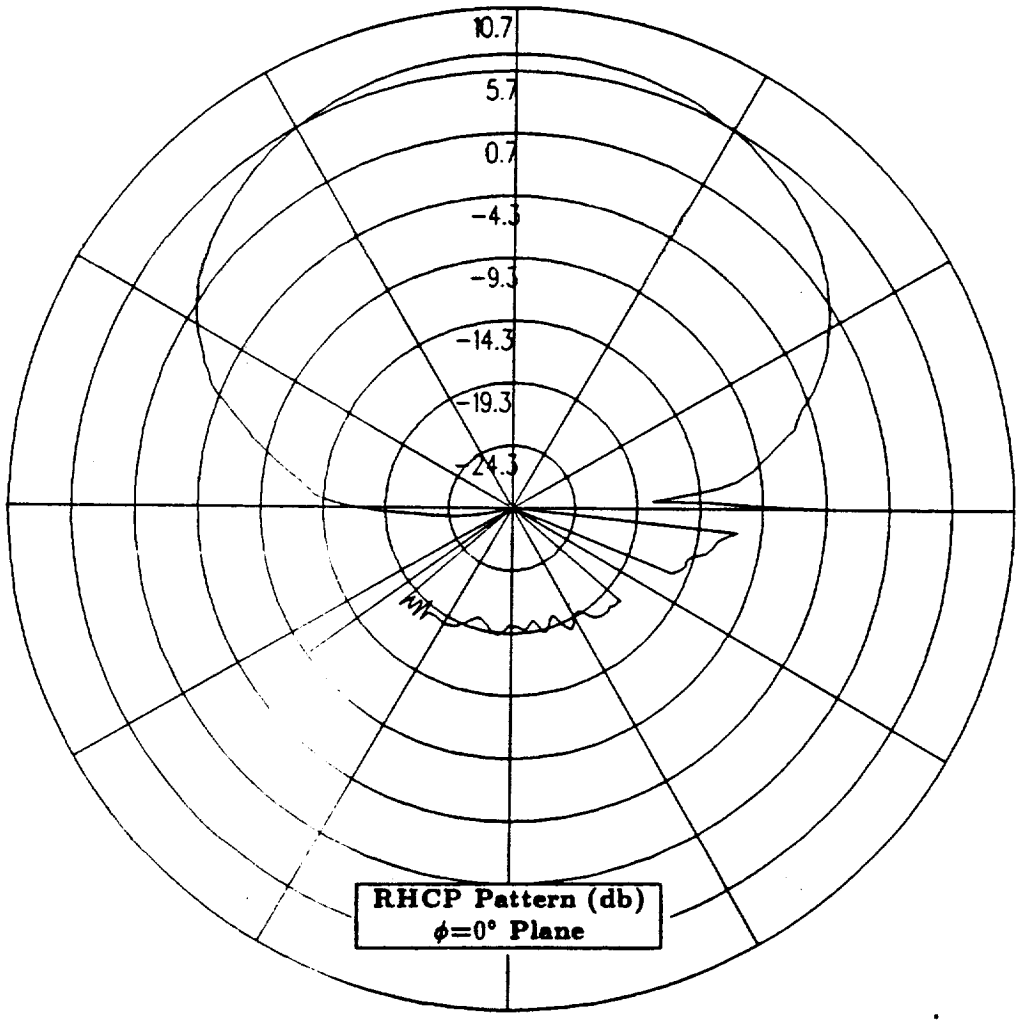

Figure 29: NEC-BSC calculated elevation plane pattern for antenna location on top center-line of the fuselage between the nose and wing for right hand circular polarization at 300 MHz. (Test Location 3)

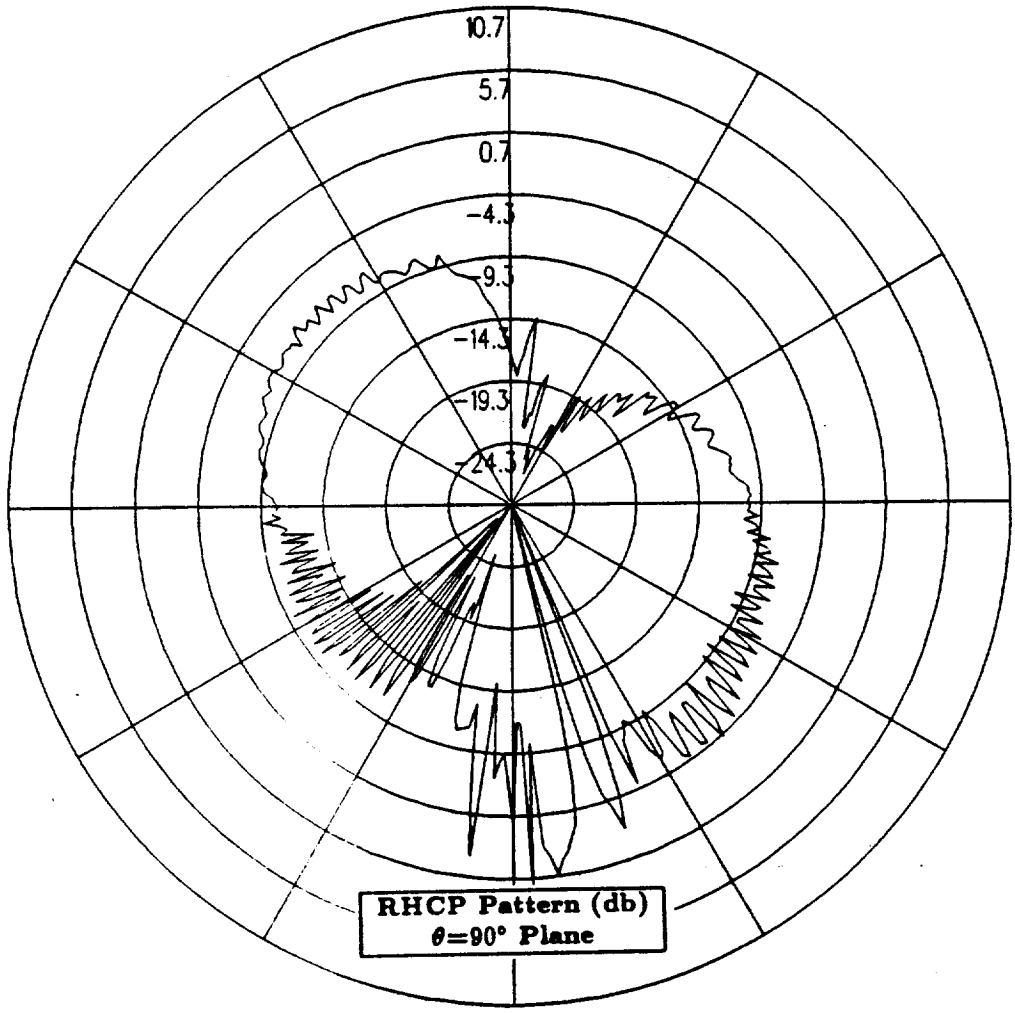

Figure 30: NEC-BSC calculated azimuth plane pattern for antenna location on top center-line of the fuselage between the nose and wing for right hand circular polarization at 300 MHz. (Test Location 3)

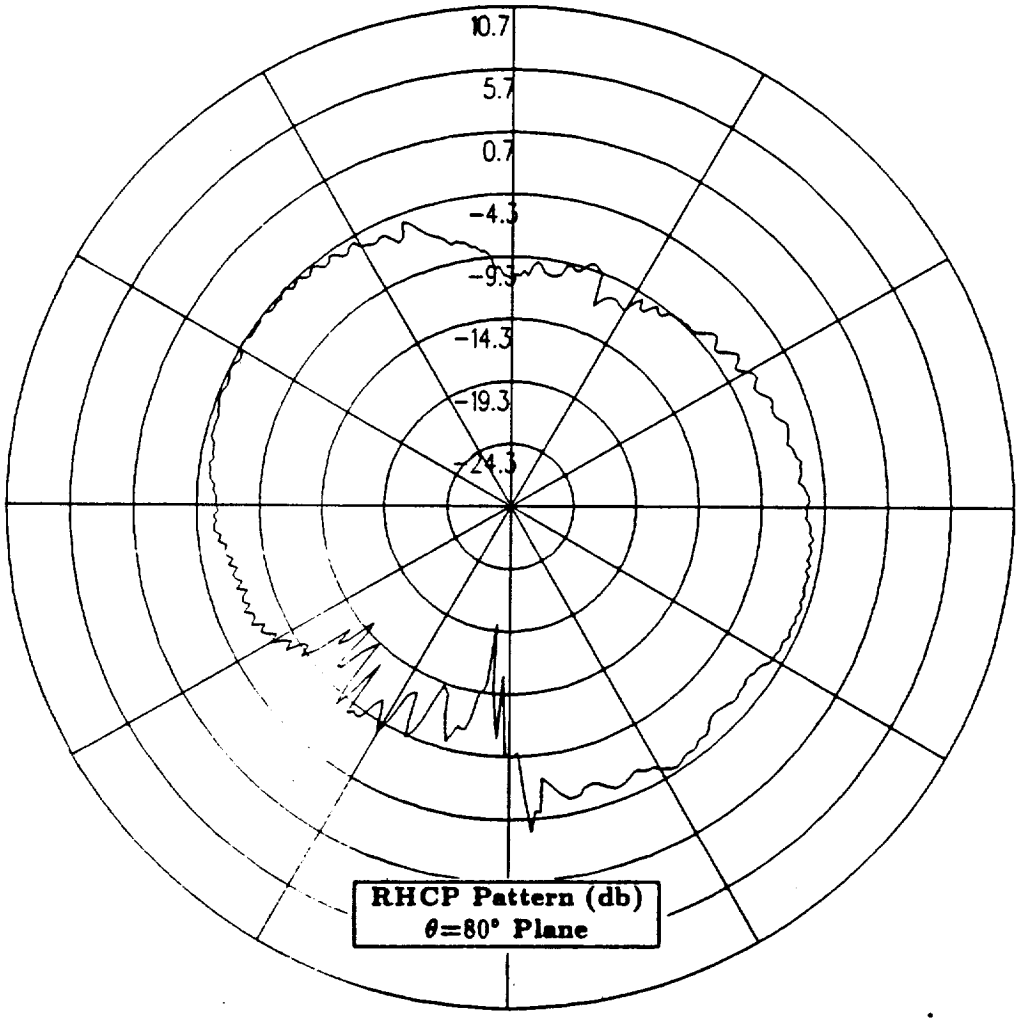

Figure 31: NEC-BSC calculated conical plane pattern 10° above the horizon for antenna location on top center-line of the fuselage between the nose and wing for right hand circular polarization at 300 MHz. (Test Location 3)

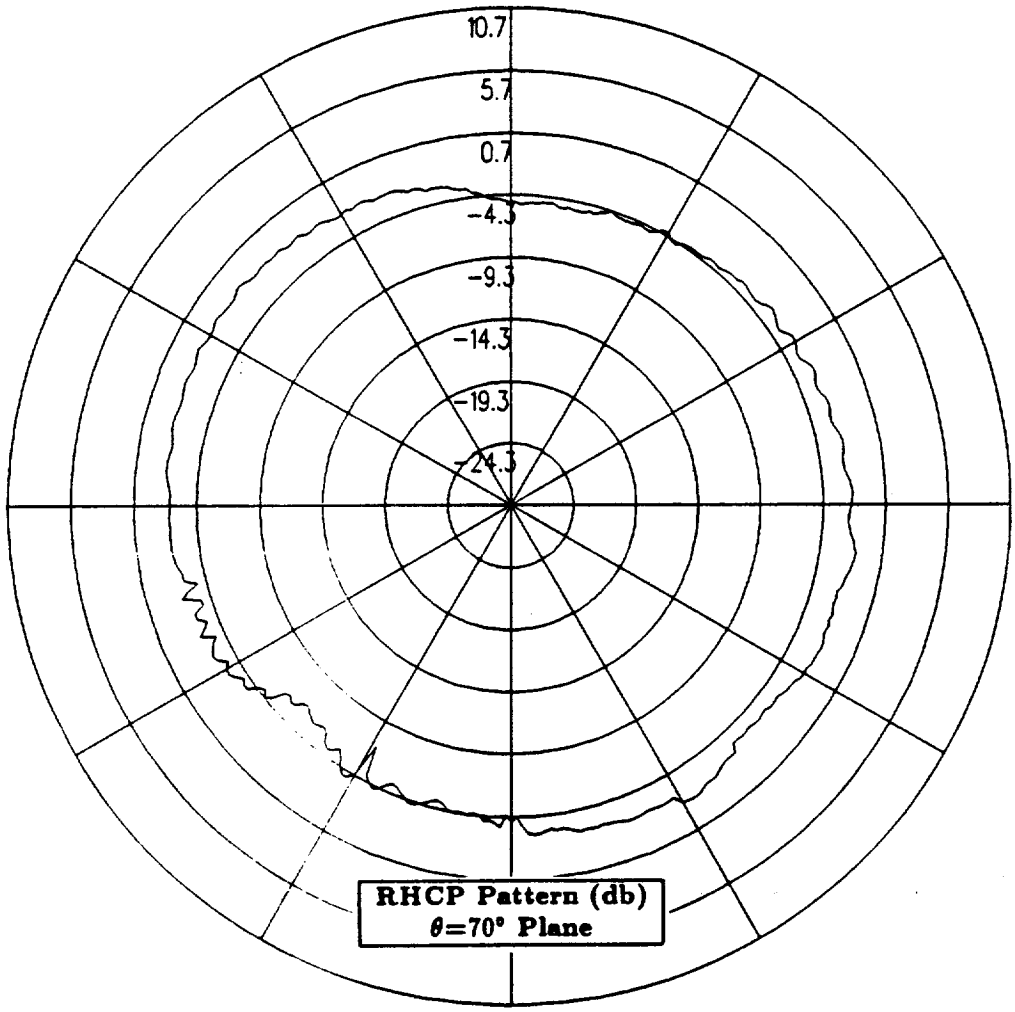

Figure 32: NEC-BSC calculated conical plane pattern 20° above the horizon for antenna location on top center-line of the fuselage between the nose and wing for right hand circular polarization at 300 MHz. (Test Location 3)

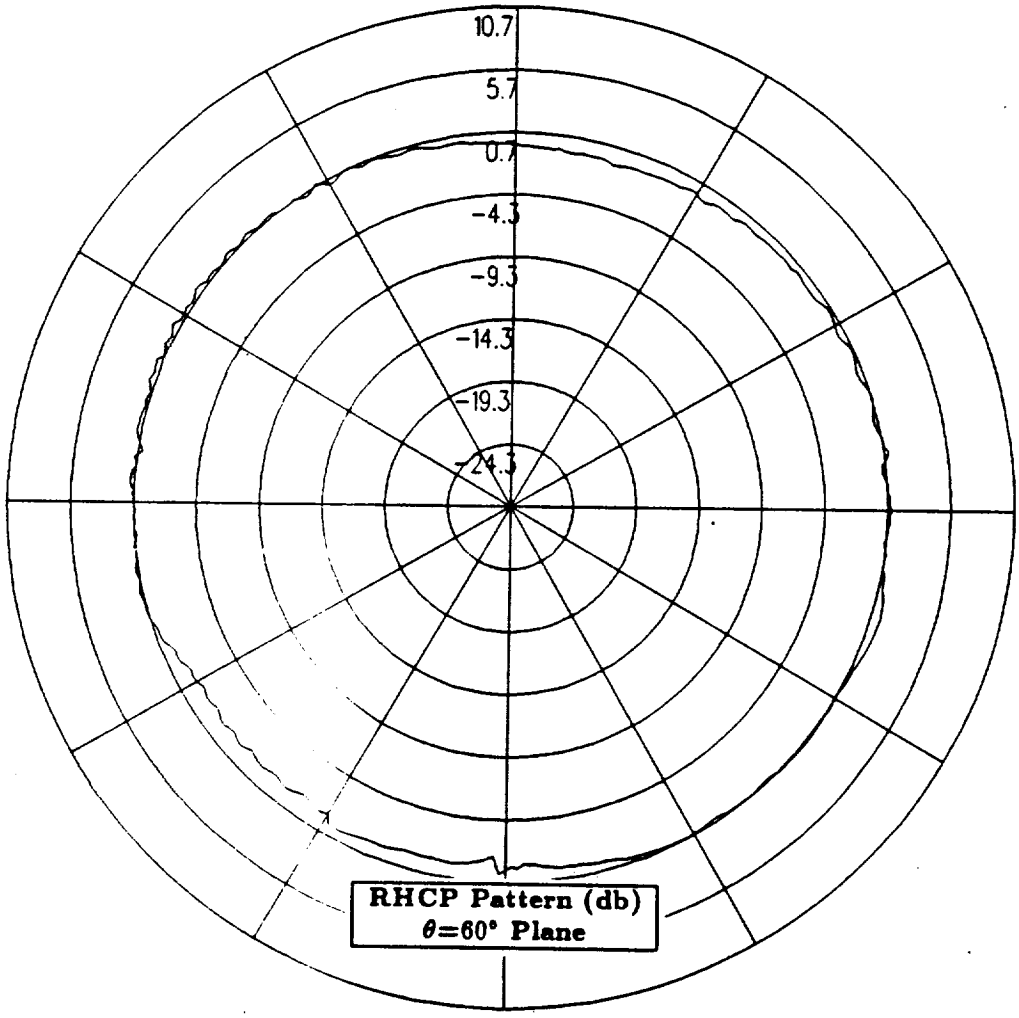

Figure 33: NEC-BSC calculated conical plane pattern 30° above the horizon for antenna location on top center-line of the fuselage between the nose and wing for right hand circular polarization at 300 MHz. (Test Location 3)

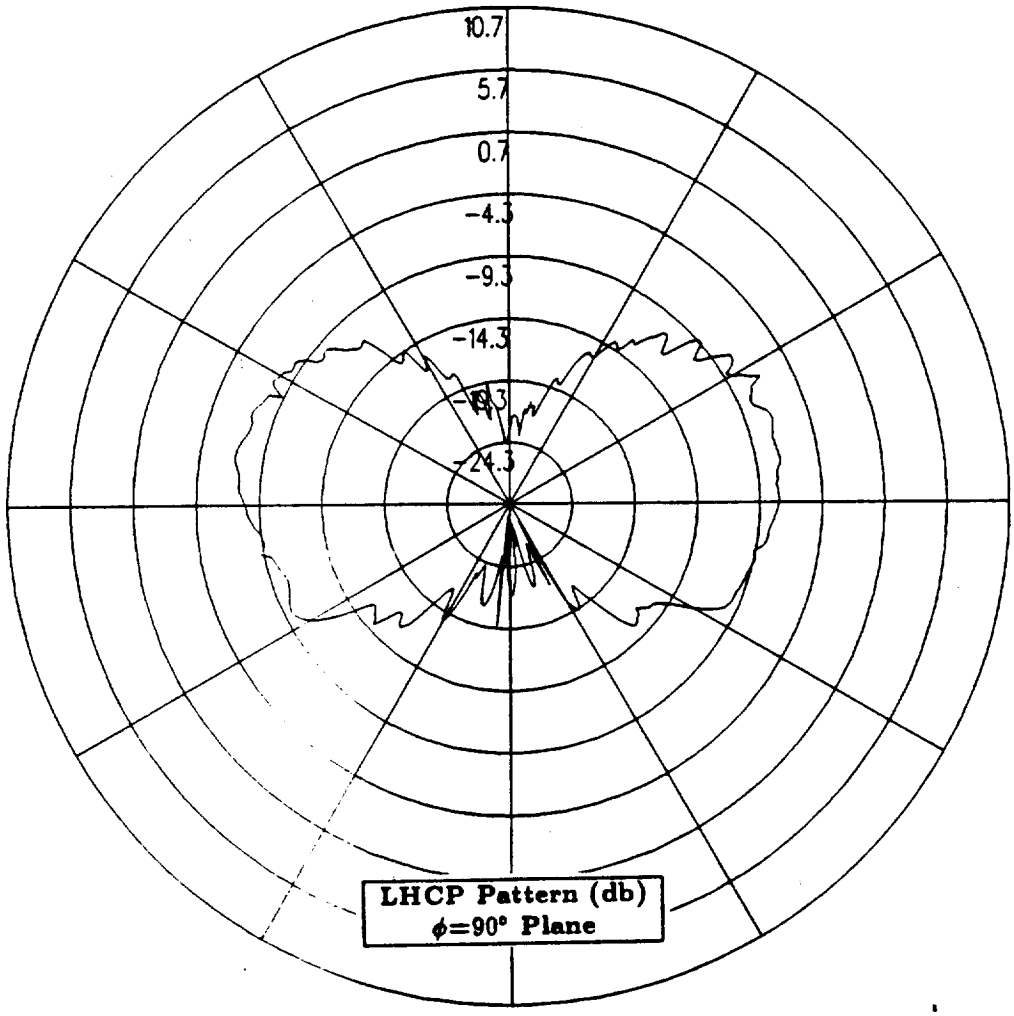

Figure 34: NEC-BSC calculated roll plane pattern for antenna location on top center-line of the fuselage between the nose and wing for left hand circular polarization at 300 MHz. (Test Location 3)

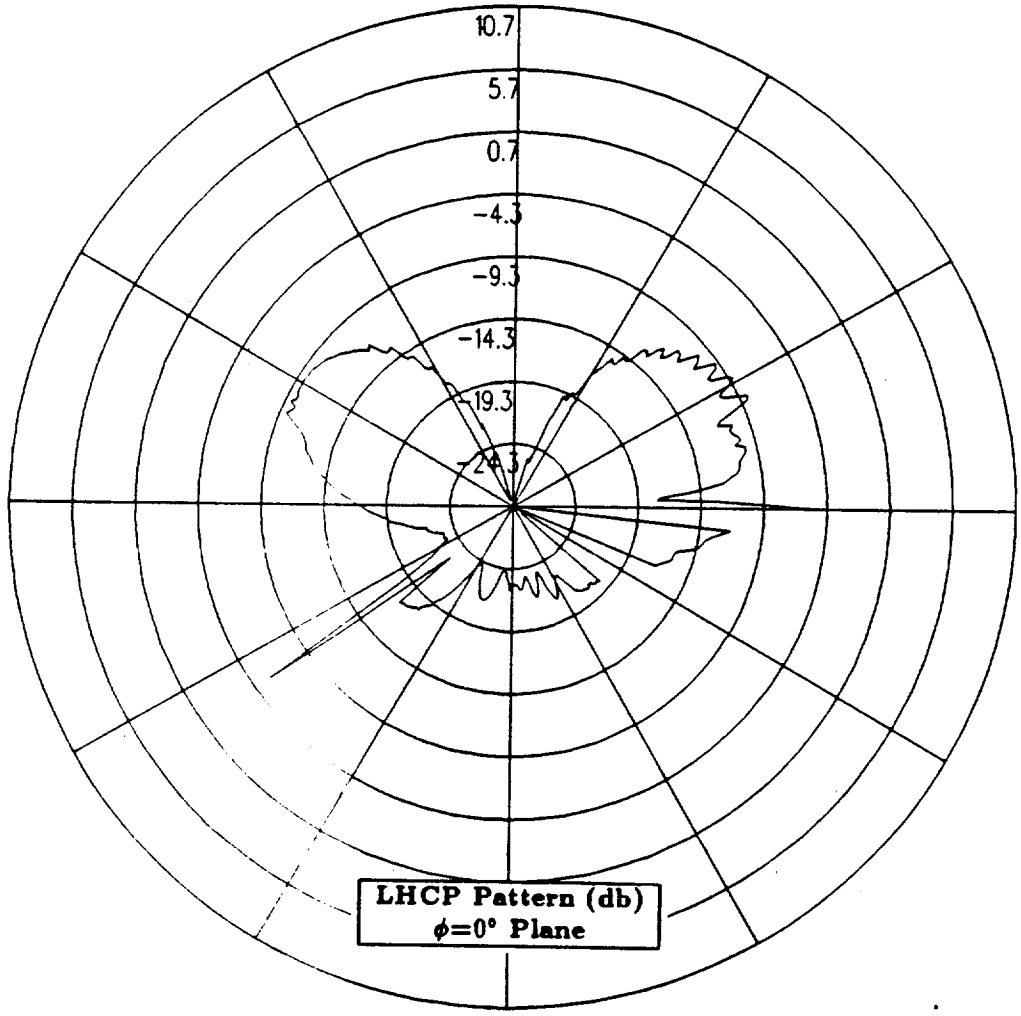

Figure 35: NEC-BSC calculated elevation plane pattern for antenna location on top center-line of the fuselage between the nose and wing for left hand circular polarization at 300 MHz. (Test Location 3)

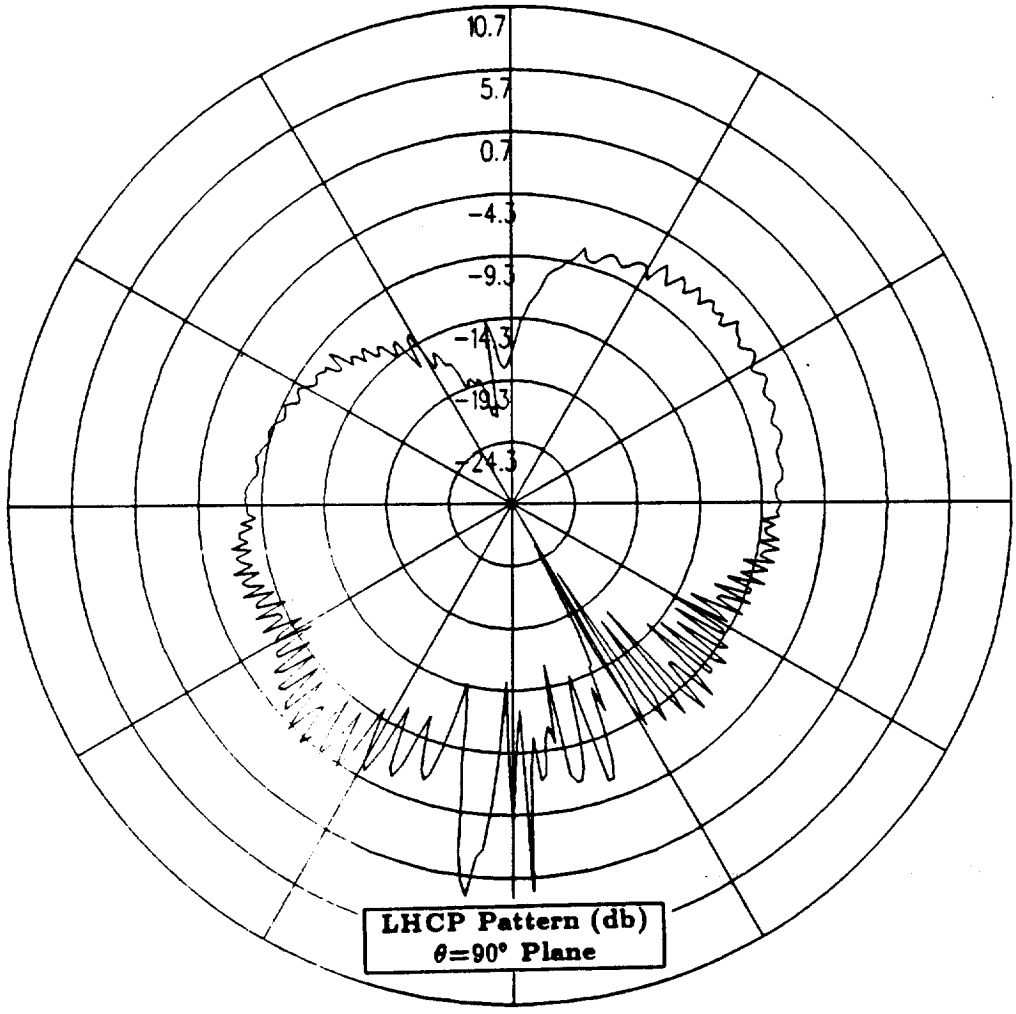

Figure 36: NEC-BSC calculated azimuth plane pattern for antenna location on top center-line of the fuselage between the nose and wing for left hand circular polarization at 300 MHz. (Test Location 3)

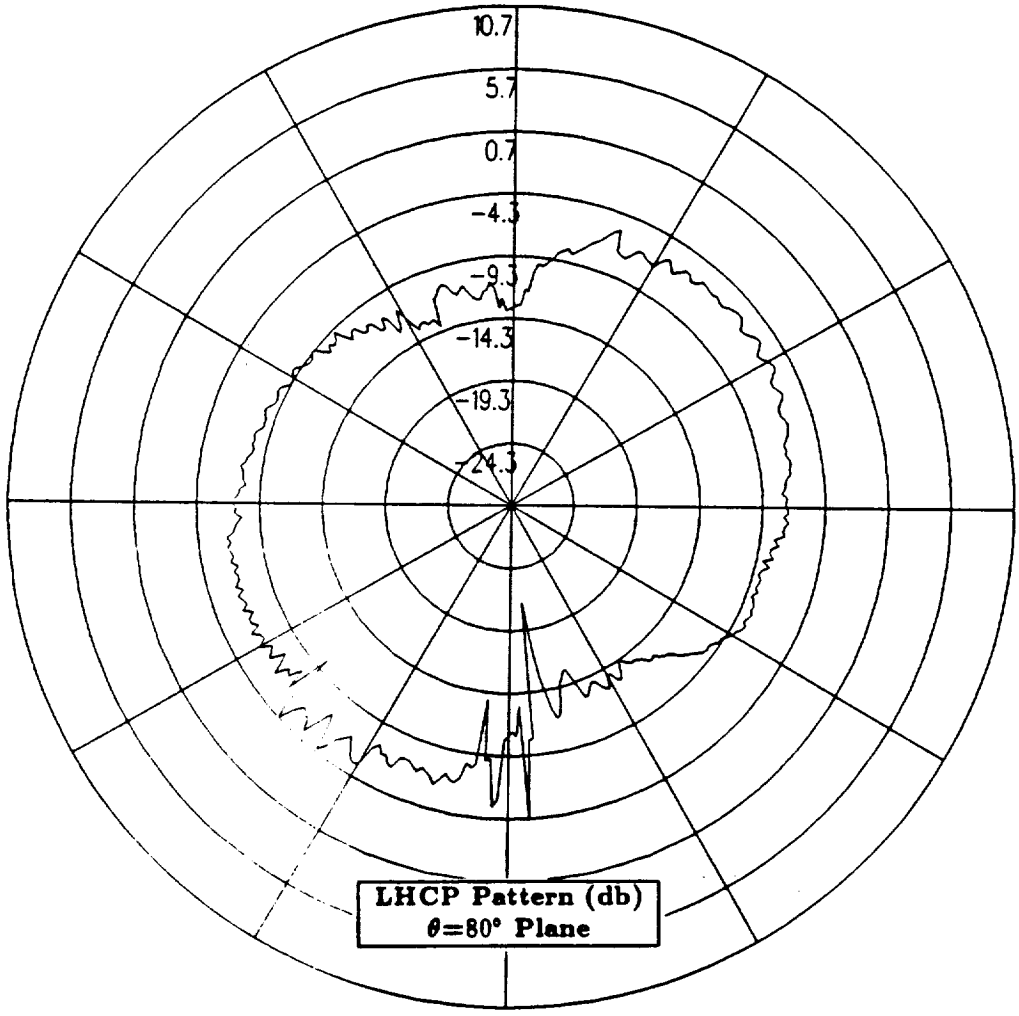

Figure 37: NEC-BSC calculated conical plane pattern 10° above the horizon for antenna location on top center-line of the fuselage between the nose and wing for left hand circular polarization at 300 MHz. (Test Location 3)

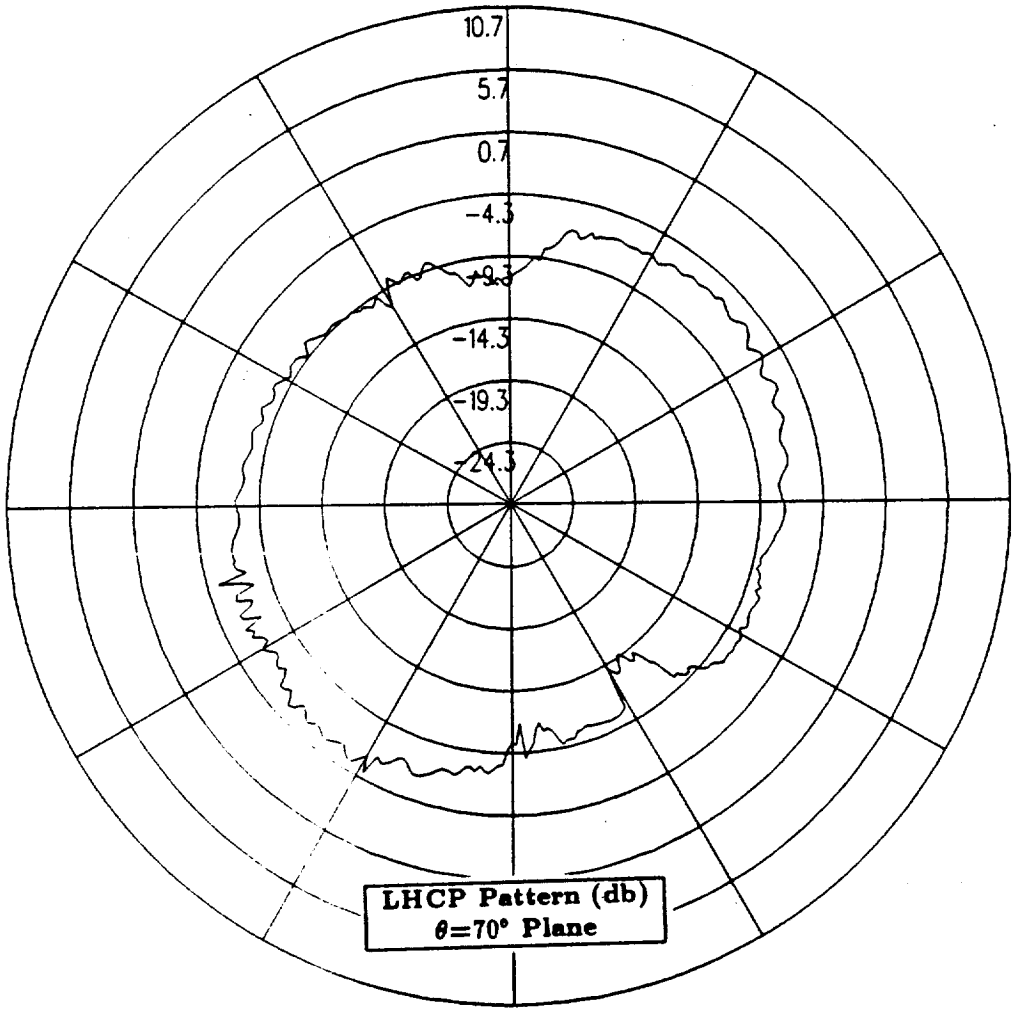

Figure 38: NEC-BSC calculated conical plane pattern 20° above the horizon for antenna location on top center-line of the fuselage between the nose and wing for left hand circular polarization at 300 MHz. (Test Location 3)

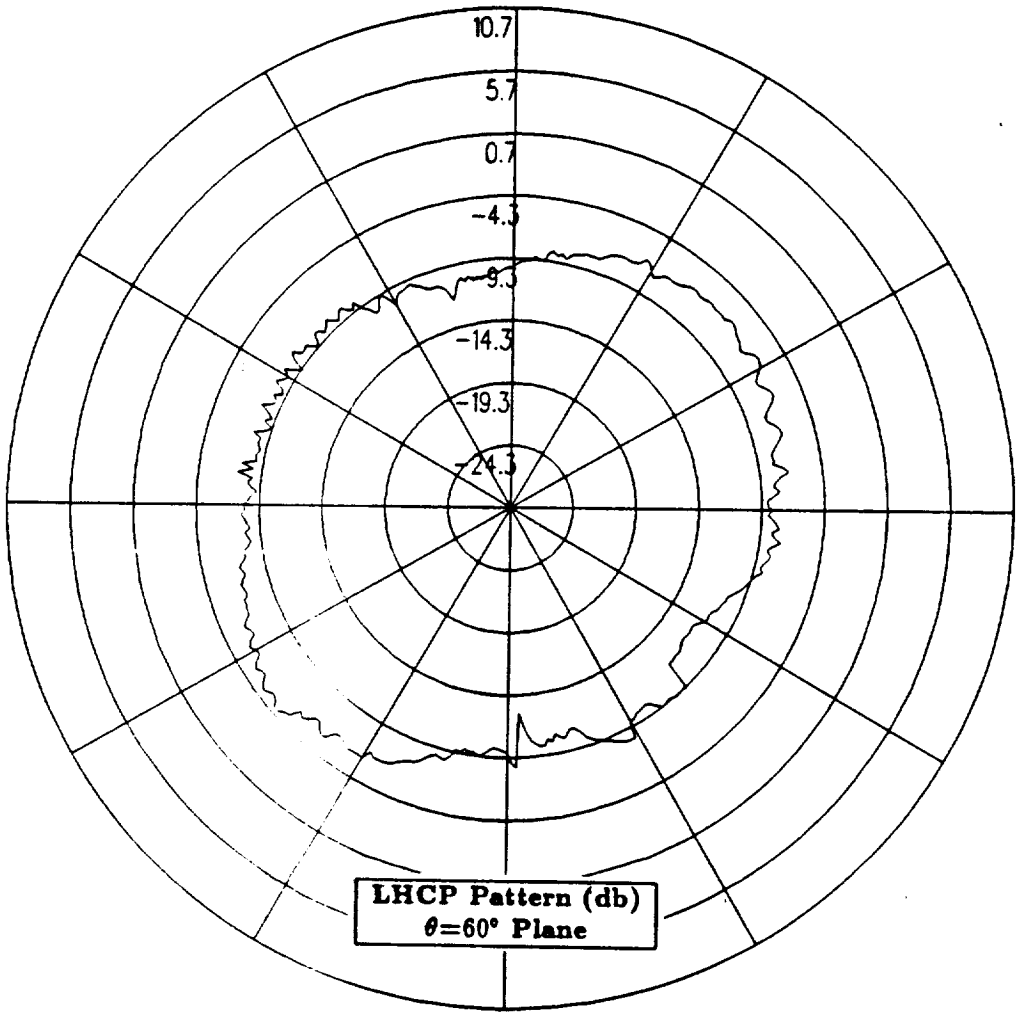

Figure 39: NEC-BSC calculated conical plane pattern 30° above the horizon for antenna location on top center-line of the fuselage between the nose and wing for left hand circular polarization at 300 MHz. (Test Location 3)

1.5 Test Location 4

In this section, the antenna is located on the center-line of the fuselage near the aircraft nose. Since the antenna location is near the nose of the aircraft and the aircraft's elliptical nose is critical to the radiation patterns, the composite ellipsoid aircraft model is used in the NEC-BSC. This composite ellipsoid aircraft model is illustrated in Figure 40, which also shows the location of the antenna on the fuselage. The improved version of the NEC-BSC does not contain plate - composite ellipsoid interactions, therefore, Version 3.1 can be used to calculate the radiation patterns for this particular antenna location.

The calculated results obtained using Version 3.1 of the NEC-BSC at 300 MHz for the right hand circular polarized or co-polarized fields are shown for the roll plane in Figure 41, for the elevation plane in Figure 42, for the azimuth plane in Figure 43 and for the conical planes 10°, 20° and 30° above the horizon in Figures 44, 45 and 46, respectively. For completeness, the left hand circular polarized or cross-polarized results are also included. These cross-polarized results are shown for the roll plane in Figure 47, for the elevation plane in Figure 48, for the azimuth plane in Figure 49 and for the conical planes 10°, 20° and 30° above the horizon in Figures 50, 51 and 52, respectively.

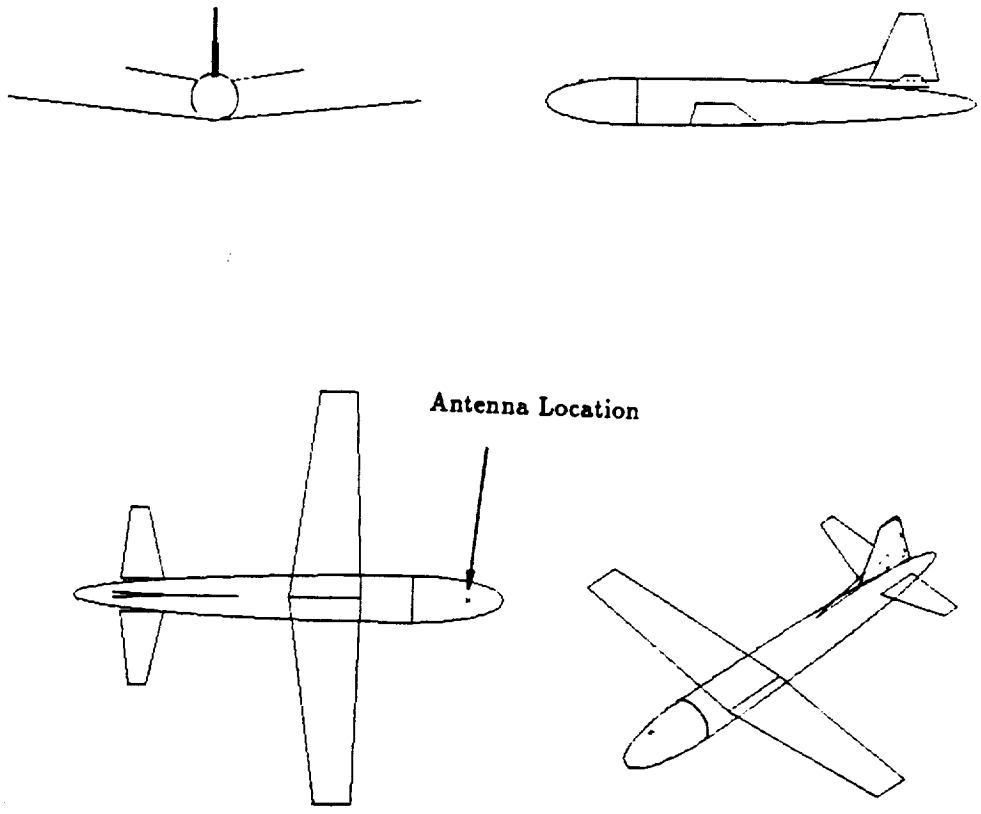

Figure 40: Geometry of the composite ellipsoid model of the P-3C aircraft used in the NEC-BSC showing the antenna location. (Test Location 4)

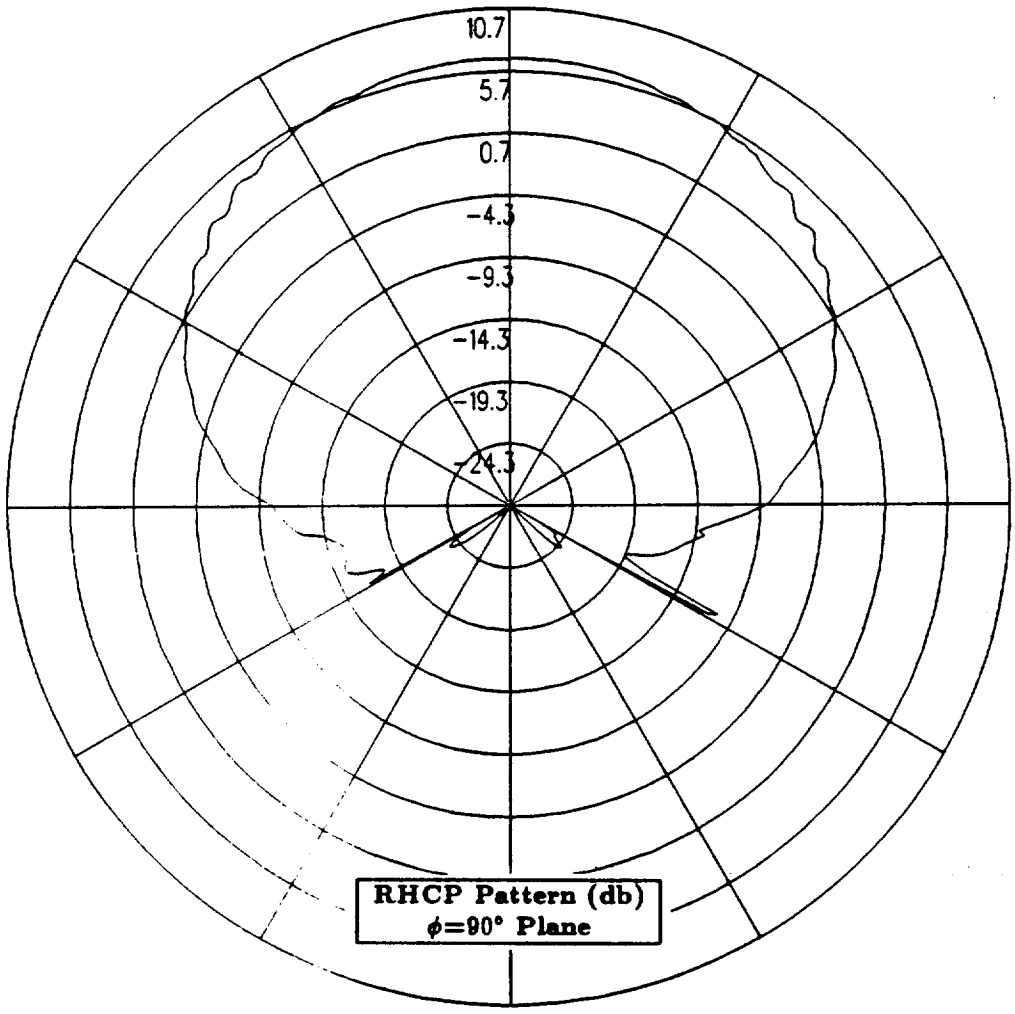

Figure 41: NEC-BSC calculated roll plane pattern for antenna location on center-line of the fuselage near the aircraft nose for right hand circular polarization at 300 MHz. (Test Location 4)

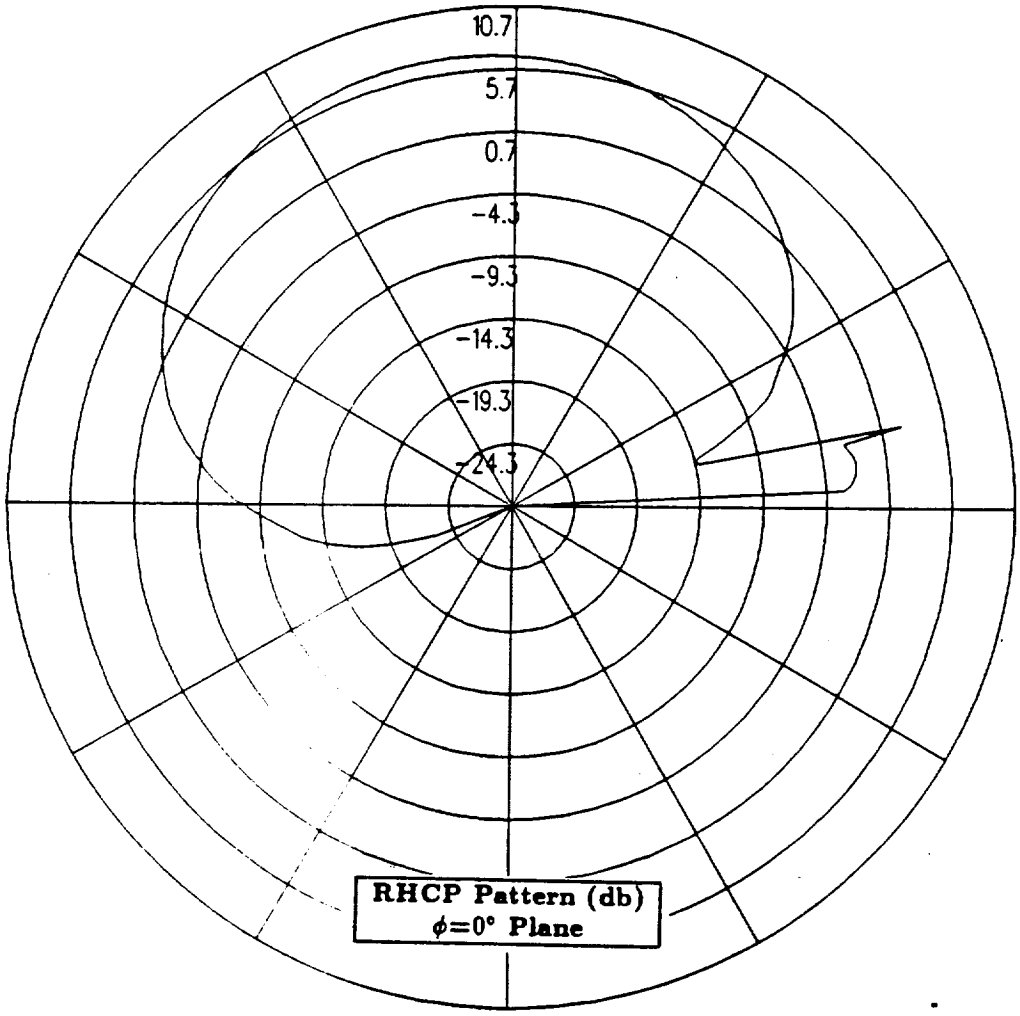

Figure 42: NEC-BSC calculated elevation plane pattern for antenna location on center-line of the fuselage near the aircraft nose for right hand circular polarization at 300 MHz. (Test Location 4)

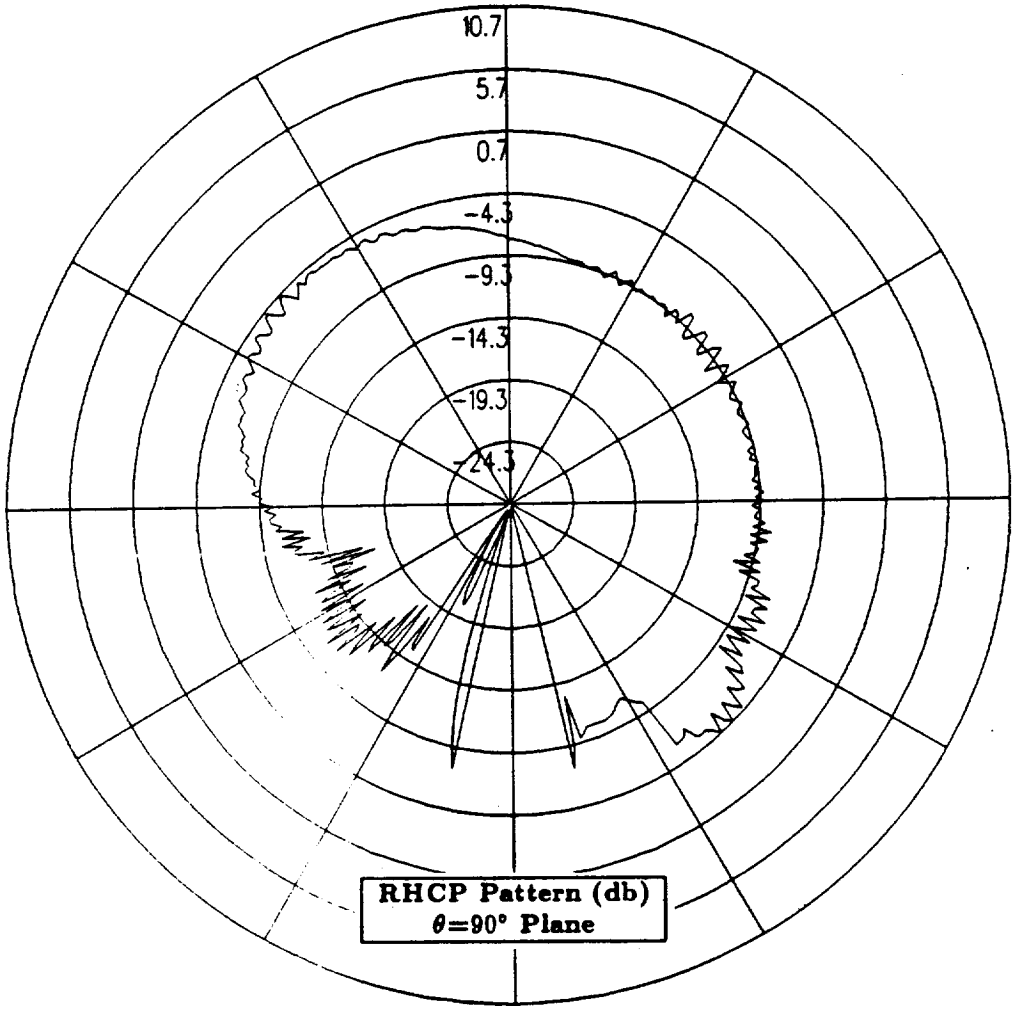

Figure 43: NEC-BSC calculated azimuth plane pattern for antenna location on center-line of the fuselage near the aircraft nose for right hand circular polarization at 300 MHz. (Test Location 4)

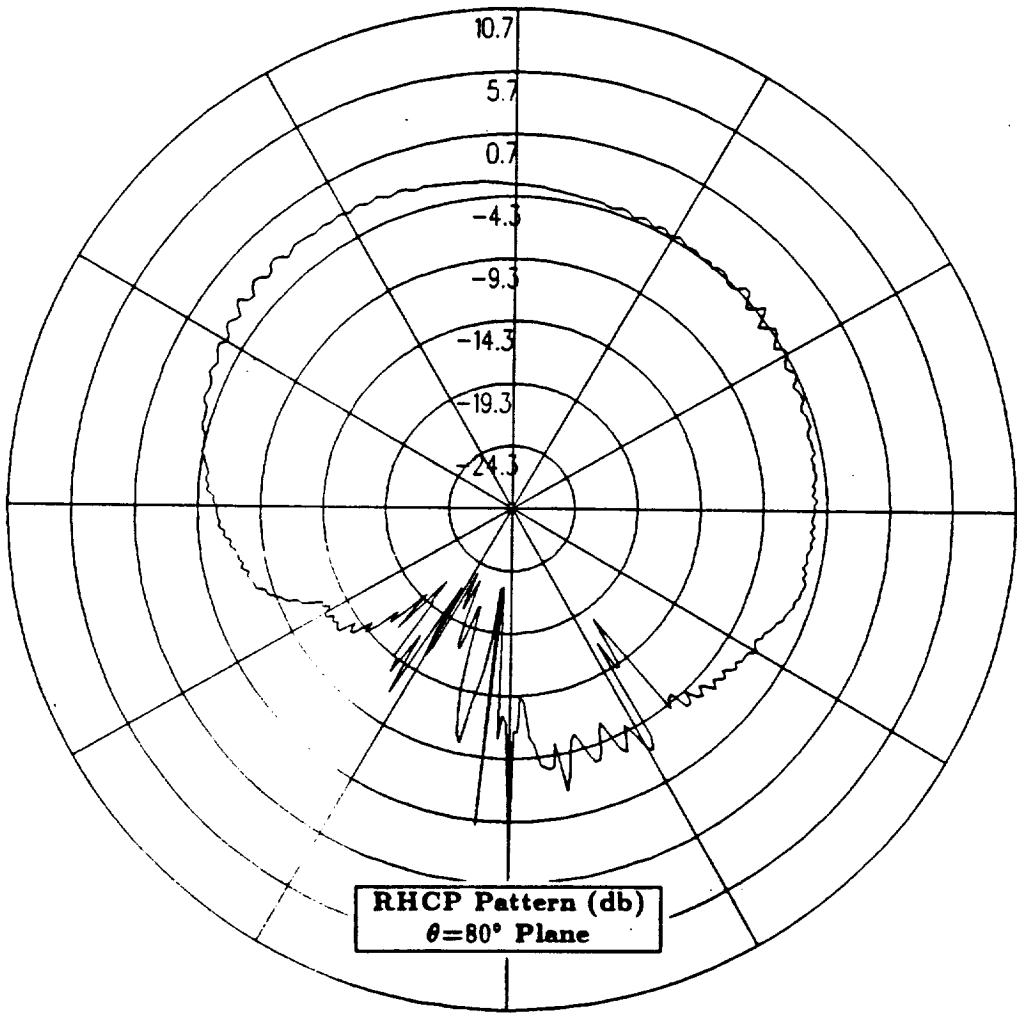

Figure 44: NEC-BSC calculated conical plane pattern 10° above the horizon for antenna location on center-line of the fuselage near the aircraft nose for right hand circular polarization at 300 MHz. (Test Location 4)

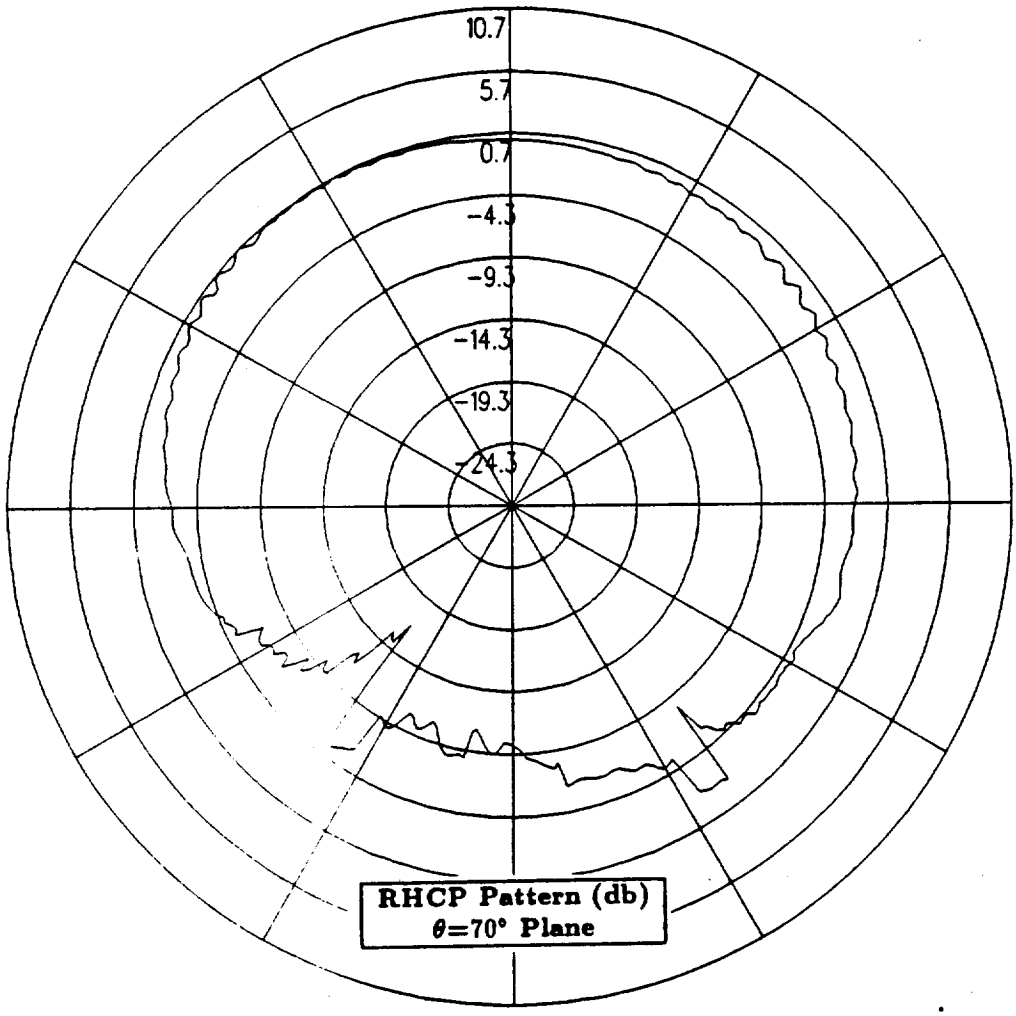

Figure 45: NEC-BSC calculated conical plane pattern 20° above the horizon for antenna location on center-line of the fuselage near the aircraft nose for right hand circular polarization at 300 MHz. (Test Location 4)

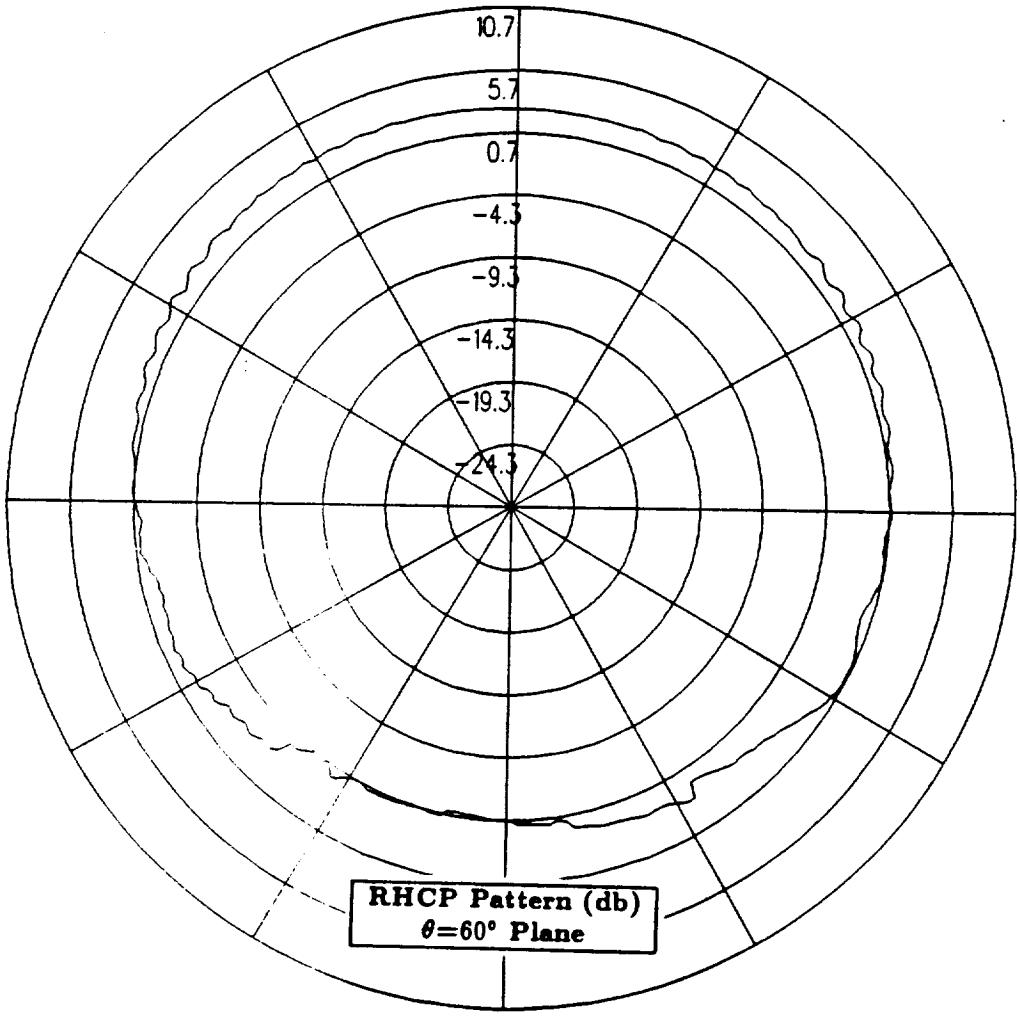

Figure 46: NEC-BSC calculated conical plane pattern 30° above the horizon for antenna location on center-line of the fuselage near the aircraft nose for right hand circular polarization at 300 MHz. (Test Location 4)

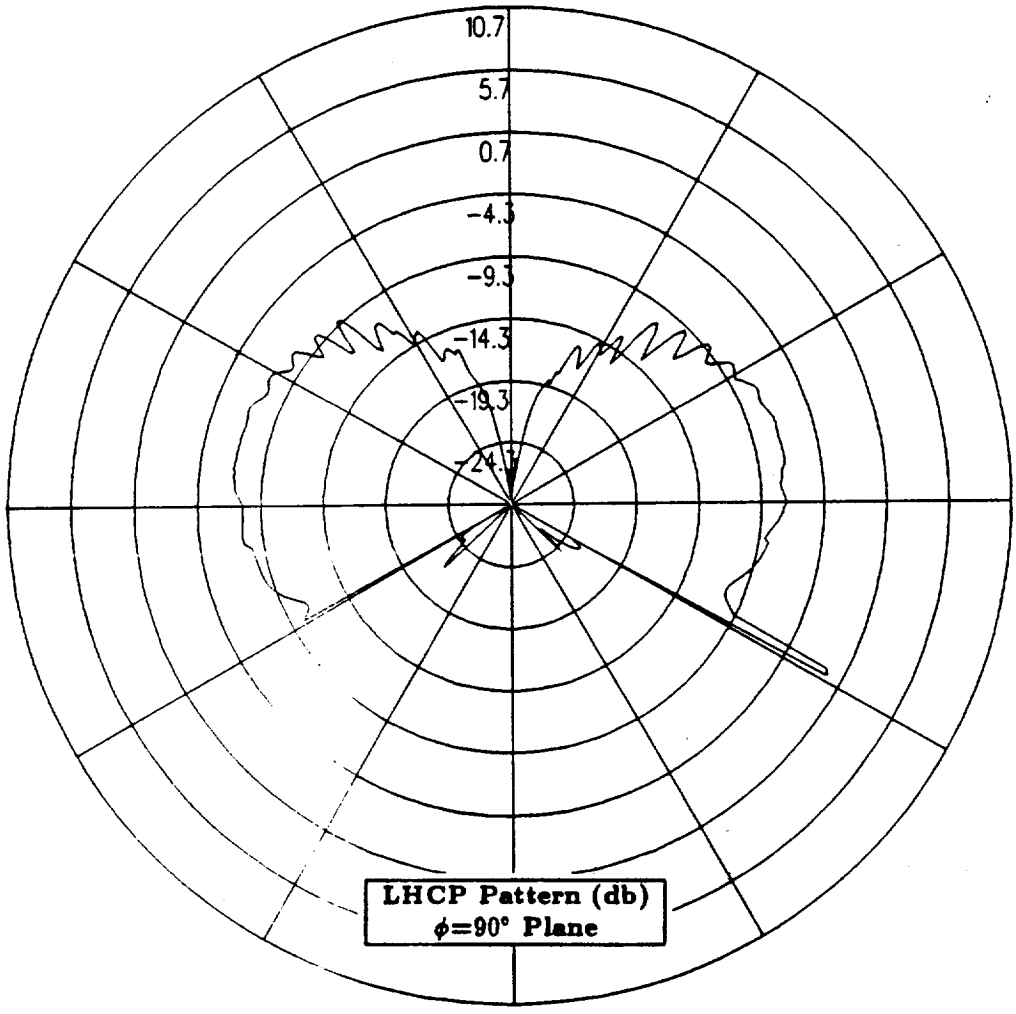

Figure 47: NEC-BSC calculated roll plane pattern for antenna location on center-line of the fuselage near the aircraft nose for left hand circular polarization at 300 MHz. (Test Location 4)

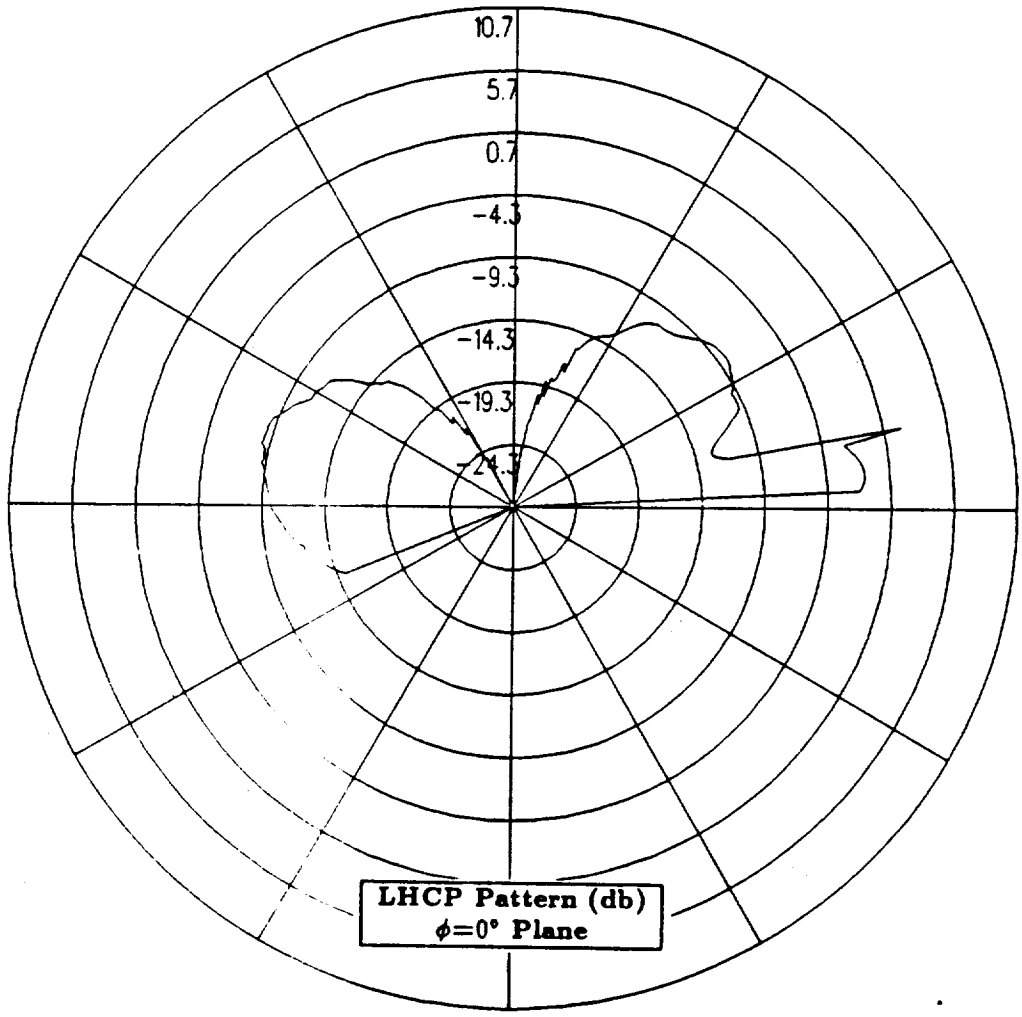

Figure 48: NEC-BSC calculated elevation plane pattern for antenna location on center-line of the fuselage near the aircraft nose for left hand circular polarization at 300 MHz. (Test Location 4)

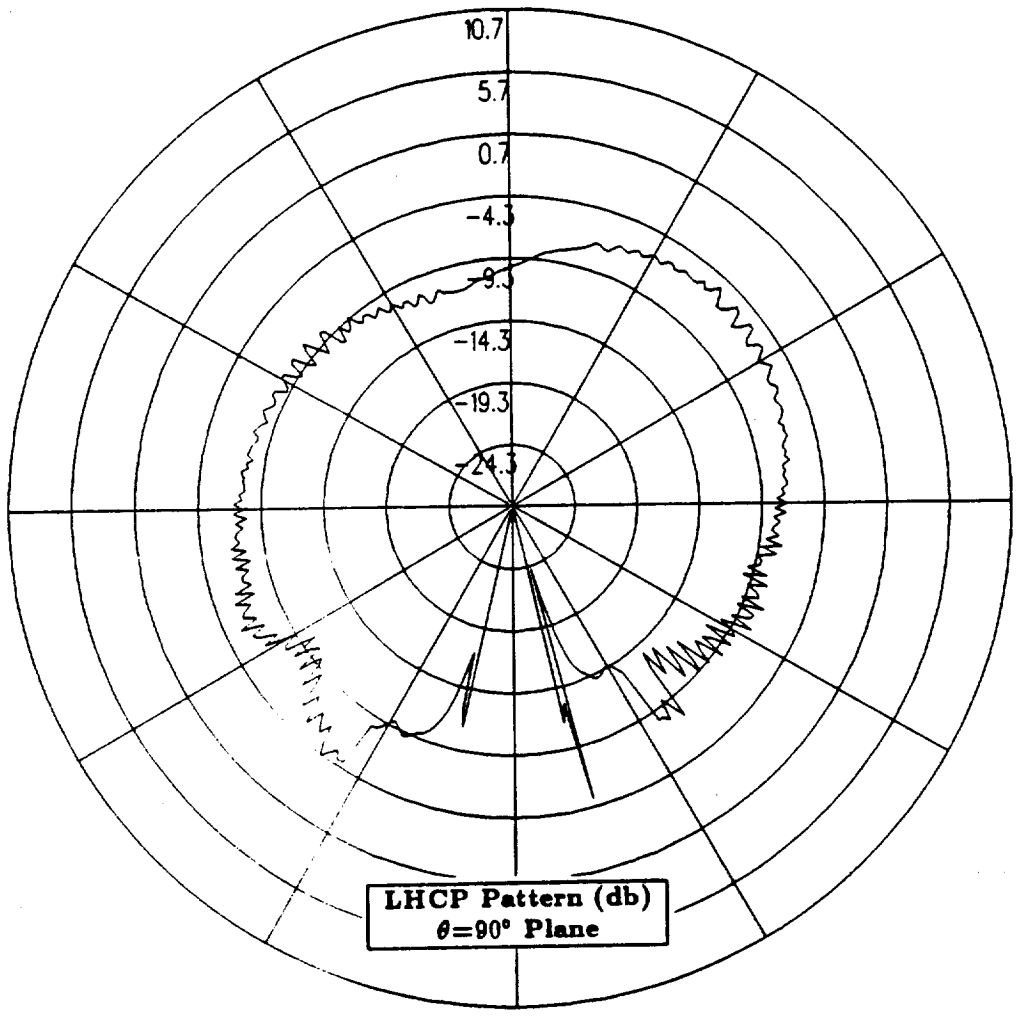

Figure 49: NEC-BSC calculated azimuth plane pattern for antenna location on center-line of the fuselage near the aircraft nose for left hand circular polarization at 300 MHz. (Test Location 4)

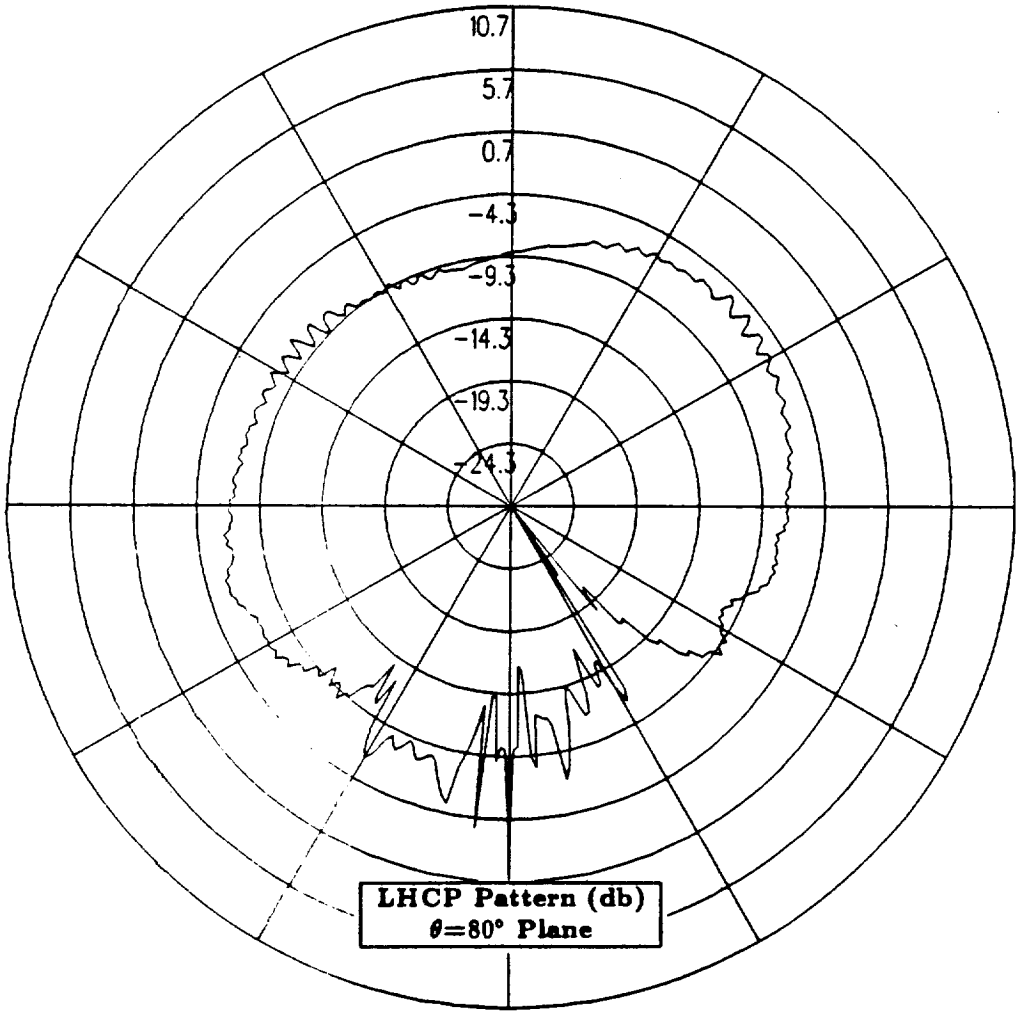

Figure 50: NEC-BSC calculated conical plane pattern 10° above the horizon for antenna location on center-line of the fuselage near the aircraft nose for left hand circular polarization at 300 MHz. (Test Location 4)

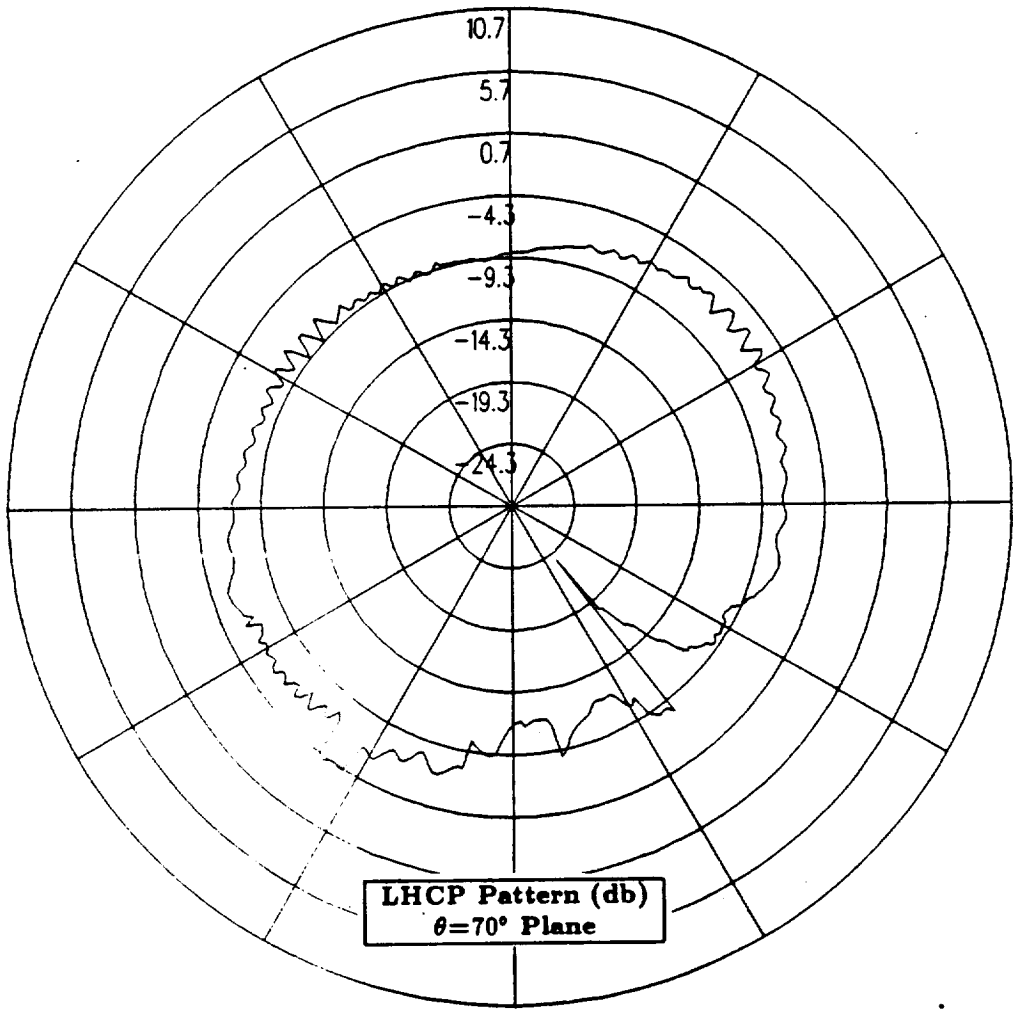

Figure 51: NEC-BSC calculated conical plane pattern 20° above the horizon for antenna location on center-line of the fuselage near the aircraft nose for left hand circular polarization at 300 MHz. (Test Location 4)

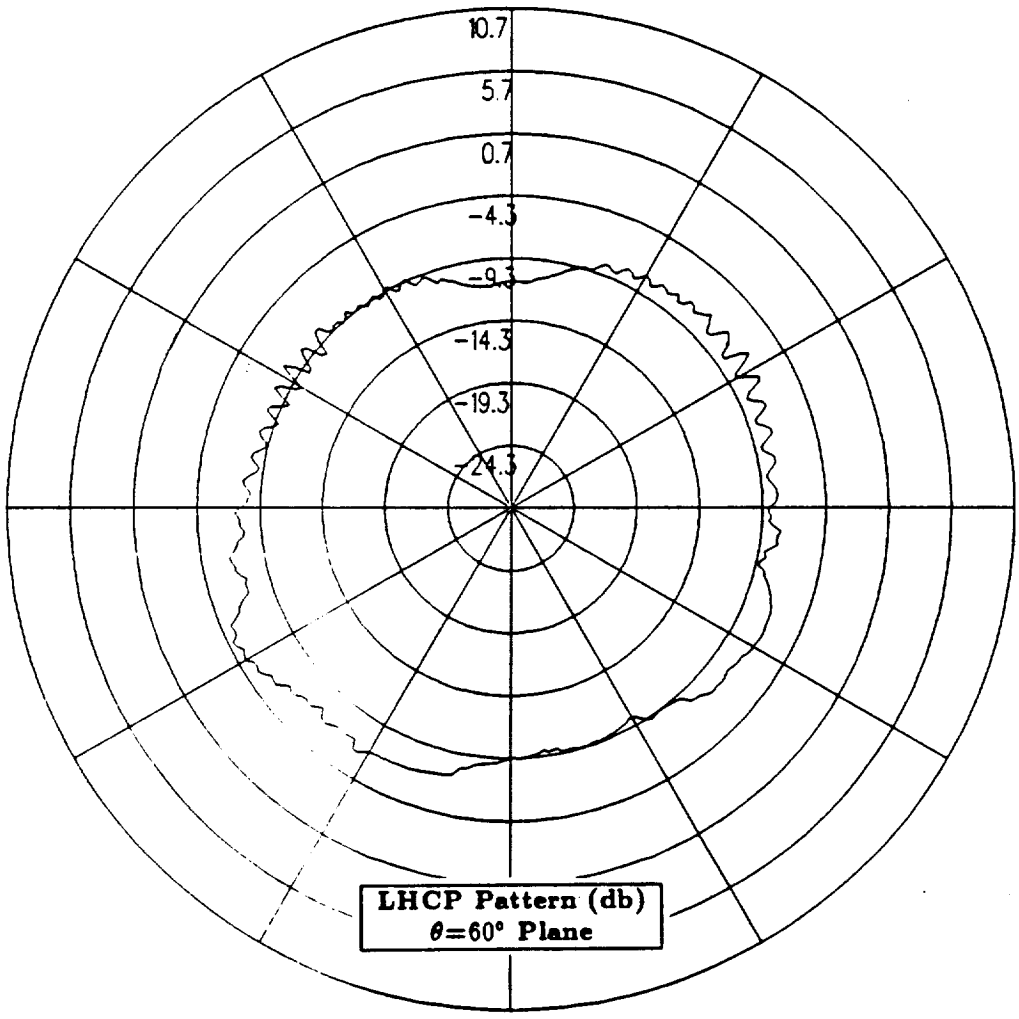

Figure 52: NEC-BSC calculated conical plane pattern 30° above the horizon for antenna location on center-line of the fuselage near the aircraft nose for left hand circular polarization at 300 MHz. (Test Location 4)

1.6 Test Location 5

In this section, the antenna is located on the center-line of the fuselage even further near the aircraft nose. Again, the composite ellipsoid aircraft model is used in the NEC-BSC. This composite ellipsoid aircraft model is illustrated in Figure 53, which also shows the location of the antenna on the fuselage. Since the improved version of the NEC-BSC does not contain plate - composite ellipsoid interactions, Version 3.1 is used to calculate the radiation patterns for this particular antenna location.

The calculated results obtained using Version 3.1 of the NEC-BSC at 300 MHz for the right hand circular polarized or co-polarized fields are shown for the roll plane in Figure 54, for the elevation plane in Figure 55, for the azimuth plane in Figure 56 and for the conical planes 10°, 20° and 30° above the horizon in Figures 57, 58 and 59, respectively. For completeness, the left hand circular polarized or cross-polarized results are also included. These cross-polarized results are shown for the roll plane in Figure 60, for the elevation plane in Figure 61, for the azimuth plane in Figure 62 and for the conical planes 10°, 20° and 30° above the horizon in Figures 63, 64 and 65, respectively.

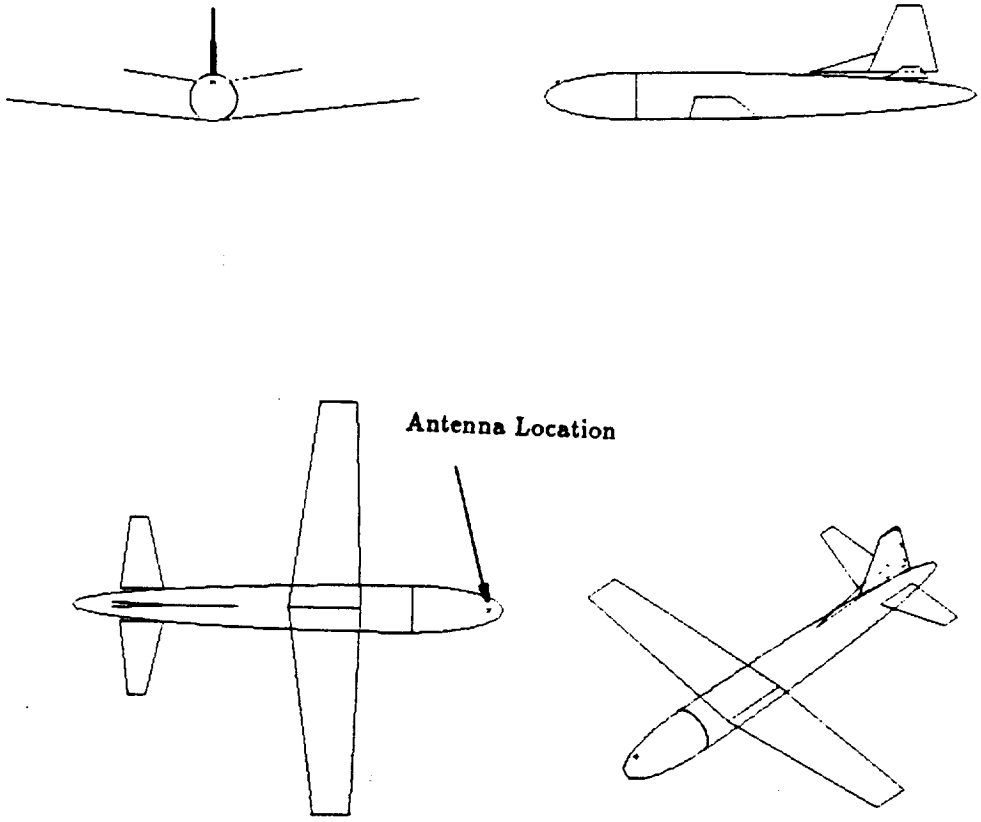

Figure 53: Geometry of the composite ellipsoid model of the P-3C aircraft used in the NEC-BSC showing the antenna location. (Test Location 5)

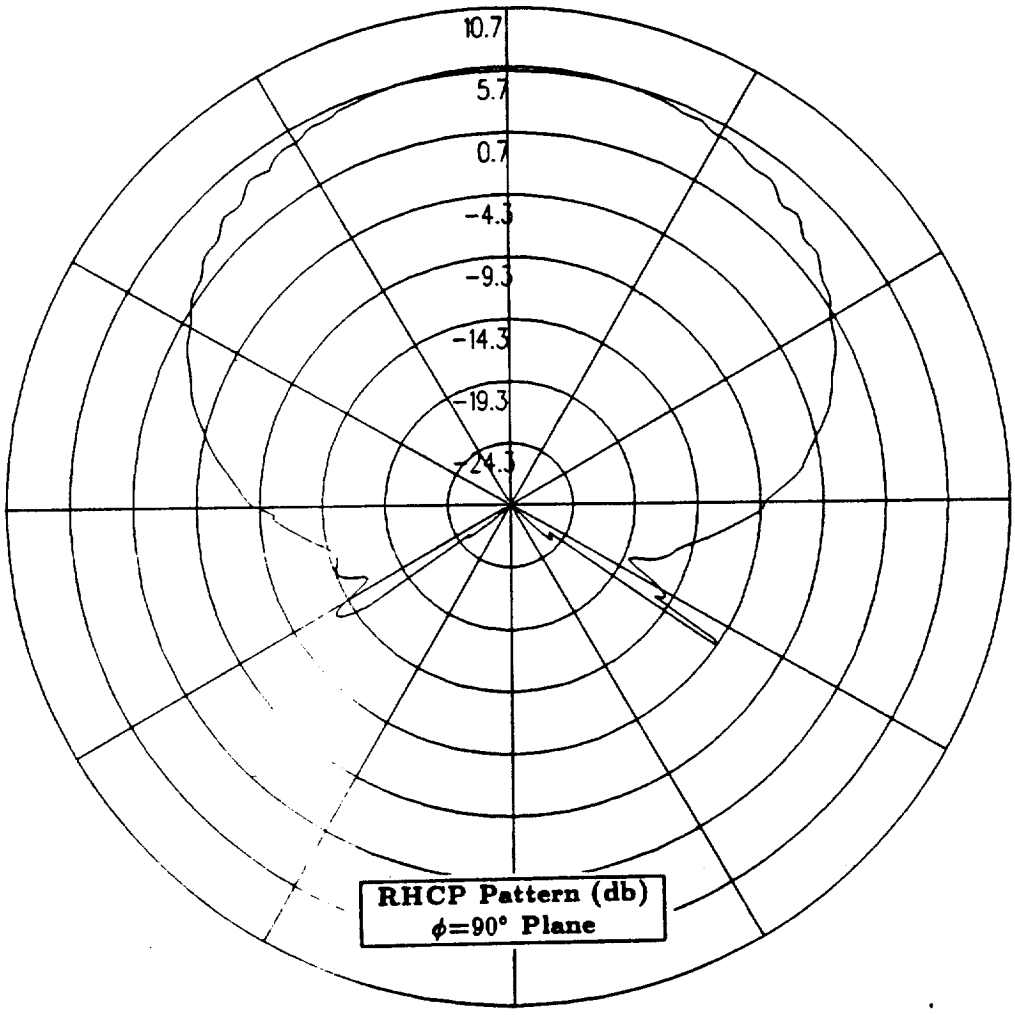

Figure 54: NEC-BSC calculated roll plane pattern for antenna location on center-line of the fuselage near the aircraft nose for right hand circular polarization at 300 MHz. (Test Location 5)

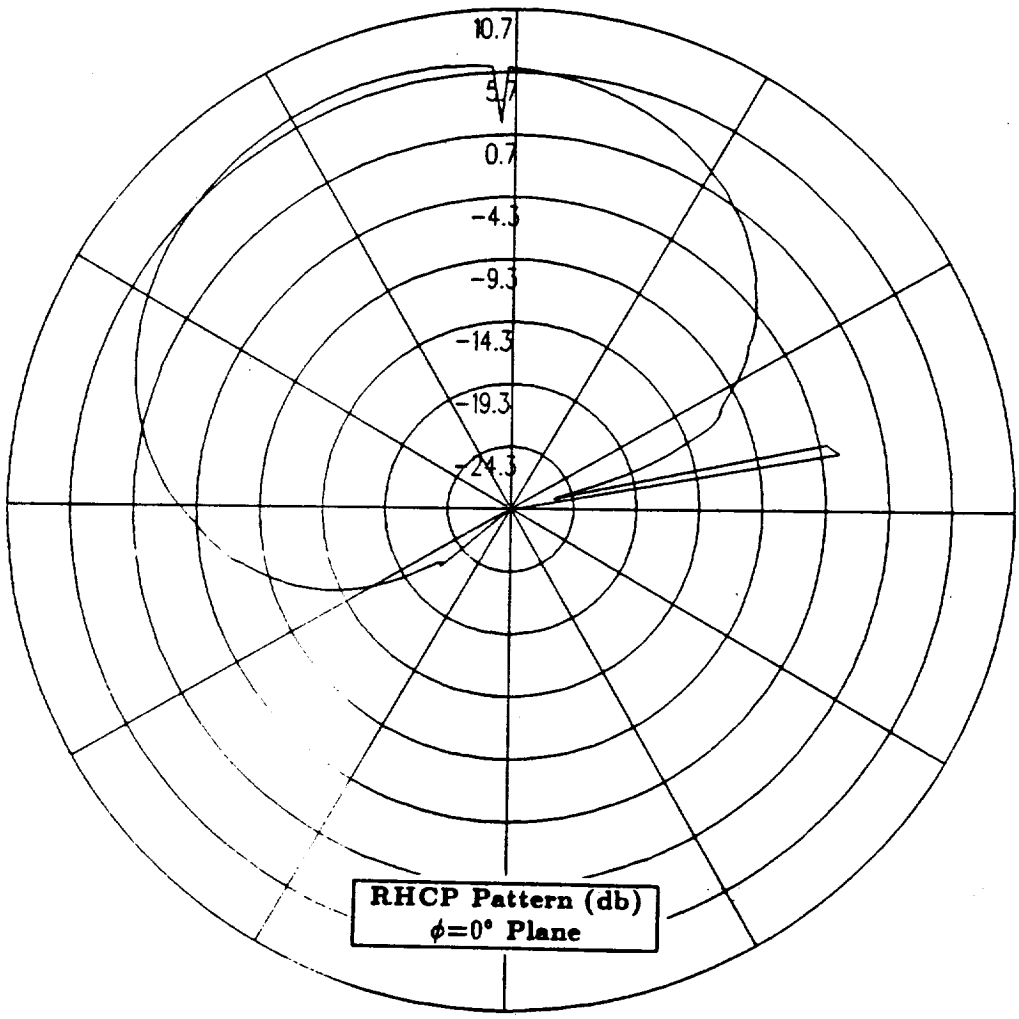

Figure 55: NEC-BSC calculated elevation plane pattern for antenna location on center-line of the fuselage near the aircraft nose for right hand circular polarization at 300 MHz. (Test Location 5)

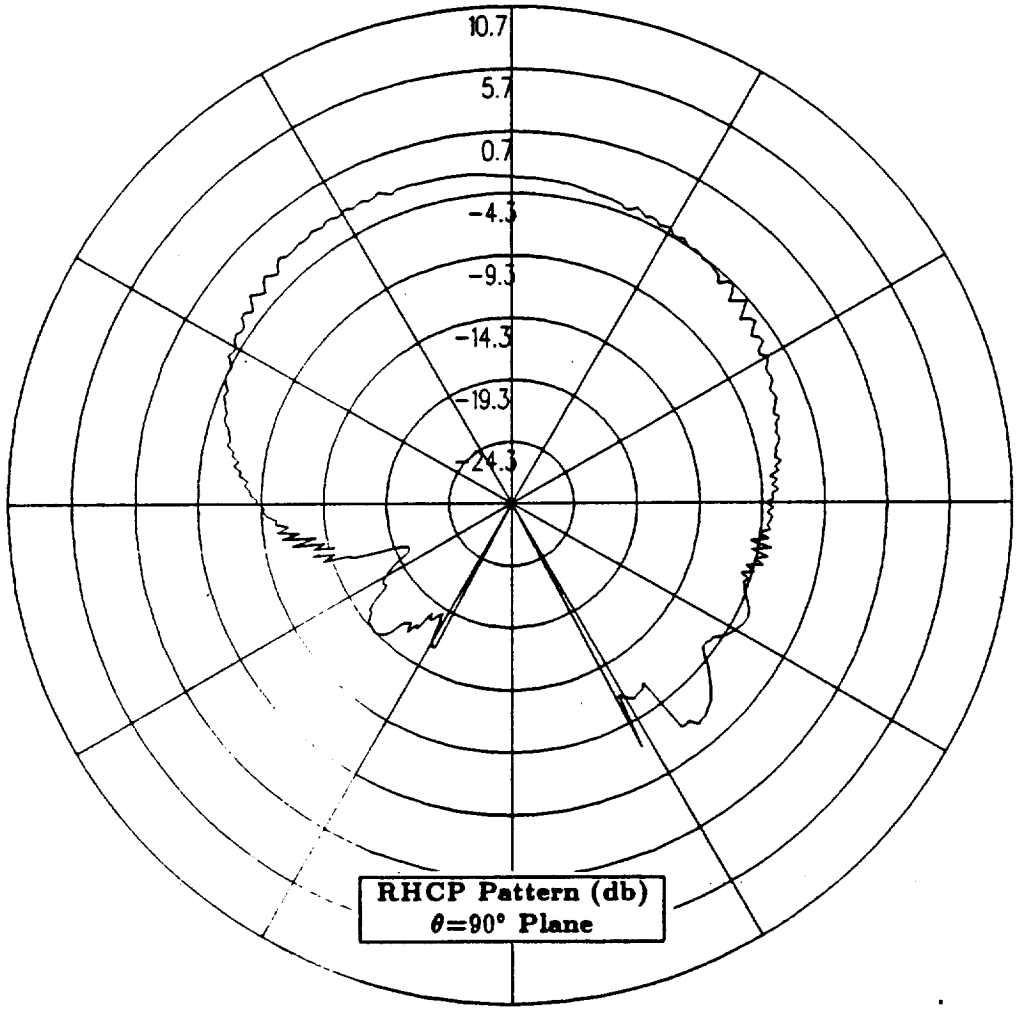

Figure 56: NEC-BSC calculated azimuth plane pattern for antenna location on center-line of the fuselage near the aircraft nose for right hand circular polarization at 300 MHz. (Test Location 5)

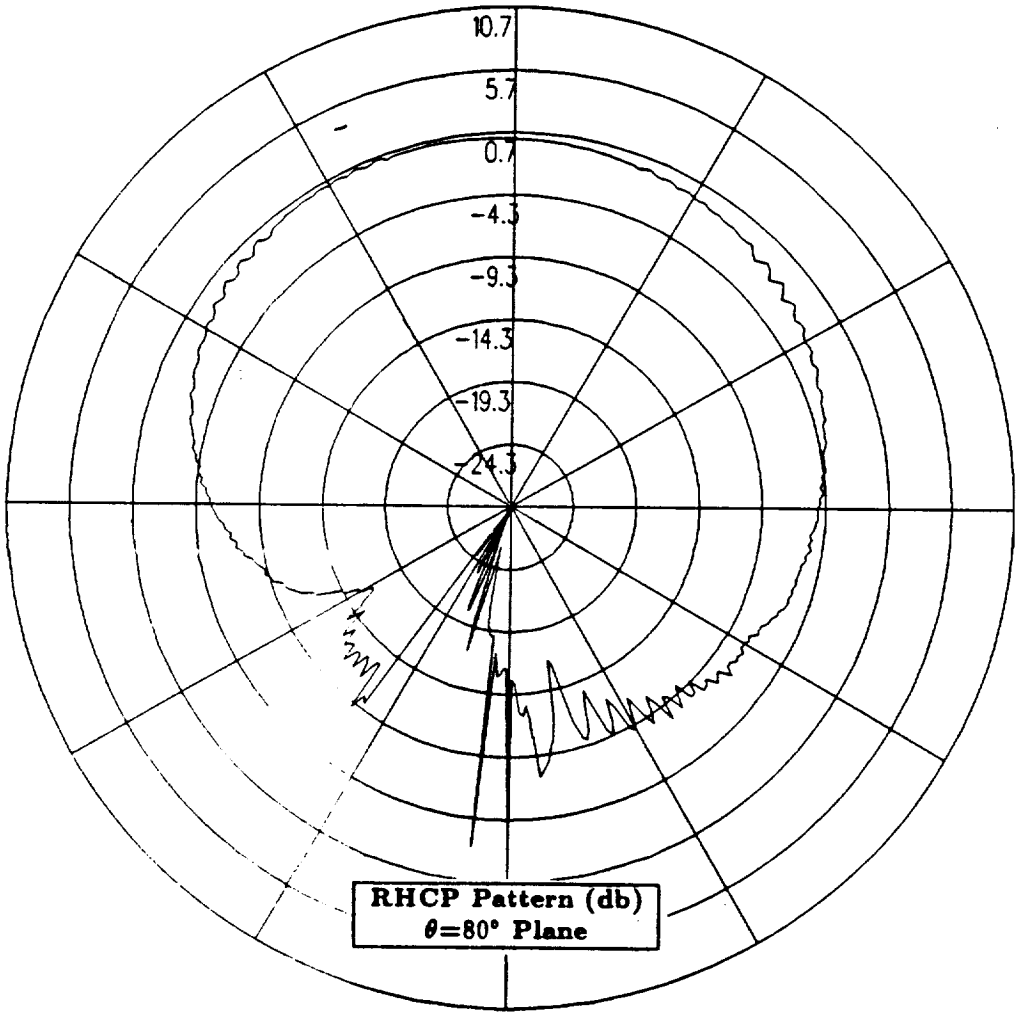

Figure 57: NEC-BSC calculated conical plane pattern 10° above the horizon for antenna location on center-line of the fuselage near the aircraft nose for right hand circular polarization at 300 MHz. (Test Location 5)

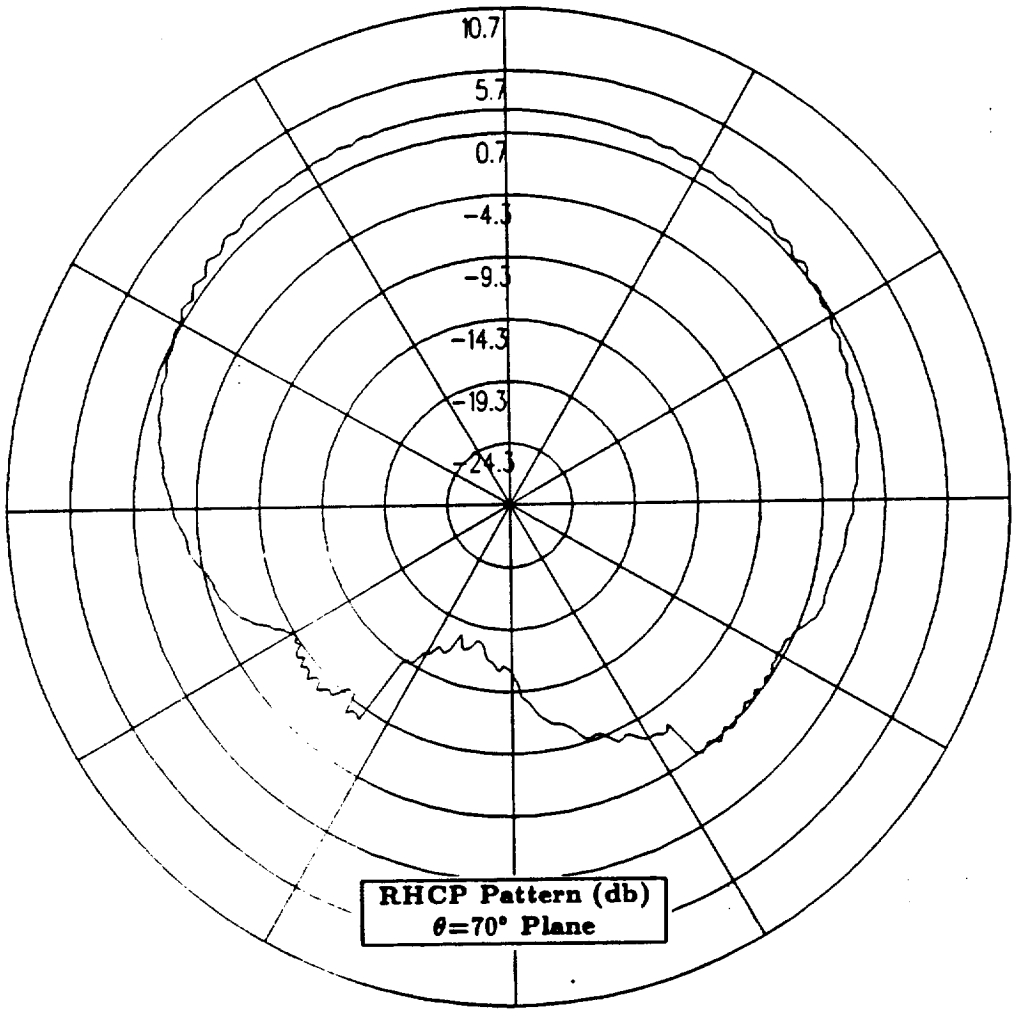

Figure 58: NEC-BSC calculated conical plane pattern 20° above the horizon for antenna location on center-line of the fuselage near the aircraft nose for right hand circular polarization at 300 MHz. (Test Location 5)

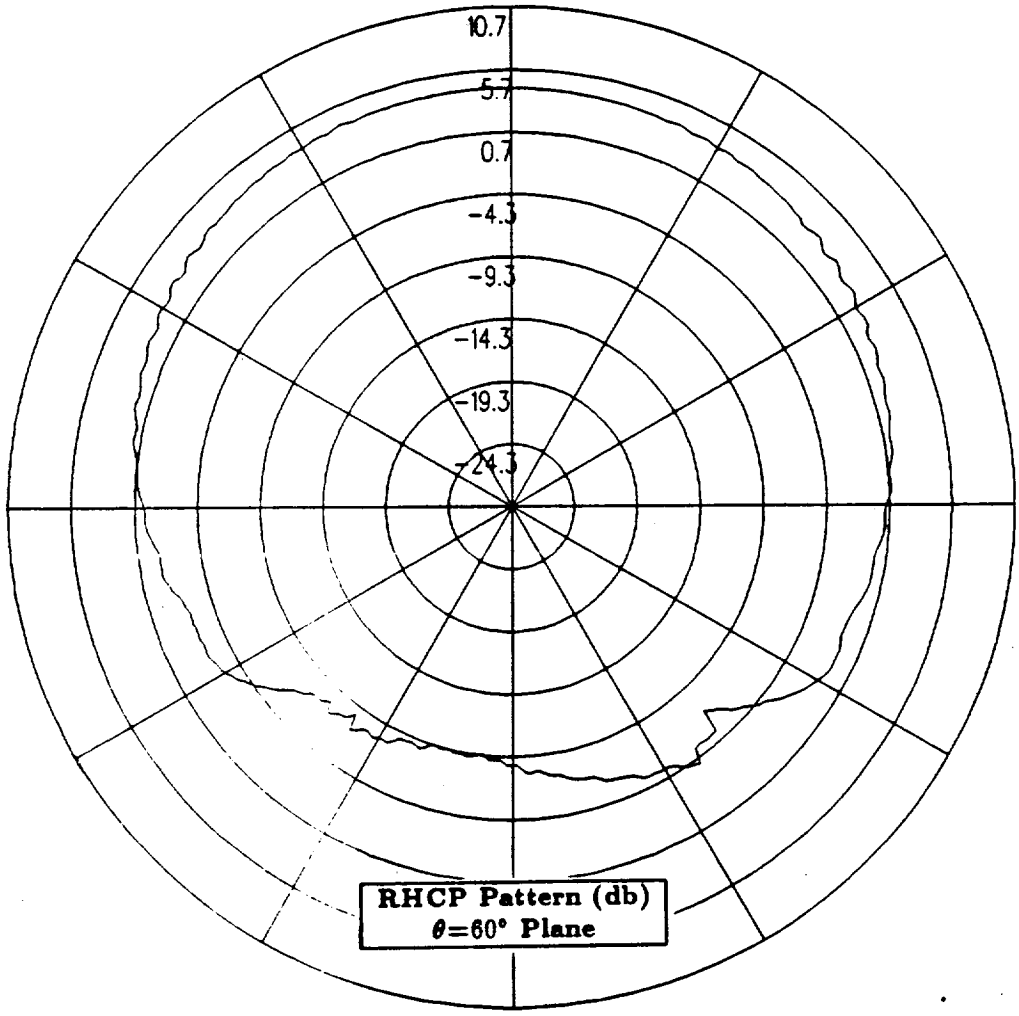

Figure 59: NEC-BSC calculated conical plane pattern 30° above the horizon for antenna location on center-line of the fuselage near the aircraft nose for right hand circular polarization at 300 MHz. (Test Location 5)

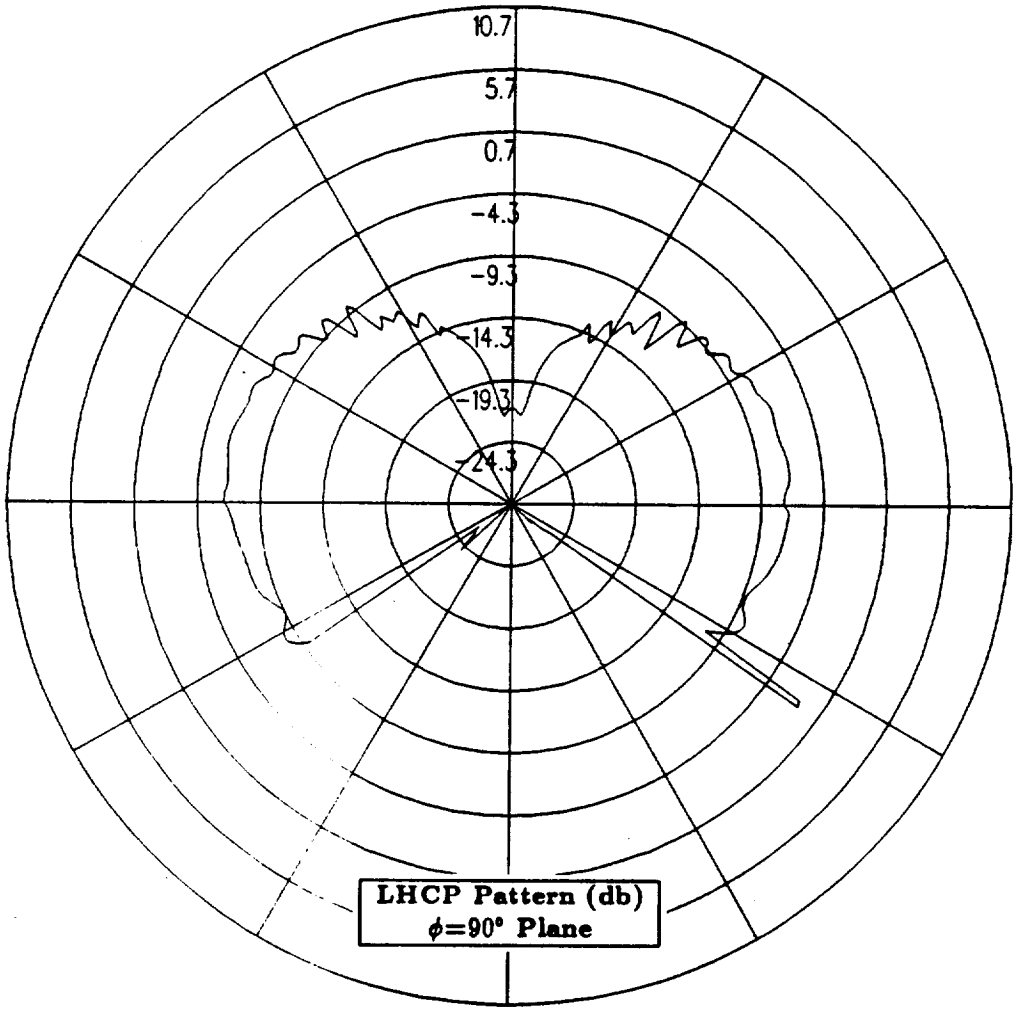

Figure 60: NEC-BSC calculated roll plane pattern for antenna location on center-line of the fuselage near the aircraft nose for left hand circular polarization at 300 MHz. (Test Location 5)

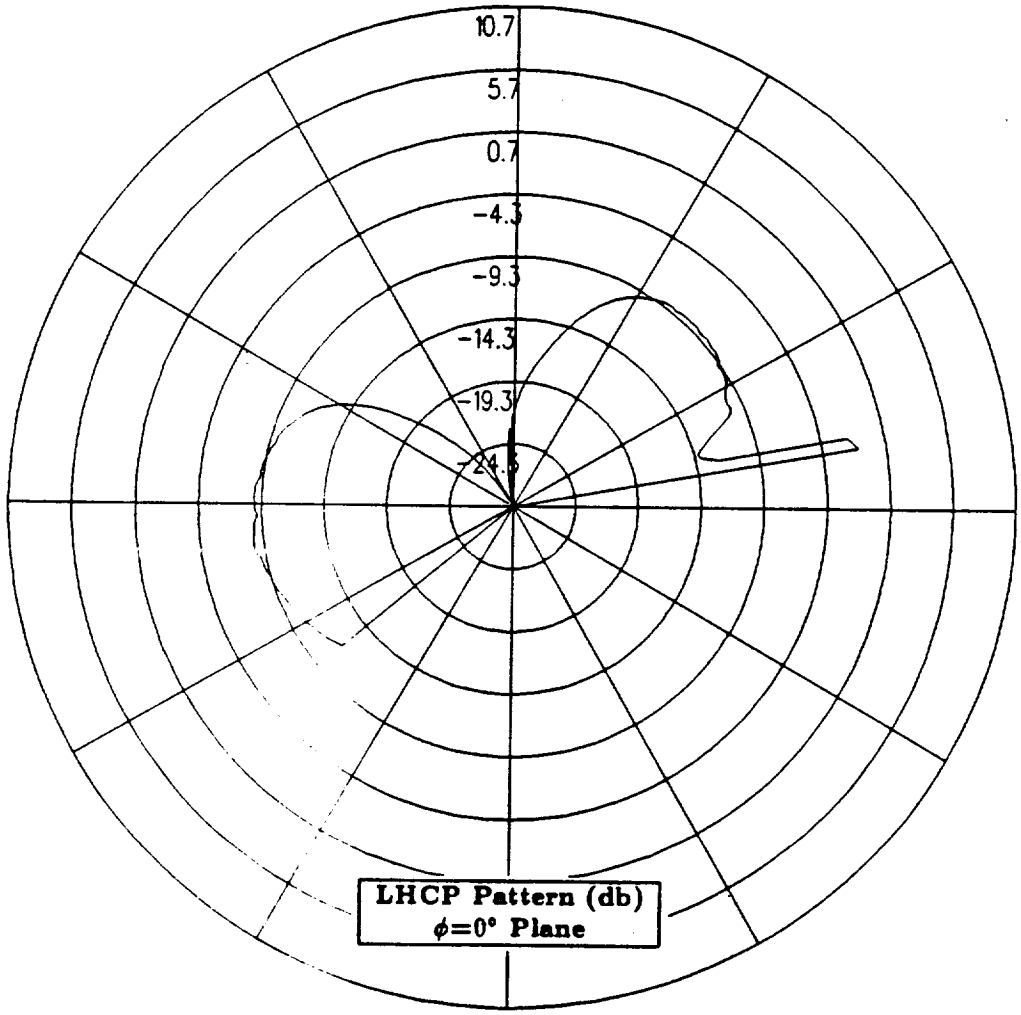

Figure 61: NEC-BSC calculated elevation plane pattern for antenna location on center-line of the fuselage near the aircraft nose for left hand circular polarization at 300 MHz. (Test Location 5)

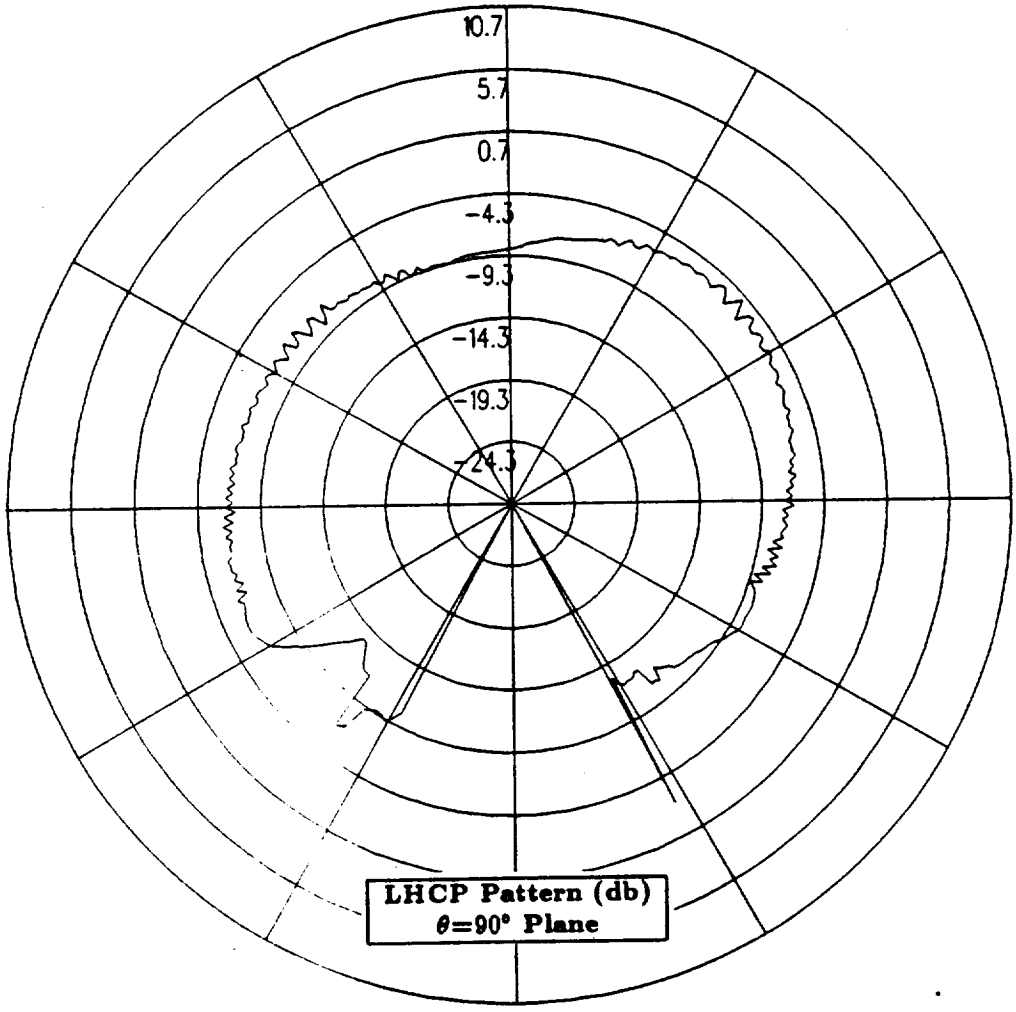

Figure 62: NEC-BSC calculated azimuth plane pattern for antenna location on center-line of the fuselage near the aircraft nose for left hand circular polarization at 300 MHz. (Test Location 5)

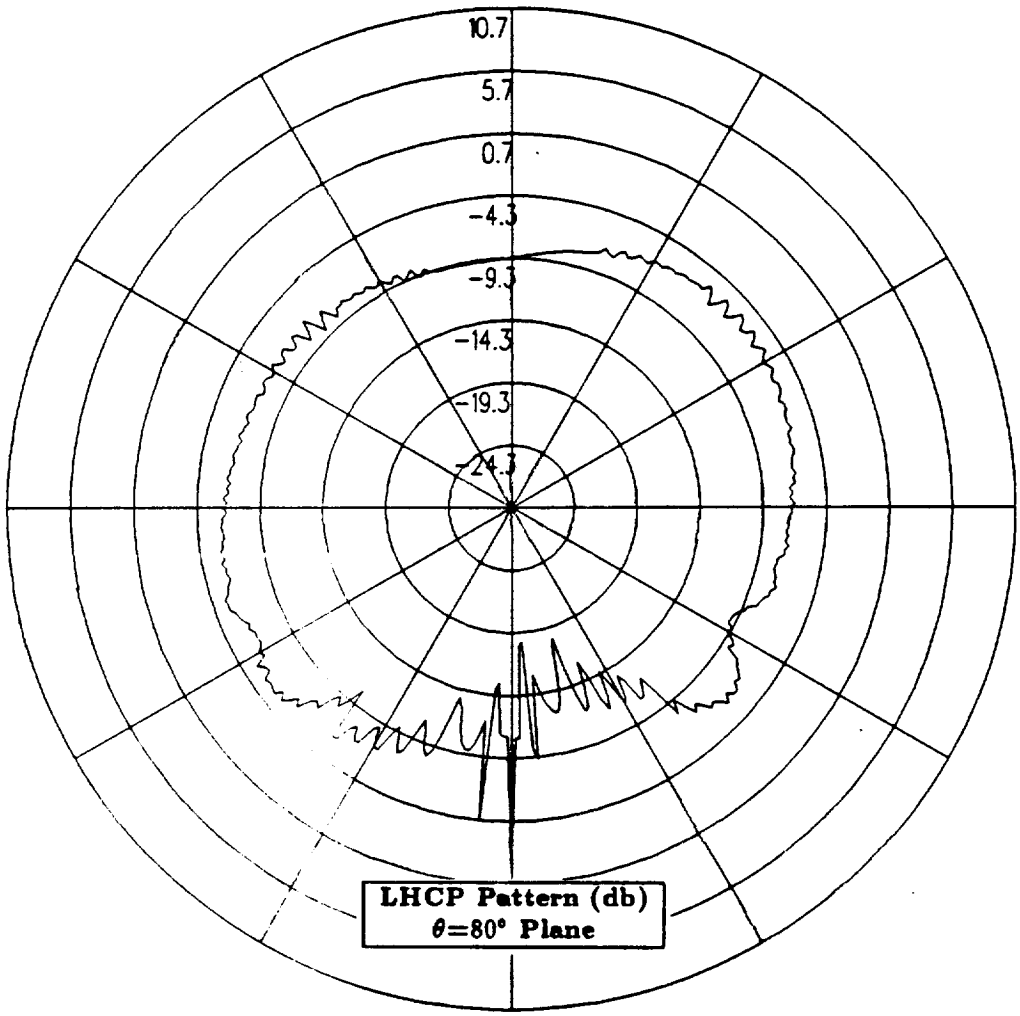

Figure 63: NEC-BSC calculated conical plane pattern 10° above the horizon for antenna location on center-line of the fuselage near the aircraft nose for left hand circular polarization at 300 MHz. (Test Location 5)

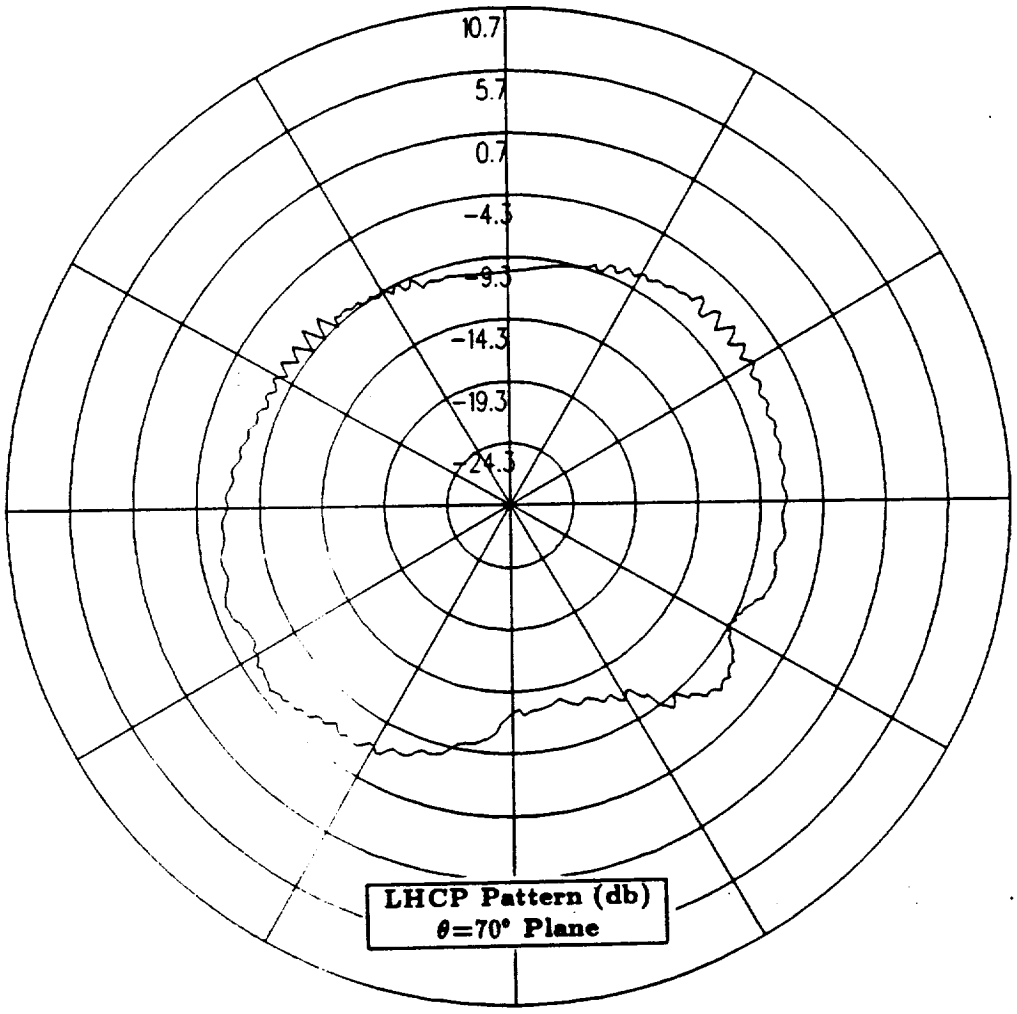

Figure 64: NEC-BSC calculated conical plane pattern 20° above the horizon for antenna location on center-line of the fuselage near the aircraft nose for left hand circular polarization at 300 MHz. (Test Location 5)

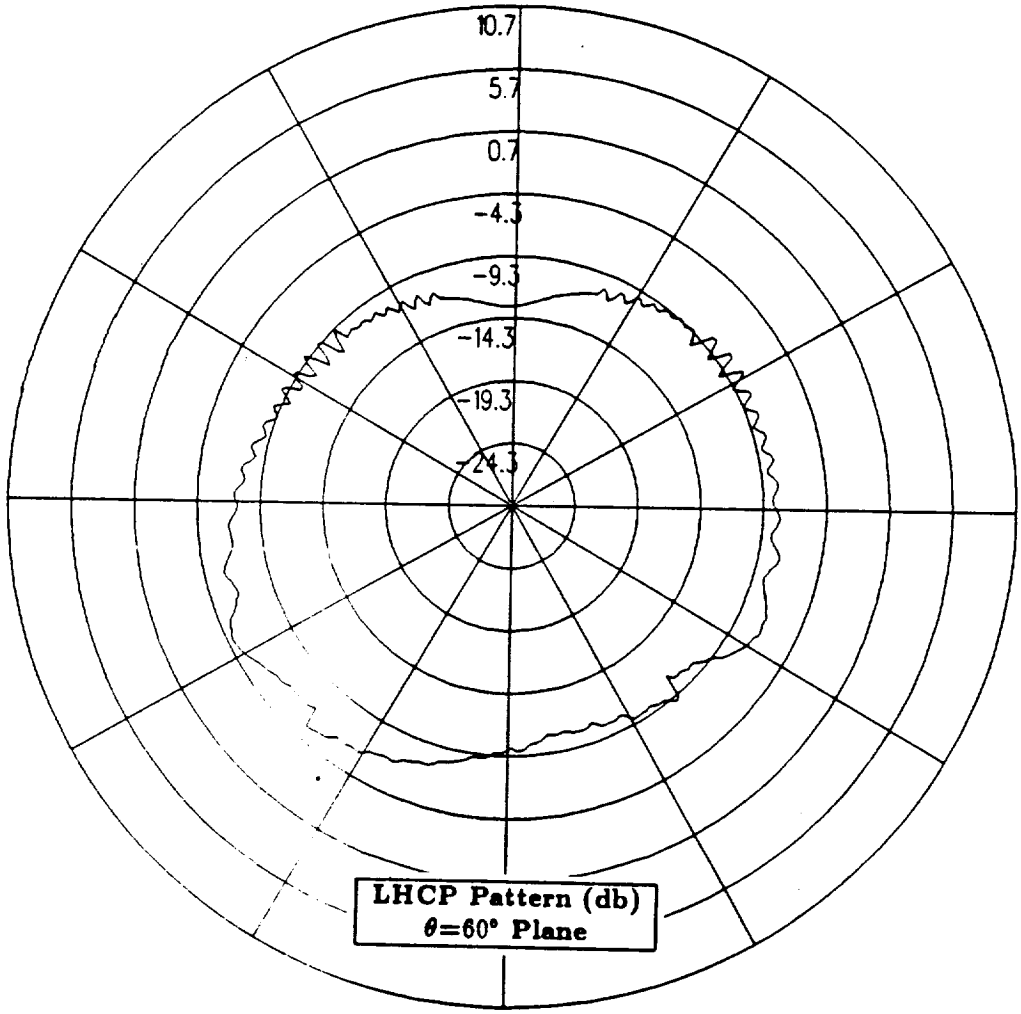

Figure 65: NEC-BSC calculated conical plane pattern 30° above the horizon for antenna location on center-line of the fuselage near the aircraft nose for left hand circular polarization at 300 MHz. (Test Location 5)

1.7 Test Location 6

In this section, the antenna is located on the port side of the fuselage above the wing and 38.7° down from the top center-line. The cylindrical aircraft model used in the NEC-BSC is illustrated in Figure 66, which also shows the location of the antenna on the fuselage. The calculated results obtained using the improved version of the NEC-BSC at 300 MHz for the right hand circular polarized or co-polarized fields are shown for the roll plane in Figure 67, for the elevation plane in Figure 68, for the azimuth plane in Figure 69 and for the conical planes 10°, 20° and 30° above the horizon in Figures 70, 71 and 72, respectively. For completeness, the left hand circular polarized or cross-polarized results are also included. These cross-polarized results are shown for the roll plane in Figure 73, for the elevation plane in Figure 74, for the azimuth plane in Figure 75 and for the conical planes 10°, 20° and 30° above the horizon in Figures 76, 77 and 78, respectively.

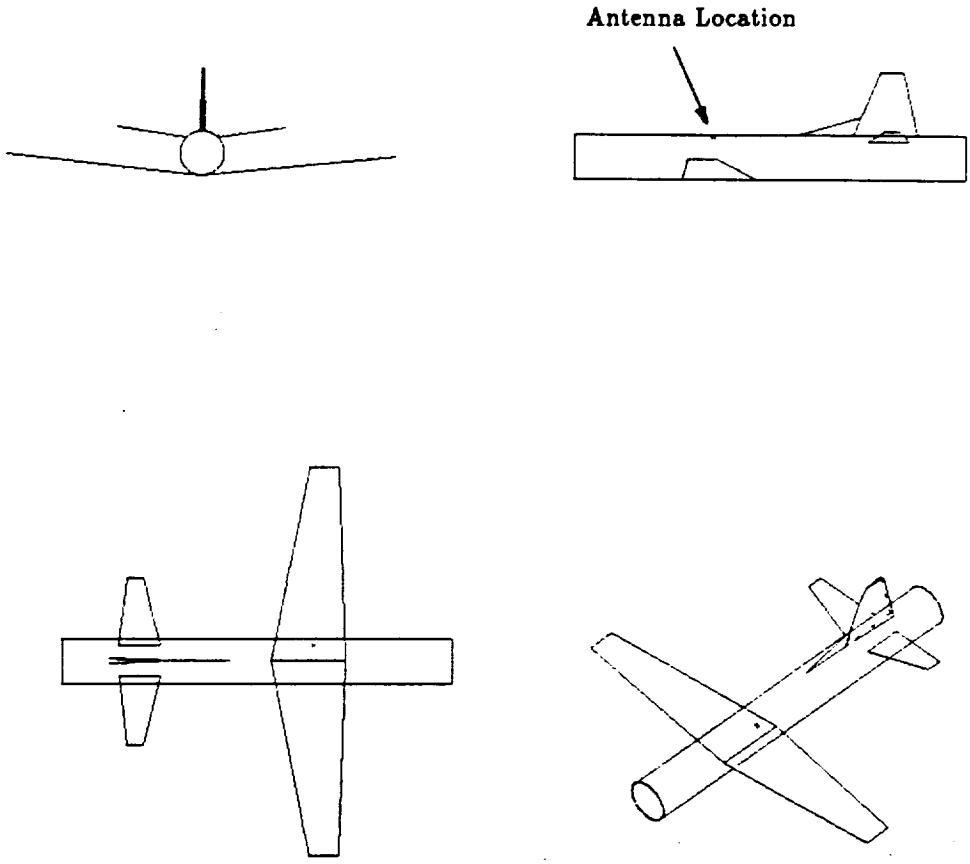

Figure 66: Geometry of the cylindrical model of the P-3C aircraft used in the NEC-BSC showing the antenna location. (Test Location 6)

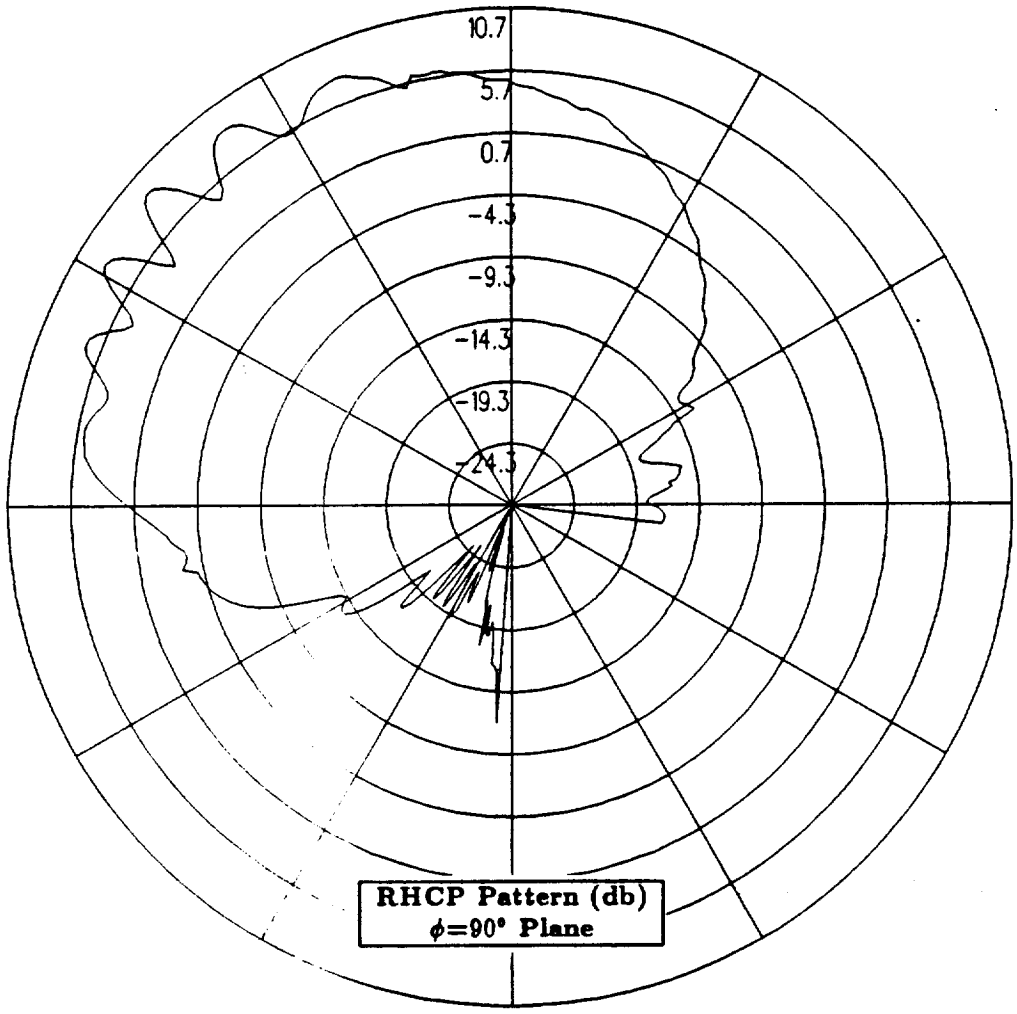

Figure 67: NEC-BSC calculated roll plane pattern for antenna location on the port side of the fuselage above the wing and 38.7° down from the top center-line for right hand circular polarization at 300 MHz. (Test Location 6)

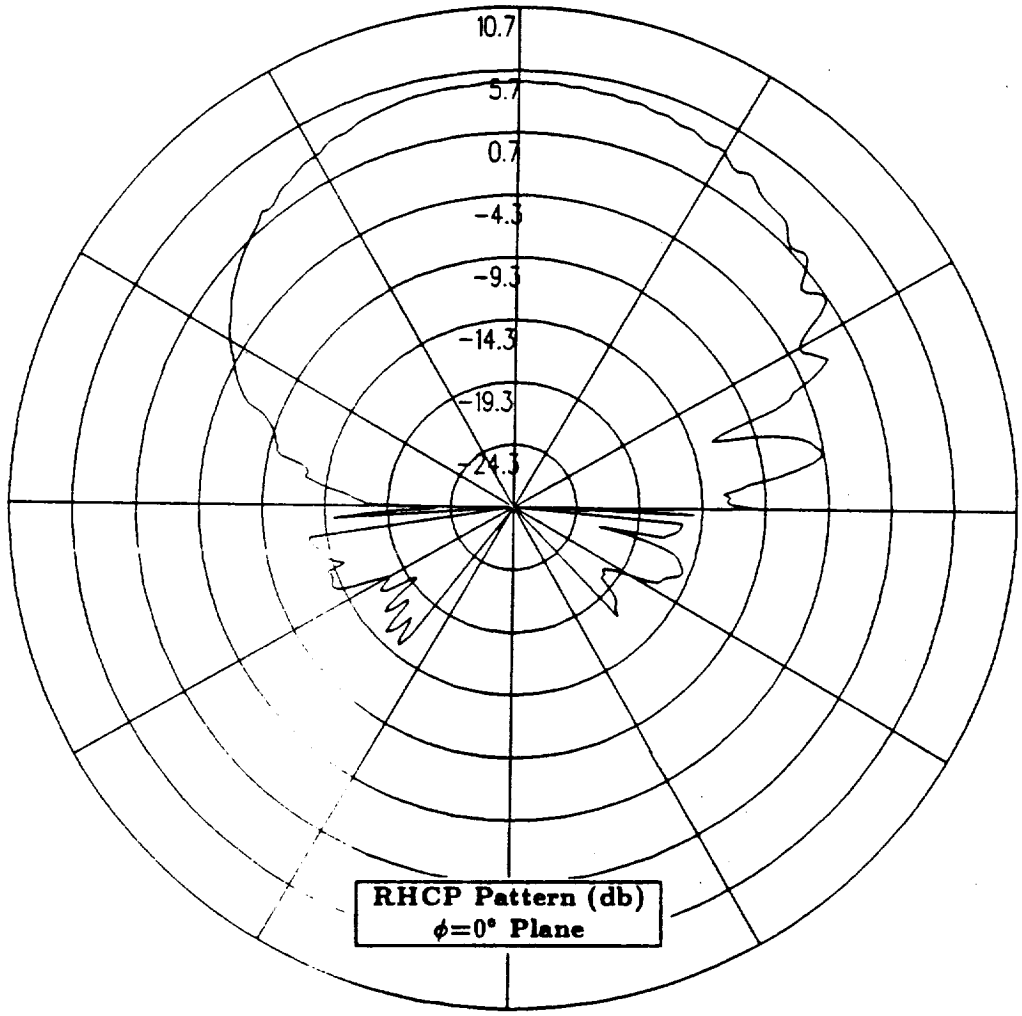

Figure 68: NEC-BSC calculated elevation plane pattern for antenna location on the port side of the fuselage above the wing and 38.7° down from the top center-line for right hand circular polarization at 300 MHz. (Test Location 6)

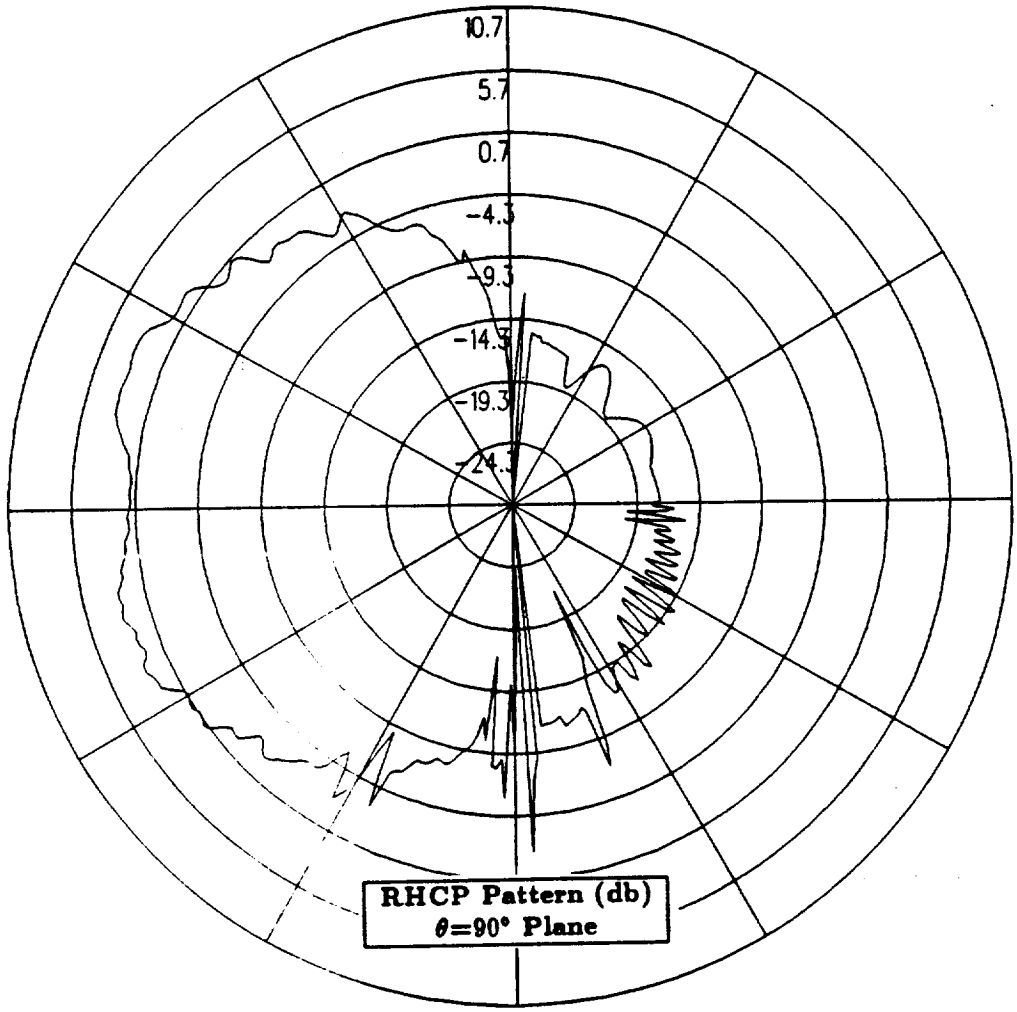

Figure 69: NEC-BSC calculated azimuth plane pattern for antenna location on the port side of the fuselage above the wing and 38.7° down from the top center-line for right hand circular polarization at 300 MHz. (Test Location 6)

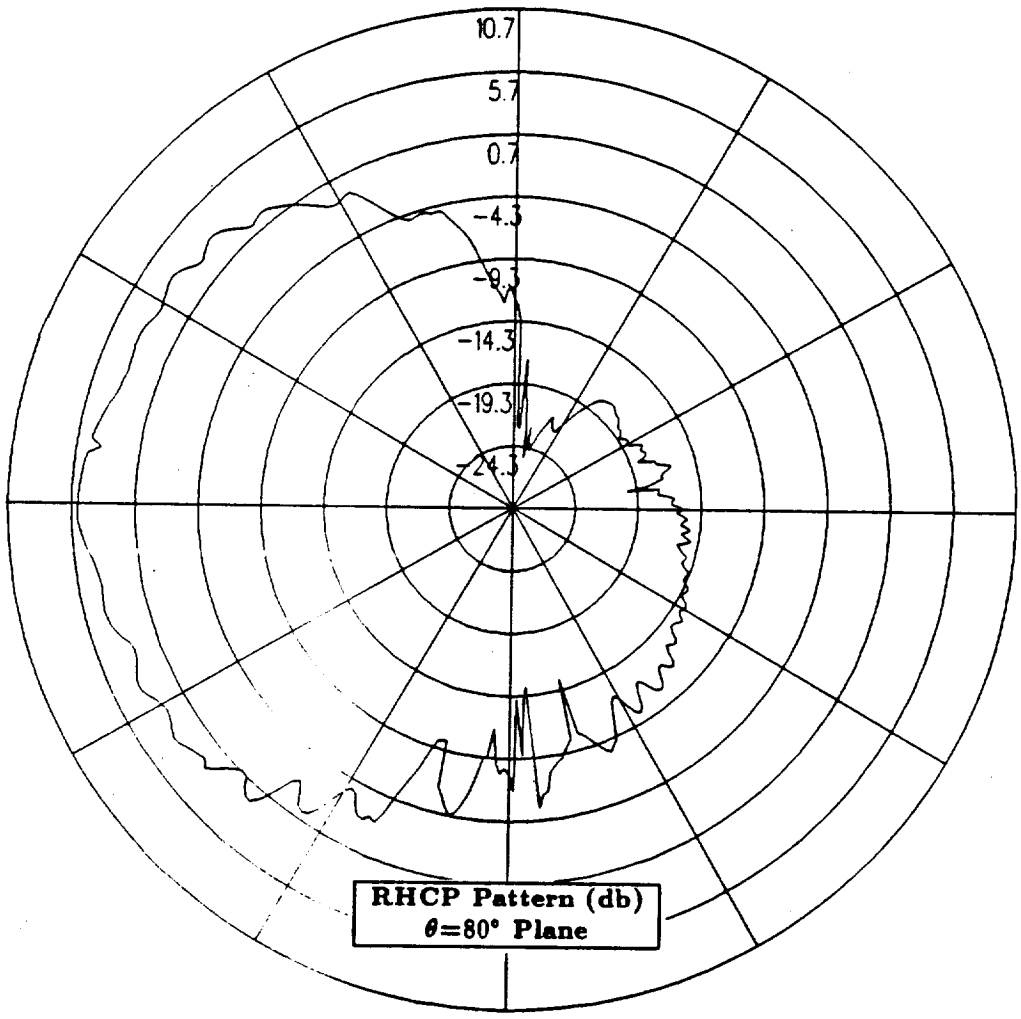

Figure 70: NEC-BSC calculated conical plane pattern 10° above the horizon for antenna location on the port side of the fuselage above the wing and 38.7° down from the top center-line for right hand circular polarization at 300 MHz. (Test Location 6)

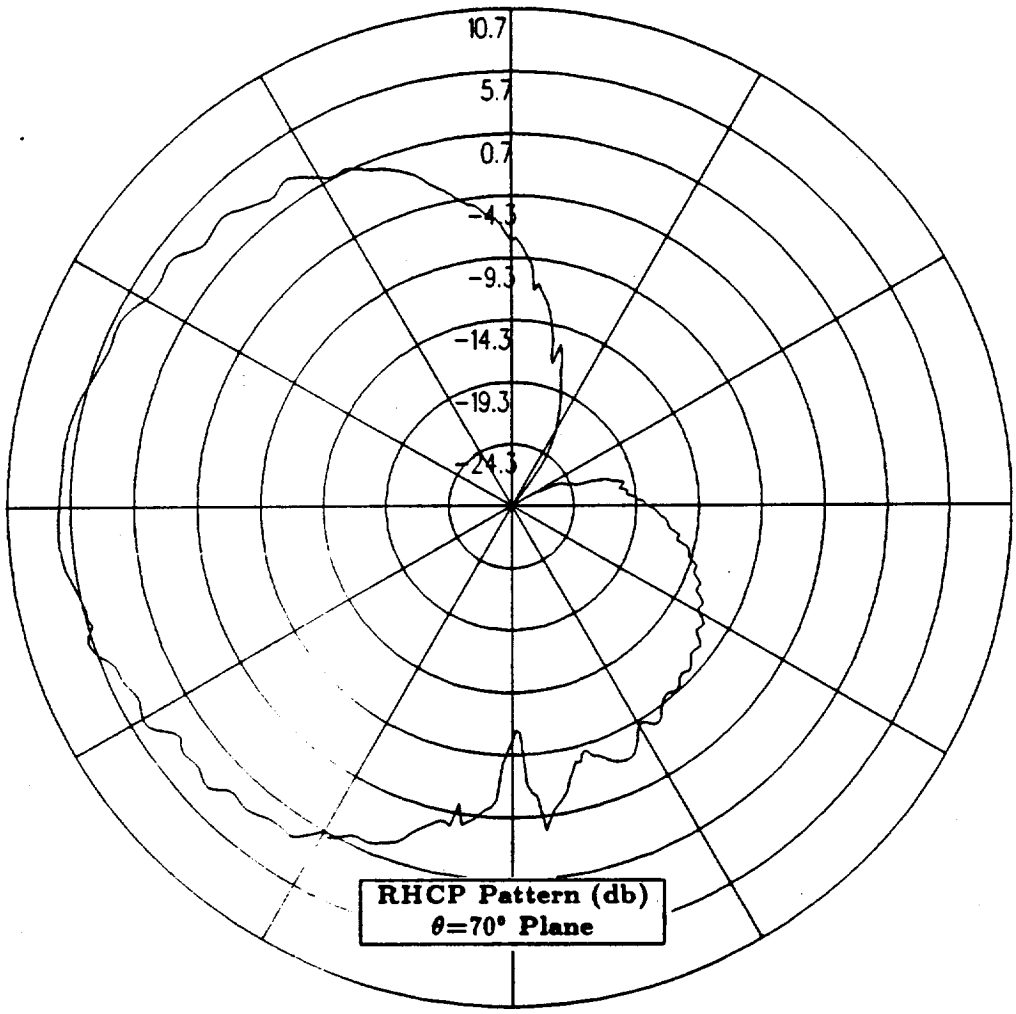

Figure 71: NEC-BSC calculated conical plane pattern 20° above the horizon for antenna location on the port side of the fuselage above the wing and 38.7° down from the top center-line for right hand circular polarization at 300 MHz. (Test Location 6)

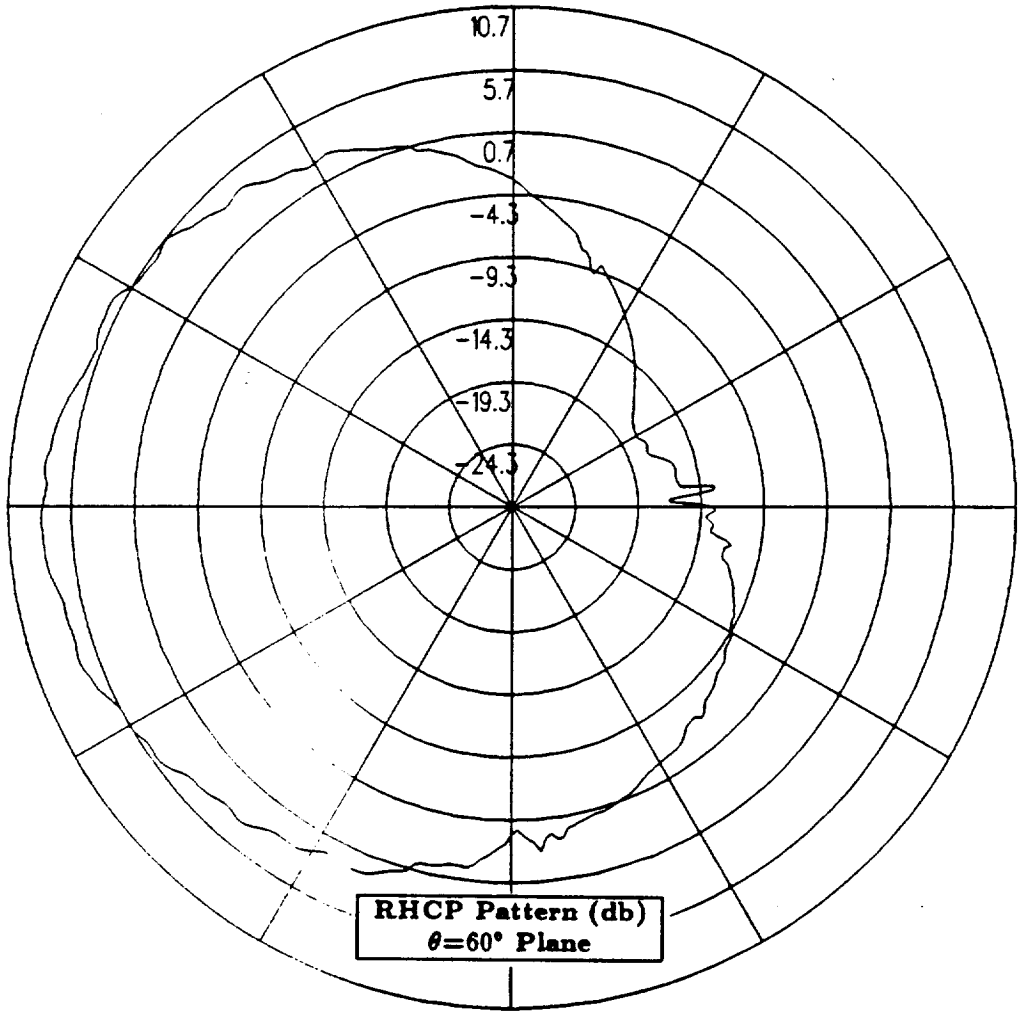

Figure 72: NEC-BSC calculated conical plane pattern 30° above the horizon for antenna location on the port side of the fuselage above the wing and 38.7° down from the top center-line for right hand circular polarization at 300 MHz. (Test Location 6)

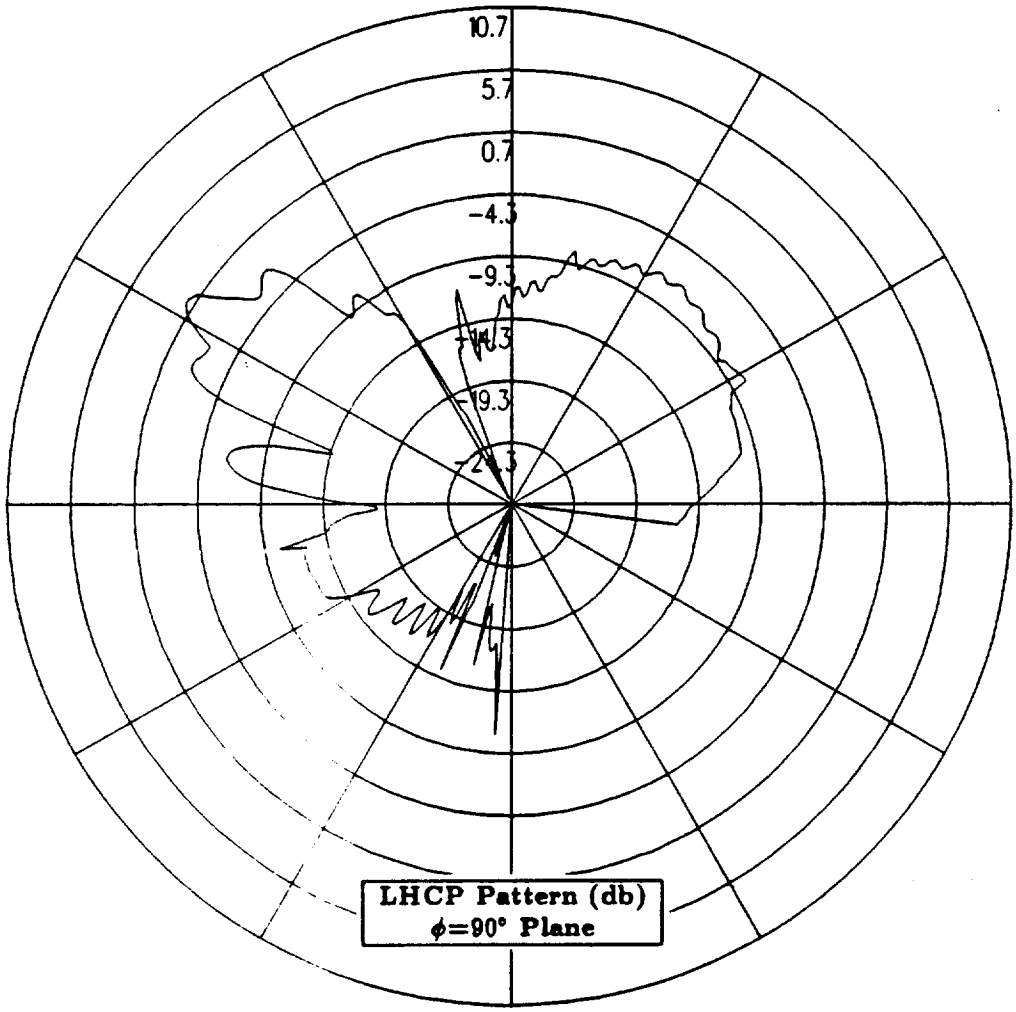

Figure 73: NEC-BSC calculated roll plane pattern for antenna location on the port side of the fuselage above the wing and 38.7° down from the top center-line for left hand circular polarization at 300 MHz. (Test Location 6)

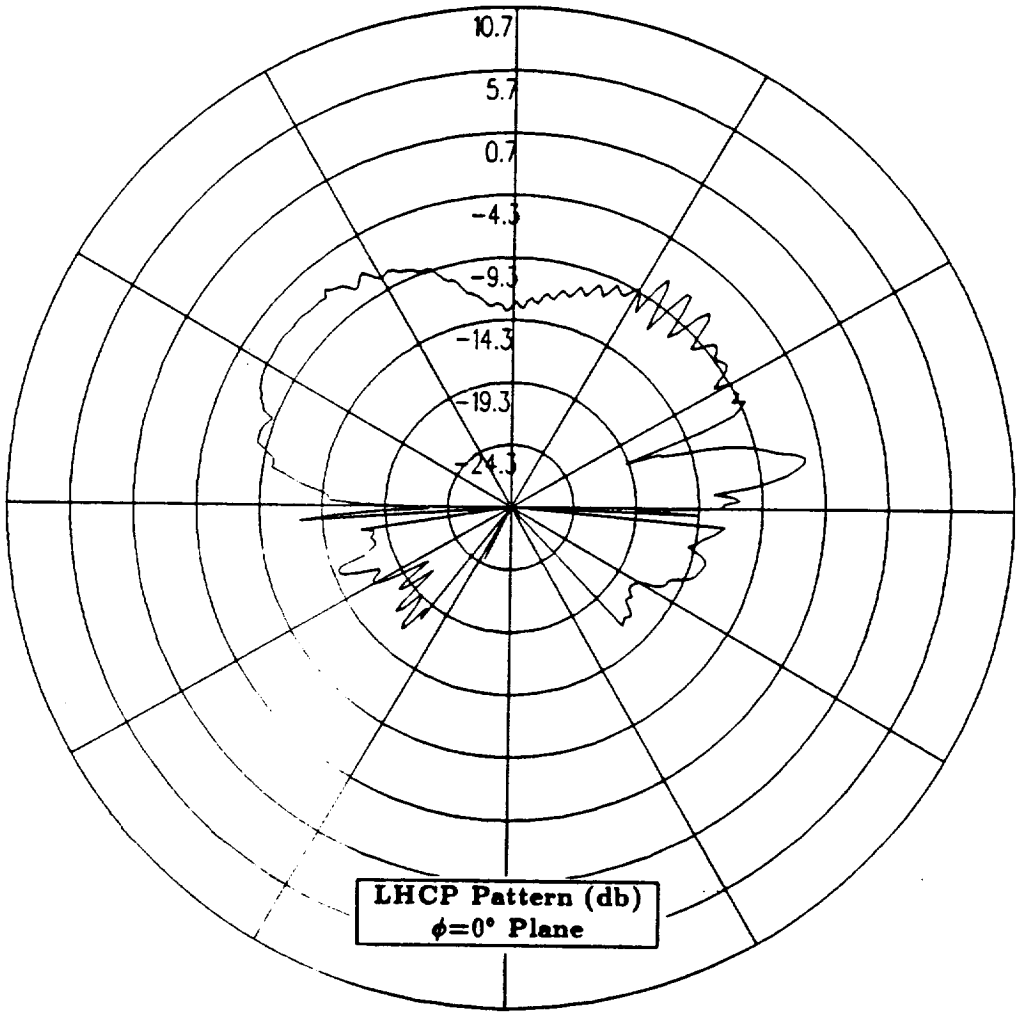

Figure 74: NEC-BSC calculated elevation plane pattern for antenna location on the port side of the fuselage above the wing and 38.7° down from the top center-line for left hand circular polarization at 300 MHz. (Test Location 6)

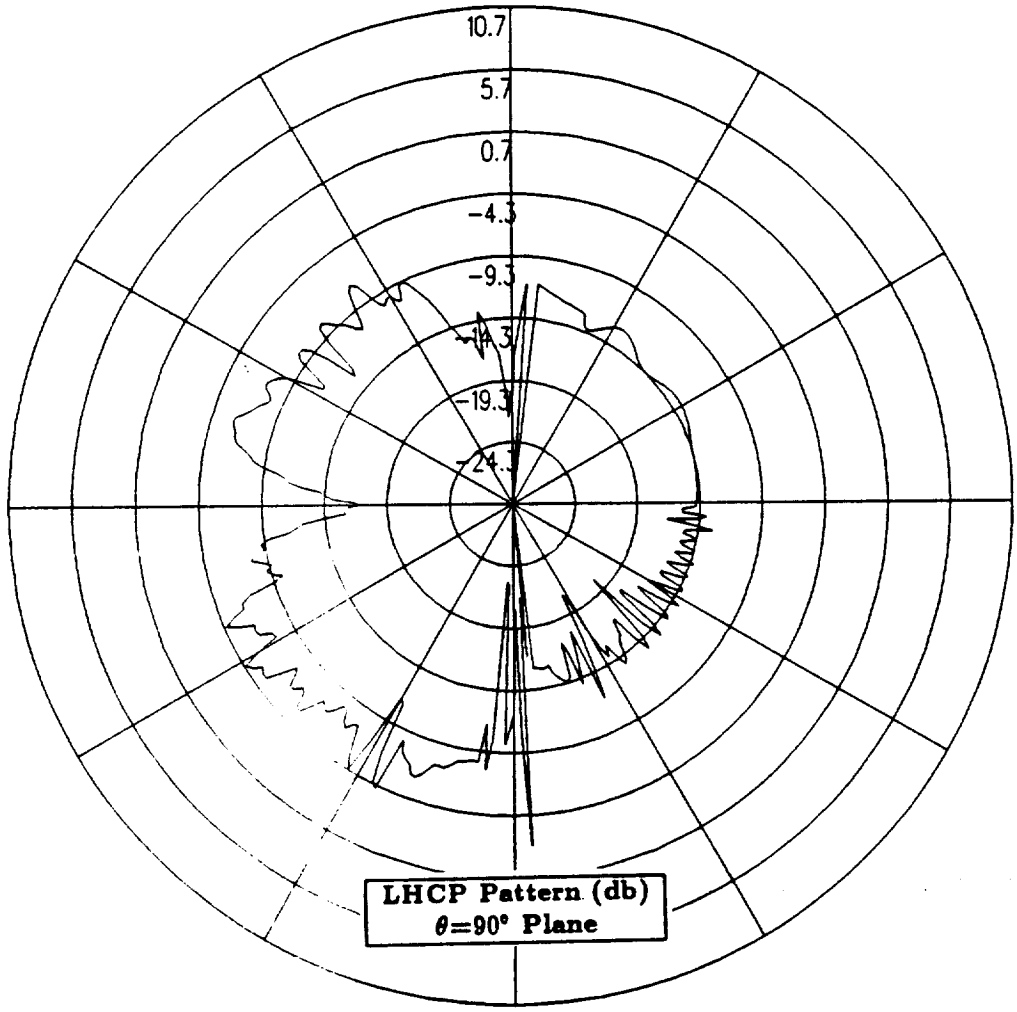

Figure 75: NEC-BSC calculated azimuth plane pattern for antenna location on the port side of the fuselage above the wing and 38.7° down from the top center-line for left hand circular polarization at 300 MHz. (Test Location 6)

C-2

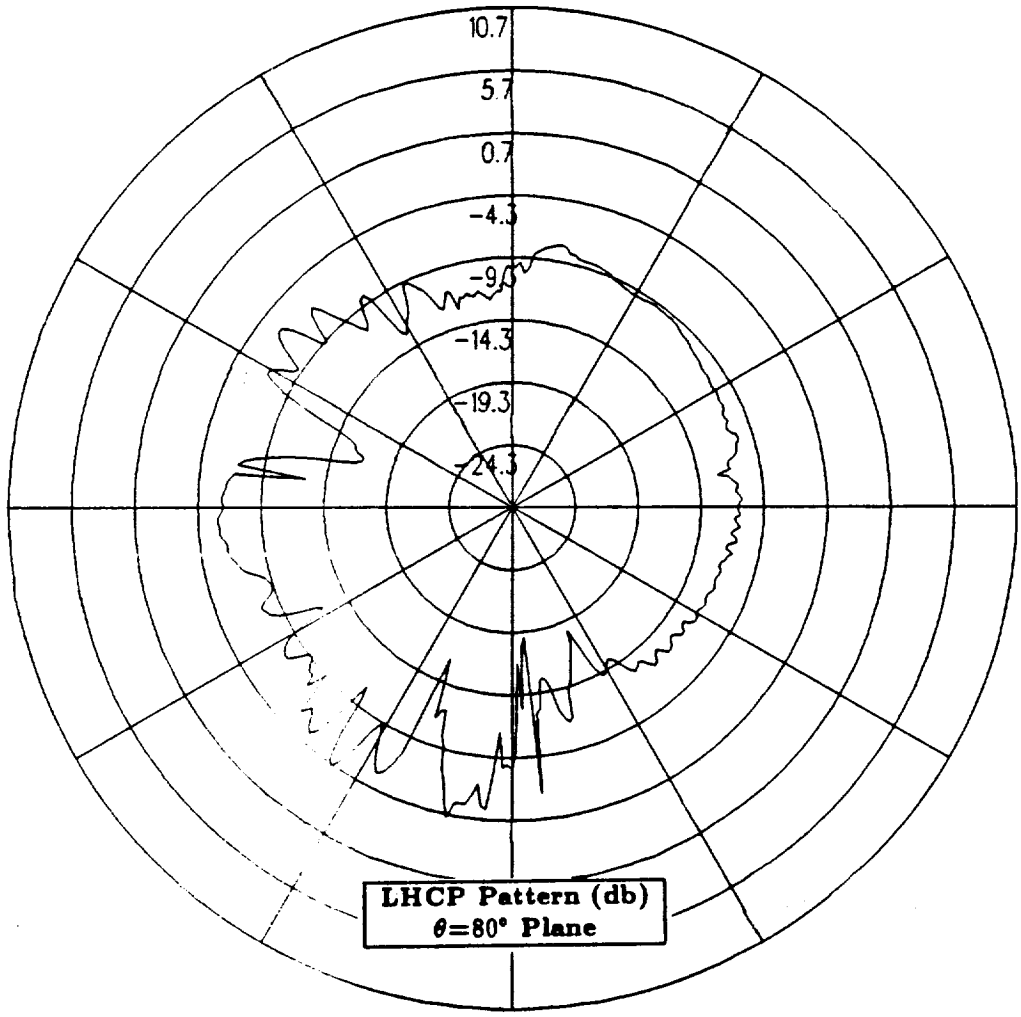

Figure 76: NEC-BSC calculated conical plane pattern 10° above the horizon for antenna location on the port side of the fuselage above the wing and 38.7° down from the top center-line for left hand circular polarization at 300 MHz. (Test Location 6)

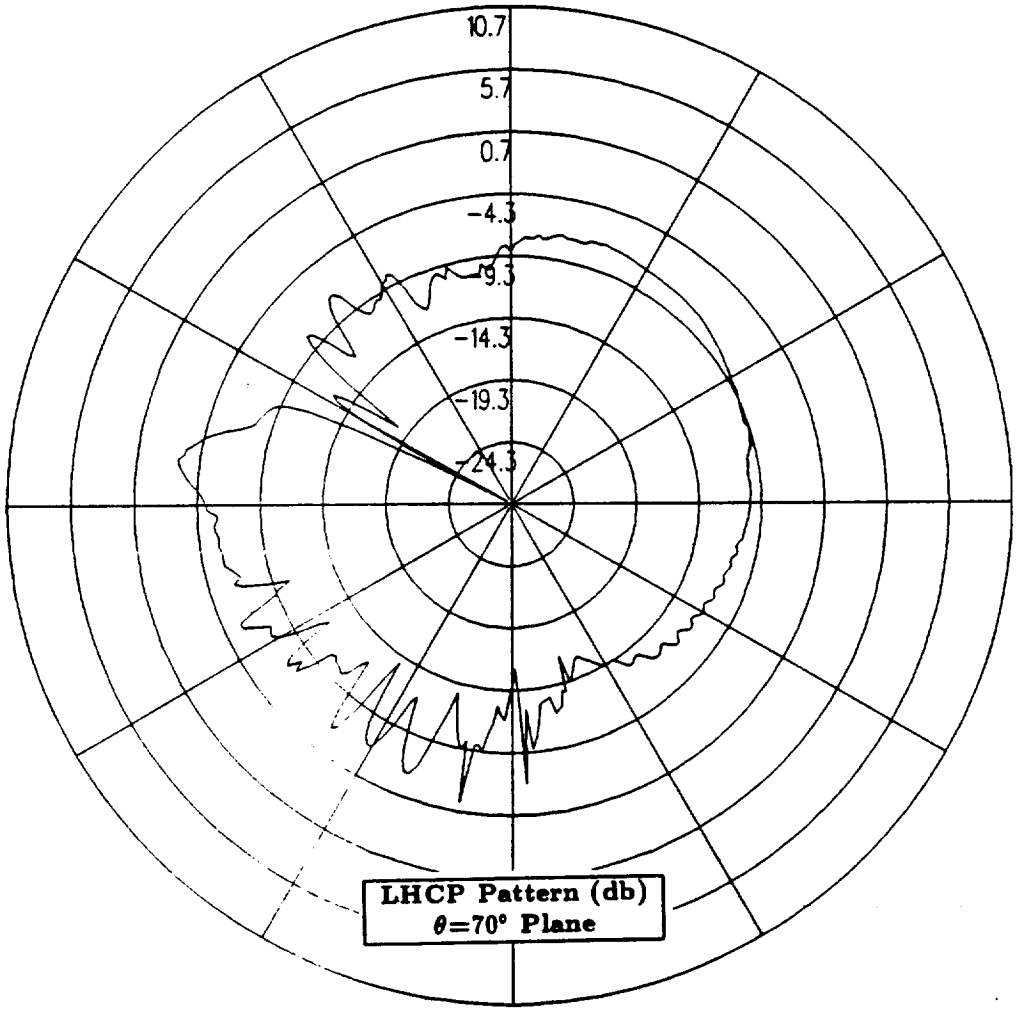

Figure 77: NEC-BSC calculated conical plane pattern 20° above the horizon for antenna location on the port side of the fuselage above the wing and 38.7° down from the top center-line for left hand circular polarization at 300 MHz. (Test Location 6)

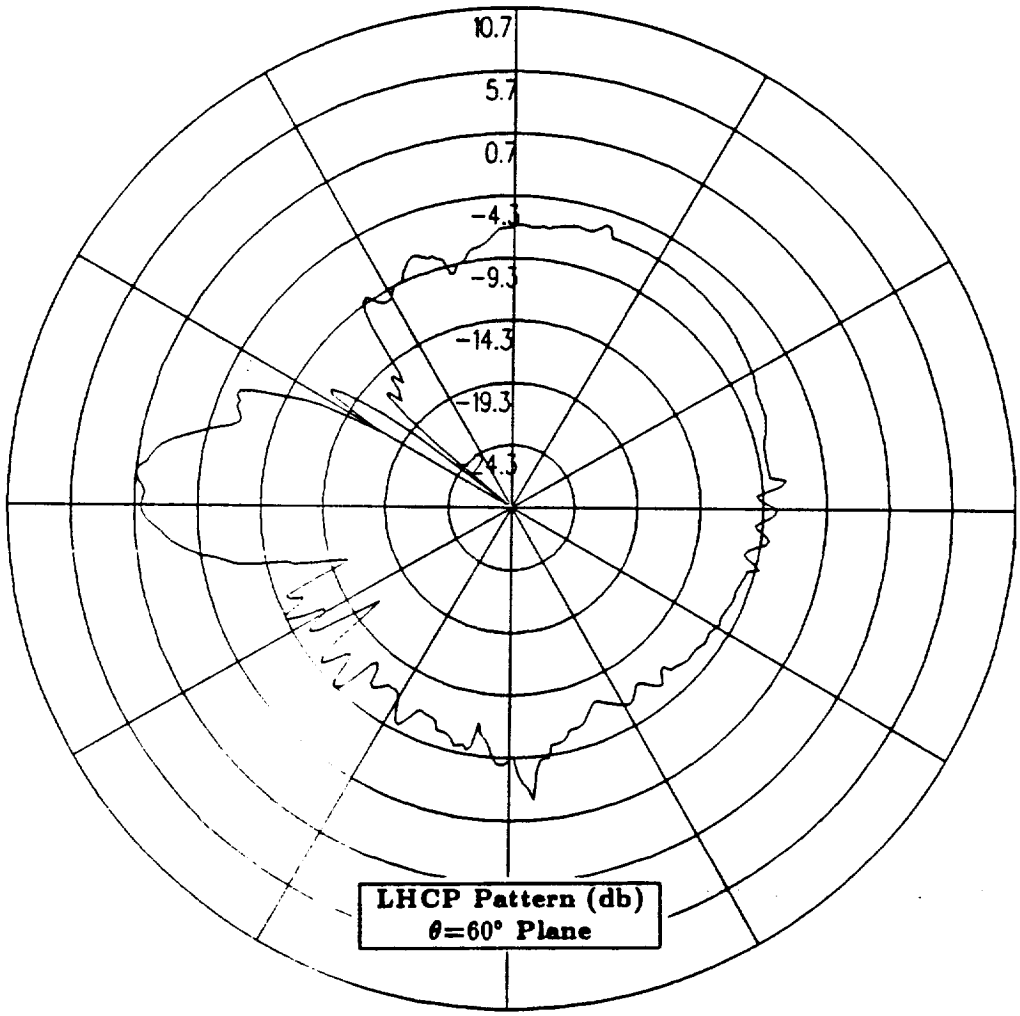

Figure 78: NEC-BSC calculated conical plane pattern 30° above the horizon for antenna location on the port side of the fuselage above the wing and 38.7° down from the top center-line for left hand circular polarization at 300 MHz. (Test Location 6)

1.8 Test Location 7

In this section, the antenna is located on the port side of the fuselage between the nose and the wing 38.7° down from the top center-line. The cylindrical aircraft model used in the NEC-BSC is illustrated in Figure 79, which also shows the location of the antenna on the fuselage. The calculated results obtained using the improved version of the NEC-BSC at 300 MHz for the right hand circular polarized or co-polarized fields are shown for the roll plane in Figure 80, for the elevation plane in Figure 81, for the azimuth plane in Figure 82 and for the conical planes 10°, 20° and 30° above the horizon in Figures 83, 84 and 85, respectively. For completeness, the left hand circular polarized or cross-polarized results are also included. These cross-polarized results are shown for the roll plane in Figure 86, for the elevation plane in Figure 87, for the azimuth plane in Figure 88 and for the conical planes 10°, 20° and 30° above the horizon in Figures 89, 90 and 91, respectively.

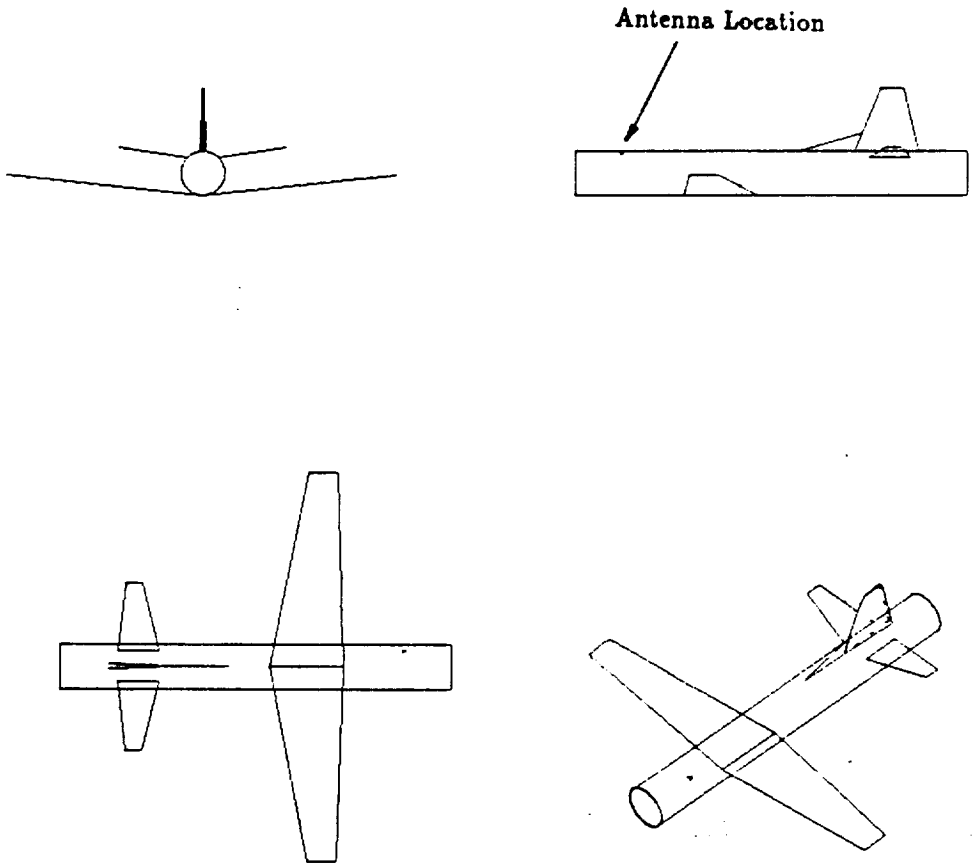

Figure 79: Geometry of the cylindrical model of the P-3C aircraft used in the NEC-BSC showing the antenna location. (Test Location 7)

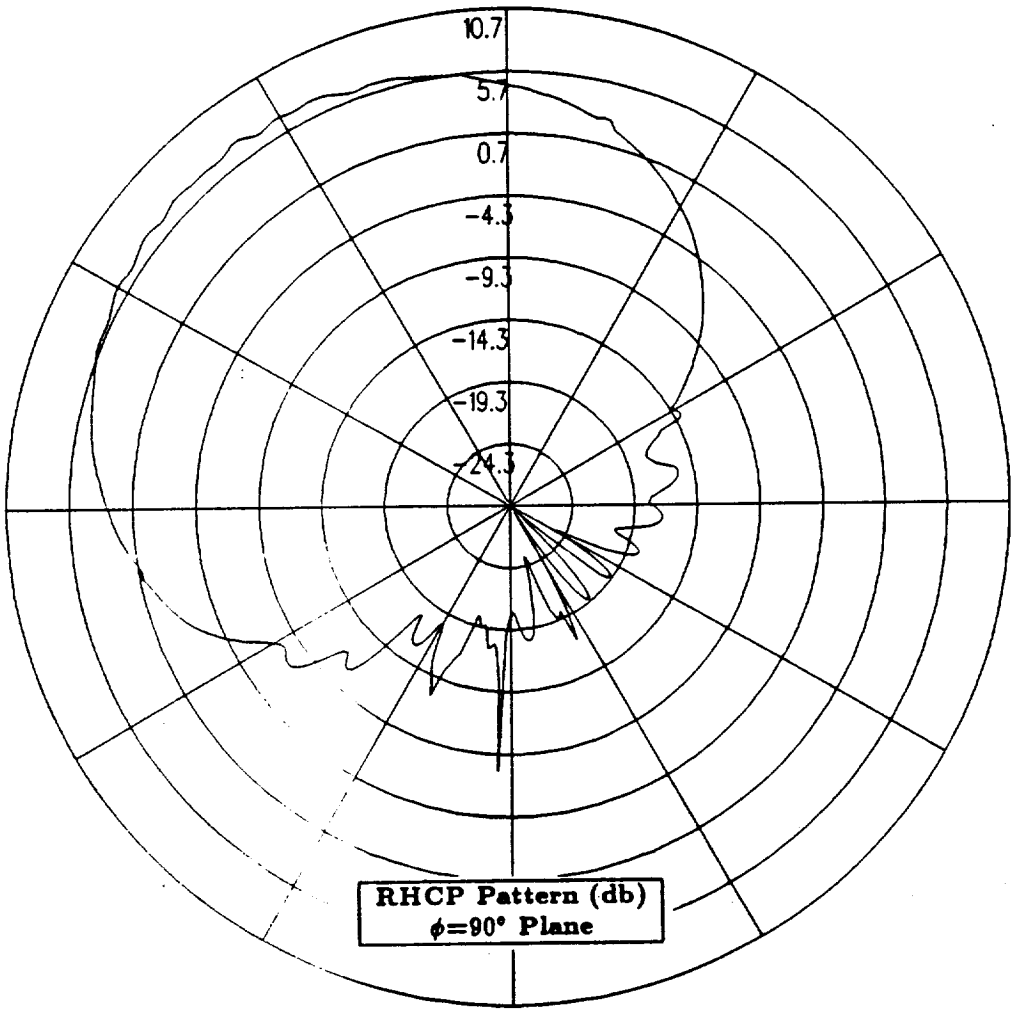

Figure 80: NEC-BSC calculated roll plane pattern for antenna location on the port side of the fuselage between the nose and the wing 38.7° down from the top center-line for right hand circular polarization at 300 MHz. (Test Location 7)

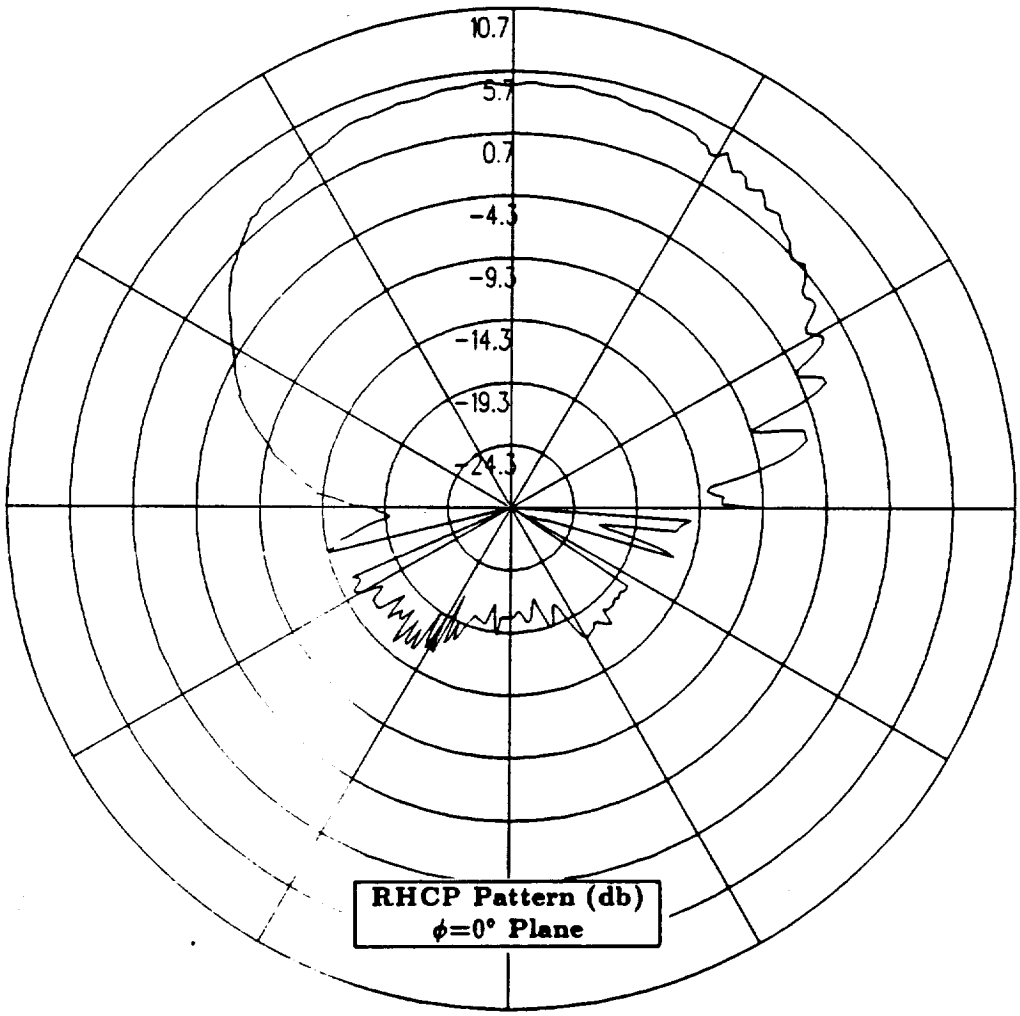

Figure 81: NEC-BSC calculated elevation plane pattern for antenna location on the port side of the fuselage between the nose and the wing 38.7° down from the top center-line for right hand circular polarization at 300 MHz. (Test Location 7)

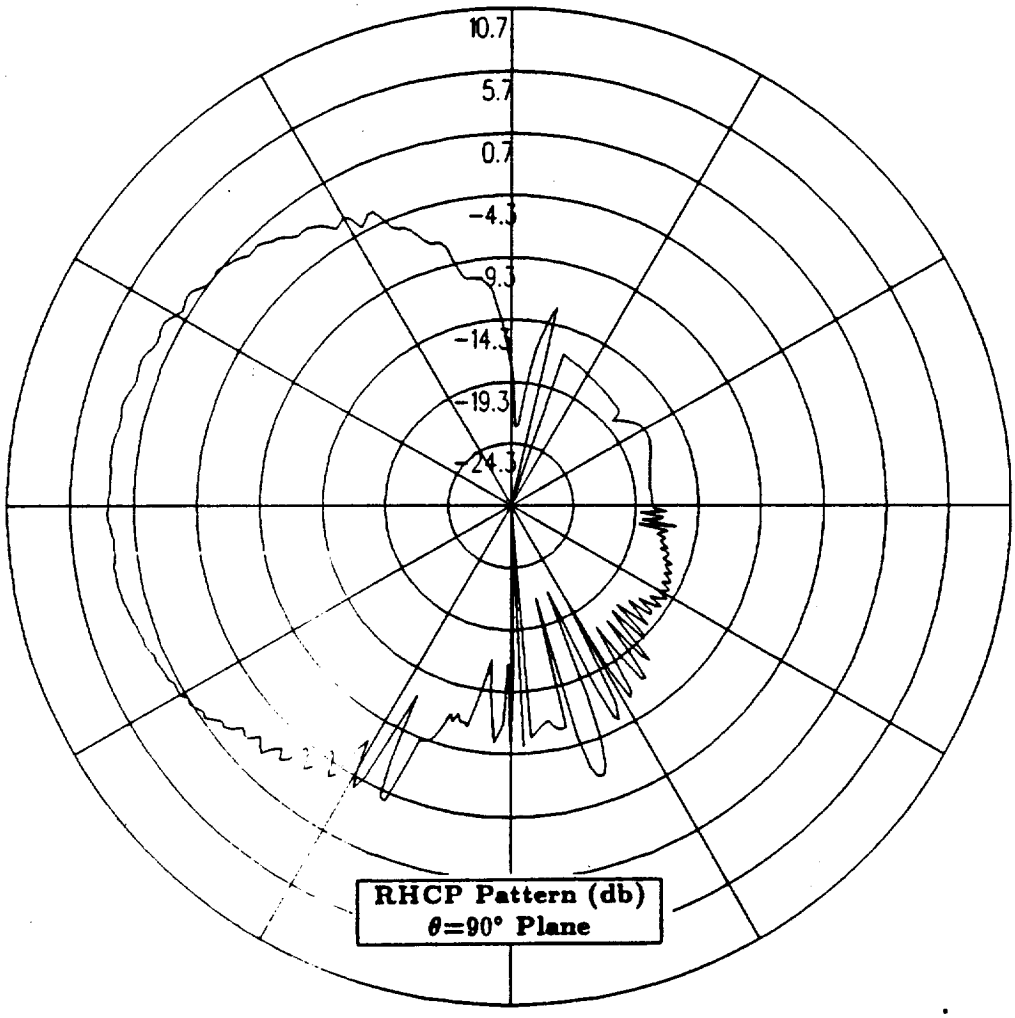

Figure 82: NEC-BSC calculated azimuth plane pattern for antenna location on the port side of the fuselage between the nose and the wing 38.7° down from the top center-line for right hand circular polarization at 300 MHz. (Test Location 7)

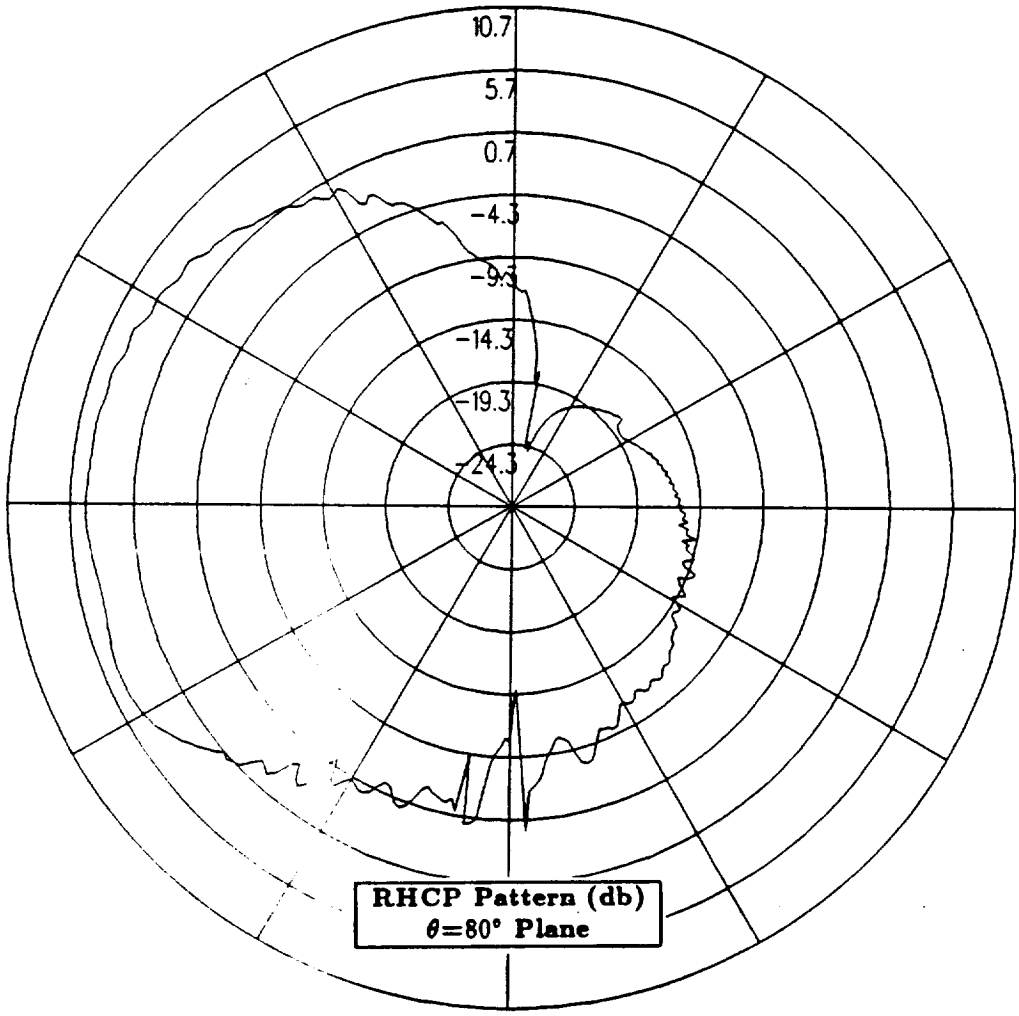

Figure 83: NEC-BSC calculated conical plane pattern 10° above the horizon for antenna location on the port side of the fuselage between the nose and the wing 38.7° down from the top center-line for right hand circular polarization at 300 MHz. (Test Location 7)

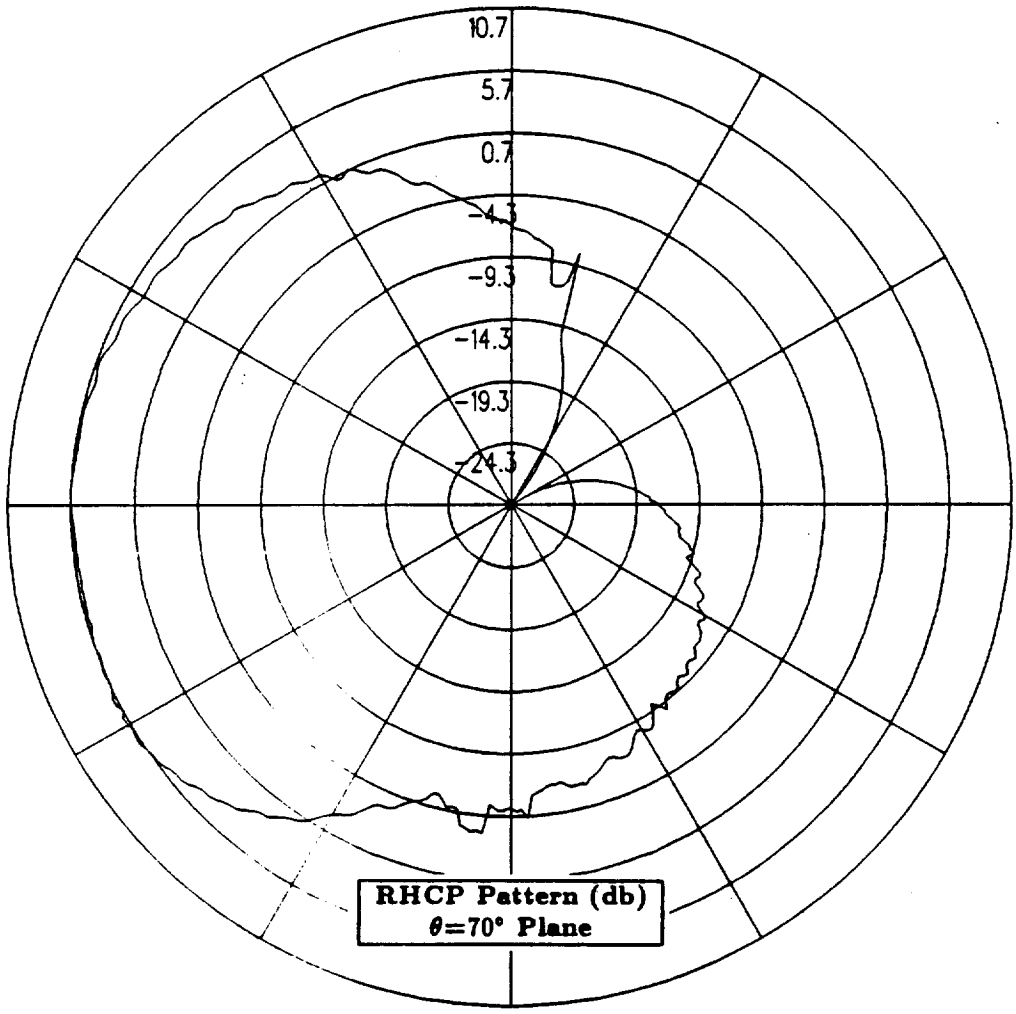

Figure 84: NEC-BSC calculated conical plane pattern 20° above the horizon for antenna location on the port side of the fuselage between the nose and the wing 38.7° down from the top center-line for right hand circular polarization at 300 MHz. (Test Location 7)

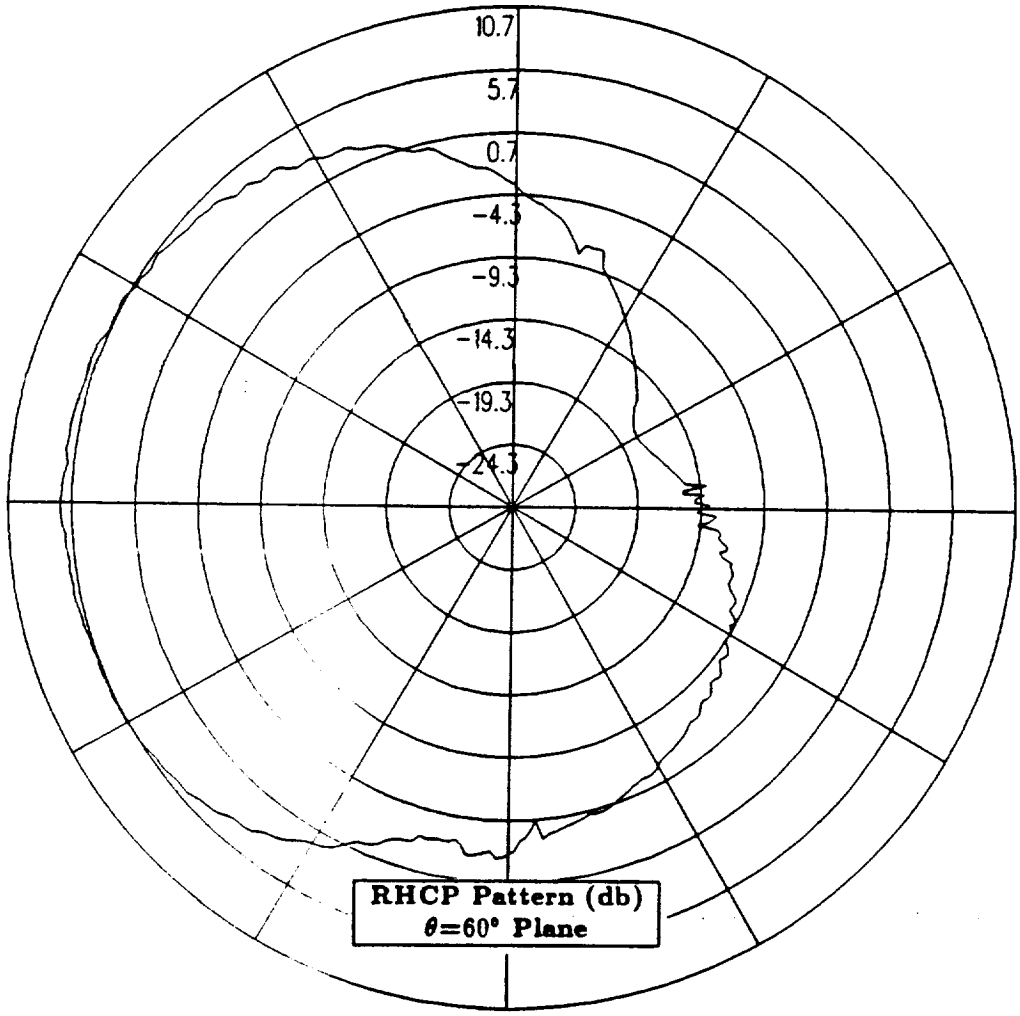

Figure 85: NEC-BSC calculated conical plane pattern 30° above the horizon for antenna location on the port side of the fuselage between the nose and the wing 38.7° down from the top center-line for right hand circular polarization at 300 MHz. (Test Location 7)

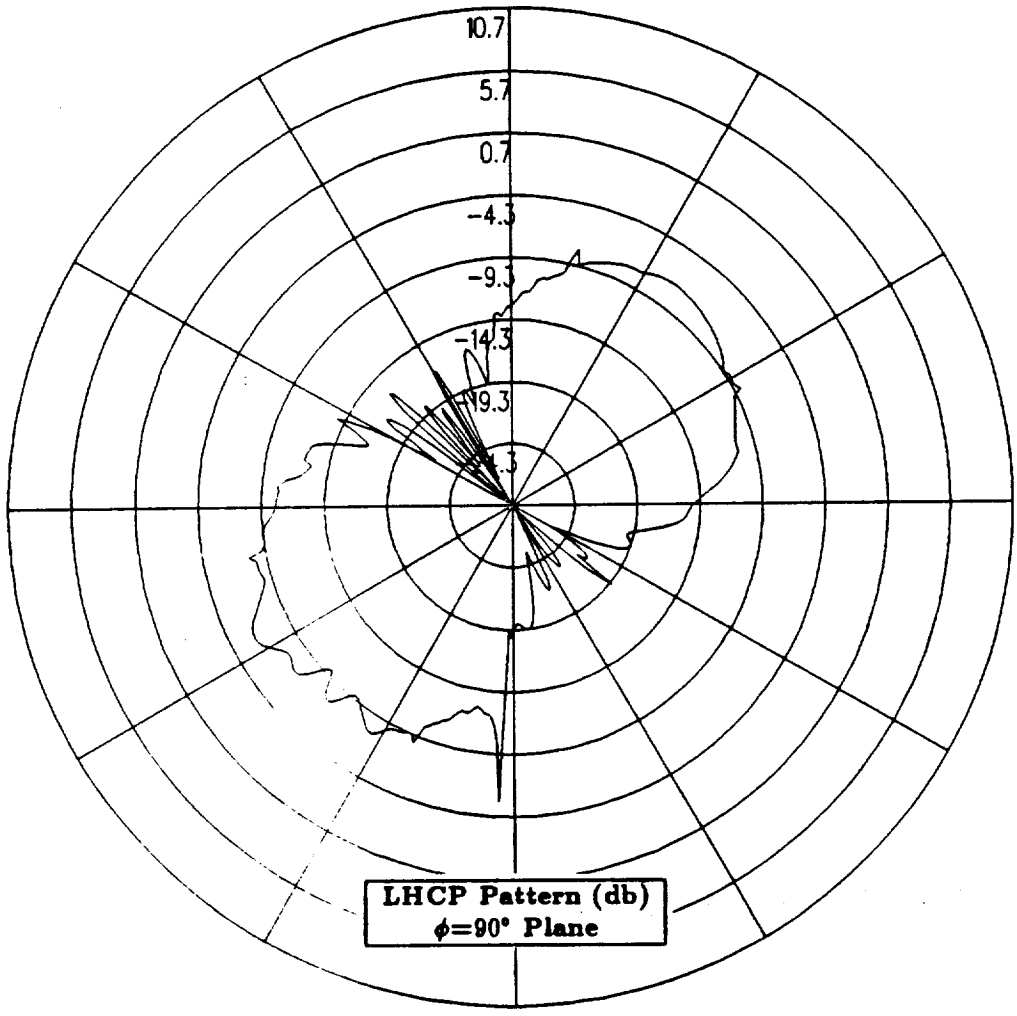

Figure 86: NEC-BSC calculated roll plane pattern for antenna location on the port side of the fuselage between the nose and the wing 38.7° down from the top center-line for left hand circular polarization at 300 MHz. (Test Location 7)

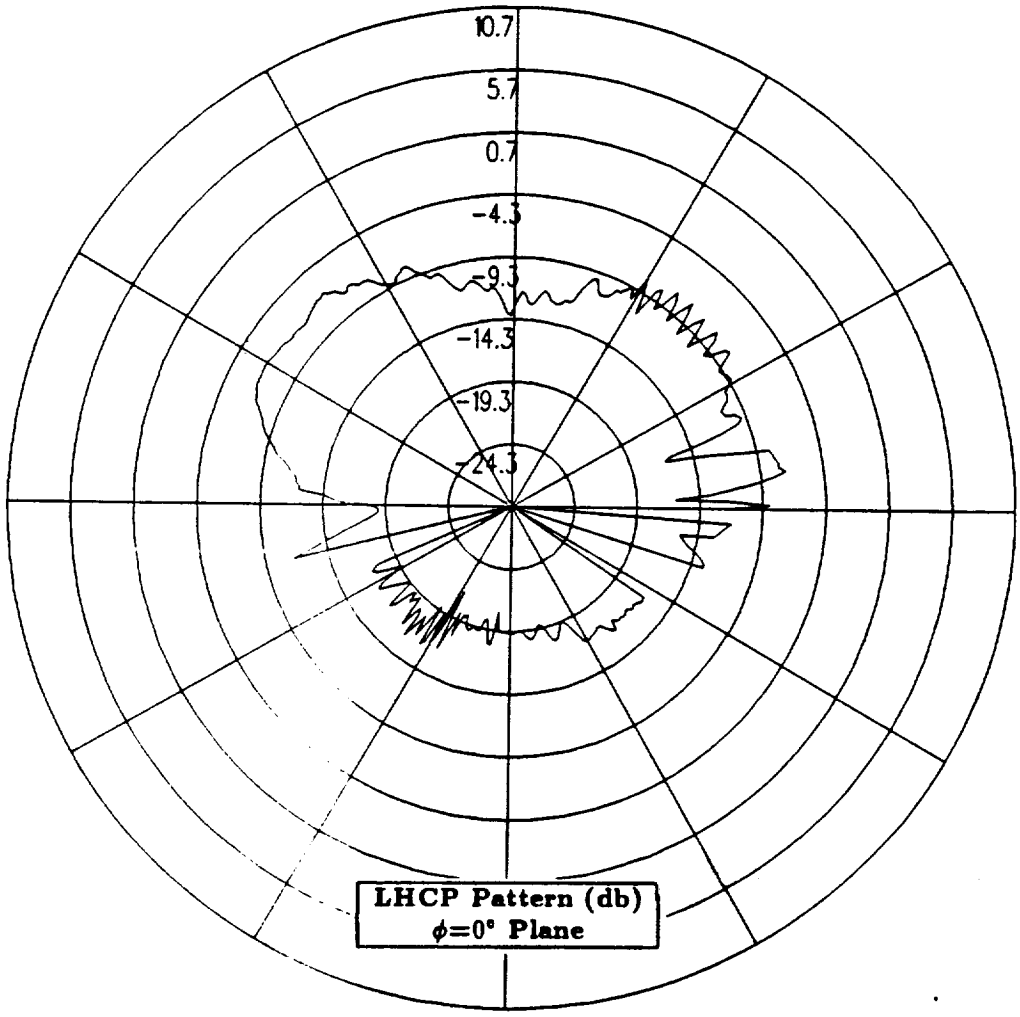

Figure 87: NEC-BSC calculated elevation plane pattern for antenna location on the port side of the fuselage between the nose and the wing 38.7° down from the top center-line for left hand circular polarization at 300 MHz. (Test Location 7)

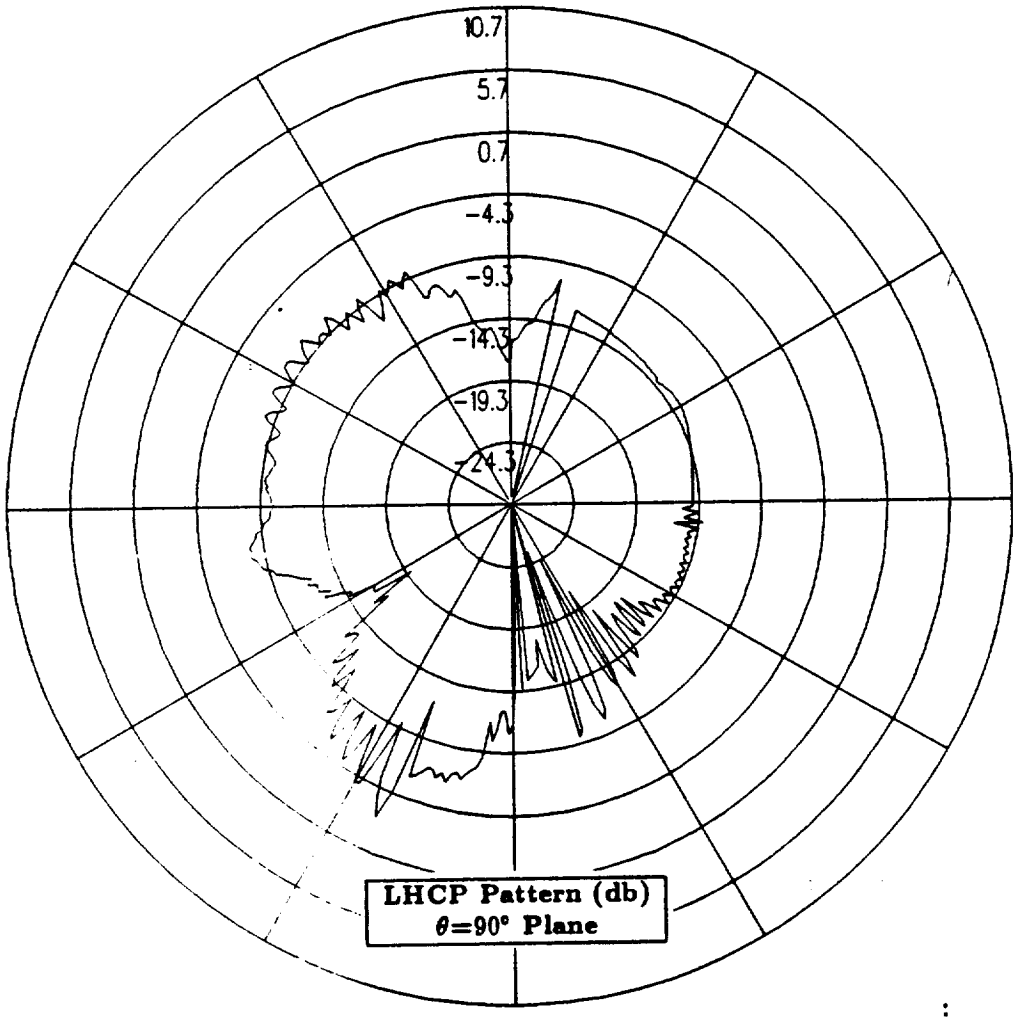

Figure 88: NEC-BSC calculated azimuth plane pattern for antenna location on the port side of the fuselage between the nose and the wing 38.7° down from the top center-line for left hand circular polarization at 300 MHz. (Test Location 7)

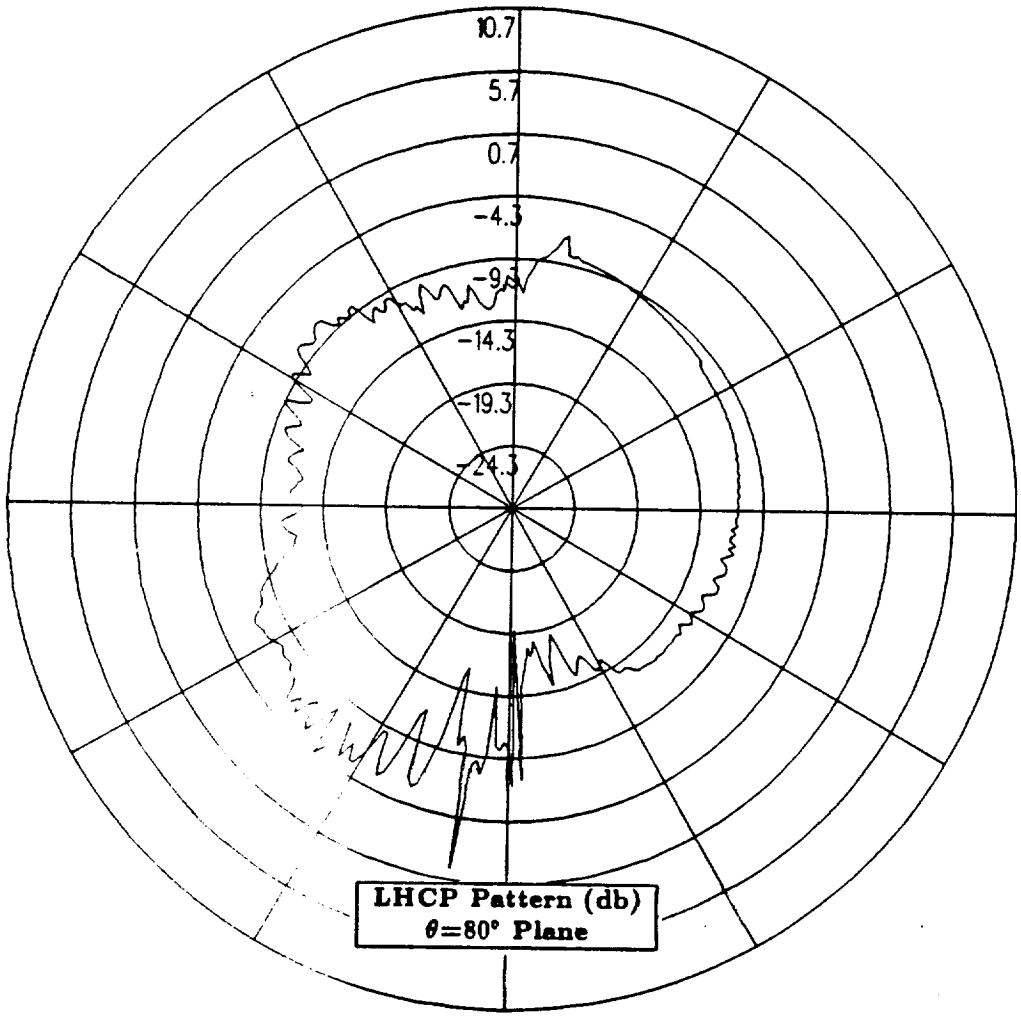

Figure 89: NEC-BSC calculated conical plane pattern 10° above the horizon for antenna location on the port side of the fuselage between the nose and the wing 38.7° down from the top center-line for left hand circular polarization at 300 MHz. (Test Location 7)

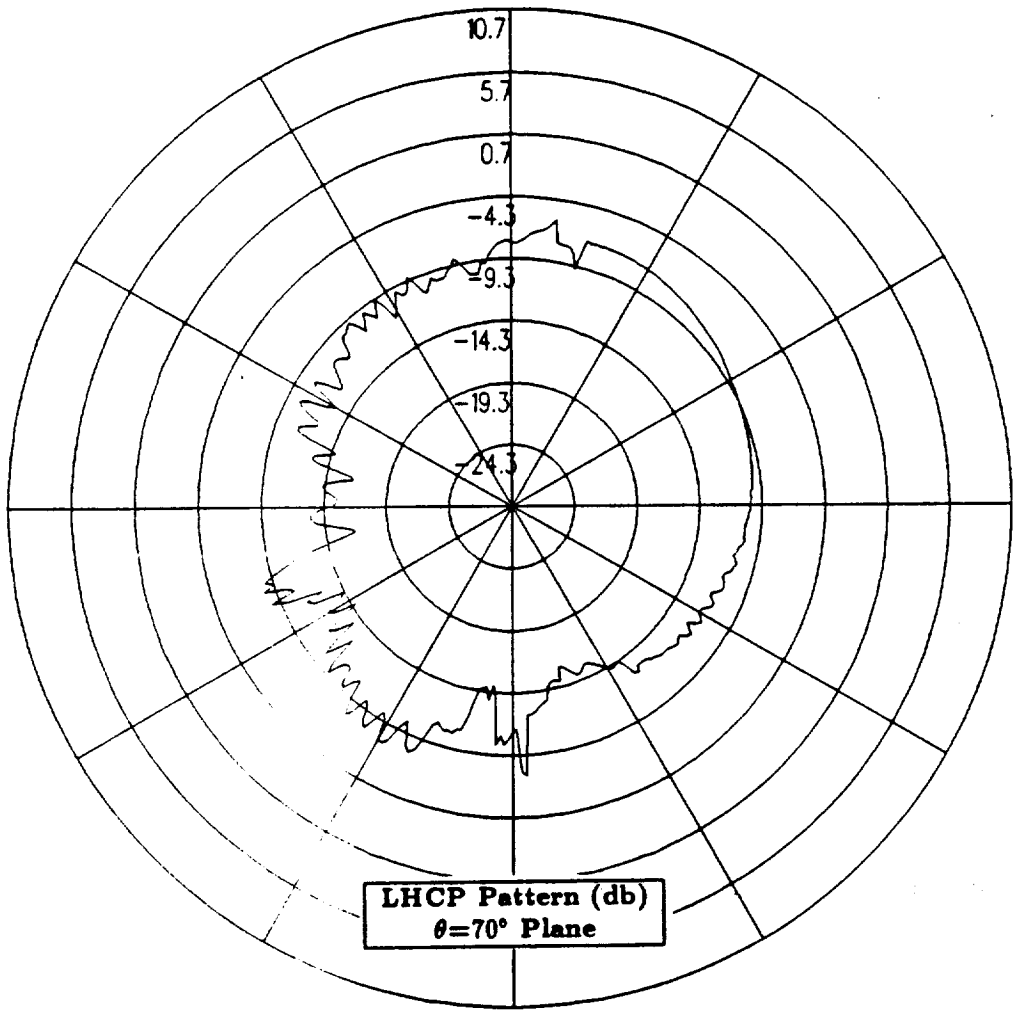

Figure 90: NEC-BSC calculated conical plane pattern 20° above the horizon for antenna location on the port side of the fuselage between the nose and the wing 38.7° down from the top center-line for left hand circular polarization at 300 MHz. (Test Location 7)

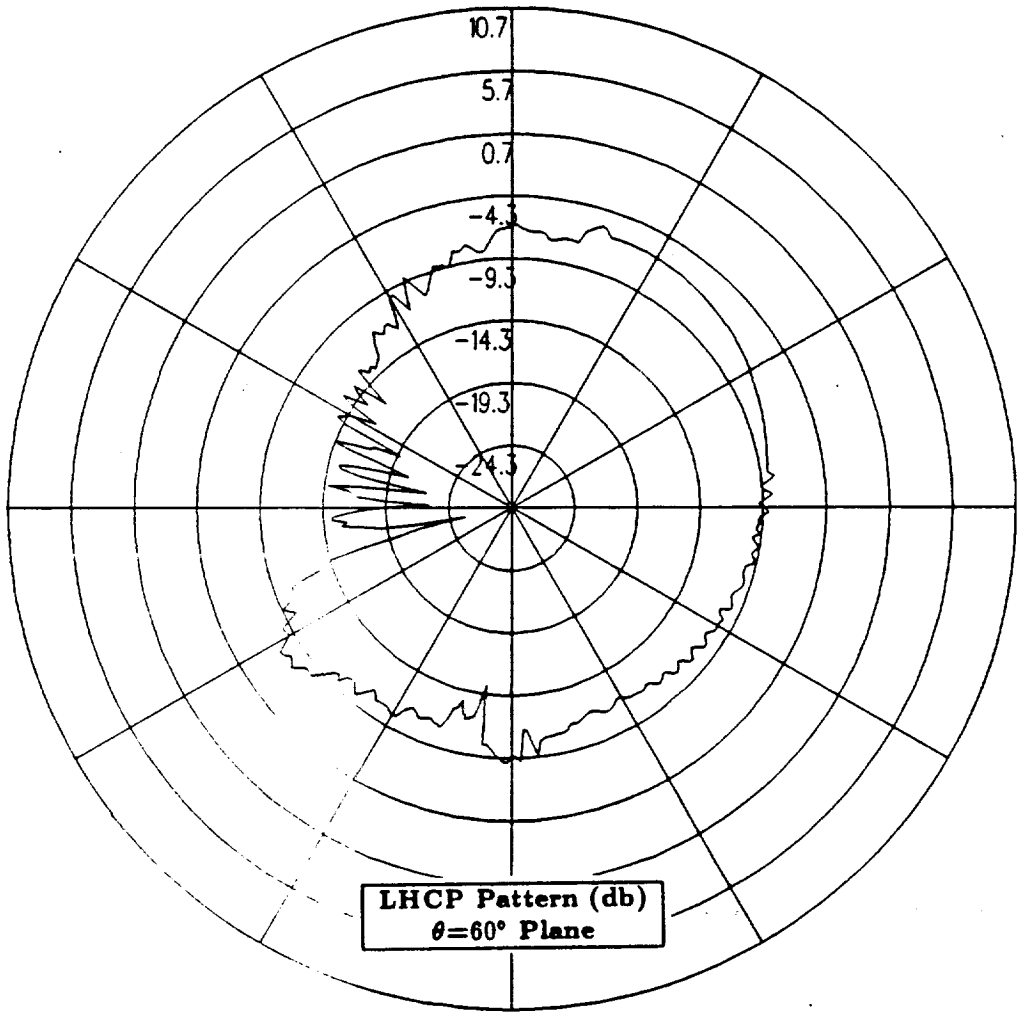

Figure 91: NEC-BSC calculated conical plane pattern 30° above the horizon for antenna location on the port side of the fuselage between the nose and the wing 38.7° down from the top center-line for left hand circular polarization at 300 MHz. (Test Location 7)

1.9 Test Location 8

In this section, the antenna is located on the port side of the vertical stabilizer. The cylindrical aircraft model used in the NEC-BSC is illustrated in Figure 92, which also shows the location of the antenna on the fuselage. The calculated results obtained using the improved version of the NEC-BSC at 300 MHz for the right hand circular polarized or co-polarized fields are shown for the roll plane in Figure 93, for the elevation plane in Figure 94, for the azimuth plane in Figure 95 and for the conical planes 10°, 20° and 30° above the horizon in Figures 96, 97 and 98, respectively. For completeness, the left hand circular polarized or cross-polarized results are also included. These cross-polarized results are shown for the roll plane in Figure 99, for the elevation plane in Figure 100, for the azimuth plane in Figure 101 and for the conical planes 10°, 20° and 30° above the horizon in Figures 102, 103 and 104, respectively.

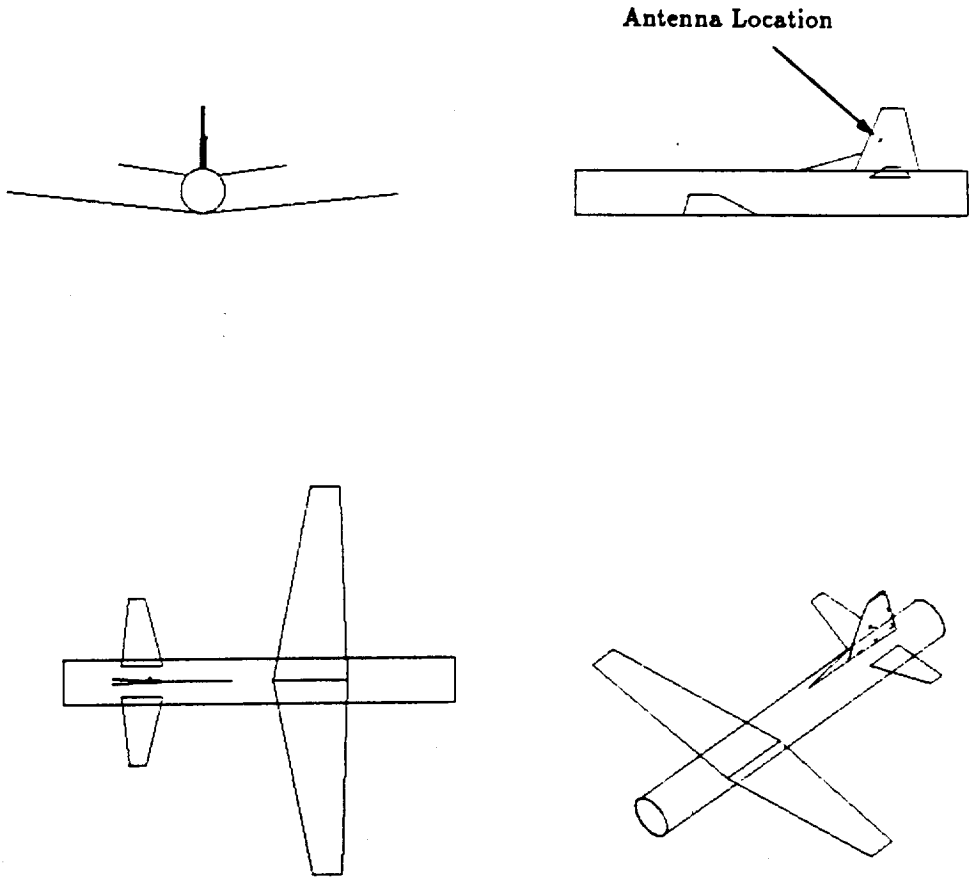

Figure 92: Geometry of the cylindrical model of the P-3C aircraft used in the NEC-BSC showing the antenna location. (Test Location 8)

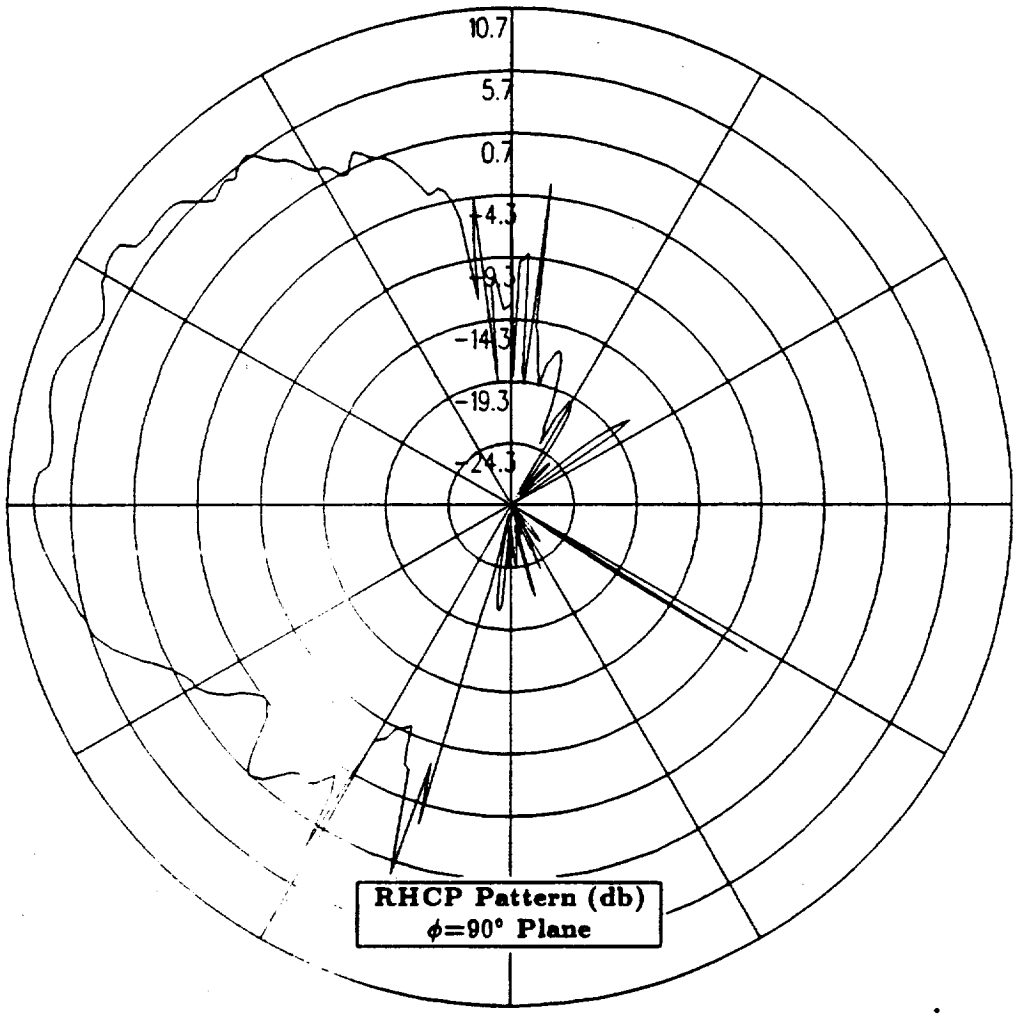

Figure 93: NEC-BSC calculated roll plane pattern for antenna location on the port side of the vertical stabilizer for right hand circular polarization at 300 MHz. (Test Location 8)

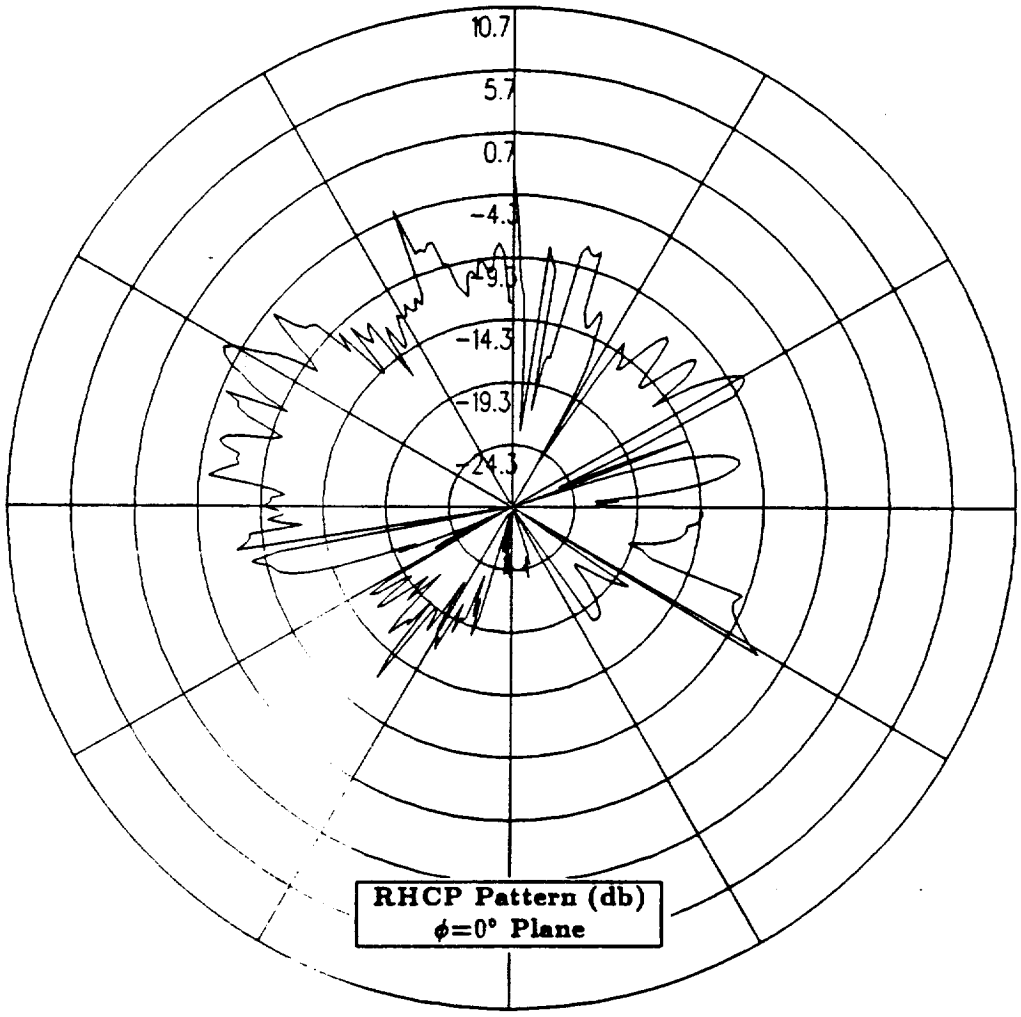

Figure 94: NEC-BSC calculated elevation plane pattern for antenna location on the port side of the vertical stabilizer for right hand circular polarization at 300 MHz. (Test Location 8)

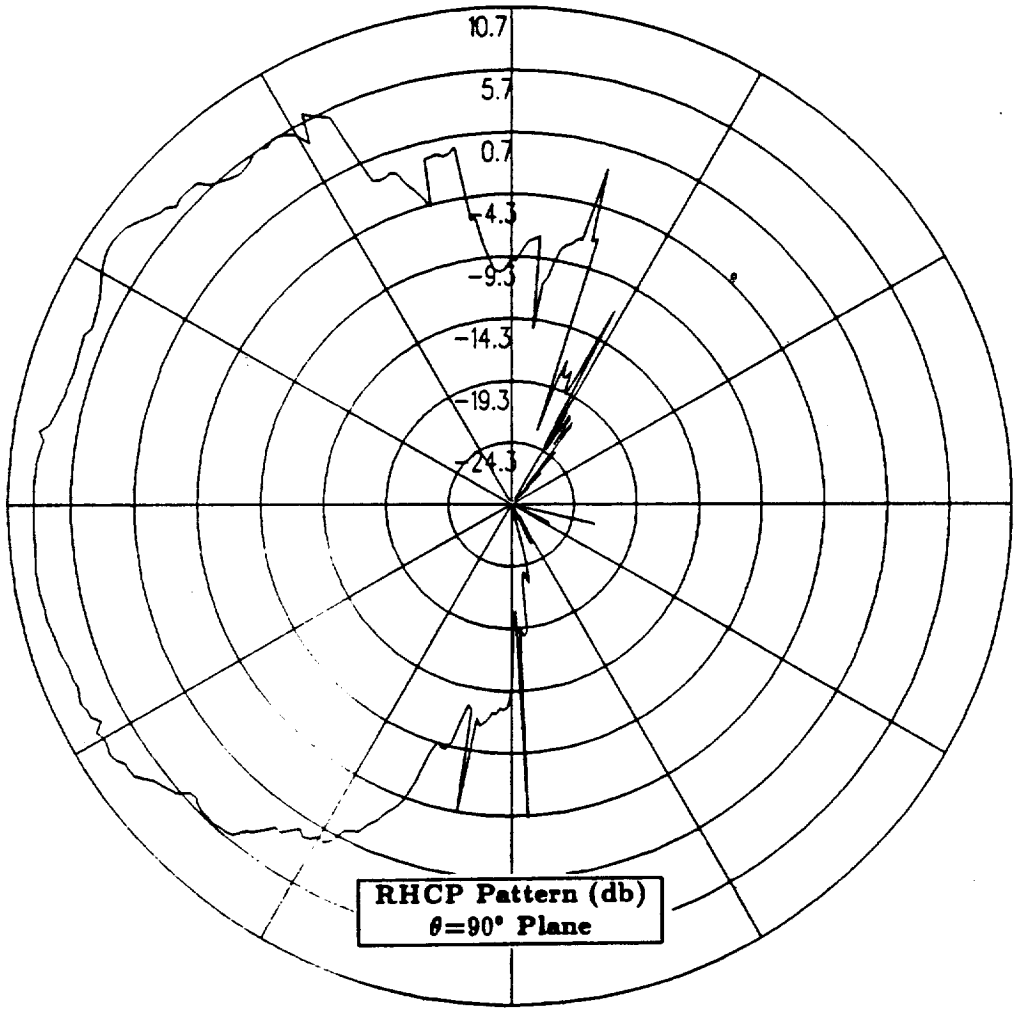

Figure 95: NEC-BSC calculated azimuth plane pattern for antenna location on the port side of the vertical stabilizer for right hand circular polarization at 300 MHz. (Test Location 8)

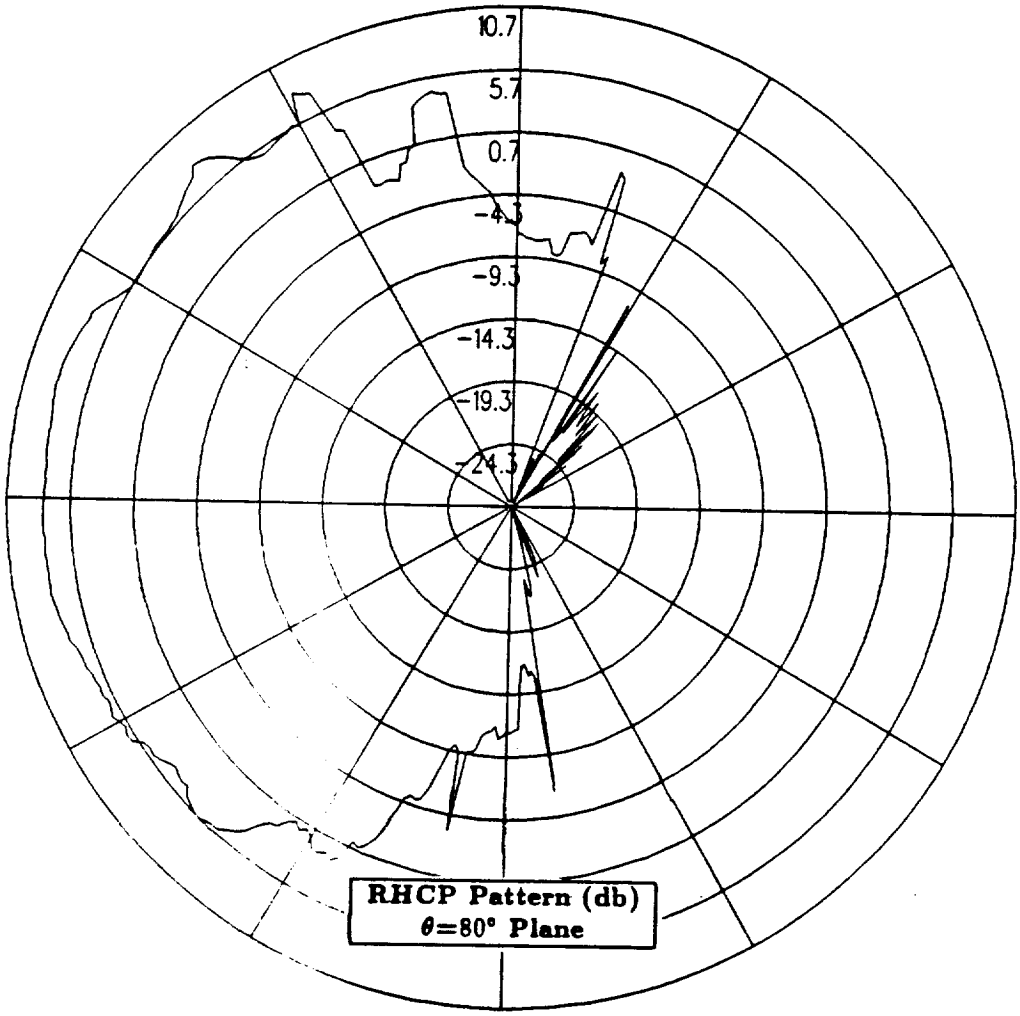

Figure 96: NEC-BSC calculated conical plane pattern 10° above the horizon for antenna location on the port side of the vertical stabilizer for right hand circular polarization at 300 MHz. (Test Location 8)

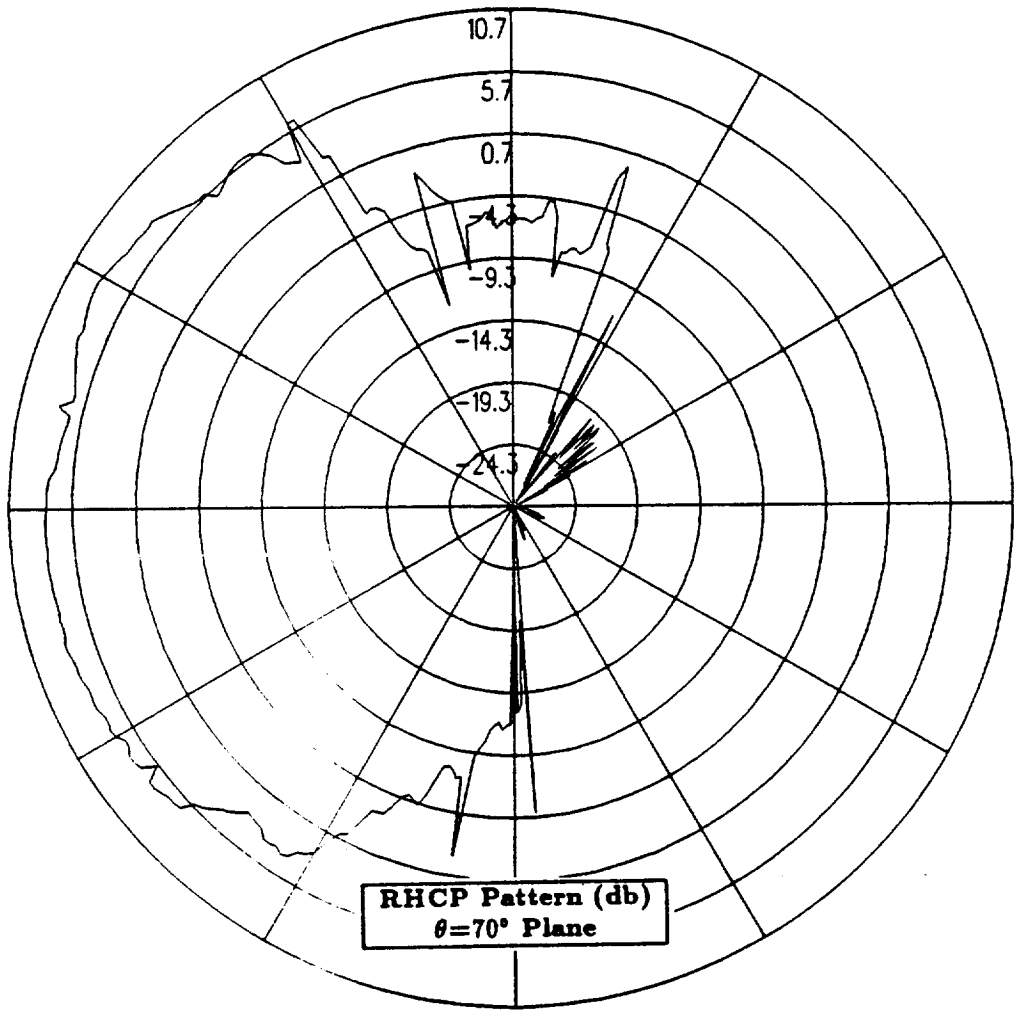

Figure 97: NEC-BSC calculated conical plane pattern 20° above the horizon for antenna location on the port side of the vertical stabilizer for right hand circular polarization at 300 MHz. (Test Location 8)

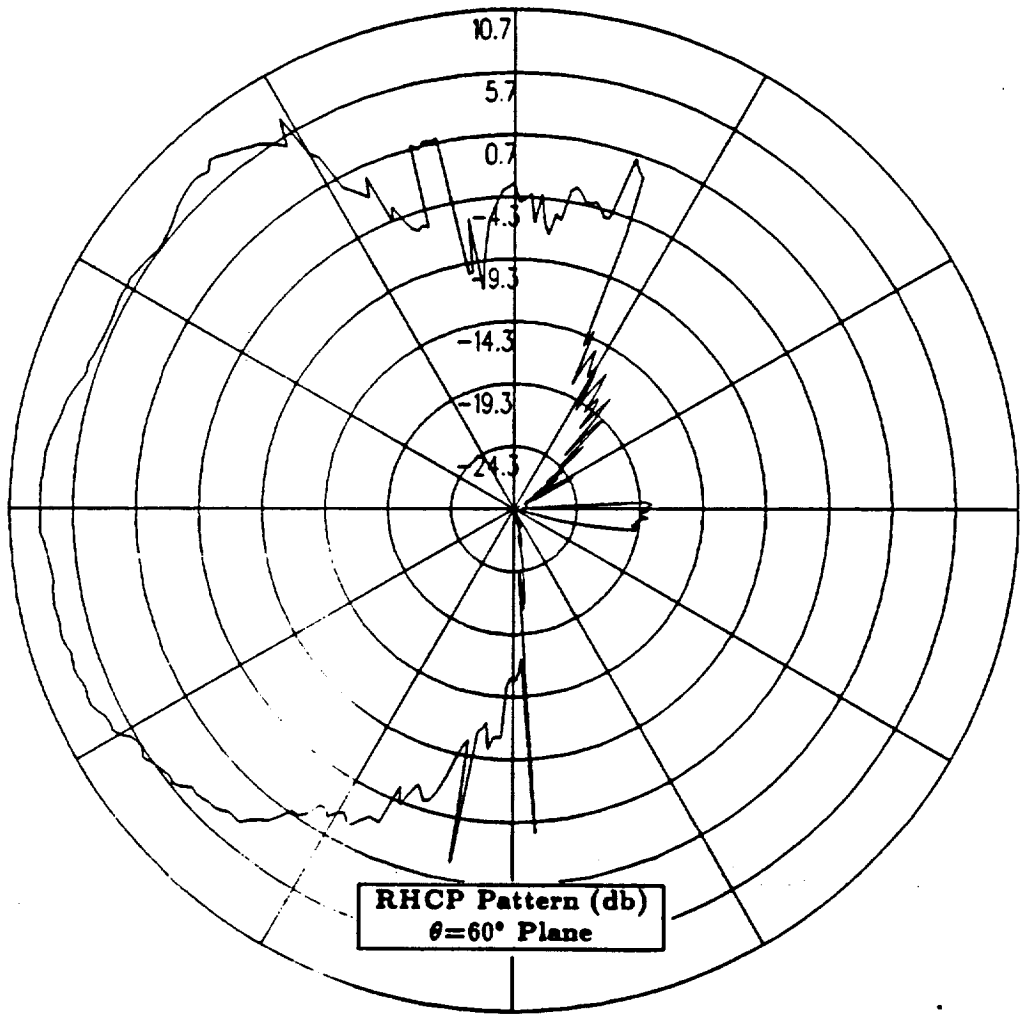

Figure 98: NEC-BSC calculated conical plane pattern 30° above the horizon for antenna location on the port side of the vertical stabilizer for right hand circular polarization at 300 MHz. (Test Location 8)

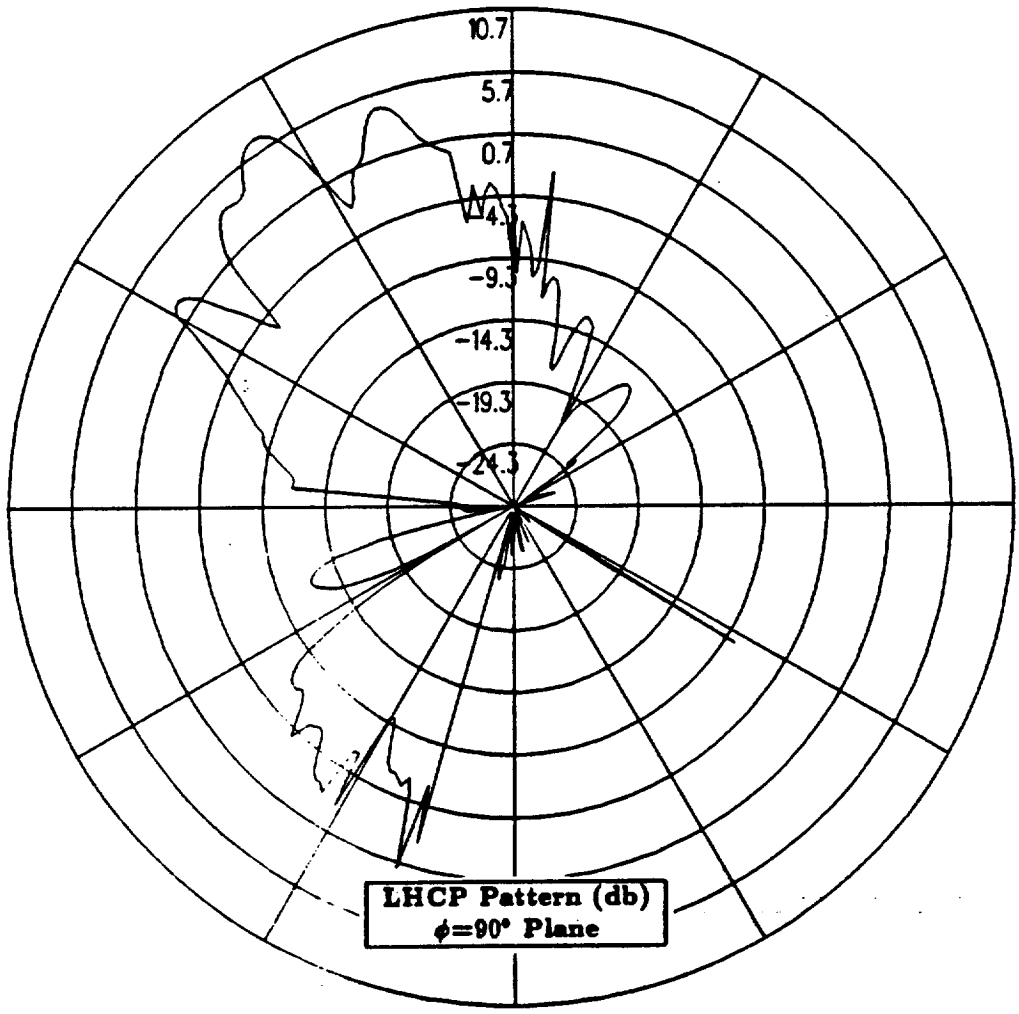

Figure 99: NEC-BSC calculated roll plane pattern for antenna location on the port side of the vertical stabilizer for left hand circular polarization at 300 MHz. (Test Location 8)

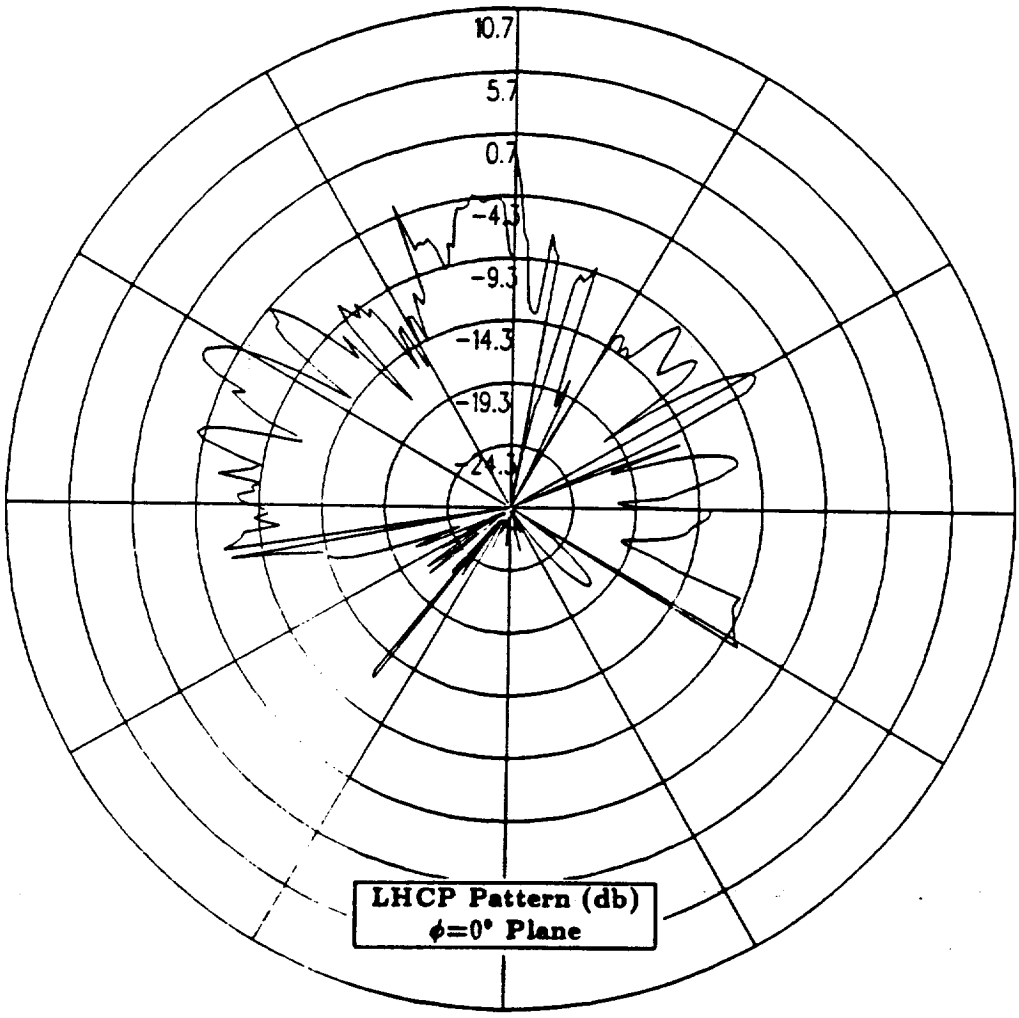

Figure 100: NEC-BSC calculated elevation plane pattern for antenna location on the port side of the vertical stabilizer for left hand circular polarization at 300 MHz. (Test Location 8)

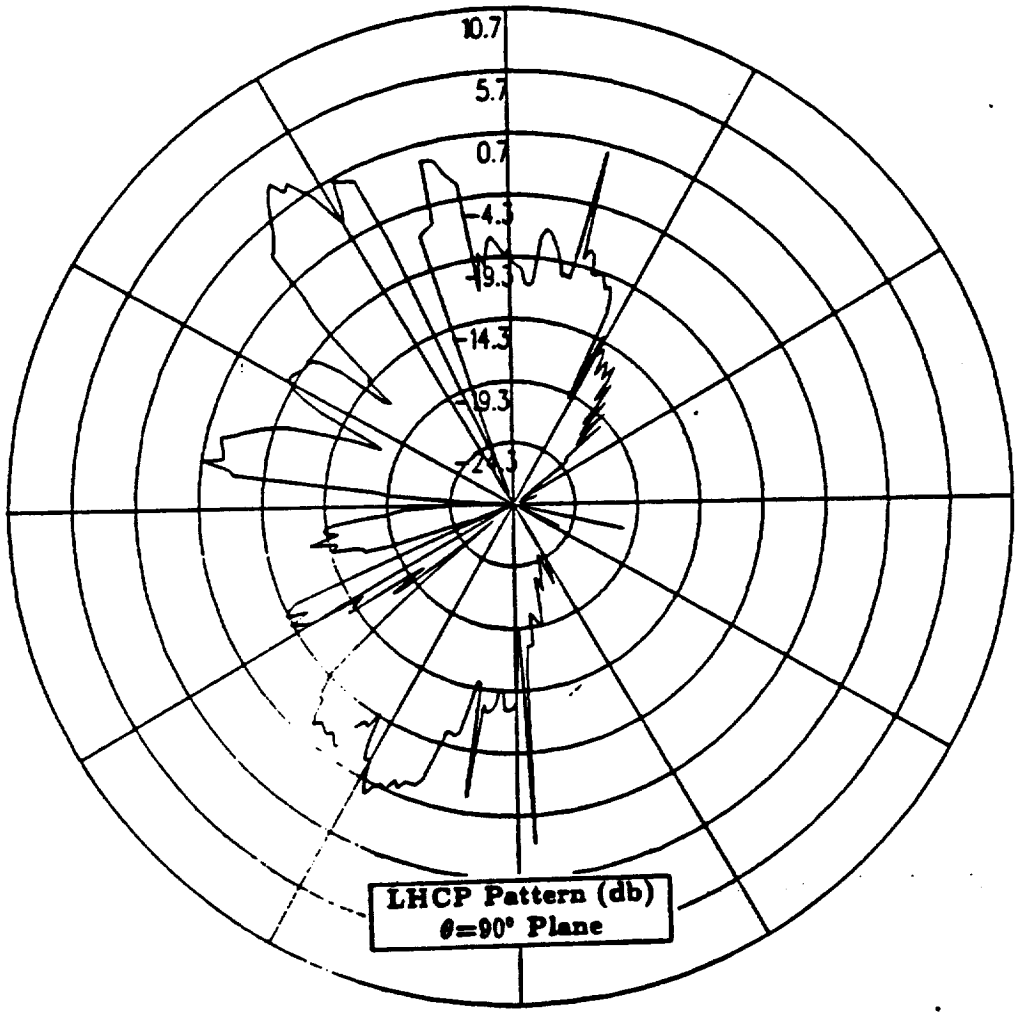

Figure 101: NEC-BSC calculated azimuth plane pattern for antenna location on the port side of the vertical stabilizer for left hand circular polarization at 300 MHz. (Test Location 8)

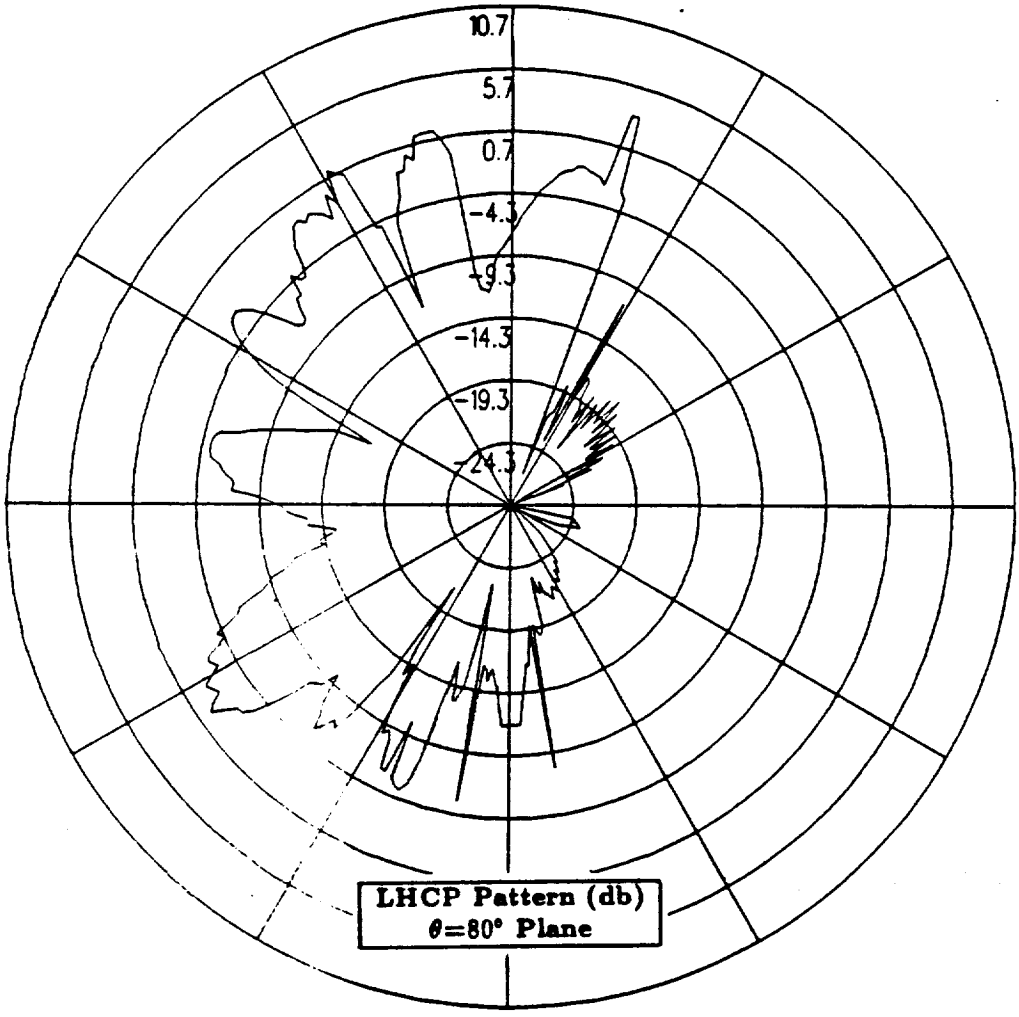

Figure 102: NEC-BSC calculated conical plane pattern 10° above the horizon for antenna location on the port side of the vertical stabilizer for left hand circular polarization at 300 MHz. (Test Location 8)

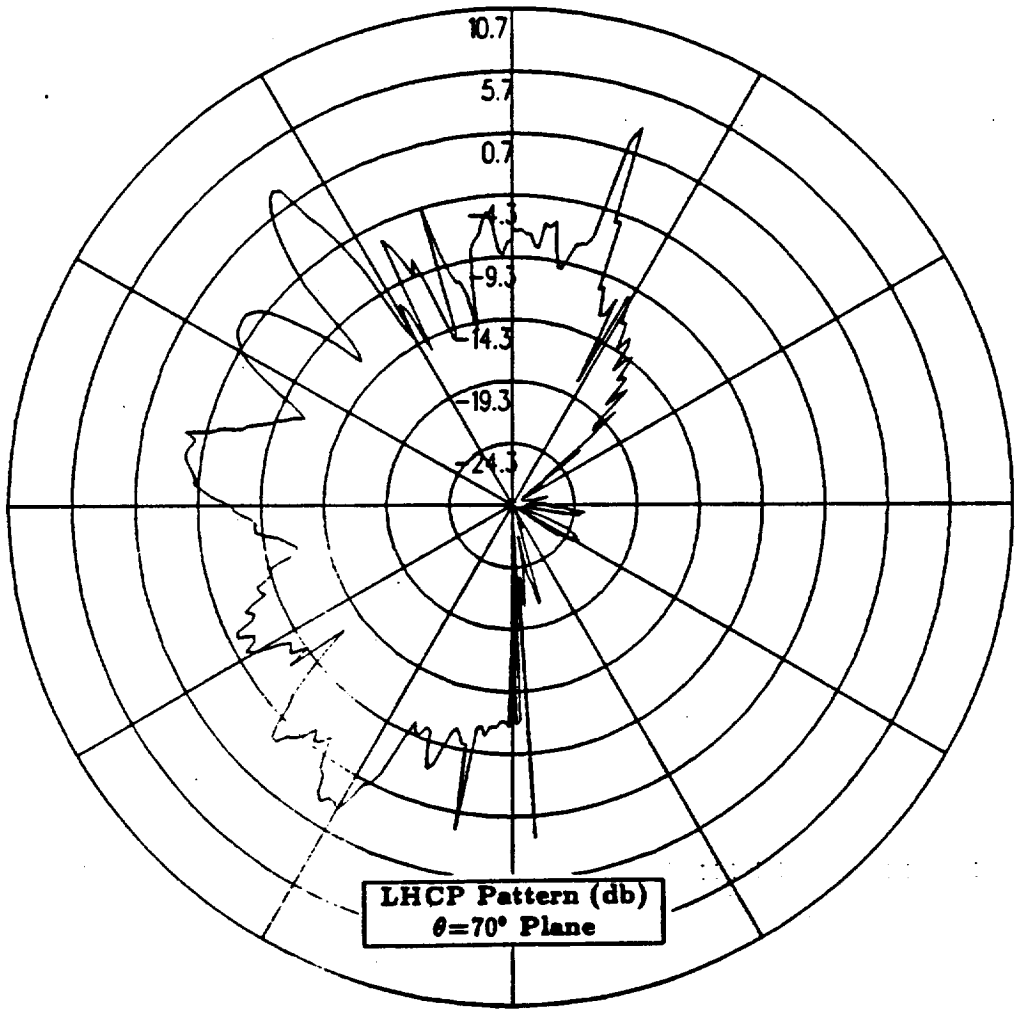

Figure 103: NEC-BSC calculated conical plane pattern 20° above the horizon for antenna location on the port side of the vertical stabilizer for left hand circular polarization at 300 MHz. (Test Location 8)

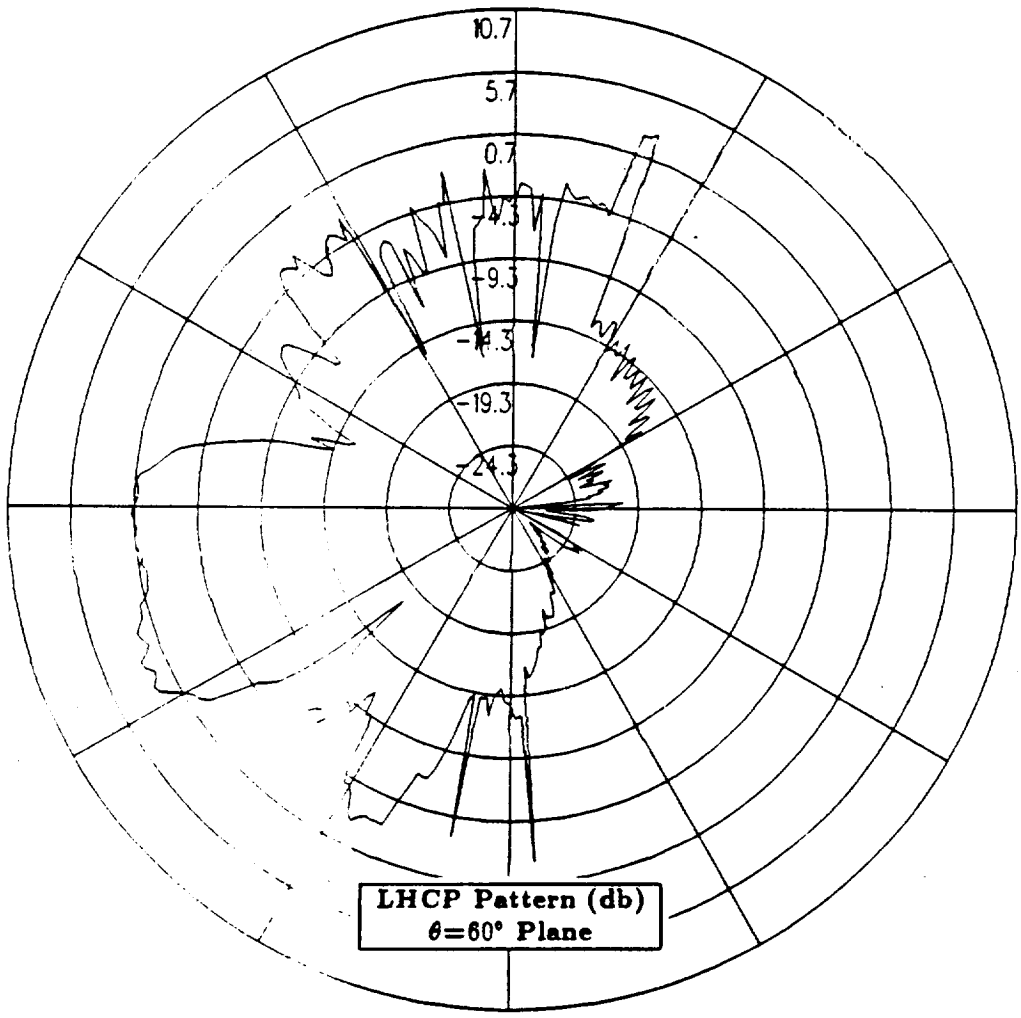

Figure 104: NEC-BSC calculated conical plane pattern 30° above the horizon for antenna location on the port side of the vertical stabilizer for left hand circular polarization at 300 MHz. (Test Location 8)

1.10 Test Location 9

In this section, the antenna is located on top of the vertical stabilizer. The cylindrical aircraft model used in the NEC-BSC is illustrated in Figure 105, which also shows the location of the antenna on the fuselage. The calculated results obtained using the improved version of the NEC-BSC at 300 MHz for the right hand circular polarized or co-polarized fields are shown for the roll plane in Figure 106, for the elevation plane in Figure 107, for the azimuth plane in Figure 108 and for the conical planes 10°, 20° and 30° above the horizon in Figures 109, 110 and 111, respectively. For completeness, the left hand circular polarized or cross-polarized results are also included. These cross-polarized results are shown for the roll plane in Figure 112, for the elevation plane in Figure 113, for the azimuth plane in Figure 114 and for the conical planes 10°, 20° and 30° above the horizon in Figures 115, 116 and 117, respectively.

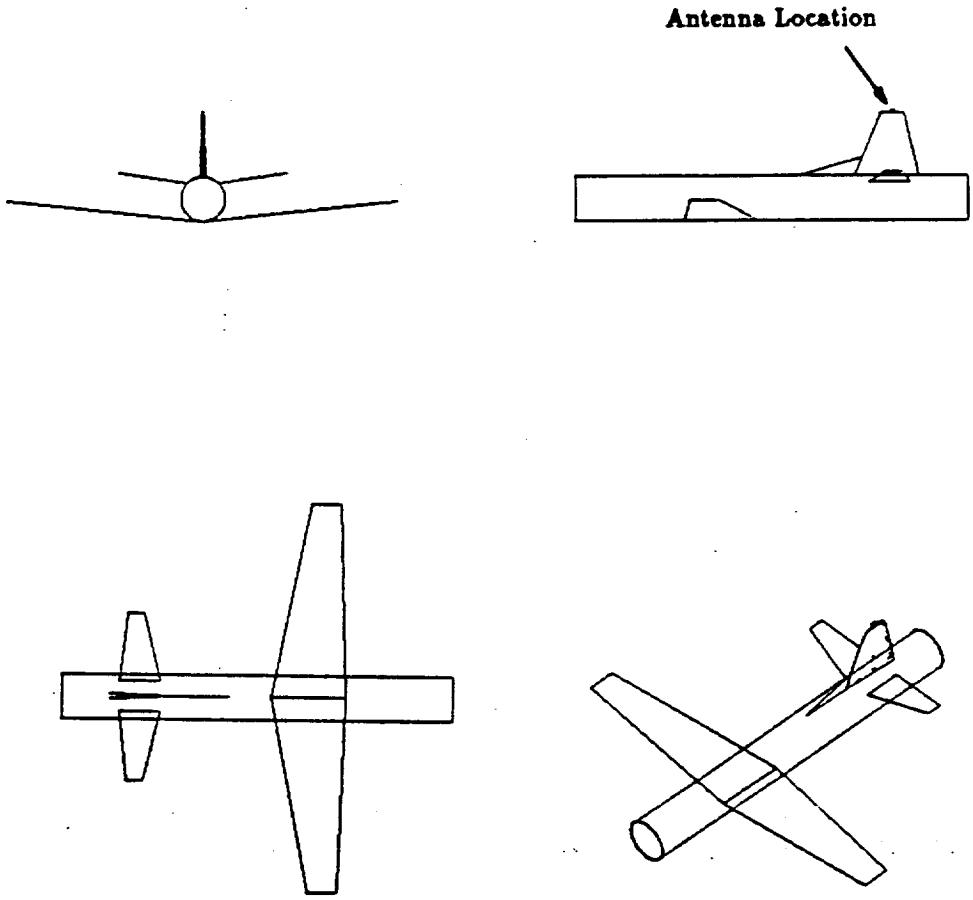

Figure 105: Geometry of the cylindrical model of the P-3C aircraft used in the NEC-BSC showing the antenna location. (Test Location 9)

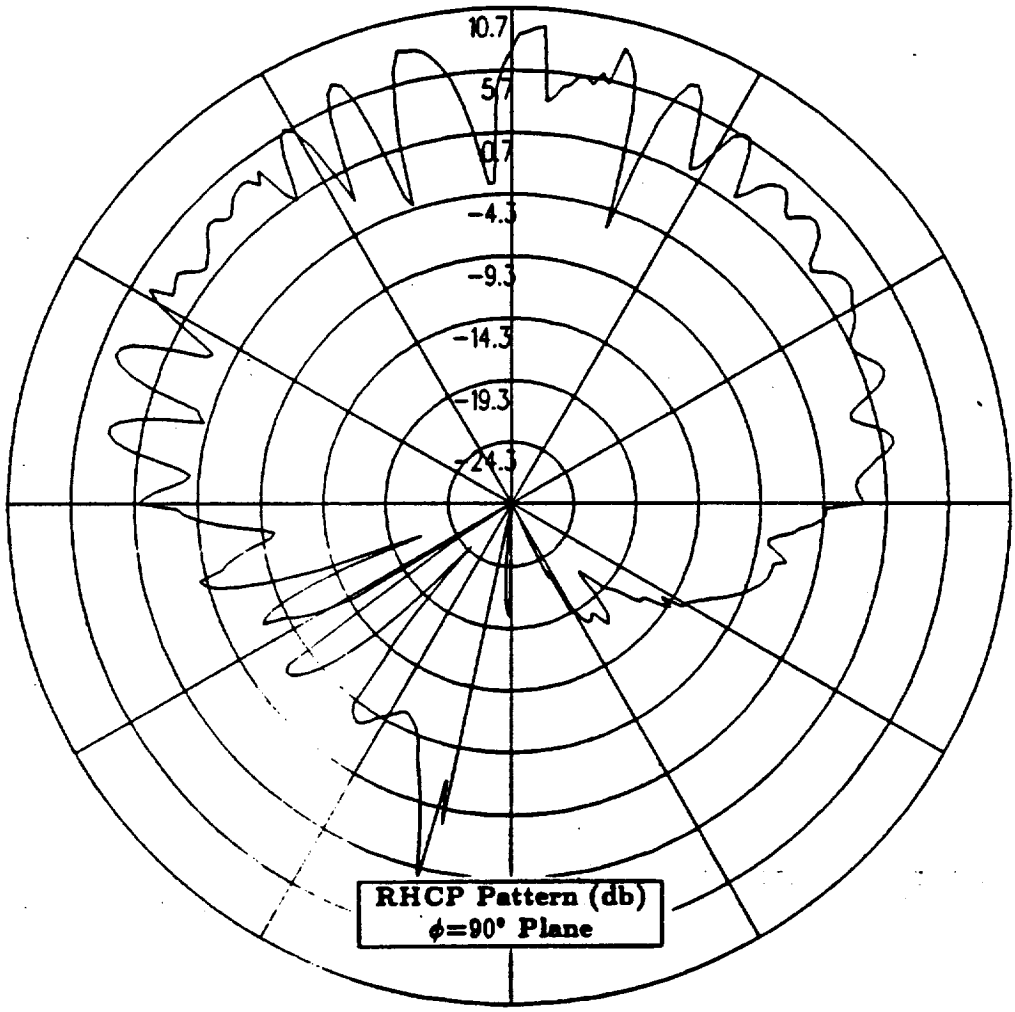

Figure 106: NEC-BSC calculated roll plane pattern for antenna location on top of the vertical stabilizer for right hand circular polarization at 300 MHz. (Test Location 9)

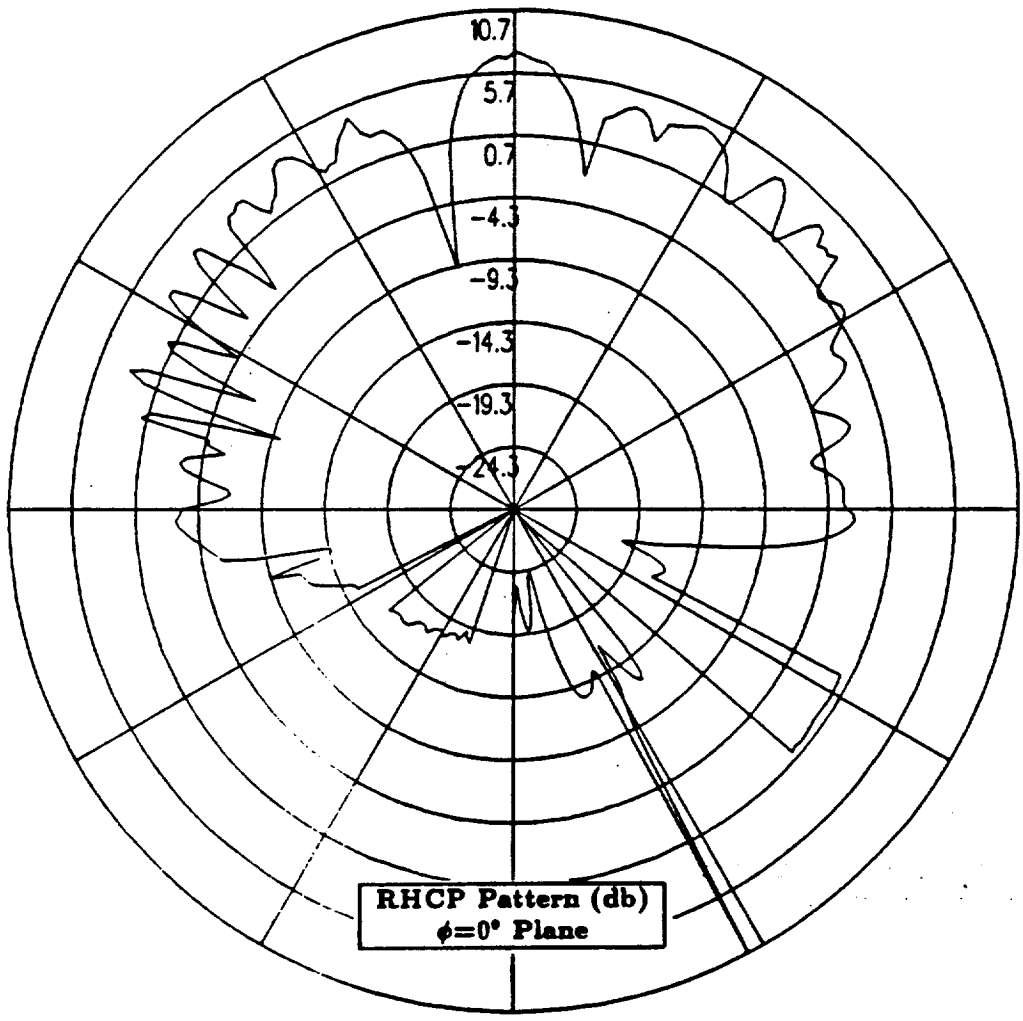

Figure 107: NEC-BSC calculated elevation plane pattern for antenna location on top of the vertical stabilizer for right hand circular polarization at 300 MHz. (Test Location 9)

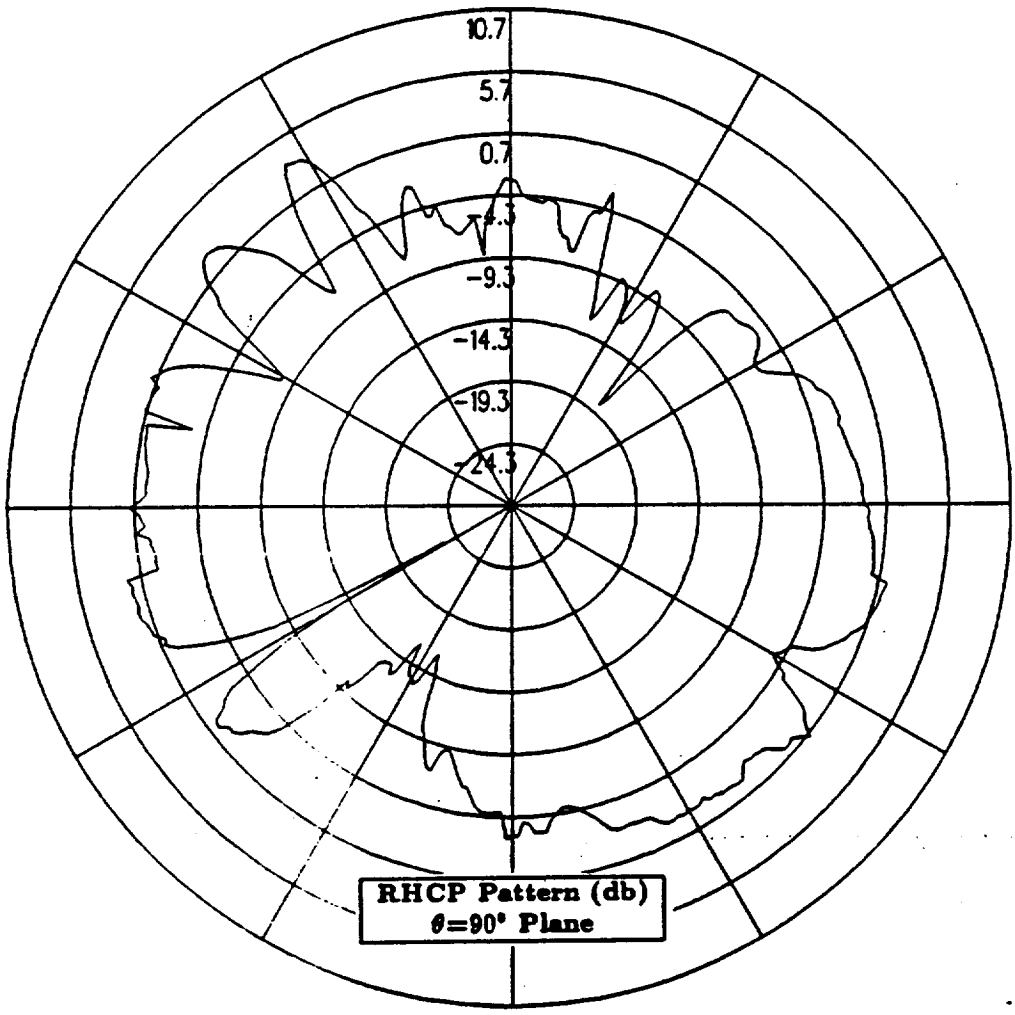

Figure 108: NEC-BSC calculated azimuth plane pattern for antenna location on top of the vertical stabilizer for right hand circular polarization at 300 MHz. (Test Location 9)

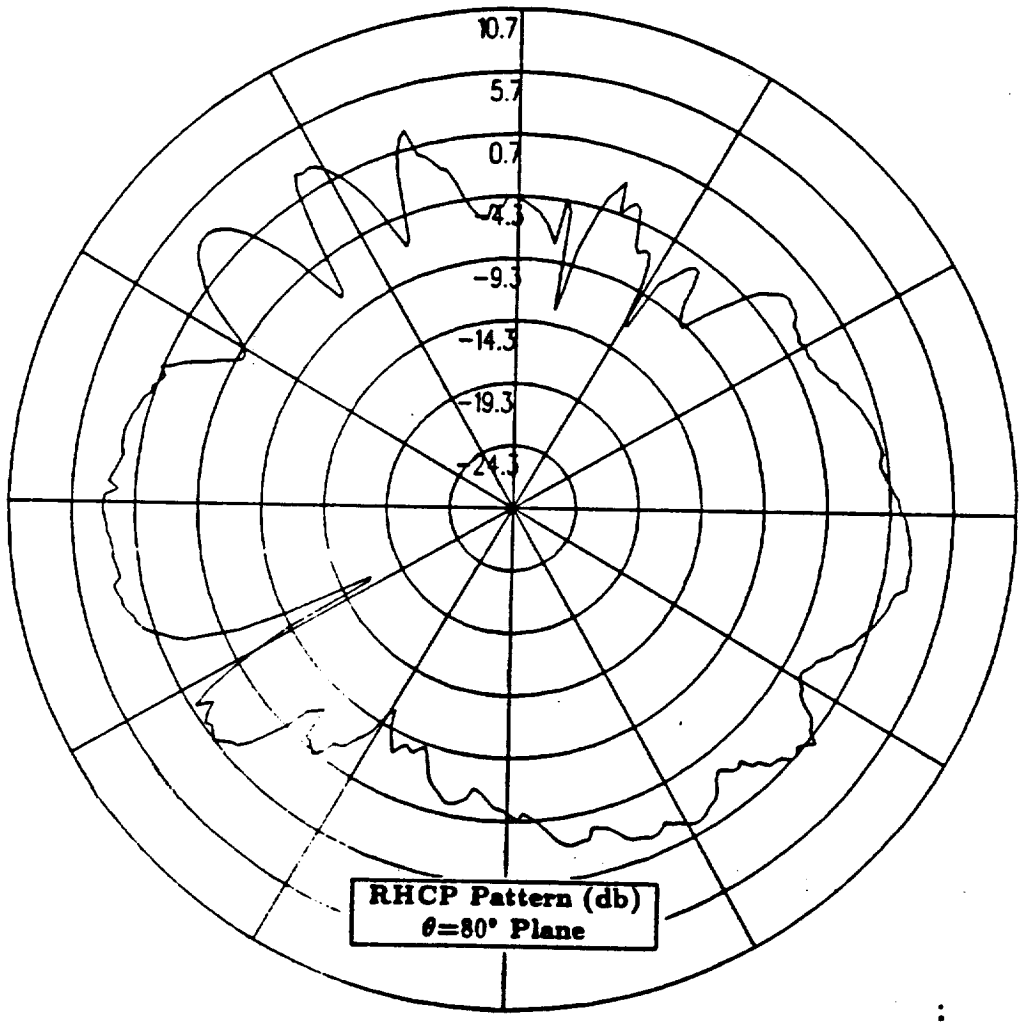

Figure 109: NEC-BSC calculated conical plane pattern 10° above the horizon for antenna location on top of the vertical stabilizer for right hand circular polarization at 300 MHz. (Test Location 9)

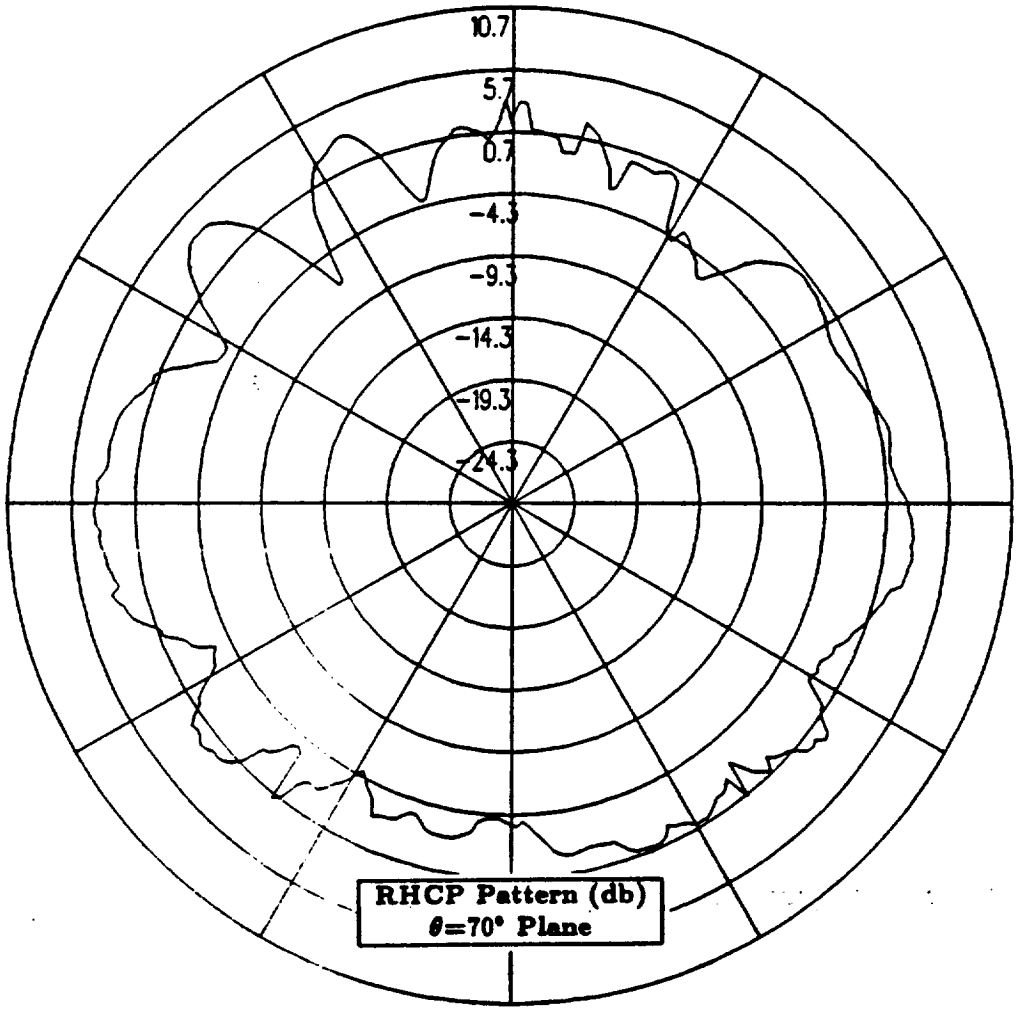

Figure 110: NEC-BSC calculated conical plane pattern 20° above the horizon for antenna location on top of the vertical stabilizer for right hand circular polarization at 300 MHz. (Test Location 9)

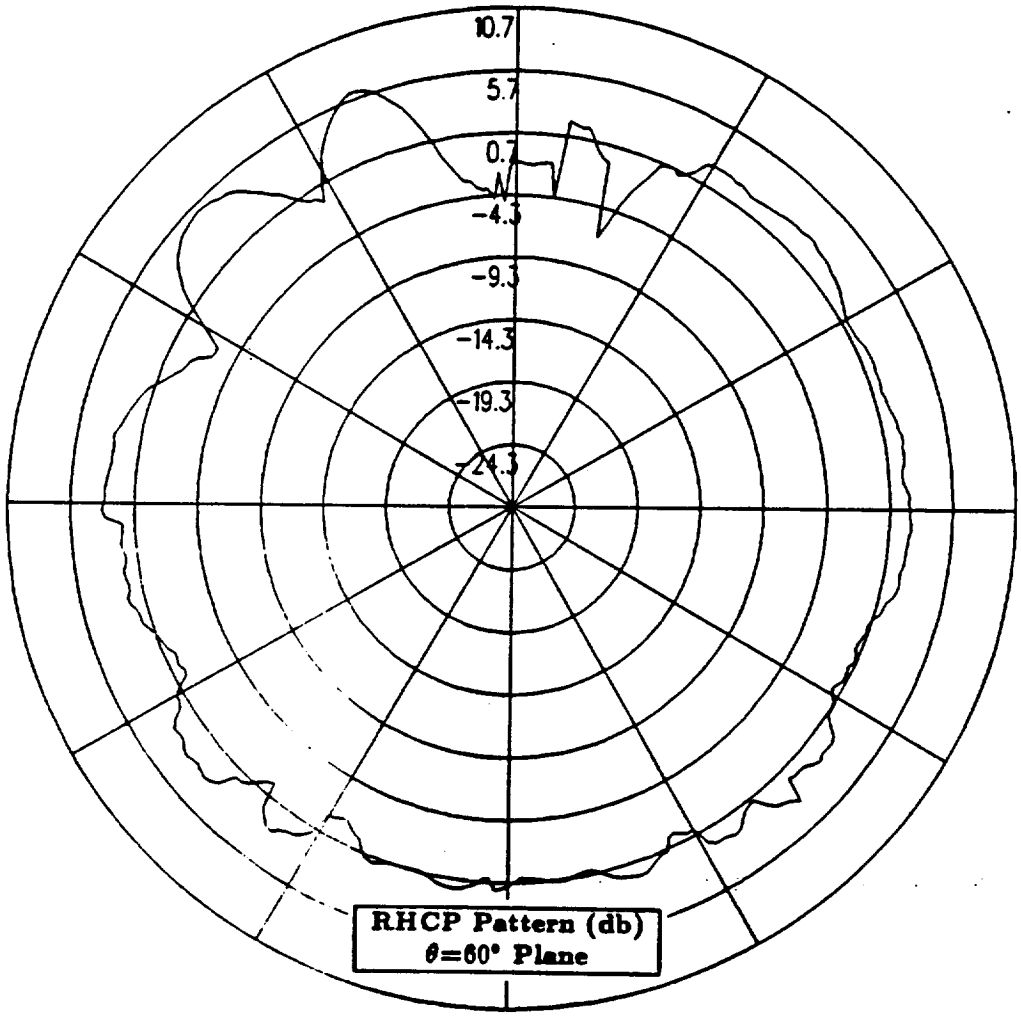

Figure 111: NEC-BSC calculated conical plane pattern 30° above the horizon for antenna location on top of the vertical stabilizer for right hand circular polarization at 300 MHz. (Test Location 9)

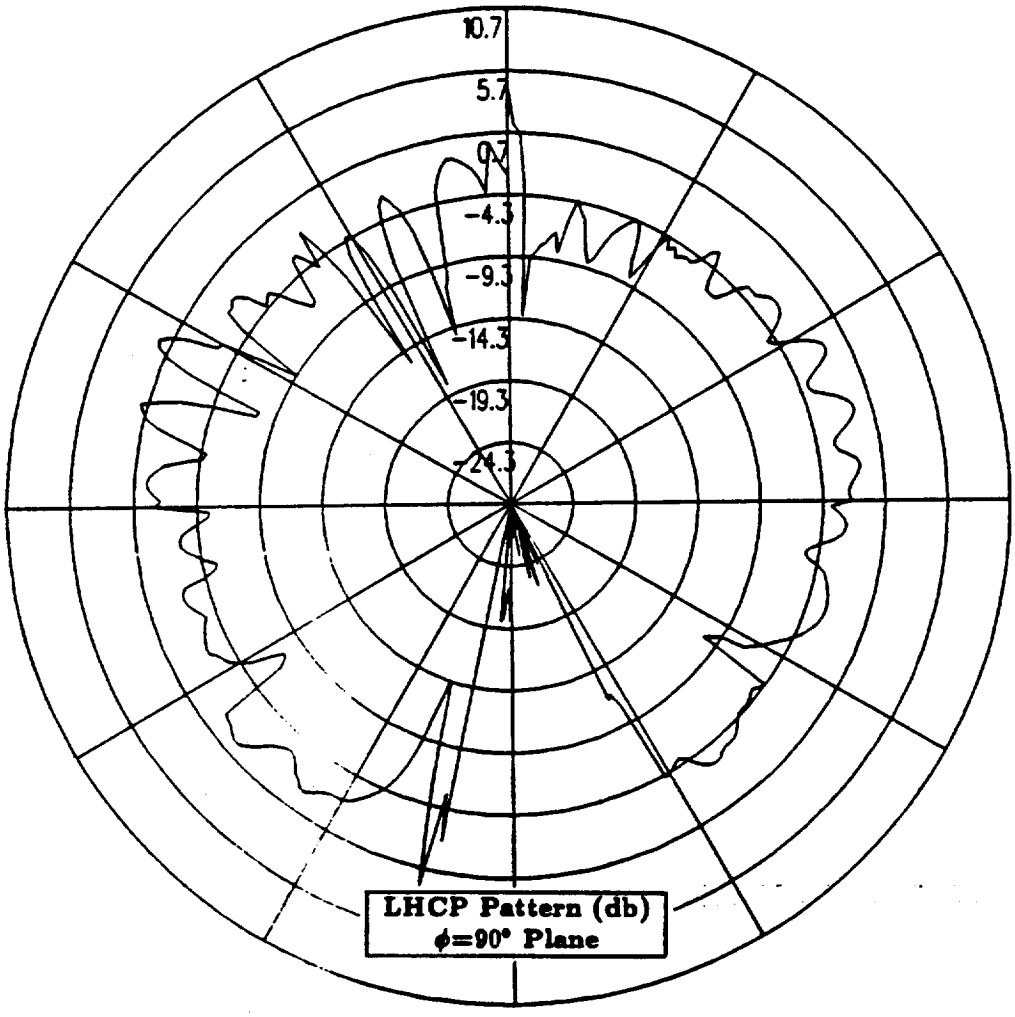

Figure 112: NEC-BSC calculated roll plane pattern for antenna location on top of the vertical stabilizer for left hand circular polarization at 300 MHz. (Test Location 9)

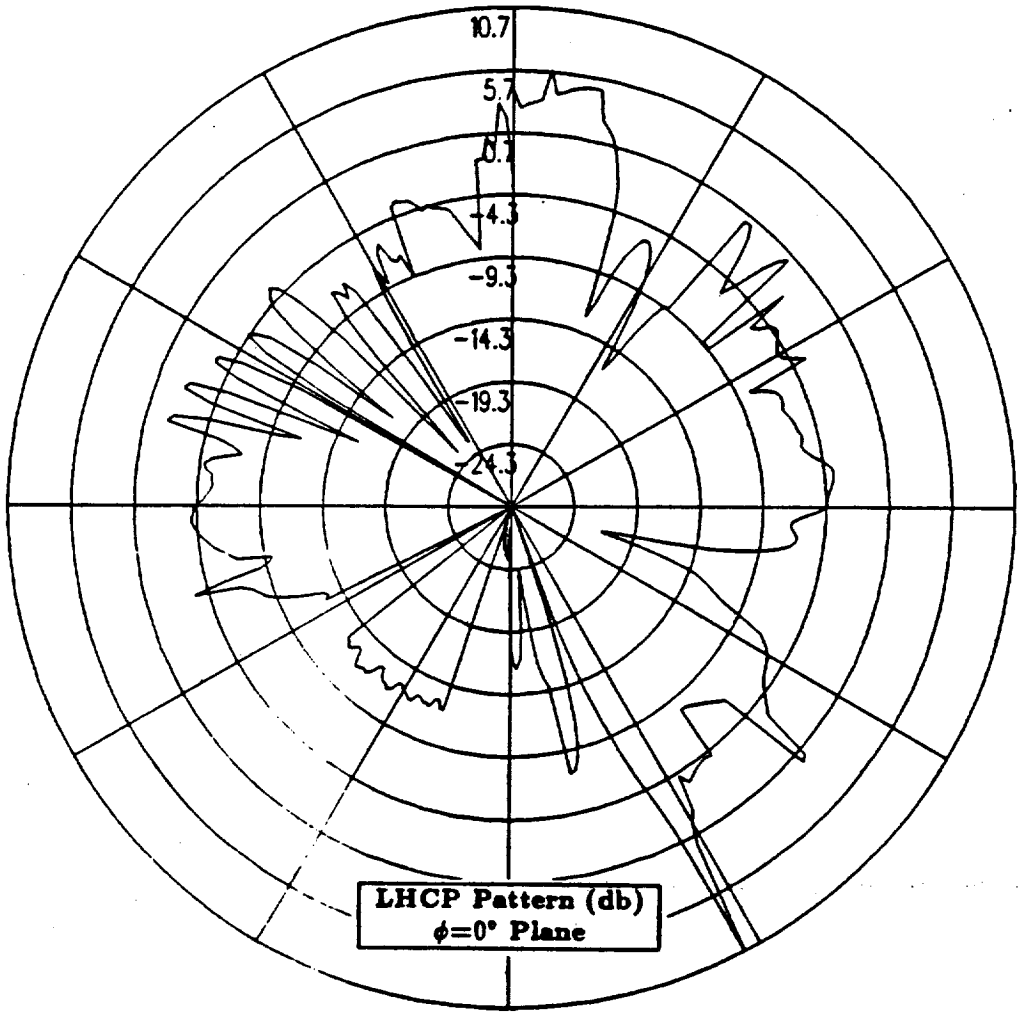

Figure 113: NEC-BSC calculated elevation plane pattern for antenna location on top of the vertical stabilizer for left hand circular polarization at 300 MHz. (Test Location 9)

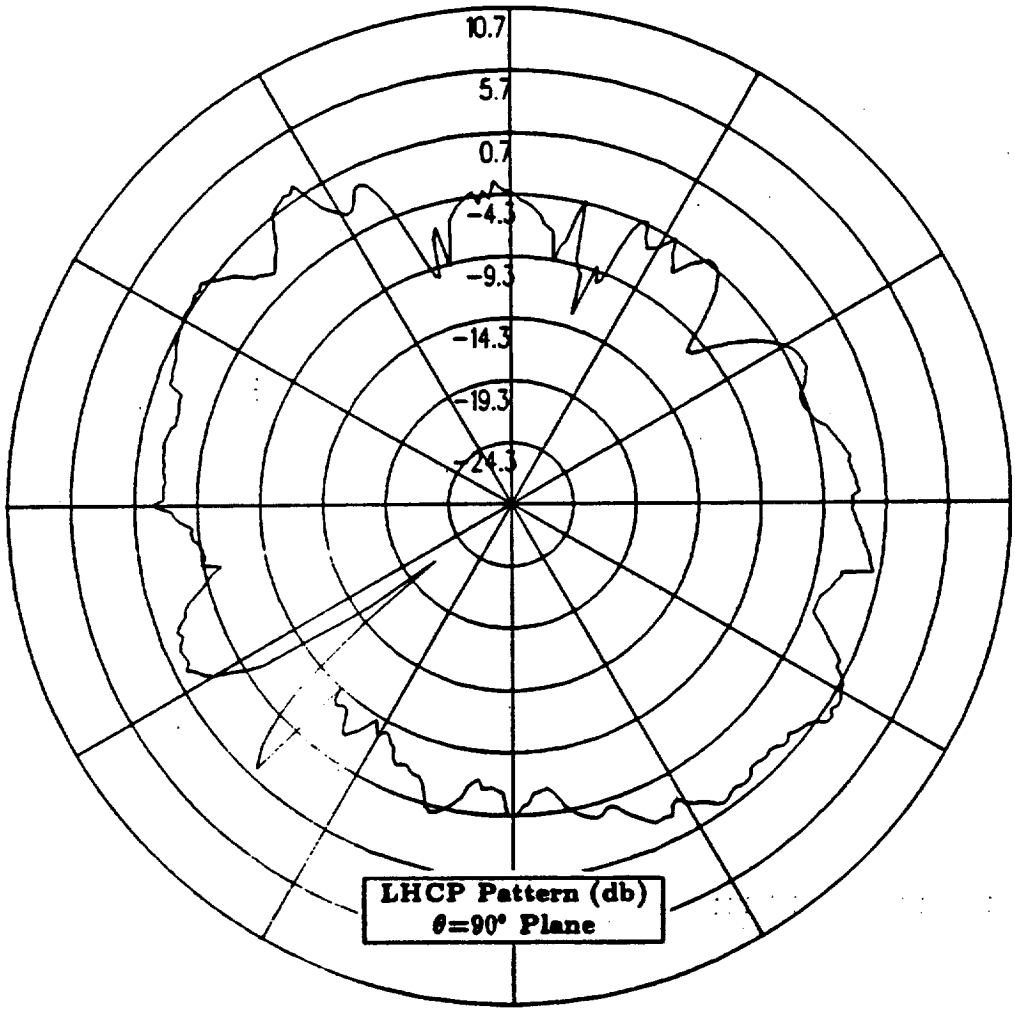

Figure 114: NEC-BSC calculated azimuth plane pattern for antenna location on top of the vertical stabilizer for left hand circular polarization at 300 MHz. (Test Location 9)

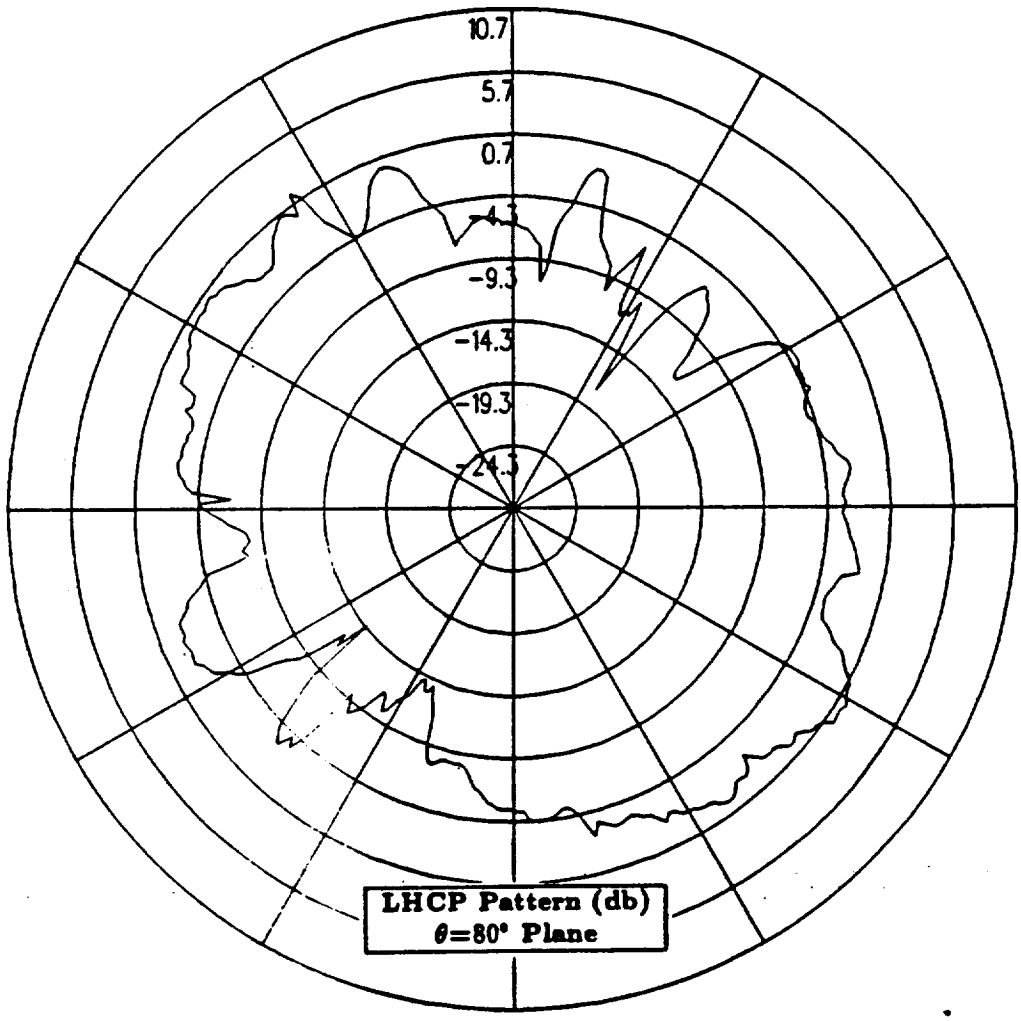

Figure 115: NEC-BSC calculated conical plane pattern 10° above the horizon for antenna location on top of the vertical stabilizer for left hand circular polarization at 300 MHz. (Test Location 9)

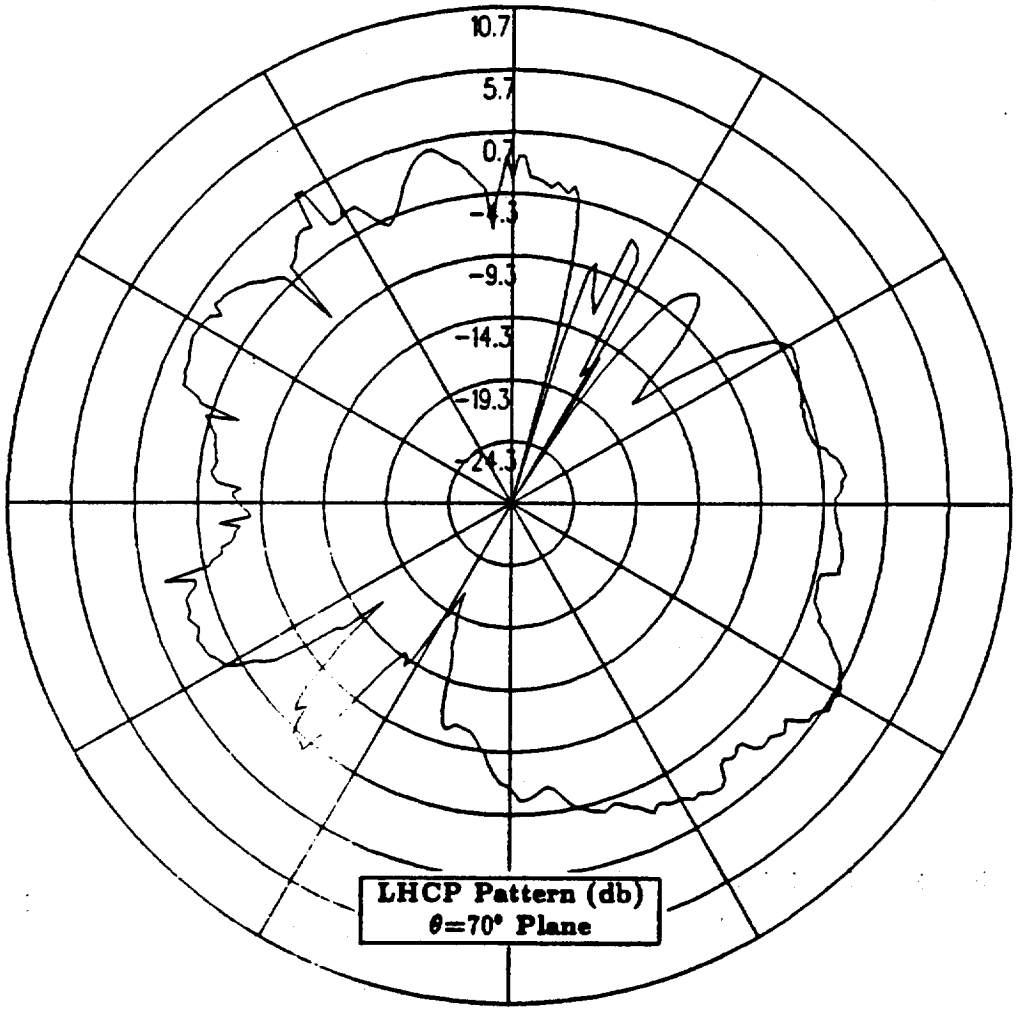

Figure 116: NEC-BSC calculated conical plane pattern 20° above the horizon for antenna location on top of the vertical stabilizer for left hand circular polarization at 300 MHz. (Test Location 9)

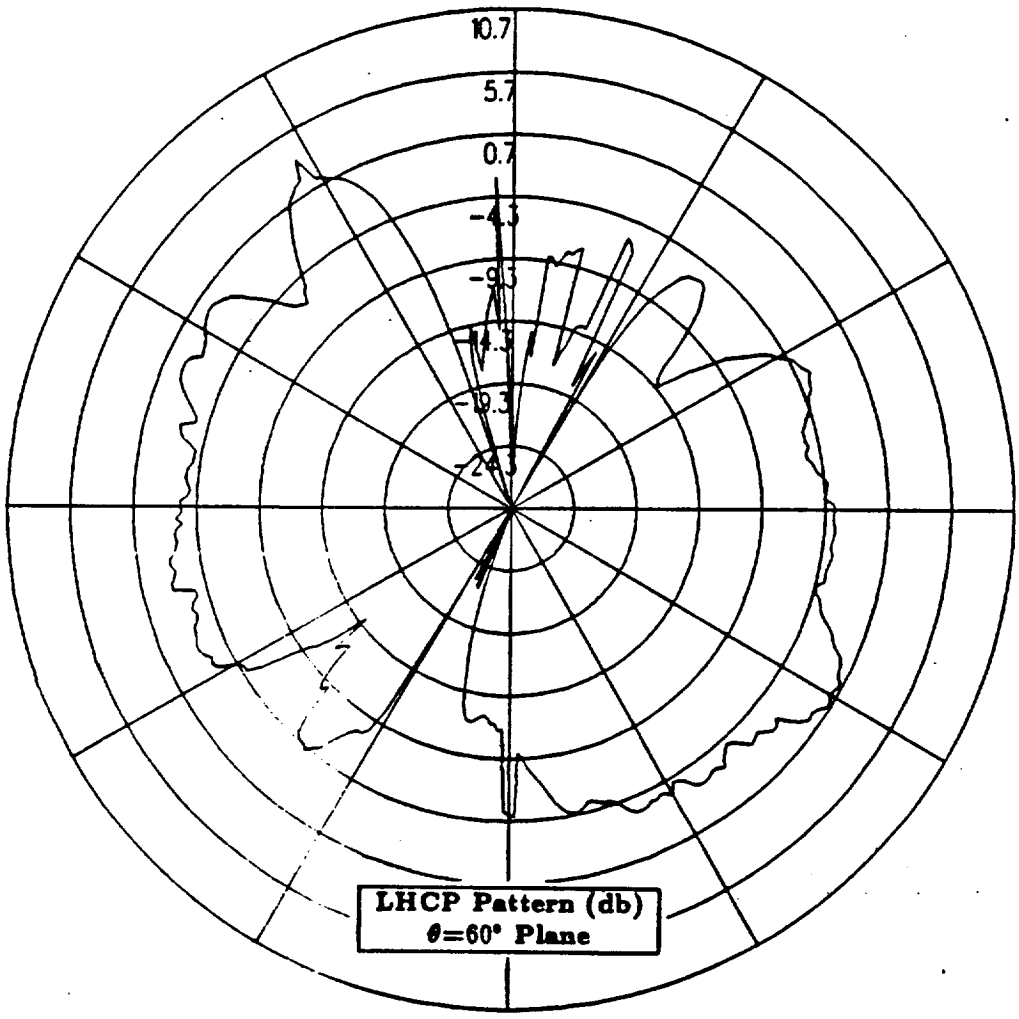

Figure 117: NEC-BSC calculated conical plane pattern 30° above the horizon for antenna location on top of the vertical stabilizer for left hand circular polarization at 300 MHz. (Test Location 9)

1.11 Test Location 10

In this section, the antenna is located on the port side horizontal stabilizer. The cylindrical aircraft model used in the NEC-BSC is illustrated in Figure 118, which also shows the location of the antenna on the fuselage. The calculated results obtained using the improved version of the NEC-BSC at 300 MHz for the right hand circular polarized or co-polarized fields are shown for the roll plane in Figure 119, for the elevation plane in Figure 120, for the azimuth plane in Figure 121 and for the conical planes 10°, 20° and 30° above the horizon in Figures 122, 123 and 124, respectively. For completeness, the left hand circular polarized or cross-polarized results are also included. These cross-polarized results are shown for the roll plane in Figure 125, for the elevation plane in Figure 126, for the azimuth plane in Figure 127 and for the conical planes 10°, 20° and 30° above the horizon in Figures 128, 129 and 130, respectively.

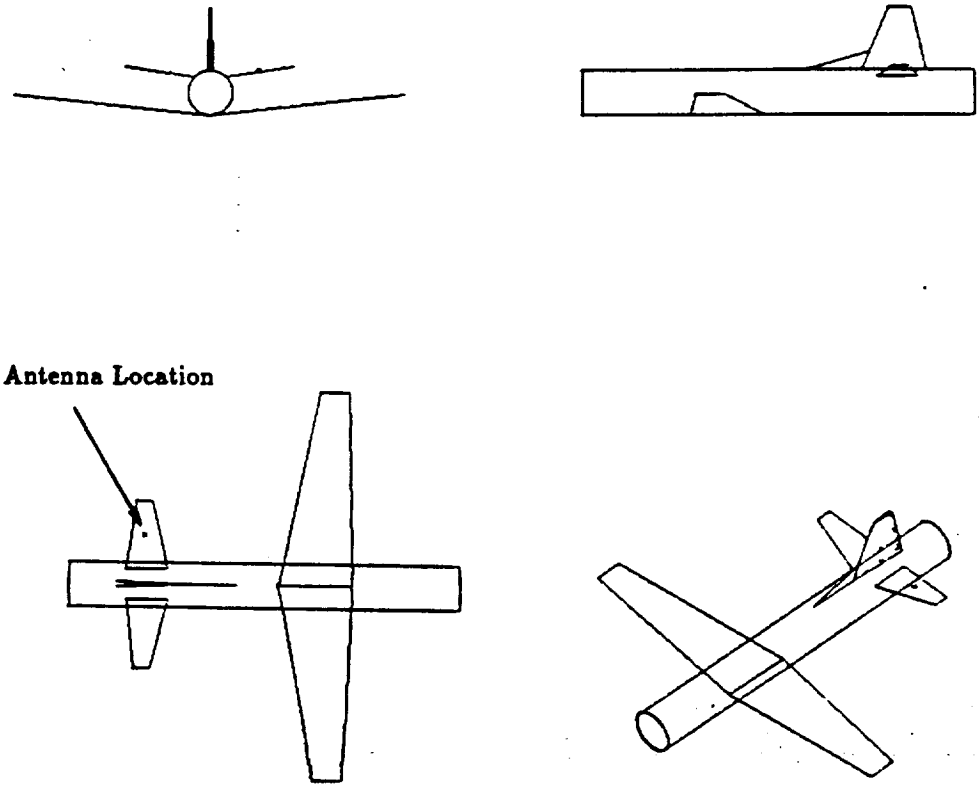

Figure 118: Geometry of the cylindrical model of the P-3C aircraft used in the NEC-BSC showing the antenna location. (Test Location 10)

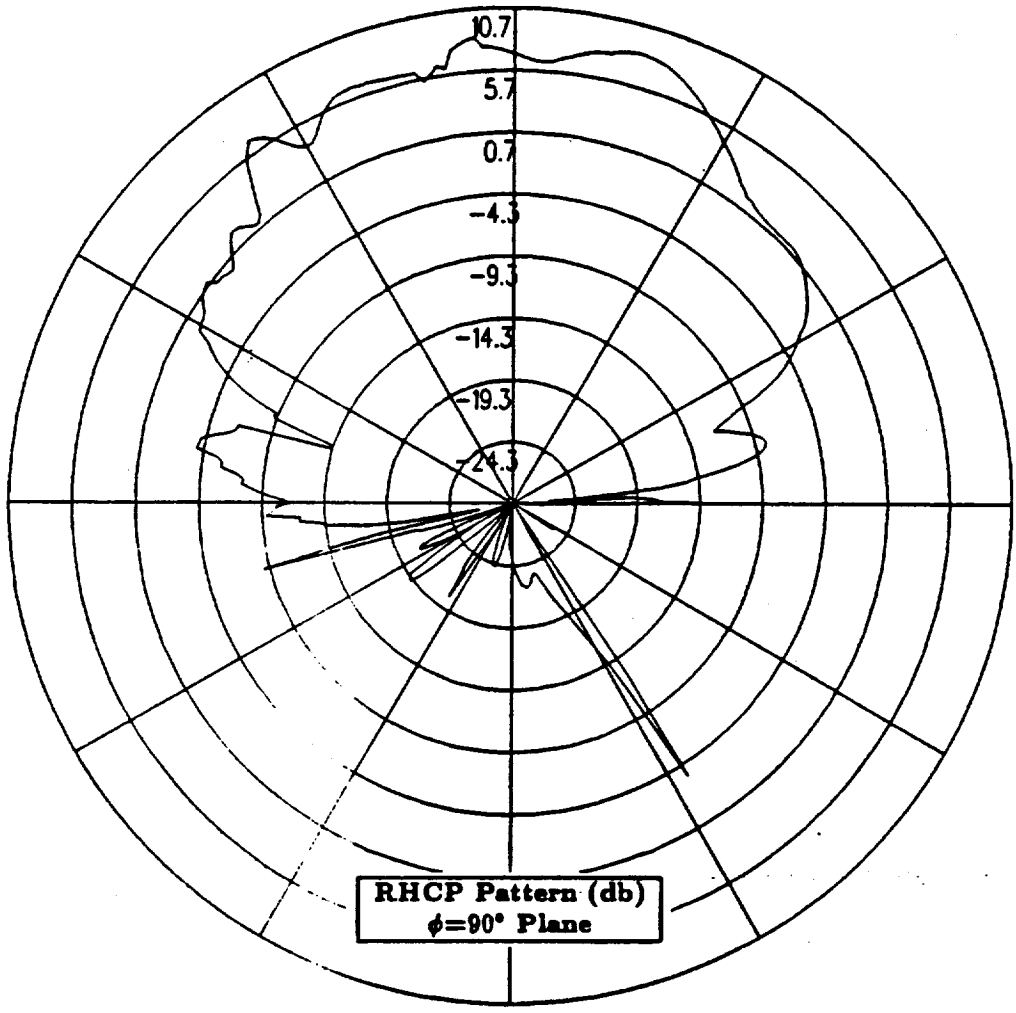

Figure 119: NEC-BSC calculated roll plane pattern for antenna location on the port side horizontal stabilizer for right hand circular polarization at 300 MHz. (Test Location 10)

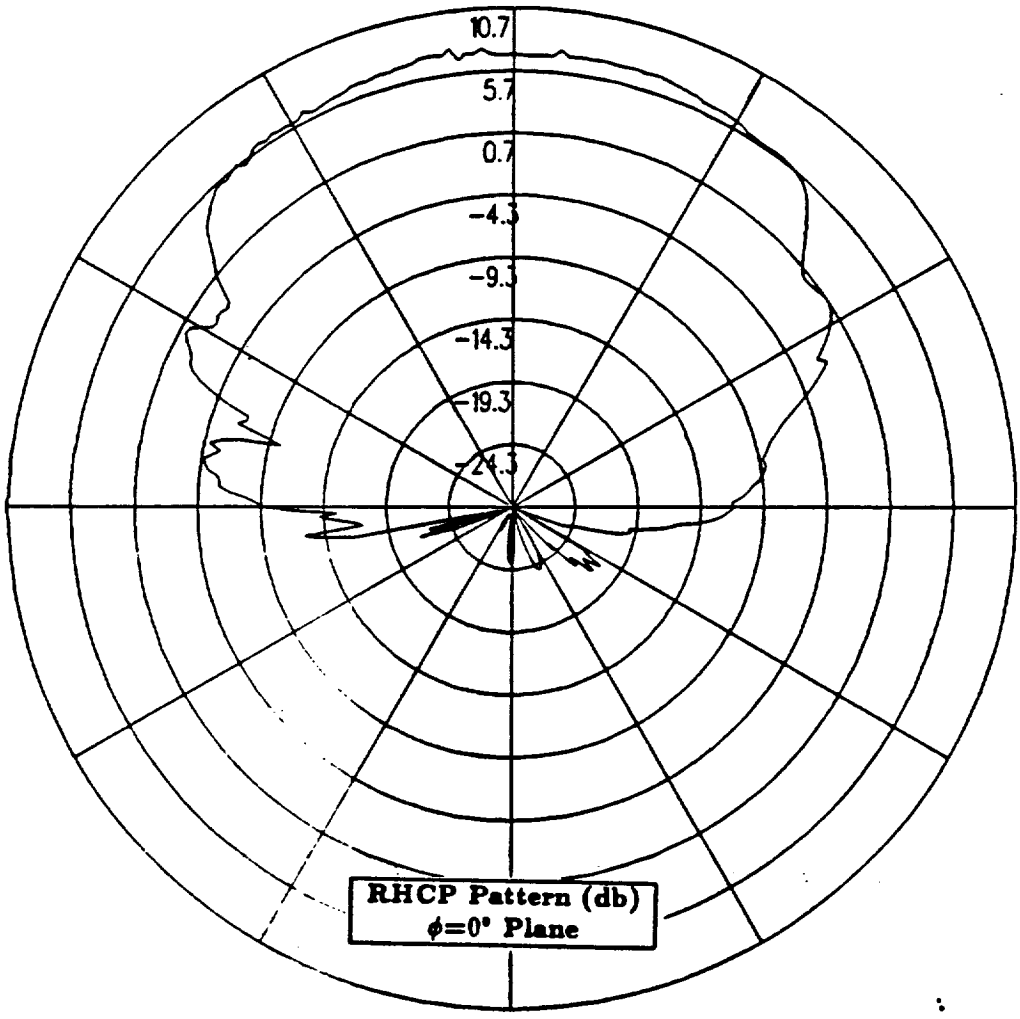

Figure 120: NEC-BSC calculated elevation plane pattern for antenna location on the port side horizontal stabilizer for right hand circular polarization at 300 MHz. (Test Location 10)

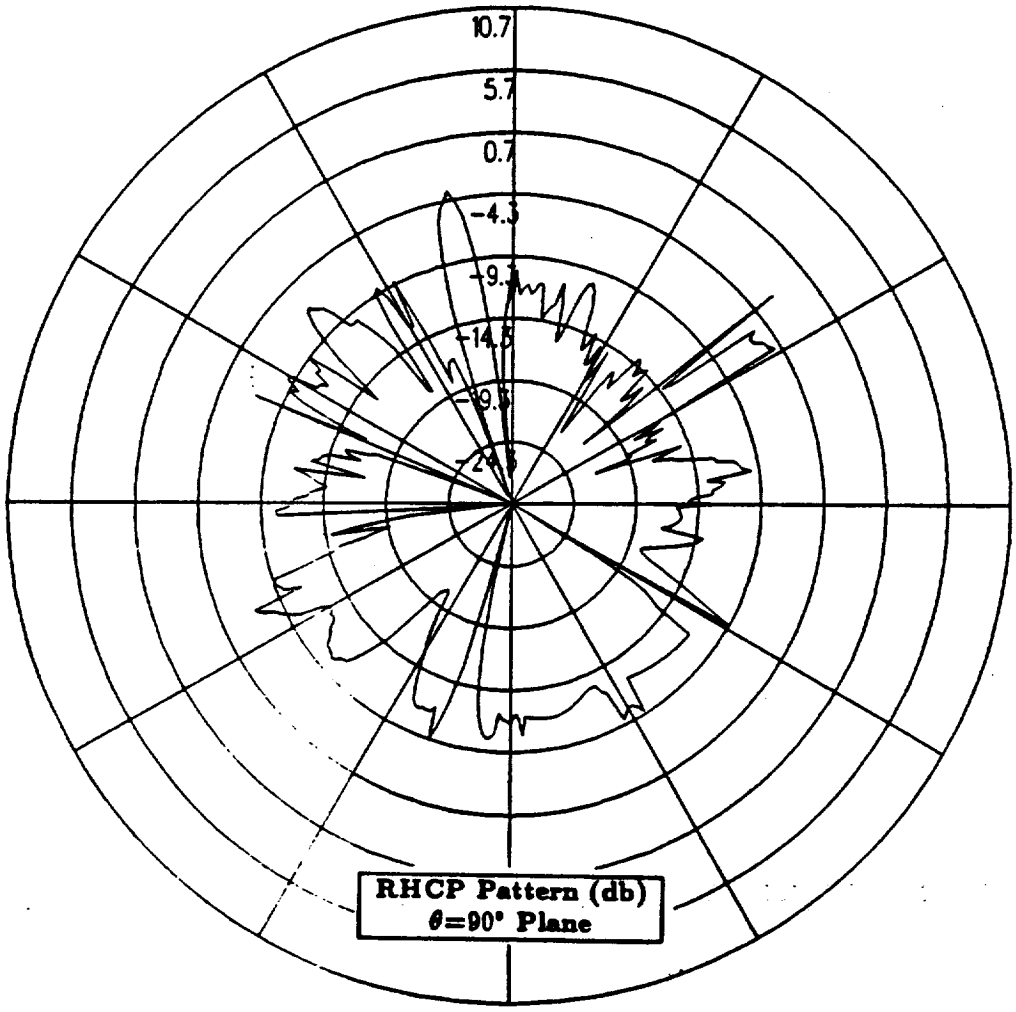

Figure 121: NEC-BSC calculated azimuth plane pattern for antenna location on the port side horizontal stabilizer for right hand circular polarization at 300 MHz. (Test Location 10)

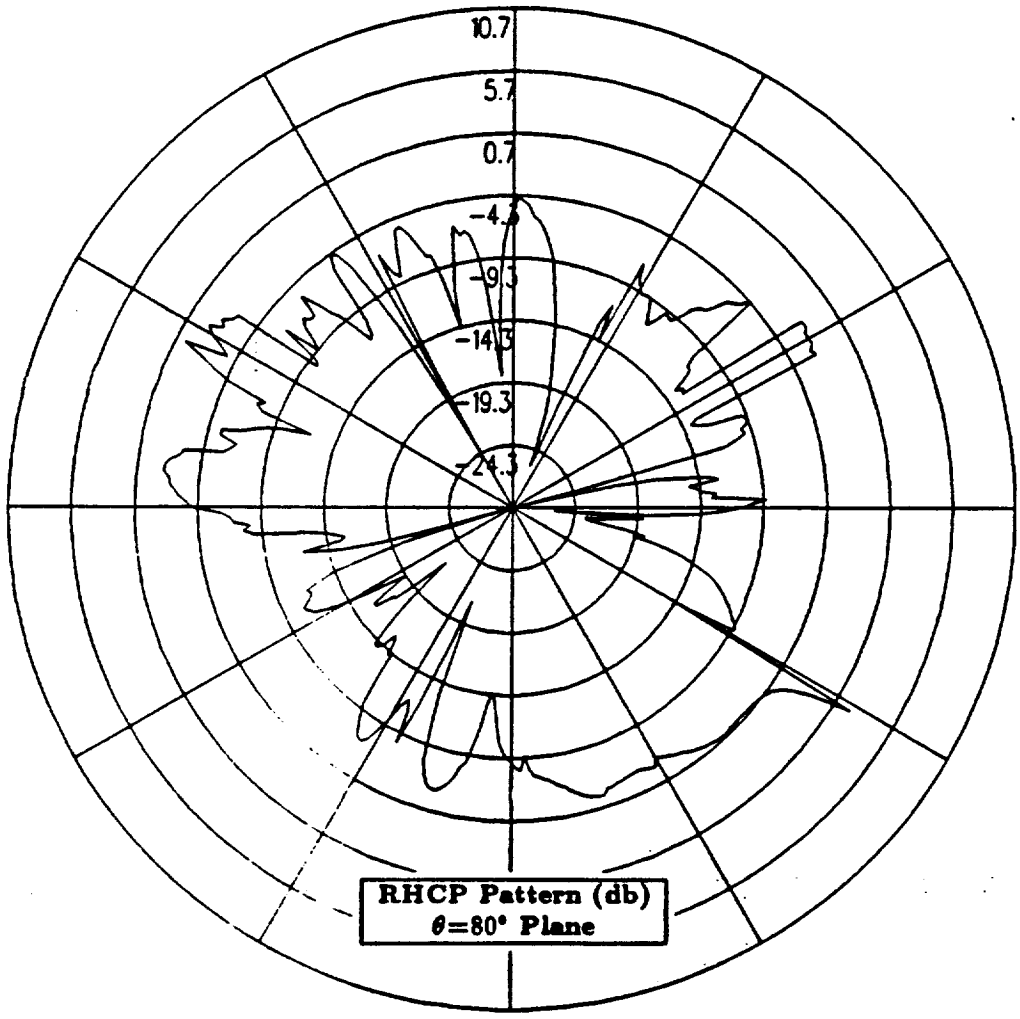

Figure 122: NEC-BSC calculated conical plane pattern 10° above the horizon for antenna location on the port side horizontal stabilizer for right hand circular polarization at 300 MHz. (Test Location 10)

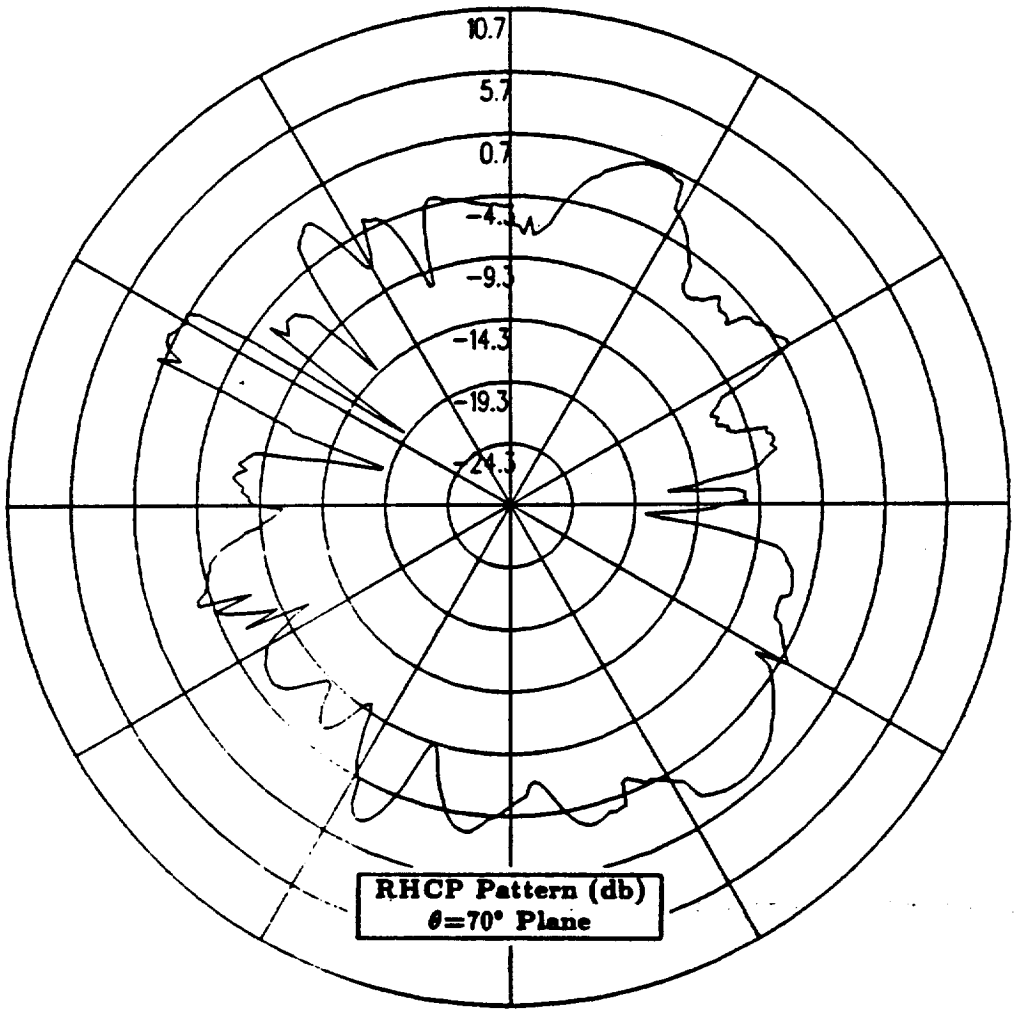

Figure 123: NEC-BSC calculated conical plane pattern 20° above the horizon for antenna location on the port side horizontal stabilizer for right hand circular polarization at 300 MHz. (Test Location 10)

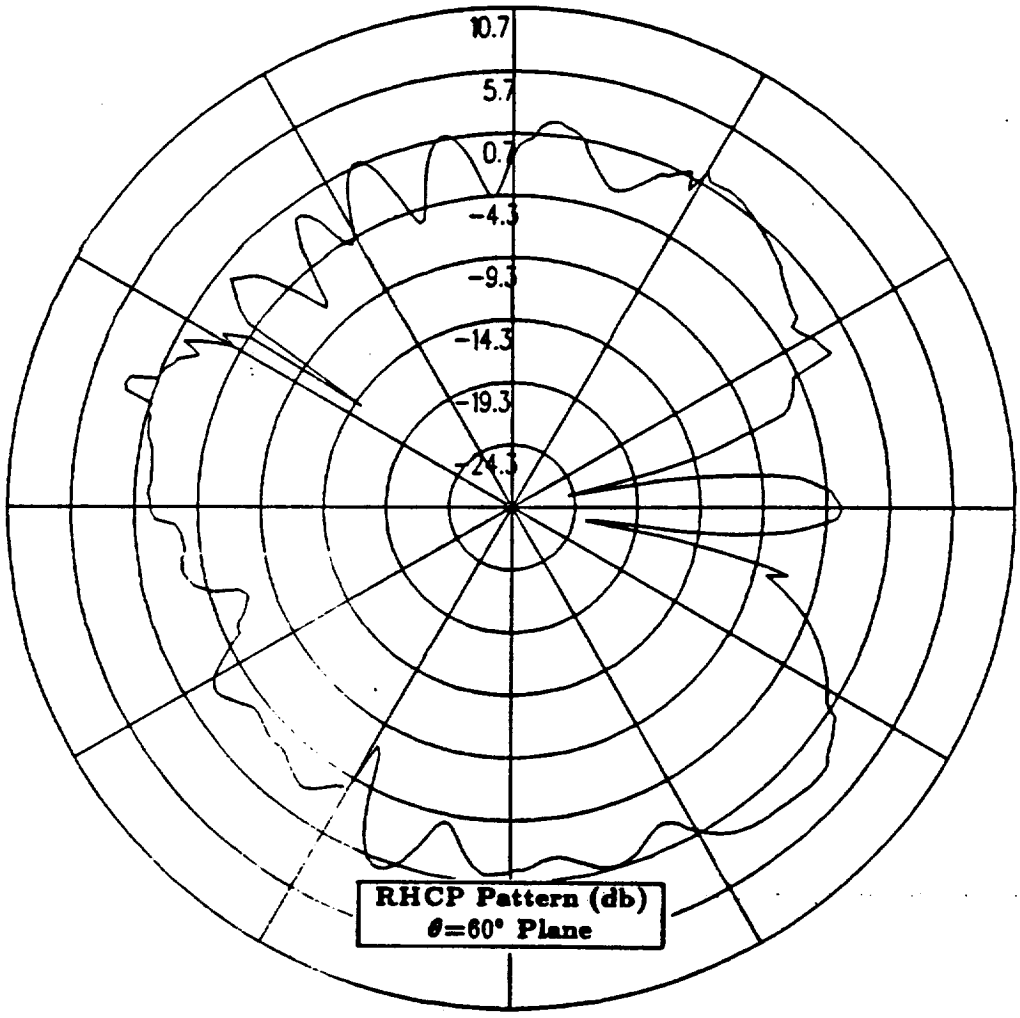

Figure 124: NEC-BSC calculated conical plane pattern 30° above the horizon for antenna location on the port side horizontal stabilizer for right hand circular polarization at 300 MHz. (Test Location 10)

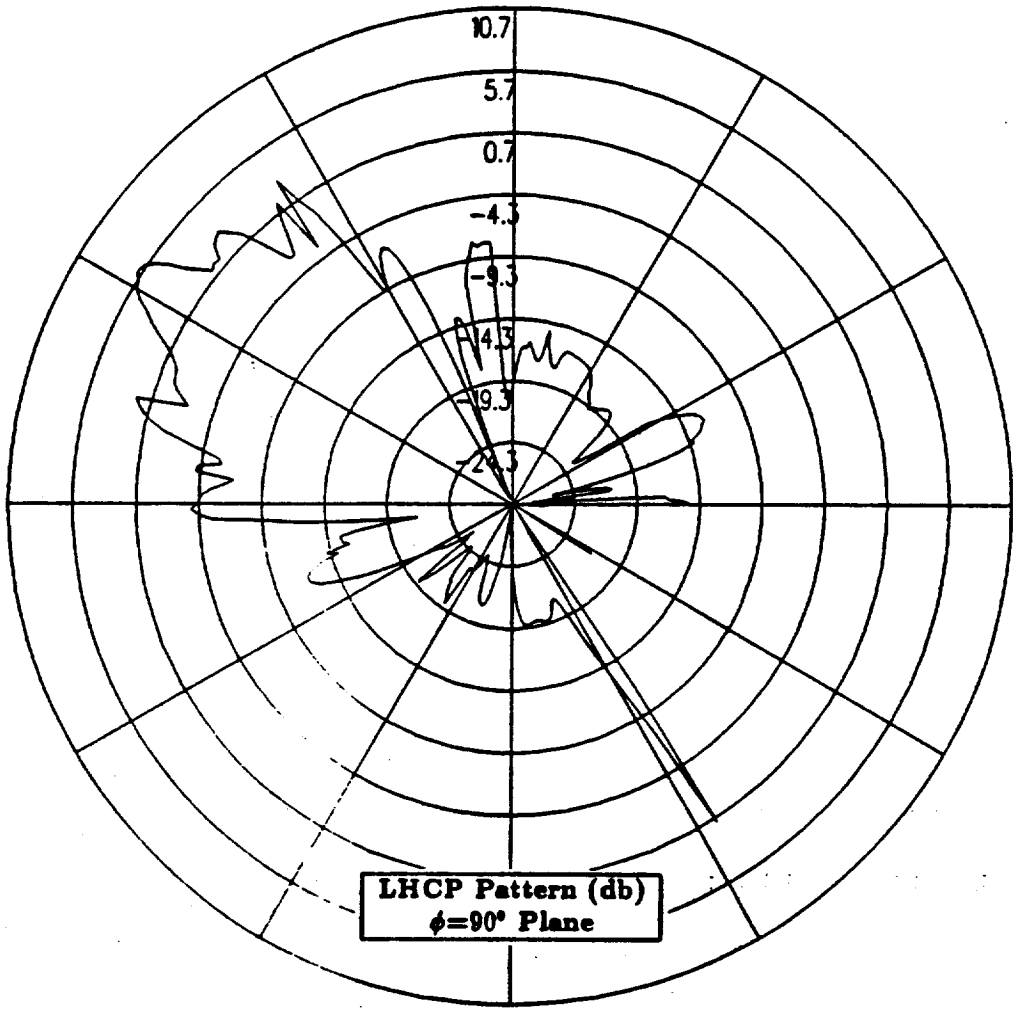

Figure 125: NEC-BSC calculated roll plane pattern for antenna location on the port side horizontal stabilizer for left hand circular polarization at 300 MHz. (Test Location 10)

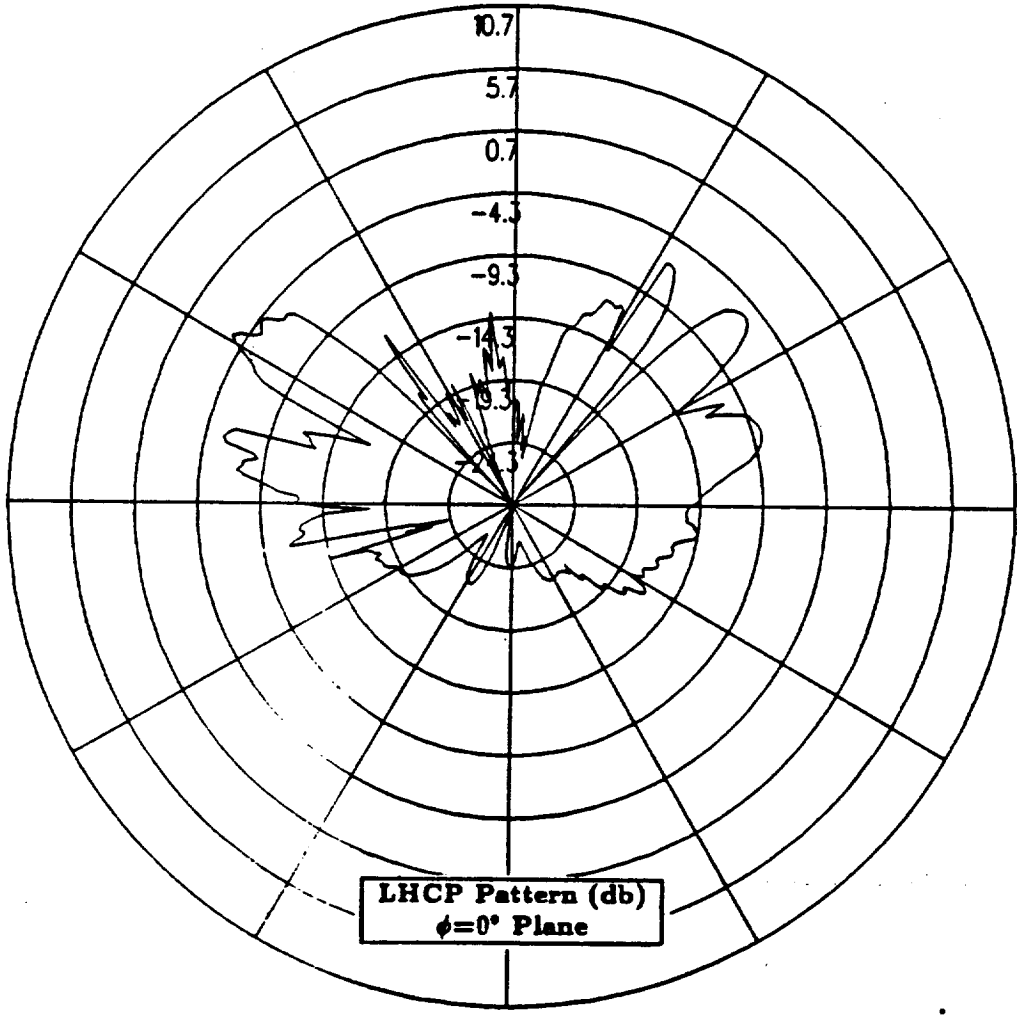

Figure 126: NEC-BSC calculated elevation plane pattern for antenna location on the port side horizontal stabilizer for left hand circular polarization at 300 MHz. (Test Location 10)

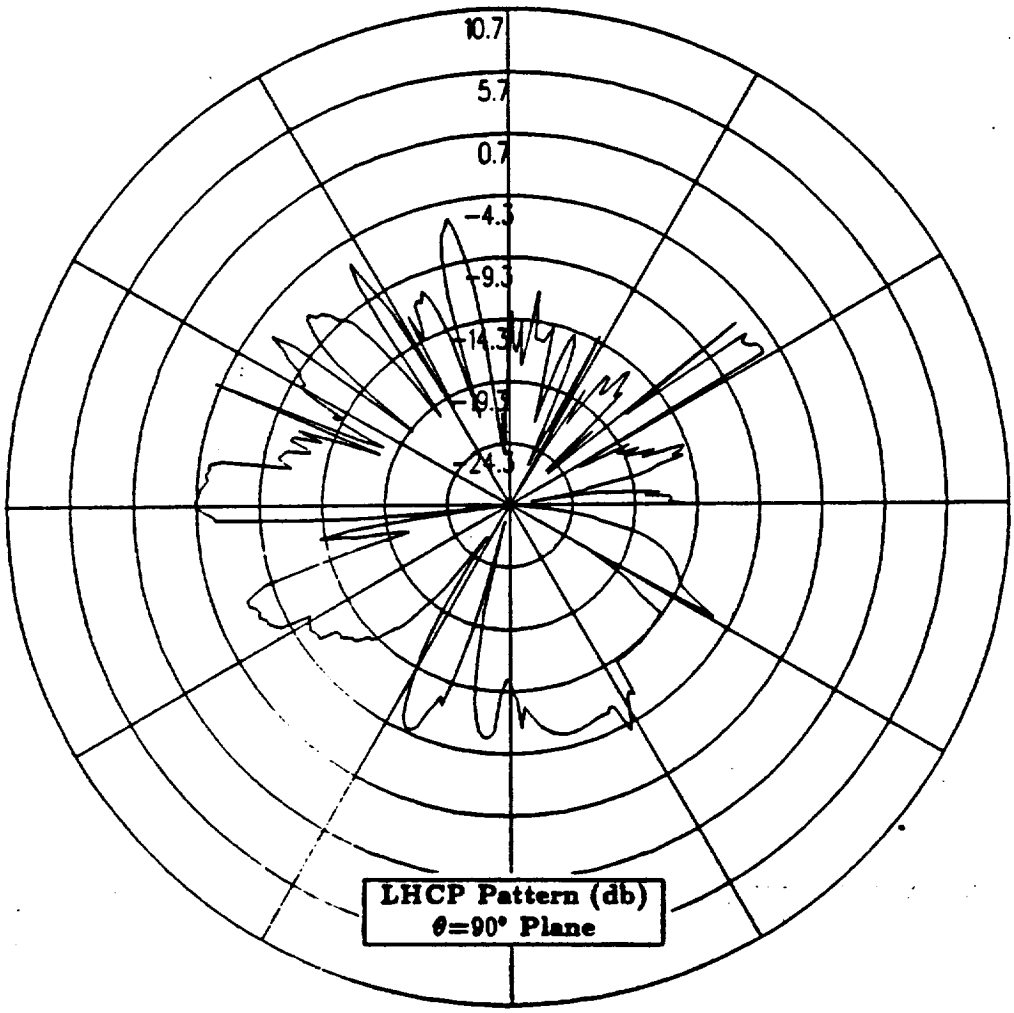

Figure 127: NEC-BSC calculated azimuth plane pattern for antenna location on the port side horizontal stabilizer for left hand circular polarization at 300 MHz. (Test Location 10)

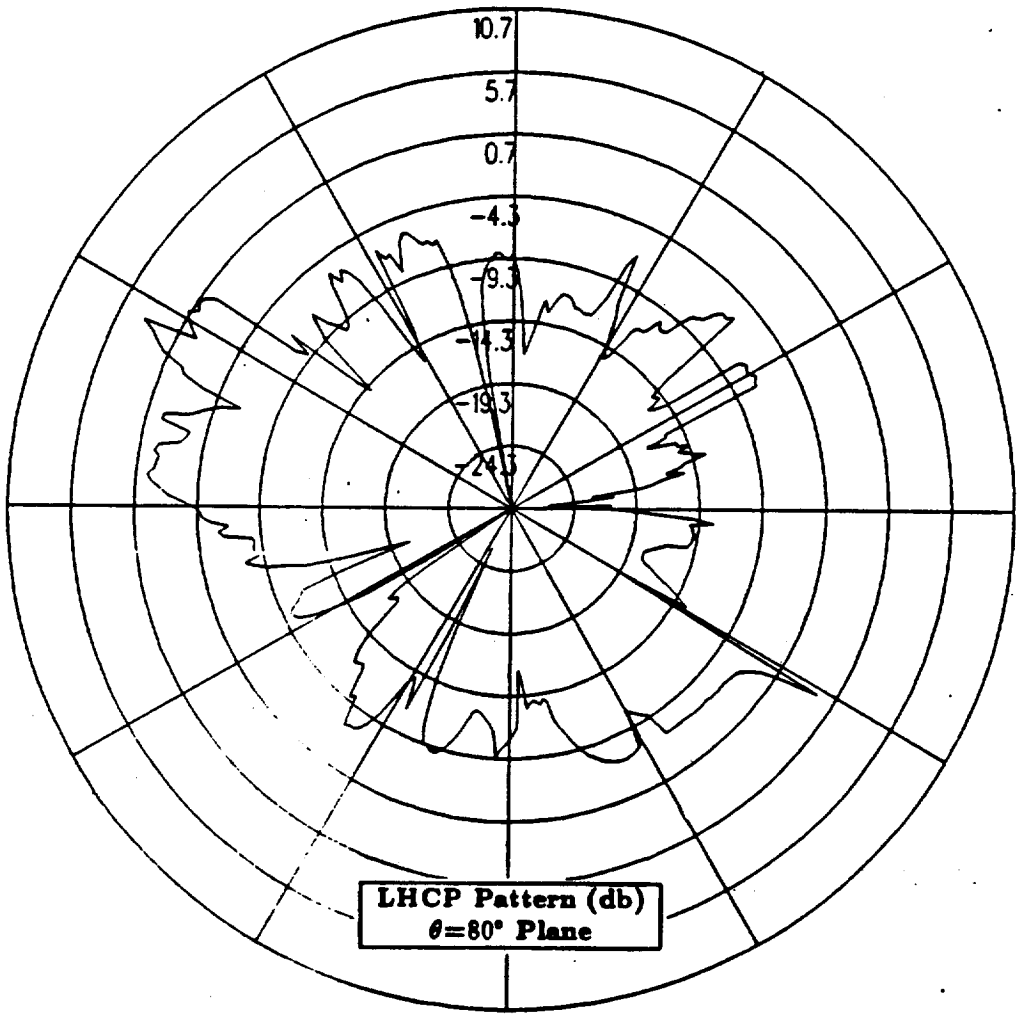

Figure 128: NEC-BSC calculated conical plane pattern 10° above the horizon for antenna location on the port side horizontal stabilizer for left hand circular polarization at 300 MHz. (Test Location 10)

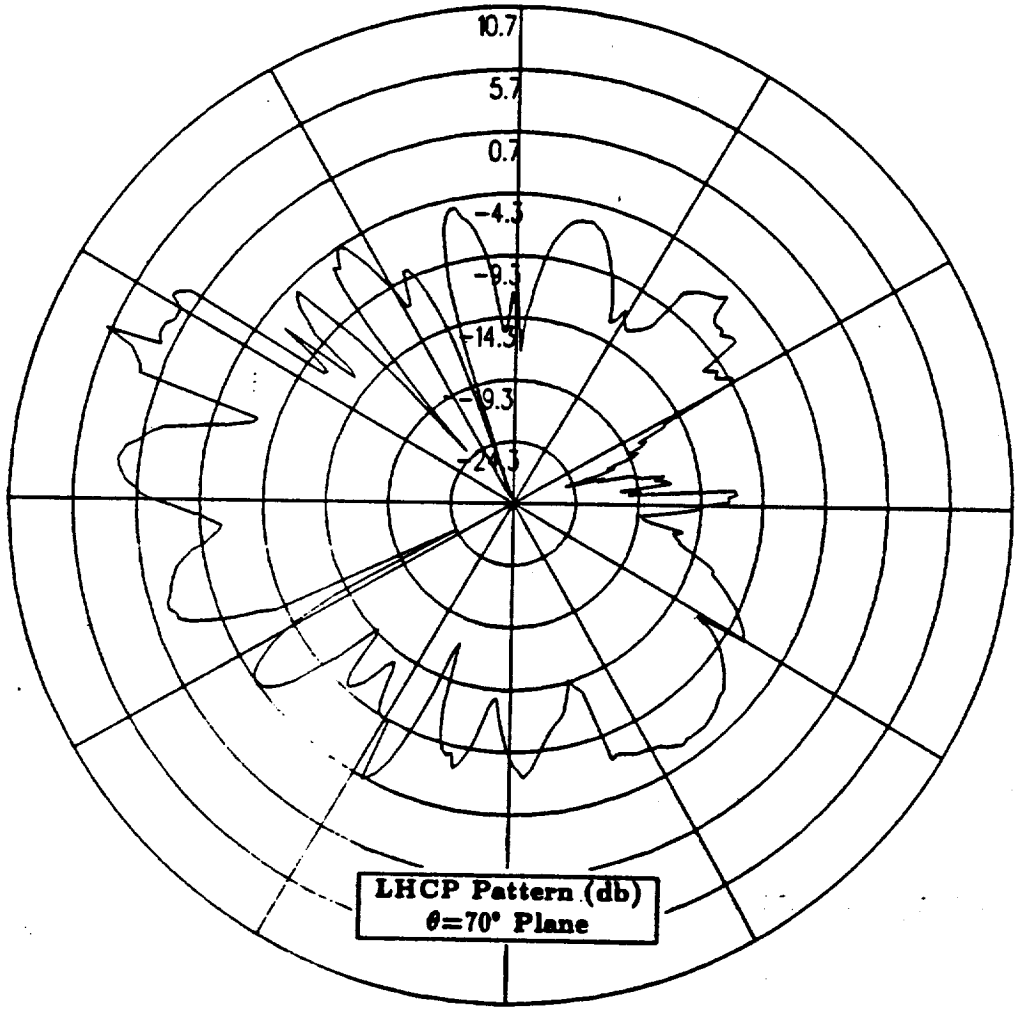

Figure 129: NEC-BSC calculated conical plane pattern 20° above the horizon for antenna location on the port side horizontal stabilizer for left hand circular polarization at 300 MHz. (Test Location 10)

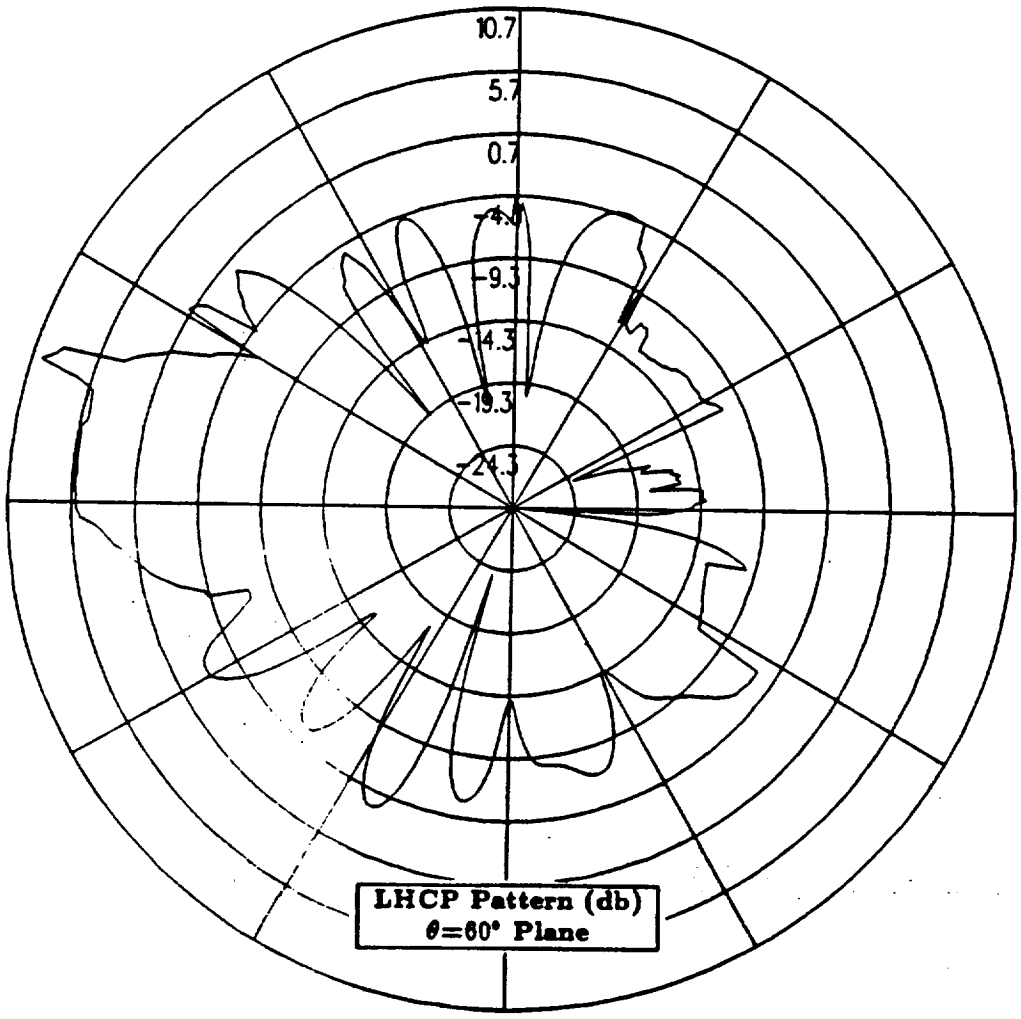

Figure 130: NEC-BSC calculated conical plane pattern 30° above the horizon for antenna location on the port side horizontal stabilizer for left hand circular polarization at 300 MHz. (Test Location 10)

1.12 Antenna Location Summary

In this section, the pattern coverage provided by each of the ten test locations is summarized. Section 1.12.1 summarizes test locations 1–3 where the antenna is located on the top center-line of the fuselage. Section 1.12.2 summarizes test locations 4–5 where the antenna is located on the center-line near the elliptical nose of the fuselage. Section 1.12.3 summarizes test locations 6–7 where the antenna is located on the fuselage 38.7° down from the top center-line. Section 1.12.4 summarizes test location 8 where the antenna is located on the port side of the vertical stabilizer. Section 1.12.5 summarizes test location 9 where the antenna is located on top of the vertical stabilizer and Section 1.12.6 summarizes test location 10 where the antenna is located on the port side horizontal stabilizer. Since the right hand circular polarized or co-polarized results are of primary importance in this report, the left hand circular polarized or cross-polarized results are not summarized here. These cross-polarized results are included only to provide additional information.

1.12.1 Test Locations 1–3

In Sections 1.2 - 1.4, the antenna is located at three different positions on the top center-line of the fuselage. The pattern coverage provided by each of the test locations is very similar. All three antenna locations provide good coverage in the region directly above the aircraft (i.e., over 30° above the horizon) as seen by the roll plane and elevation plane results. The patterns reach levels as high as 7–8 dB above the isotropic level directly above the aircraft. However in the horizon of the aircraft near the nose and the tail, the radiation levels are 15–20 dB below the levels in the main region and up to 12 dB below the isotropic level. The azimuth plane results demonstrate that the coverage in the horizon of the aircraft is very

poor with radiation levels which are as much as 10 dB below the isotropic level. As the conic cuts are taken further above the horizon of the aircraft, the levels gradually increase until they reach the isotropic level in the cut 30° above the horizon.

Comparing the patterns in Sections 1.2 - 1.4 with the patterns presented in Section 5.2 of Volume I shows that these test locations provide better coverage directly above the aircraft than the primary Boeing location. However, these test locations provide much worse coverage throughout the horizon of the aircraft. Also, the test locations do not provide adequate coverage in the horizon of the aircraft near the nose and tail which could compensate for the lack of coverage provided by the primary Boeing location in these regions. Therefore, none of these three antennas located on the top center-line of the fuselage can be combined with the primary Boeing location in order to achieve the pattern and polarization coverage required of the antenna system.

1.12.2 Test Locations 4–5

In Sections 1.5 and 1.6, the antenna is located at two different positions on the center-line of the fuselage near the aircraft nose. The pattern coverage provided by both of the test locations is very similar. Both antenna locations provide good coverage in the region directly above the aircraft and towards the nose as seen by the roll plane and elevation plane results. The patterns reach levels as high as 6–7 dB above the isotropic level directly above the aircraft. In the horizon of the aircraft near the nose, the radiation levels are improved so that they are as little as 4 dB below the isotropic level. However, the radiation levels in the horizon of the aircraft near the tail are up to as much as 20 dB below the isotropic level. The azimuth plane results demonstrate that the coverage in the horizon of the aircraft is still poor with radiation levels which are as much as 5 dB below the isotropic

level near the nose of the aircraft. As the conic cuts are taken further above the horizon of the aircraft, however, these levels gradually increase until they are up to 5 dB above the isotropic level in the cut 30° above the horizon.

Comparing the patterns in Sections 1.5 and 1.6 with the patterns presented in Section 5.2 of Volume I shows that these test locations provide slightly better coverage directly above the aircraft than the primary Boeing location. These test locations also provide slightly better coverage in the horizon of the aircraft near the nose. Although the test locations do not provide adequate coverage in the horizon of the aircraft near the tail which could compensate for the lack of coverage provided by the primary Boeing location in this region, they do improve the coverage in the horizon of the aircraft near the nose. Therefore, either one of these antennas located on the center-line of the fuselage near the nose can be combined with the primary Boeing location in order to improve the pattern and polarization coverage of the antenna system.

1.12.3 Test Locations 6–7

In Sections 1.7 and 1.8, the antenna is located at two different positions on the port side of fuselage 38.7° down from the top center-line. The pattern coverage provided by both of the test locations is very similar. Both antenna locations provide good coverage in the region directly above the aircraft as seen by the roll plane and elevation plane results. The patterns reach levels as high as 5 dB above the isotropic level directly above the aircraft. The azimuth plane results demonstrate that the coverage in the horizon of the aircraft is adequate with radiation levels near the isotropic level in the main region. However in the horizon of the aircraft near the nose and the tail, the radiation levels are up to 15 dB below the isotropic level. As the conic cuts are taken further above the horizon of the

aircraft, the levels near the nose and tail gradually increase, however, they still are 5–10 dB below the levels in the main region of these patterns.

Comparing the patterns in Sections 1.7 and 1.8 with the patterns presented in Section 5.2 of Volume I shows that these test locations provide very similar coverage to that provided by the primary Boeing location. Therefore, these test locations provide good coverage throughout all regions except in the horizon of the aircraft near the nose and tail. Since these test locations contain the same problems as the primary Boeing location in these regions, neither of these antennas located on the port side of fuselage 38.7° down from the top center-line can be combined with the primary Boeing location in order to achieve the pattern and polarization coverage required of the antenna system.

1.12.4 Test Location 8

In Section 1.9, the antenna is located on the port side of the vertical stabilizer. This antenna location provides good coverage in the region directly to the left of the aircraft as seen by the roll plane and azimuth plane results. The patterns reach levels as high as 8–9 dB above the isotropic level in this region. However, the radiation levels in the elevation plane are up to 12 dB below the isotropic level. Therefore, the coverage is very poor in the region directly above the aircraft and in the horizon of the aircraft near the nose and tail.

Comparing the patterns in Section 1.9 with the patterns presented in Section 5.2 of Volume I shows that this test location provides better coverage directly to the left of the aircraft than the primary Boeing location. However, this test location provides much worse coverage throughout the elevation plane. The test location does not provide adequate coverage in the horizon of the aircraft near the nose and tail which could compensate for the lack of coverage provided by the primary Boeing location in these regions. Therefore, this antenna located on the

port side of the vertical stabilizer cannot be combined with the primary Boeing location in order to achieve the pattern and polarization coverage required of the antenna system.

1.12.5 Test Location 9

In Section 1.10, the antenna is located on top of the vertical stabilizer. In the roll plane, the elevation plane and the azimuth plane, the radiation patterns all contain significant lobes. Although the overall radiation levels are above the isotropic level in the majority of the roll plane and the elevation plane, the lobing which is present is not desirable. The radiation levels in the azimuth plane and the conic cuts are below the isotropic level and also contain these lobes. Because of the lobing, this antenna located on top of the vertical stabilizer is not viable and cannot be combined with the primary Boeing location in order to achieve the pattern and polarization coverage required of the antenna system.

1.12.6 Test Location 10

In Section 1.11, the antenna is located on the port side horizontal stabilizer. This antenna location provides good coverage in the region directly above the aircraft as seen by the roll plane and elevation plane results. The patterns reach levels as high as 8 dB above the isotropic level directly above the aircraft. However in the horizon of the aircraft near the nose and the tail, the radiation levels are 15–20 dB below the levels in the main region and up to 12 dB below the isotropic level. The azimuth plane results demonstrate that the coverage in the horizon of the aircraft is very poor with radiation levels which are as much as 15 dB below the isotropic level. As the conic cuts are taken further above the horizon of the aircraft, the levels gradually increase up to 5 dB below the isotropic level.

Comparing the patterns in Section 1.11 with the patterns presented in Section 5.2 of Volume I shows that this test location provides better coverage directly above the aircraft than the primary Boeing location. However, this test location provides much worse coverage throughout the horizon of the aircraft. Also, the test location does not provide adequate coverage in the horizon of the aircraft near the nose and tail which could compensate for the lack of coverage provided by the primary Boeing location in these regions. Therefore, this antenna located on the port side horizontal stabilizer cannot be combined with the primary Boeing location in order to achieve the pattern and polarization coverage required of the antenna system.

1.13 Conclusions

This chapter illustrates that none of the test locations provide adequate coverage in the horizon of the aircraft near both the nose and the tail which could compensate for the lack of coverage provided by the primary Boeing location in these regions. Therefore, none of the test locations investigated achieves the desired pattern and polarization coverage when combined with the primary Boeing location. However, Sections 1.5 and 1.6 contain antenna locations on the center-line of the fuselage near the nose which improve the coverage in the horizon of the aircraft near the nose. By combining one of these antenna locations with the primary Boeing location, the desired pattern and polarization coverage can be achieved in all regions except in the horizon of the aircraft near the tail.

However, the test locations investigated in Sections 1.5 and 1.6 which involve the presence of the antenna on the center-line of the fuselage near the nose of the aircraft are not physically realizable on the actual P-3C aircraft. These test locations are not acceptable because placing an antenna at these positions would

interfere with the aerodynamics of the aircraft. Therefore, the Naval Air Test Center suggested that an alternative circular polarized antenna be placed in the radome which is located in the nose of the P-3C aircraft. This is done in the following chapter.

Chapter 2

Alternative Antenna

2.1 Introduction

In this chapter, a model for an alternative circular polarized antenna placed in the radome located in the nose of the P-3C aircraft is developed using the NEC-BSC. The NEC-BSC is then used to determine the pattern and polarization coverage which is provided by this antenna configuration. The antenna to be modeled represents a Dorne & Margolin DM C99-series airborne UHF satellite communications antenna. The objective is to determine whether this antenna placed in the nose of the P-3C aircraft will provide the desired coverage in the horizon of the aircraft near the nose. All of the results found in this chapter have been referenced to an isotropic radiator.

Section 2.2 defines the procedure used in the NEC-BSC to model the DM C99-series UHF SATCOM antenna and validates this model. In Section 2.3, a model is developed to represent the DM C99-4 antenna placed in the radome located in the nose of the P-3C aircraft. This model could potentially be made to fit in the radome area. In Section 2.4, this model is used and radiation patterns are calculated in the roll plane, the elevation plane, the azimuth plane and conical cuts from 10° to 30° above the horizon for both right hand and left hand circular polarizations.

2.2 DM C99-series Antenna Model

The Dorne & Margolin DM C99-4 airborne UHF satellite communications antenna is shown in Figure 131. This antenna is designed to produce a very broad beam radiation pattern with minimal gain variation over the entire upper hemisphere. The radiation patterns of the DM C99-series UHF SATCOM antenna could not be matched using any of the six built-in antenna types available in the NEC-BSC. Therefore, the linear interpolated table look-up feature of the NEC-BSC had to be used in order to match the calculated patterns with the measured patterns provided by Dorne & Margolin. The procedure used to implement the table look-up feature is as follows. First, the magnitude and phase of both the E_θ and E_ϕ components must be read from the manufacturers antenna pattern and input into the NEC-BSC. Then the right hand circular polarized pattern must be calculated using the NEC-BSC. If this calculated right hand circular polarized pattern matches the measured pattern provided by the manufacturer, then the model for the antenna is accurate.

Dorne & Margolin has provided antenna system information for the DM C99-series airborne UHF satellite communication antenna in free space. The measured results for the E_θ and E_ϕ components at 244 MHz are compared to the data input in the NEC-BSC in Figures 132 and 133, respectively. From these E_θ and E_ϕ components, the right hand circular polarization is calculated using the NEC-BSC. The calculated and measured patterns at 244 MHz for right hand circular polarization are shown for the DM C99-series antenna in Figure 134. The measured results for the E_θ and E_ϕ components at 318 MHz are compared to the data input in the NEC-BSC in Figures 135 and 136, respectively. From these E_θ and E_ϕ components, the right hand circular polarization is calculated using the NEC-BSC. The calculated and measured patterns at 318 MHz for right hand circular polarization are shown for the DM C99-series antenna in Figure 137. Note that

the results are plotted in relative gain. The calculated and measured right hand circular polarized results agree to within 1 dB throughout the pattern at both 244 MHz and 318 MHz. Therefore, the table look-up feature of the NEC-BSC provides an accurate representation of the actual DM C99-series antenna.

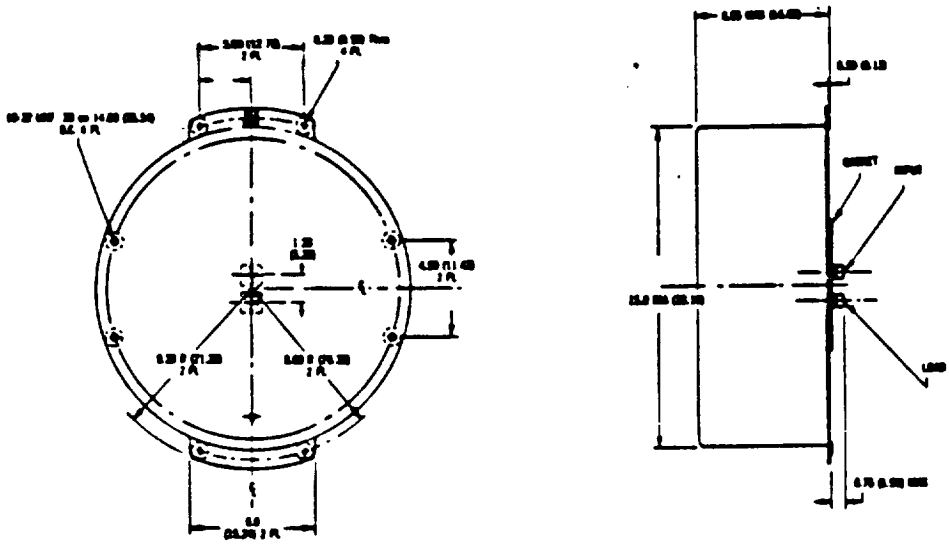

Figure 131: DM C99-4 airborne UHF satellite communication antenna of Dorne & Margolin.

ORIGINAL PAGE IS
OF POOR QUALITY

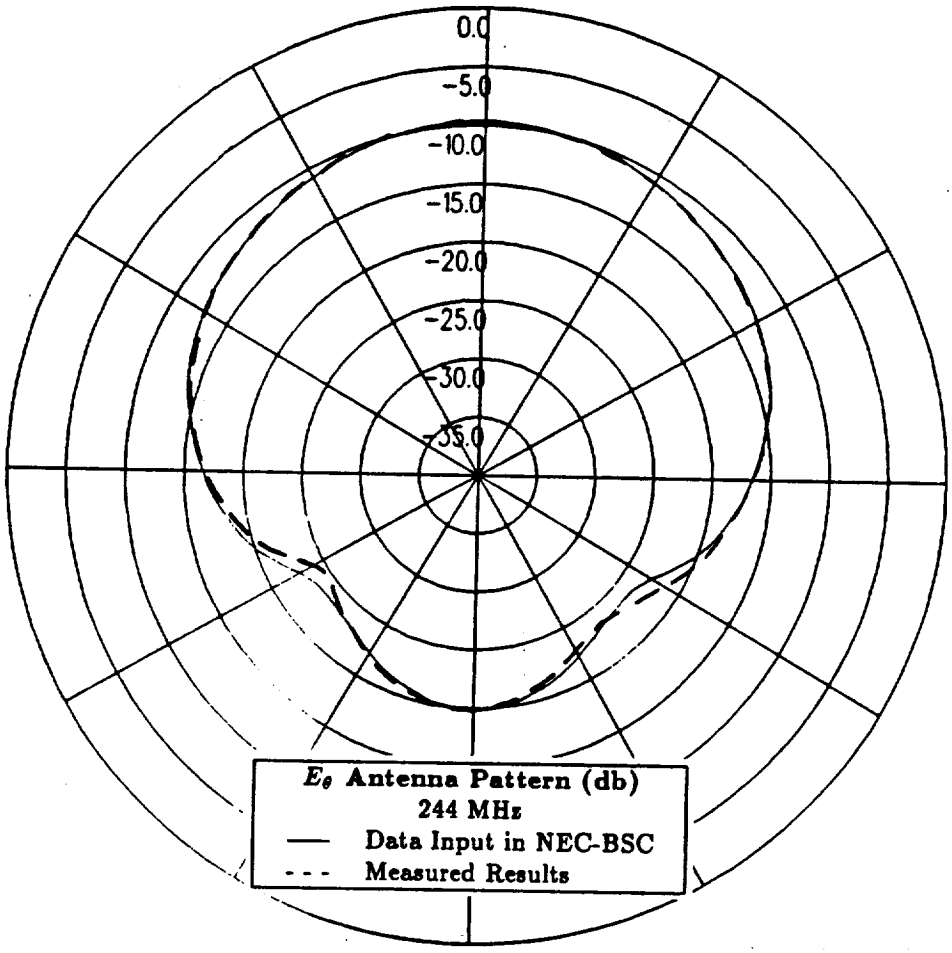

Figure 132: E_θ antenna pattern at 244 MHz for DM C99-series antenna in free space.

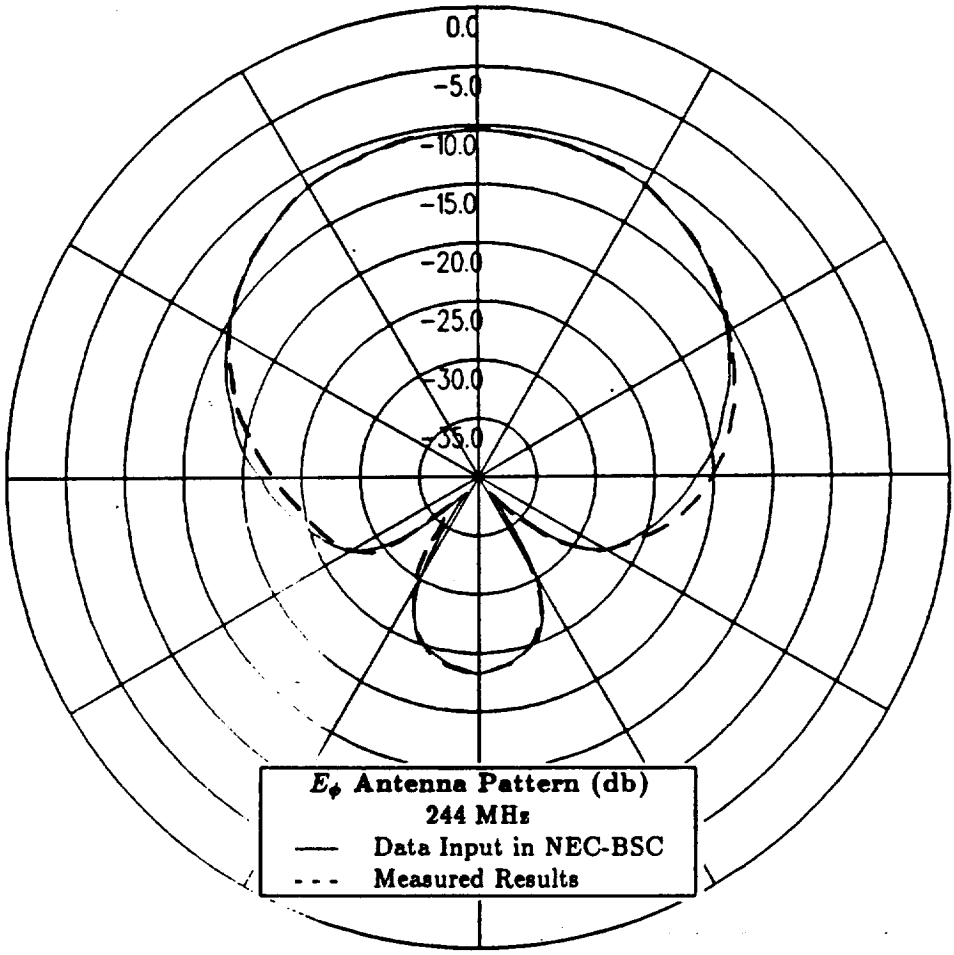

Figure 133: E_ϕ antenna pattern at 244 MHz for DM C99-series antenna in free space.

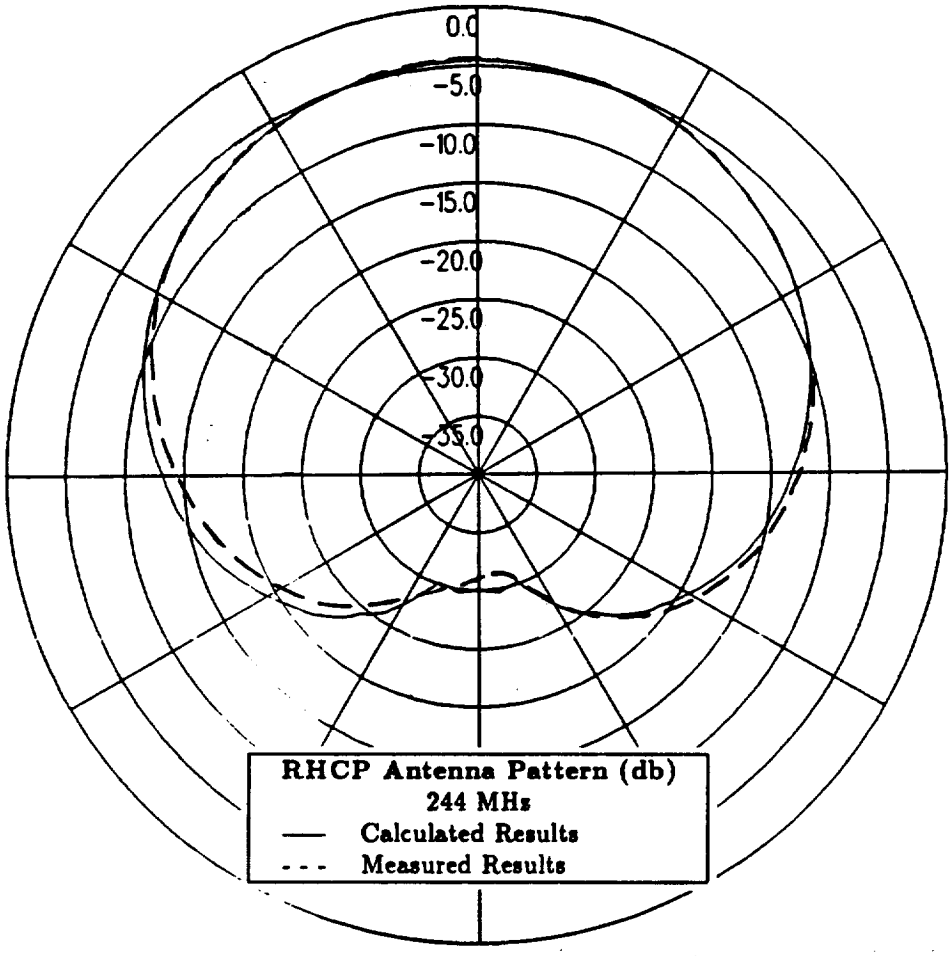

Figure 134: Right hand circular polarized antenna pattern at 244 MHz for DM C99-series antenna in free space.

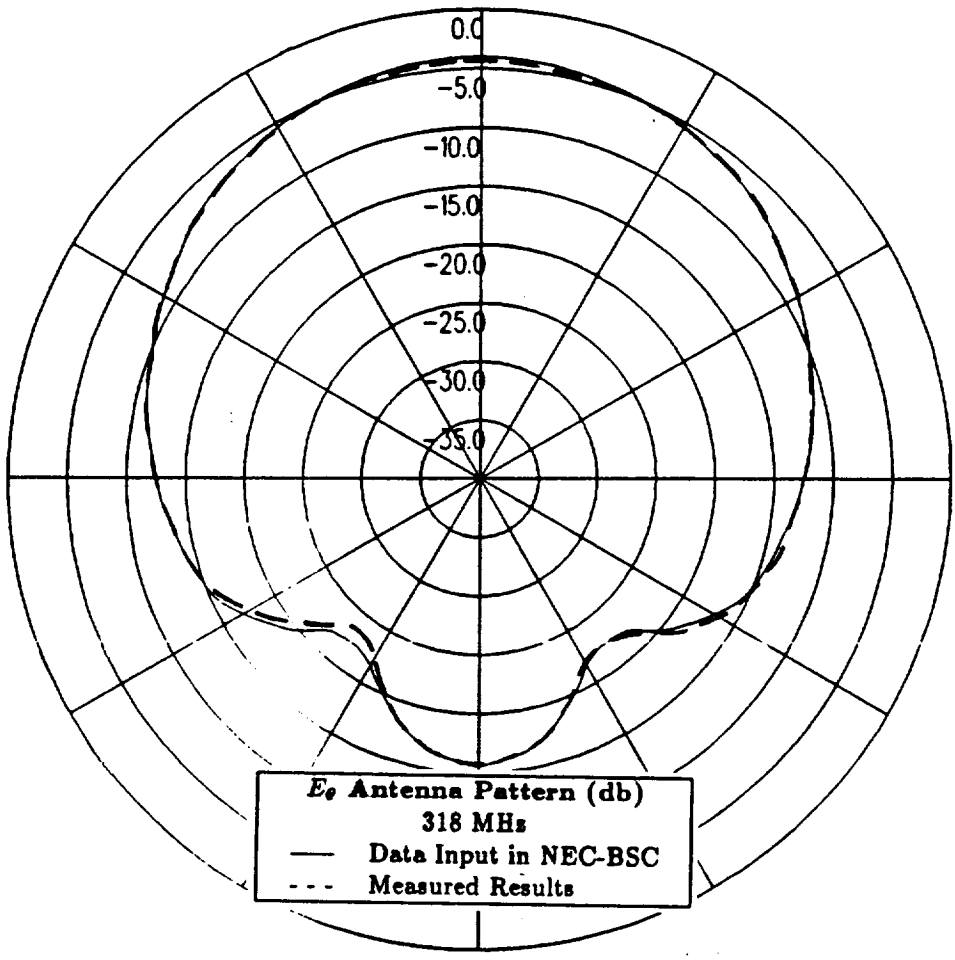

Figure 135: E_θ antenna pattern at 318 MHz for DM C99-series antenna in free space.

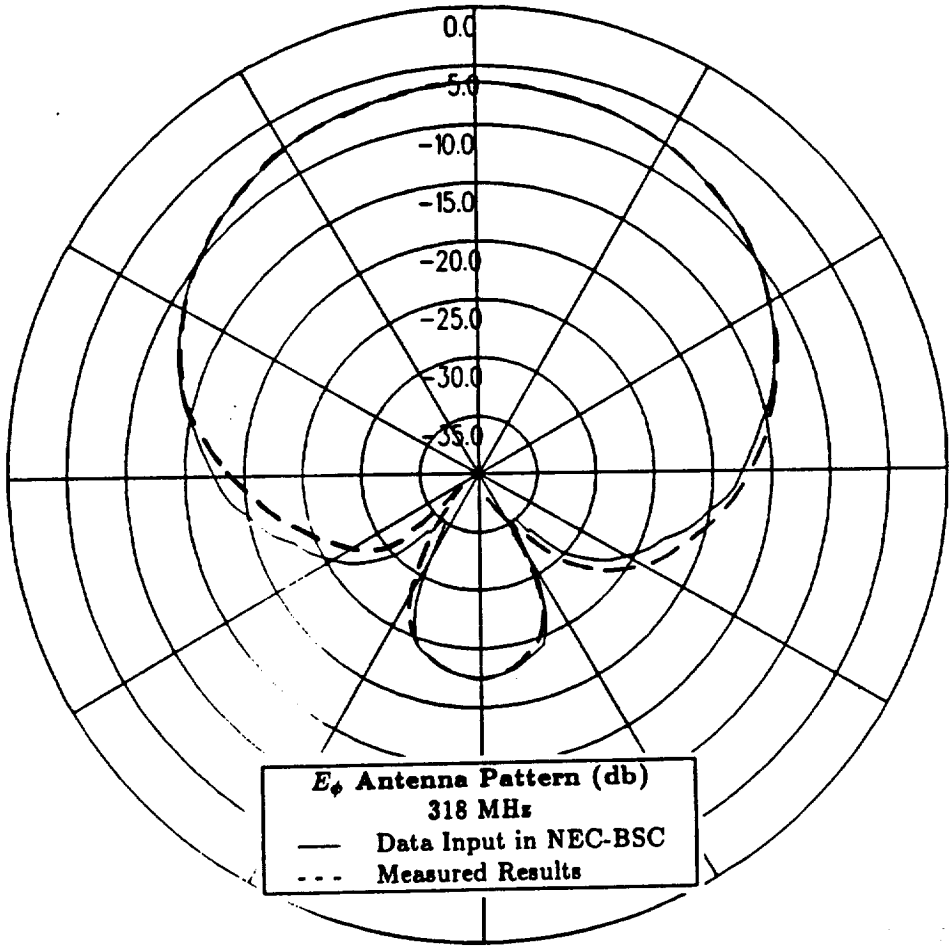

Figure 136: E_ϕ antenna pattern at 318 MHz for DM C99-series antenna in free space.

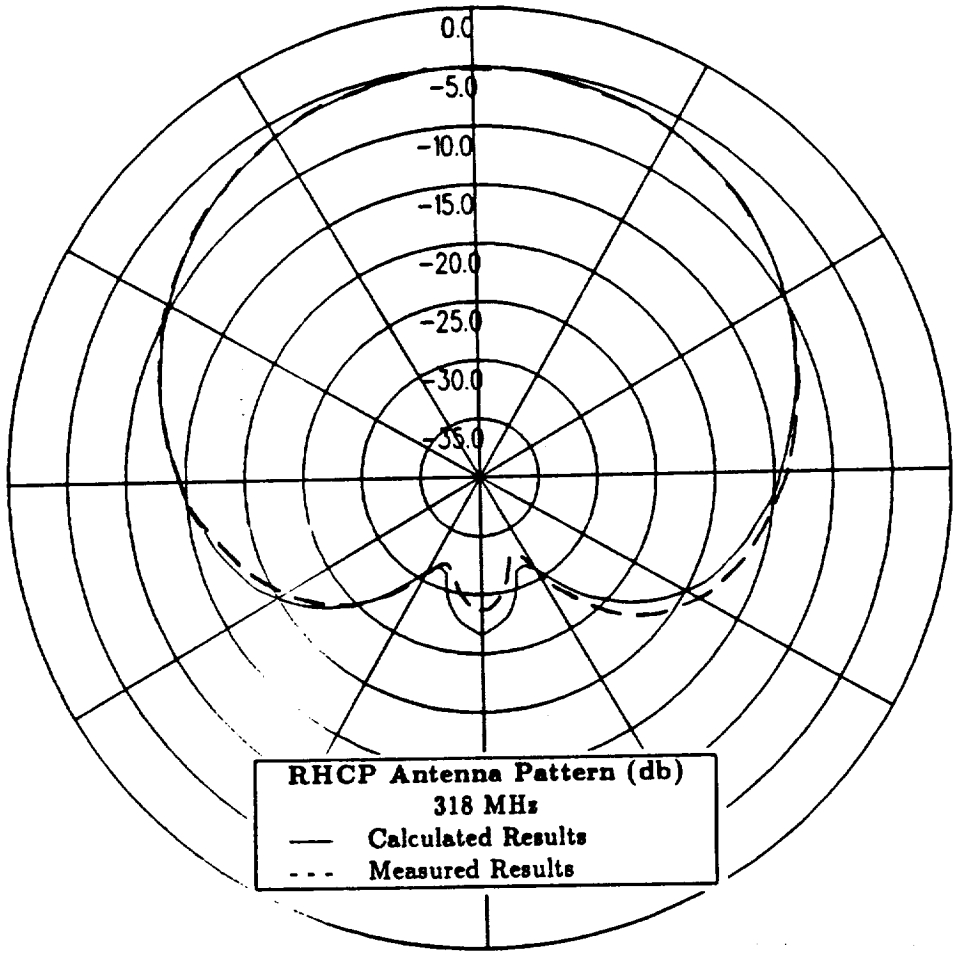

Figure 137: Right hand circular polarized antenna pattern at 318 MHz for DM C99-series antenna in free space.

2.3 DM C99-series Antenna in Radome

In this section, a model is developed to represent the DM C99-series antenna placed in the radome located in the nose of the P-3C aircraft. An illustration of the forward section of the actual P-3C aircraft which includes a visual model for the antenna is given in Figure 138. The visual model used to represent the DM C99-series is a drooped crossed dipole antenna which is curved to approximate the domed surface of a DM C99-2 antenna. Because the table look-up feature of the NEC-BSC is used to represent the antenna, this drooped crossed dipole antenna is not used when the radiation patterns are calculated. It is only included in the figure for visualizing the location of the antenna in the radome.

Because of the location of the antenna in the nose of the aircraft, the antenna will not interact with the fuselage of the aircraft, the wings or the vertical and horizontal stabilizers. Therefore, these details of the actual P-3C aircraft do not need to be included in the aircraft model. Also, the surface of the radome shown in Figure 138 is electrically invisible and does not need to be included in the aircraft model. Therefore, the only significant structure which will affect the radiation patterns for this antenna location is the surface of the fuselage to which the radome is attached.

To model this fuselage surface, a twelve-sided flat plate is tilted at an angle of 66° corresponding to the actual tilt of the fuselage surface. An illustration of this surface with the antenna model present includes both a side view and a front view and is given in Figure 139. The important physical aspects as pertains to positioning this antenna are that the antenna is located 18.5 inches to the right of and 10 inches above the radome center-line and that the angle which the antenna makes with the center-line of the aircraft fusleage is 40° as denoted in the figure.

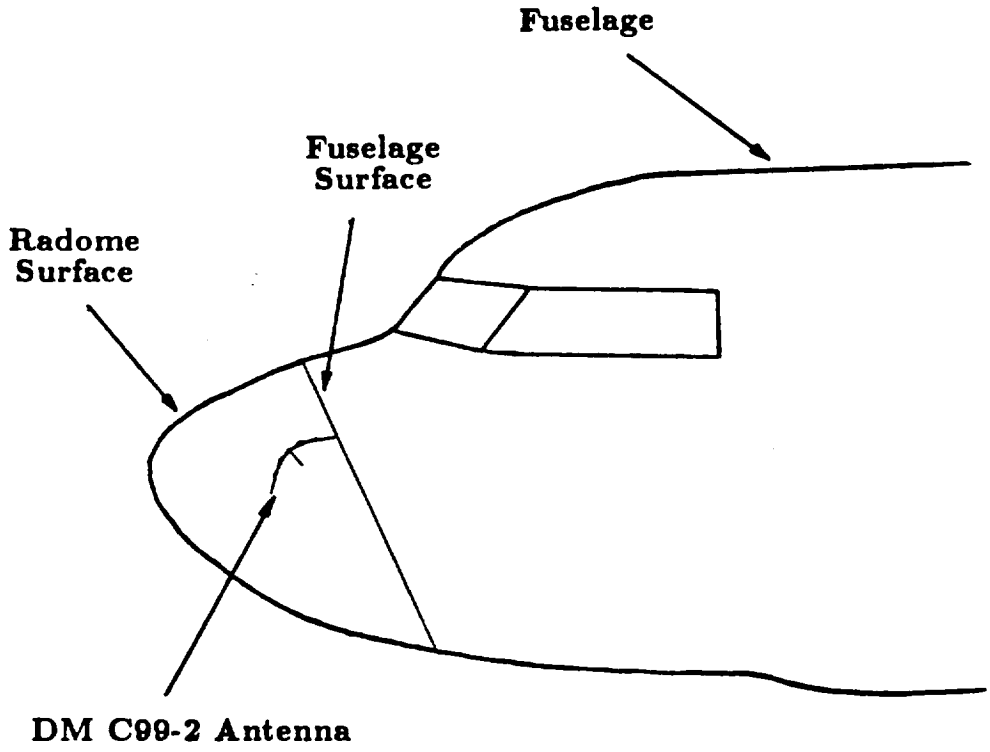

Figure 138: Geometry of the forward section of the actual P-3C aircraft which includes a model for the DM C99-series antenna.

Side View

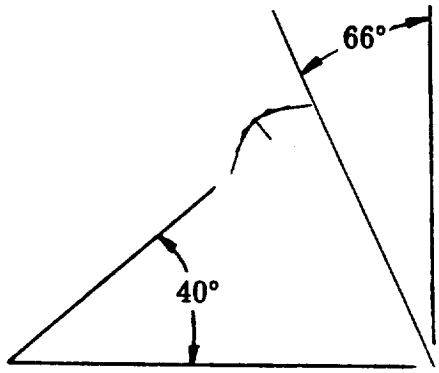

Front View

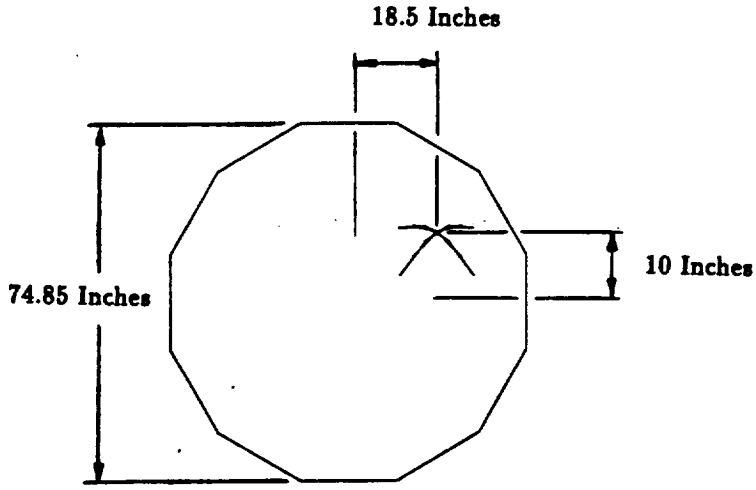

Figure 139: Geometry of twelve-sided flat plate used to model the fuselage surface which includes a model for the DM C99-series antenna.

2.4 Radiation Patterns for DM C99-series Antenna in Radome

In this section, the radiation patterns are computed with the NEC-BSC for the model developed in the previous section to represent the DM C99-series antenna placed in the radome located in the nose of the P-3C aircraft. The calculated results at 244 MHz for the right hand circular polarized or co-polarized fields are shown for the roll plane in Figure 140, for the elevation plane in Figure 141, for the azimuth plane in Figure 142 and for the conical planes 10°, 20° and 30° above the horizon in Figures 143, 144 and 145, respectively. For completeness, the left hand circular polarized or cross-polarized results are also included. These cross-polarized results are shown for the roll plane in Figure 146, for the elevation plane in Figure 147, for the azimuth plane in Figure 148 and for the conical planes 10°, 20° and 30° above the horizon in Figures 149, 150 and 151, respectively.

The results at 318 MHz also have been calculated using the NEC-BSC. These results are almost identical to the results calculated at 244 MHz for each of the pattern cuts taken. Therefore, the results calculated at 318 MHz are not included here.

For this antenna configuration, the radiation patterns maintain levels which are above the isotropic level in the 30° conic section directly off the nose of the aircraft as seen by the elevation plane and azimuth plane results. Although this antenna configuration does not provide the desired coverage directly above the aircraft or in the region near the tail of the aircraft, it does provide the desired coverage in the region directly off the nose. Therefore, the DM C99-4 antenna, which is the most likely candidate of this series for a radome location, combined with the Batwing antenna located at the primary Boeing location, which is investigated in Chapter 5 of Volume I, will provide the desired pattern and polarization coverage in all regions except in the horizon of the aircraft near the tail.

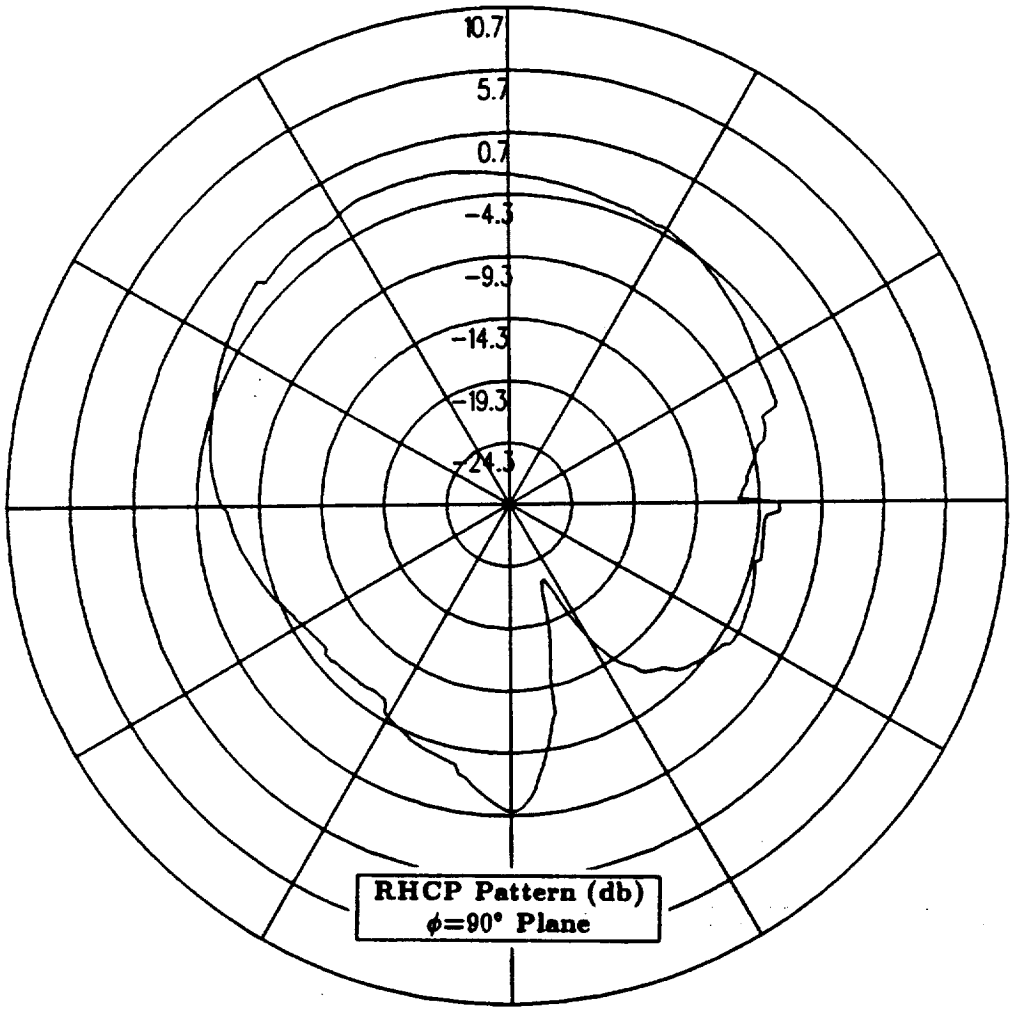

Figure 140: Roll plane pattern for DM C99-series antenna placed in radome located in the nose of the P-3C aircraft for right hand circular polarization at 244 MHz.

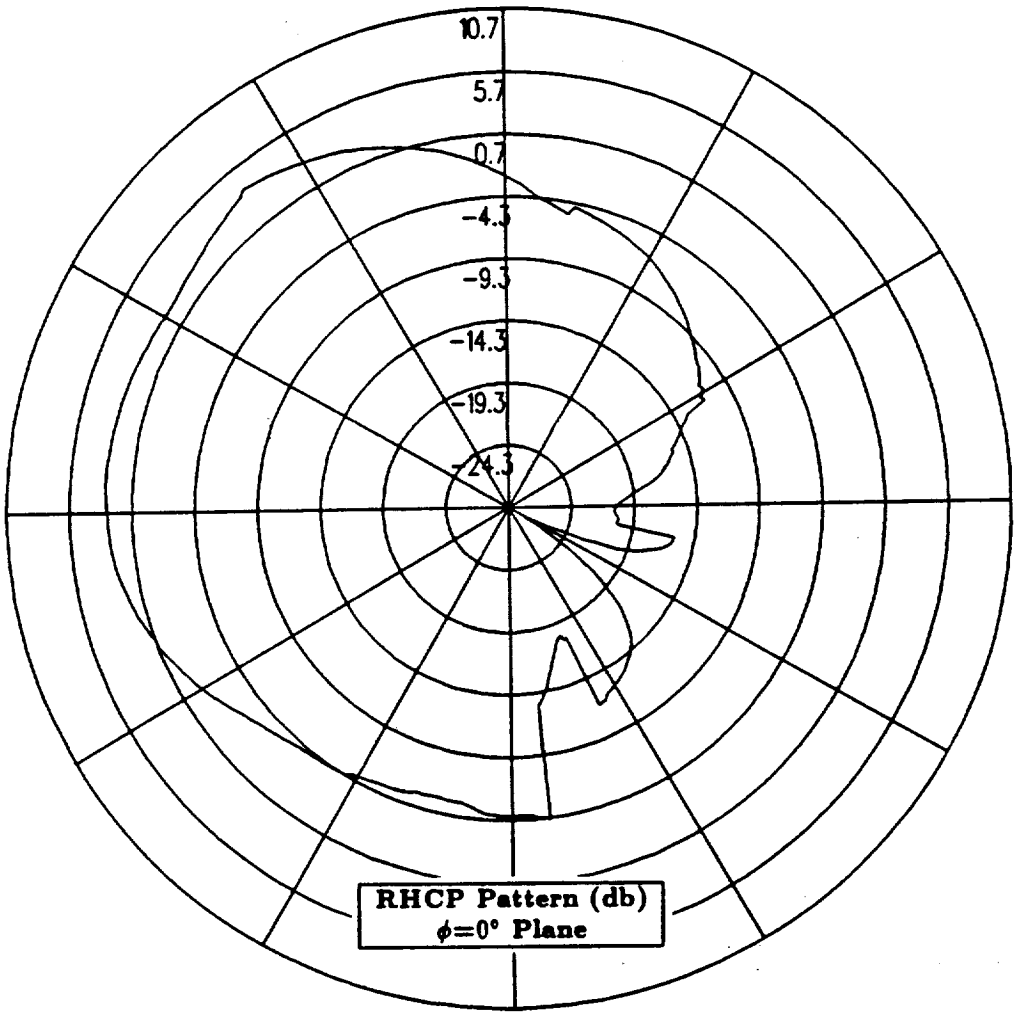

Figure 141: Elevation plane pattern for DM C99-series antenna placed in radome located in the nose of the P-3C aircraft for right hand circular polarization at 244 MHz.

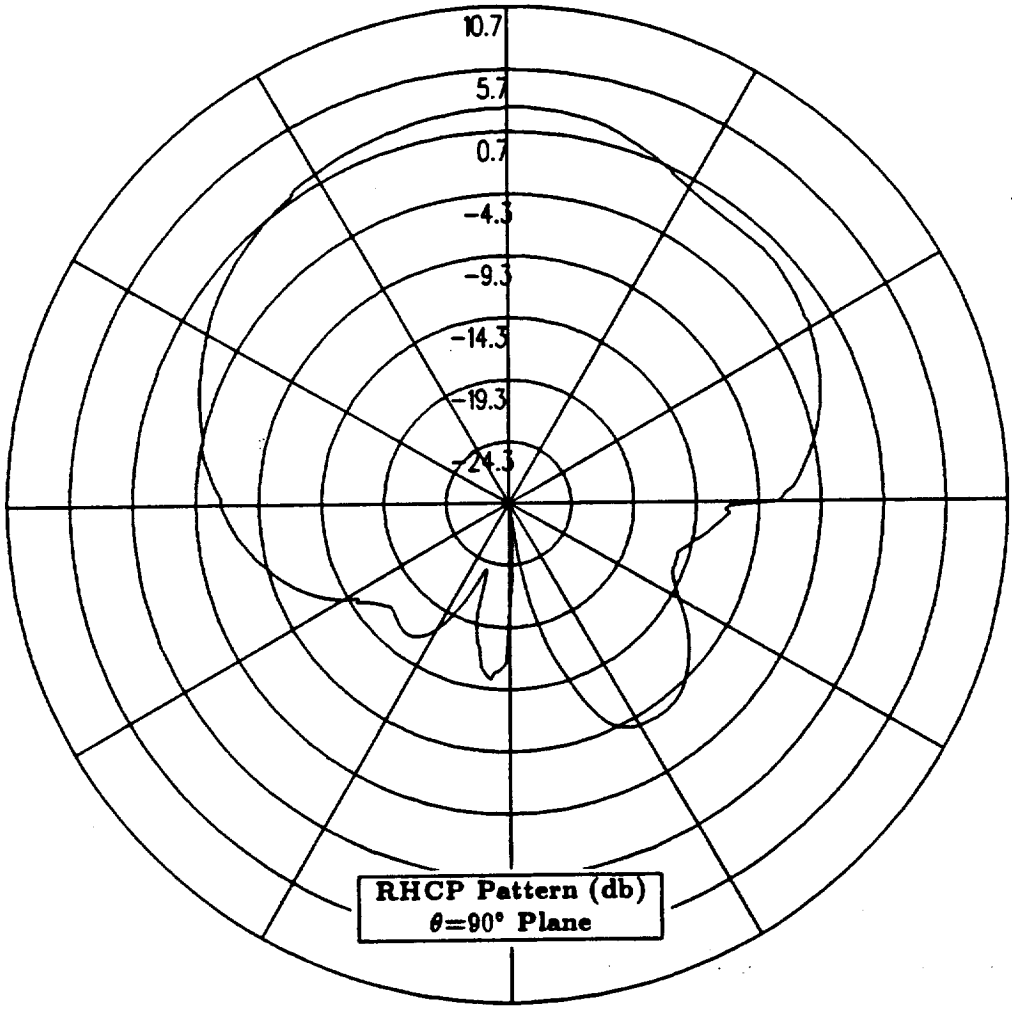

Figure 142: Azimuth plane pattern for DM C99-series antenna placed in radome located in the nose of the P-3C aircraft for right hand circular polarization at 244 MHz.

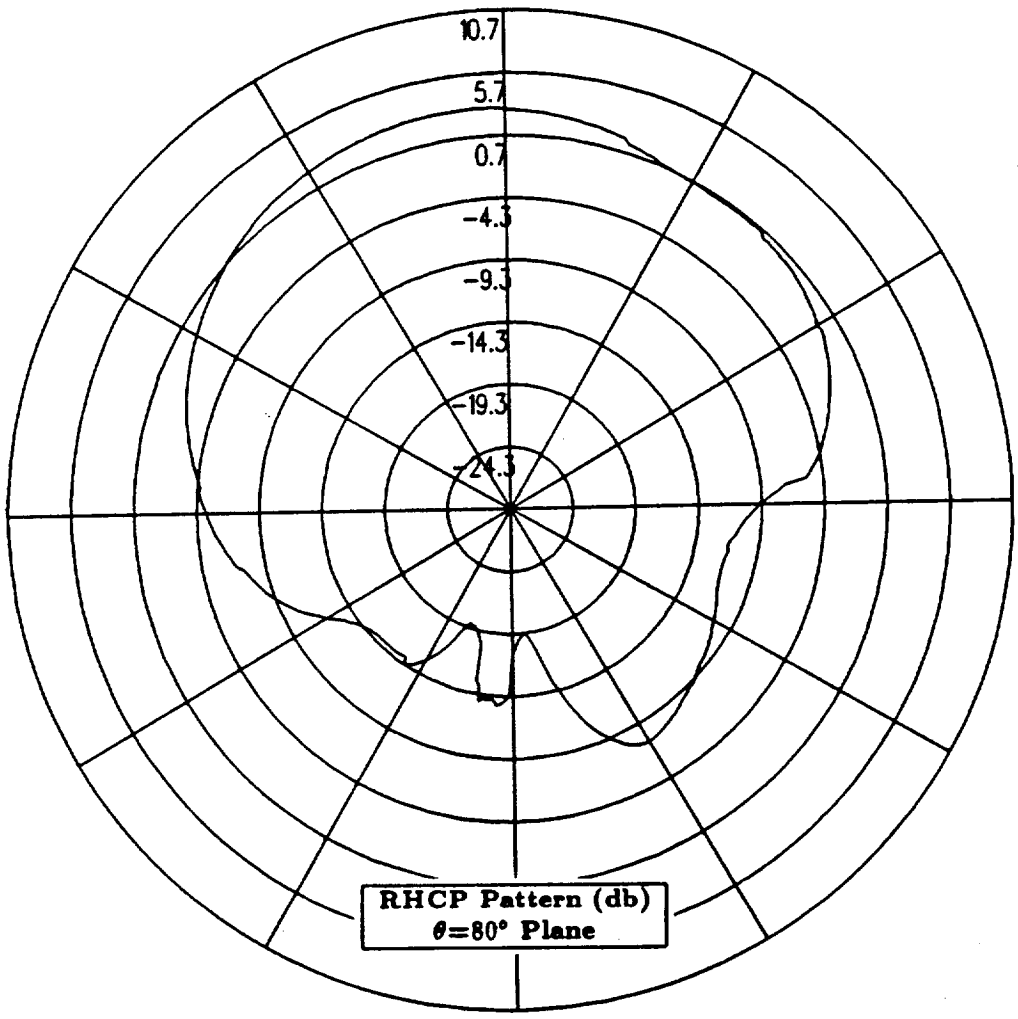

Figure 143: Conical plane pattern 10° above the horizon for DM C99-series antenna placed in radome located in the nose of the P-3C aircraft for right hand circular polarization at 244 MHz.

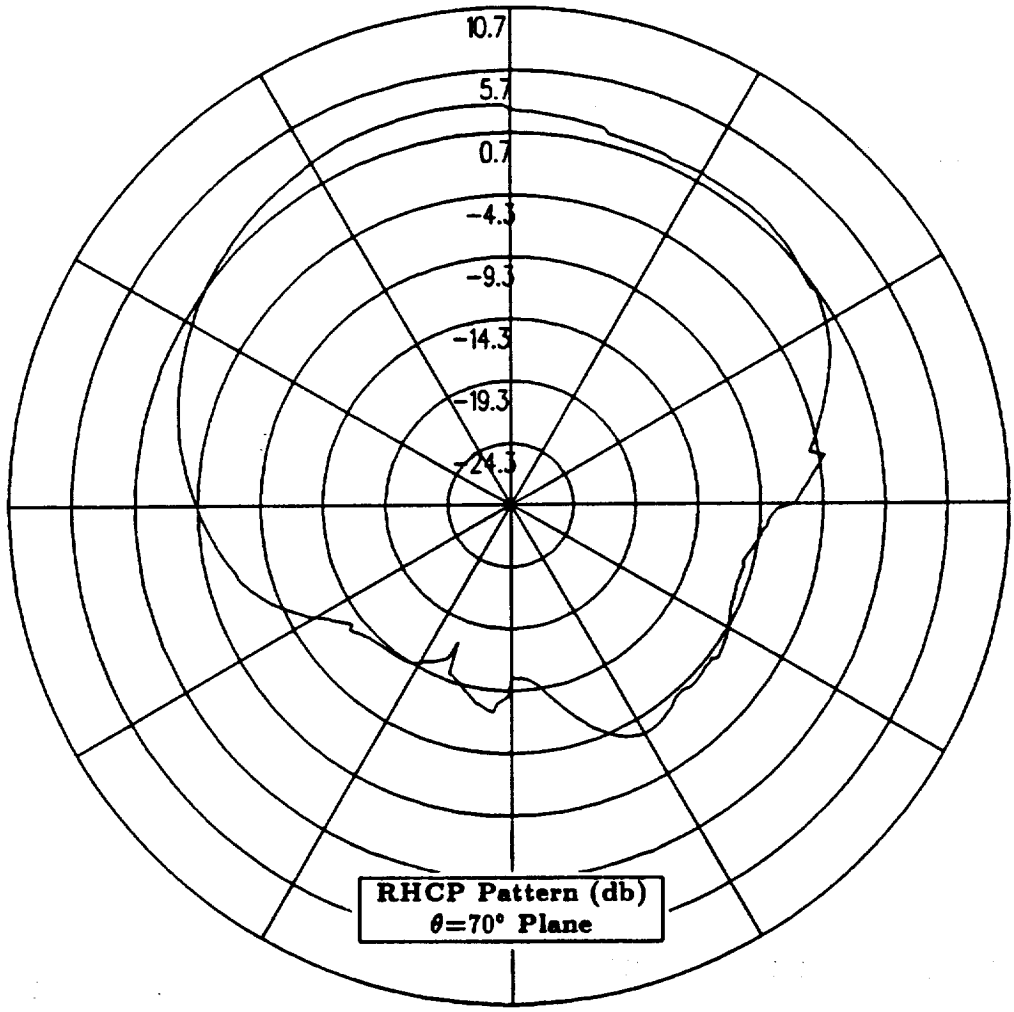

Figure 144: Conical plane pattern 20° above the horizon for DM C99-series antenna placed in radome located in the nose of the P-3C aircraft for right hand circular polarization at 244 MHz.

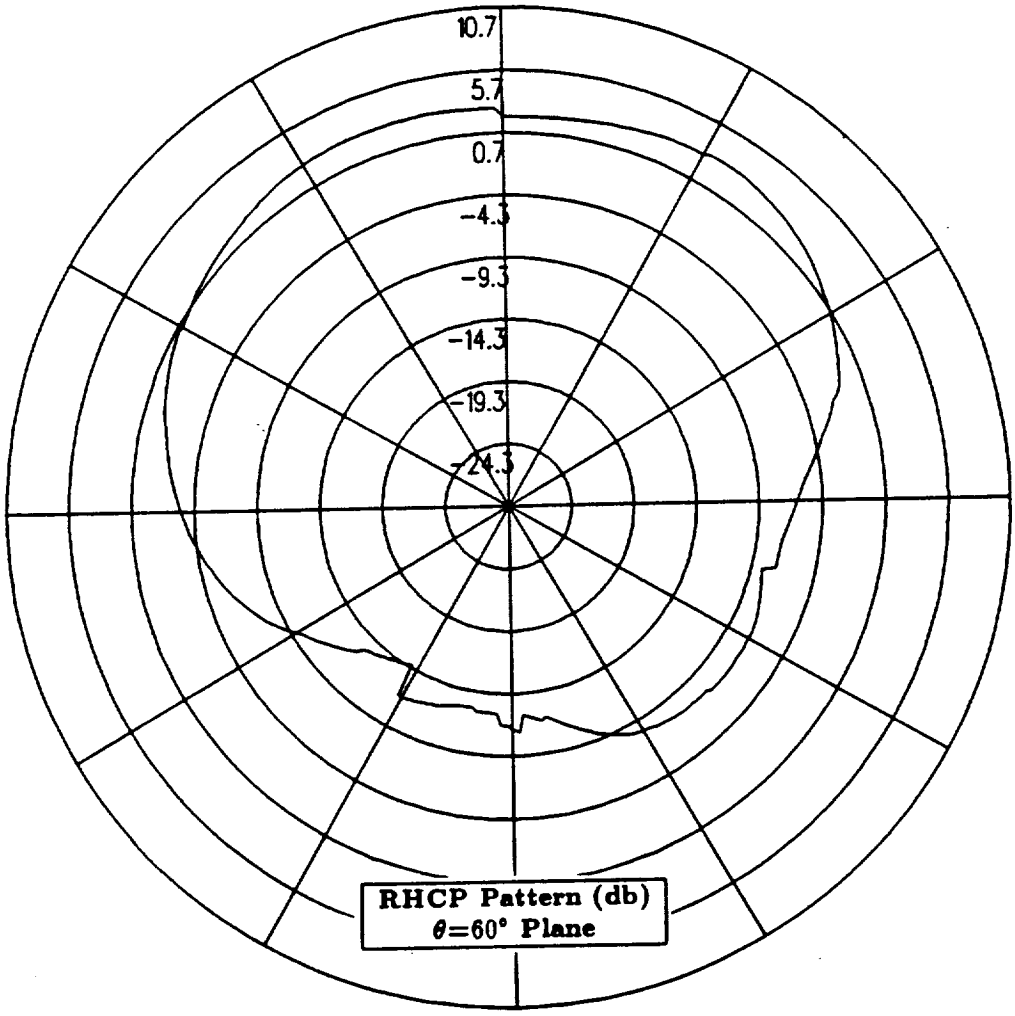

Figure 145: Conical plane pattern 30° above the horizon for DM C99-series antenna placed in radome located in the nose of the P-3C aircraft for right hand circular polarization at 244 MHz.

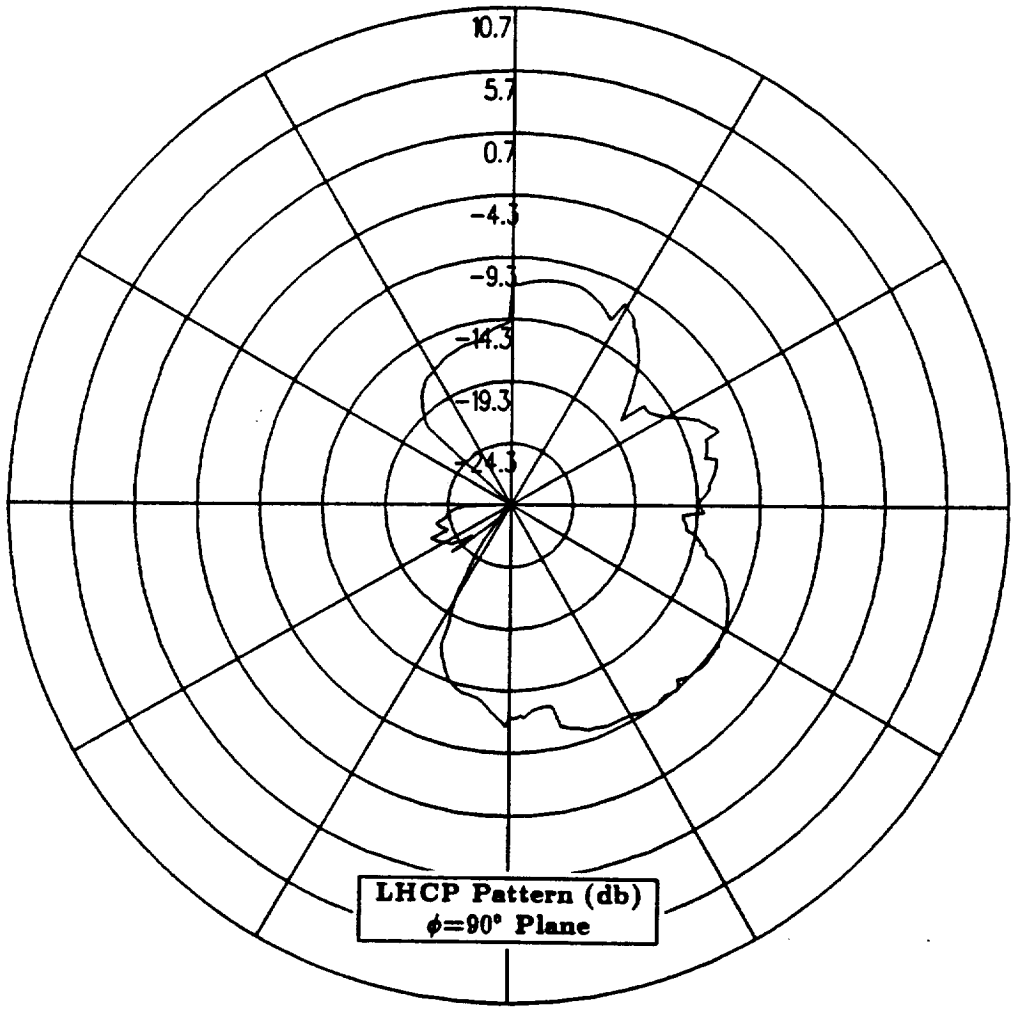

Figure 146: Roll plane pattern for DM C99-series antenna placed in radome located in the nose of the P-3C aircraft for left hand circular polarization at 244 MHz.

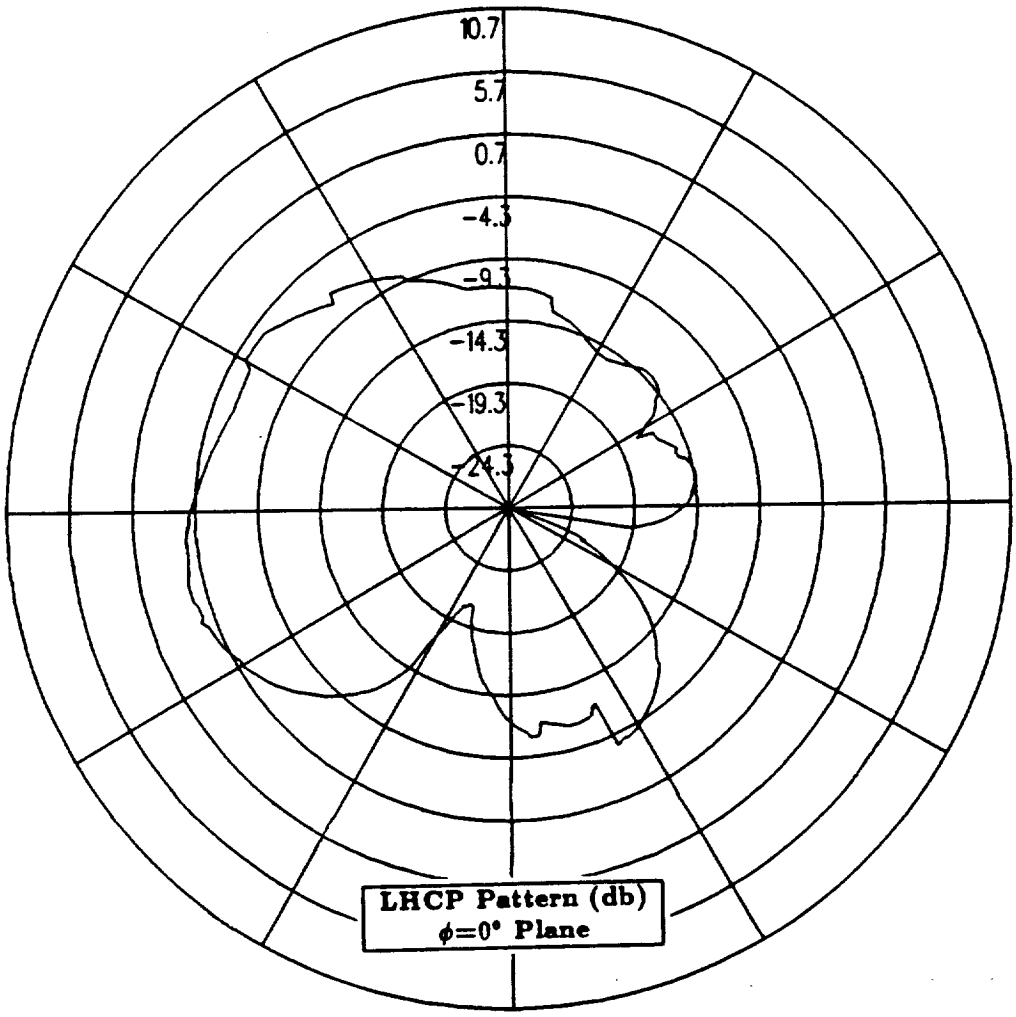

Figure 147: Elevation plane pattern for DM C99-series antenna placed in radome located in the nose of the P-3C aircraft for left hand circular polarization at 244 MHz.

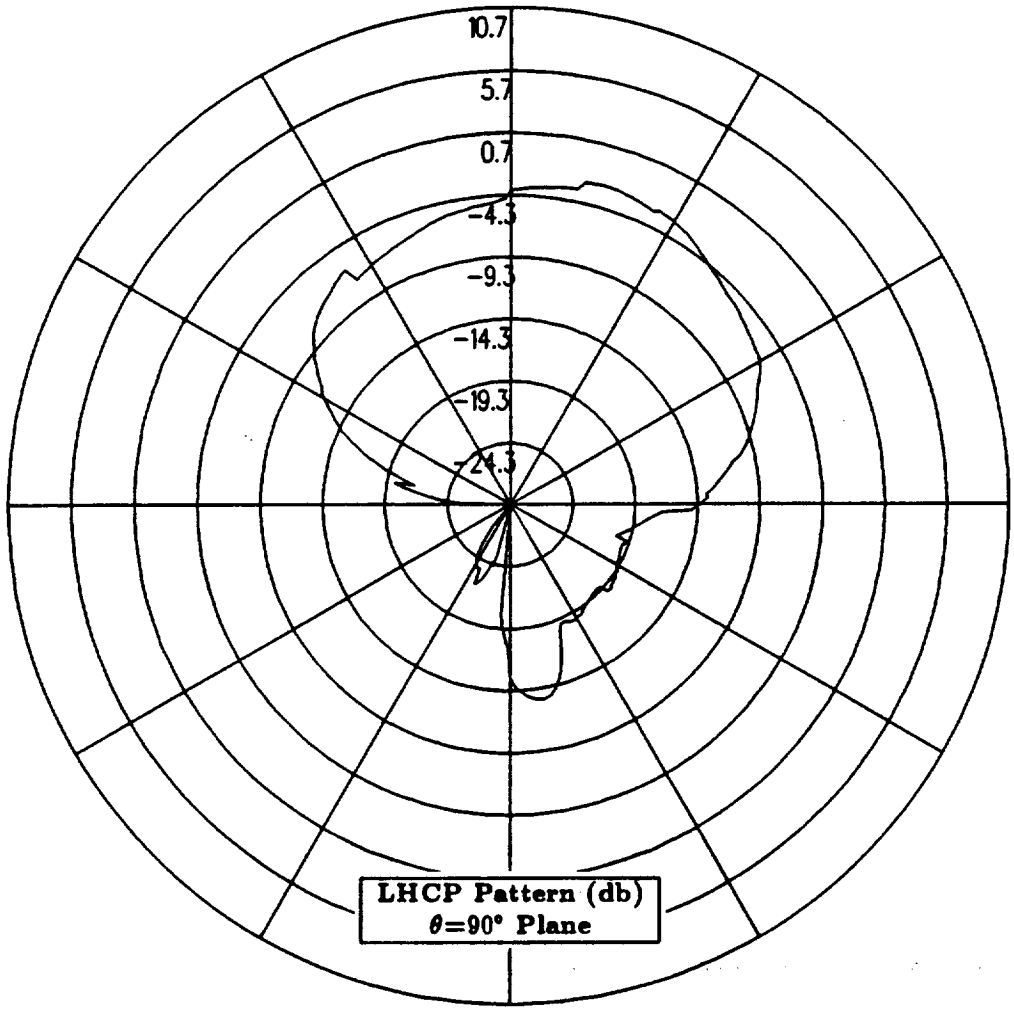

Figure 148: Azimuth plane pattern for DM C99-series antenna placed in radome located in the nose of the P-3C aircraft for left hand circular polarization at 244 MHz.

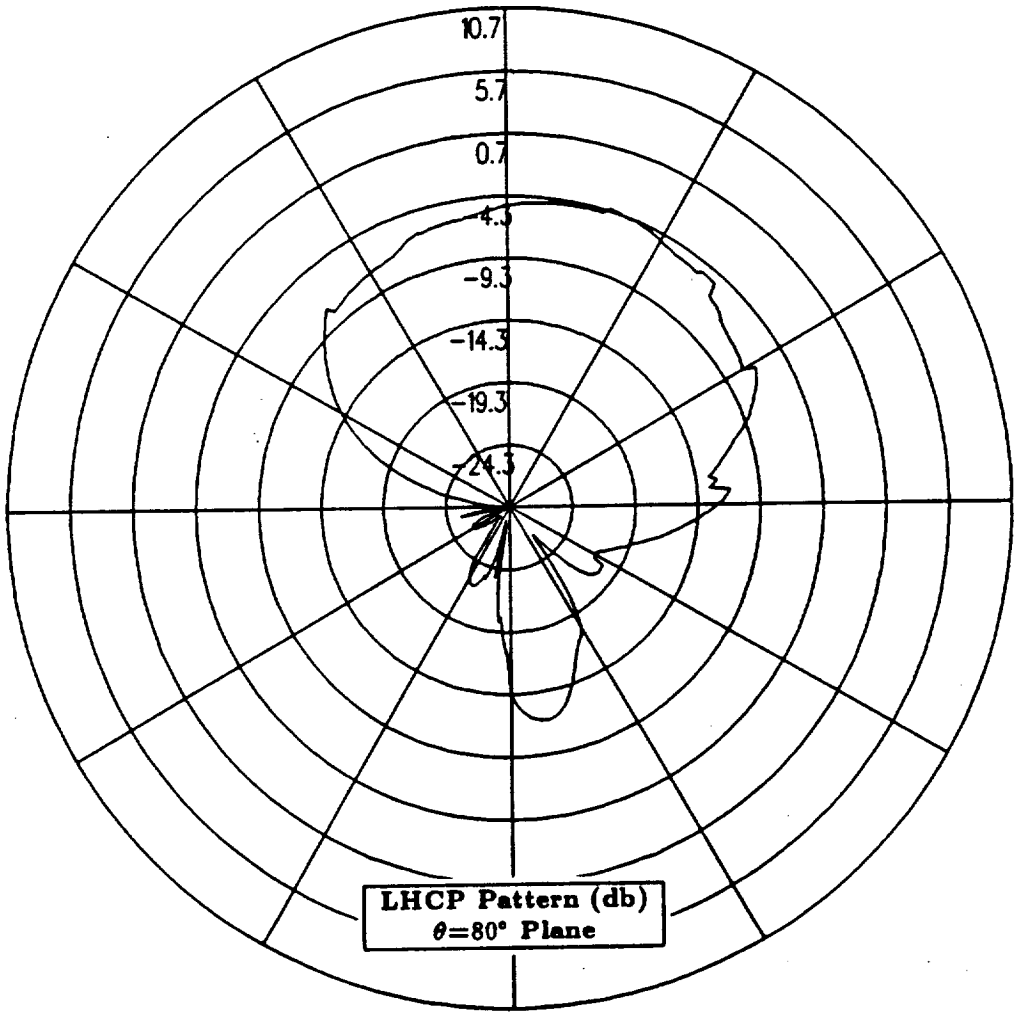

Figure 149: Conical plane pattern 10° above the horizon for DM C99-series antenna placed in radome located in the nose of the P-3C aircraft for left hand circular polarization at 244 MHz.

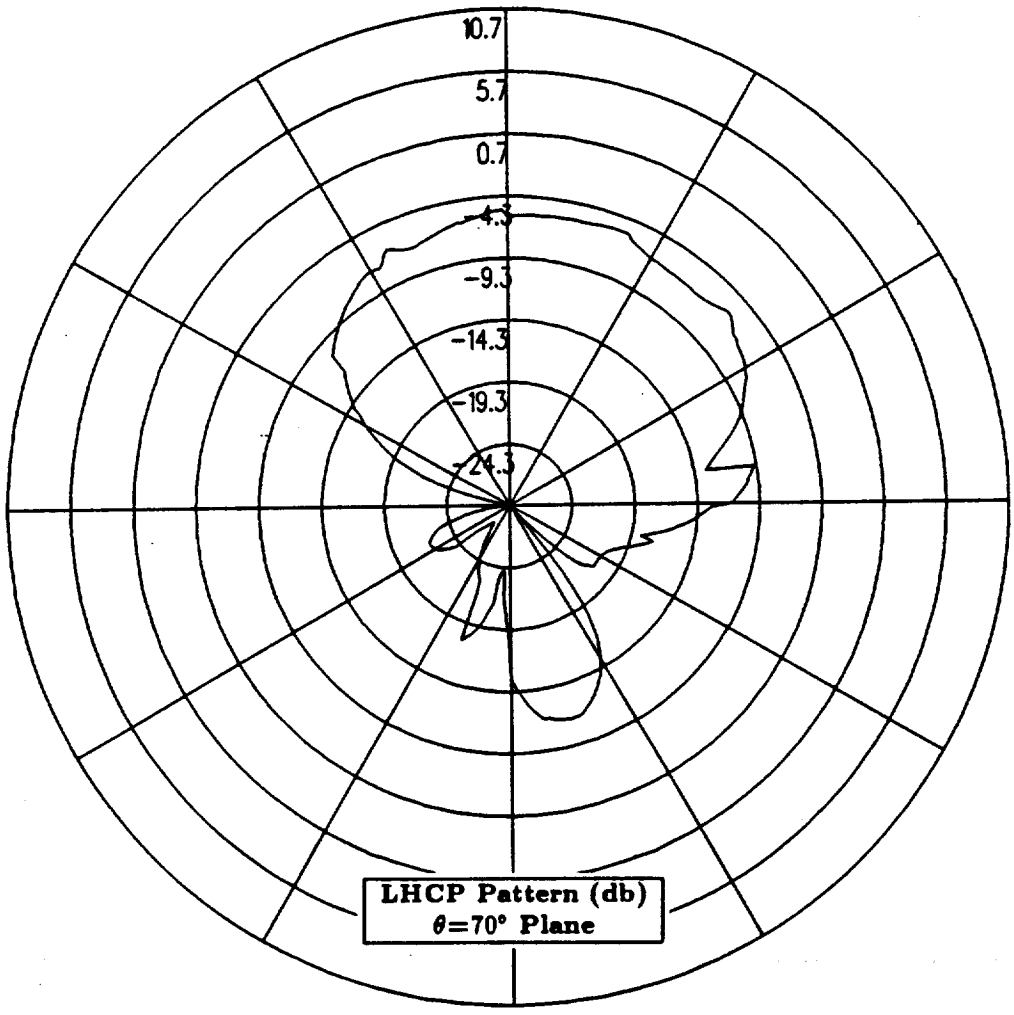

Figure 150: Conical plane pattern 20° above the horizon for DM C99-series antenna placed in radome located in the nose of the P-3C aircraft for left hand circular polarization at 244 MHz.

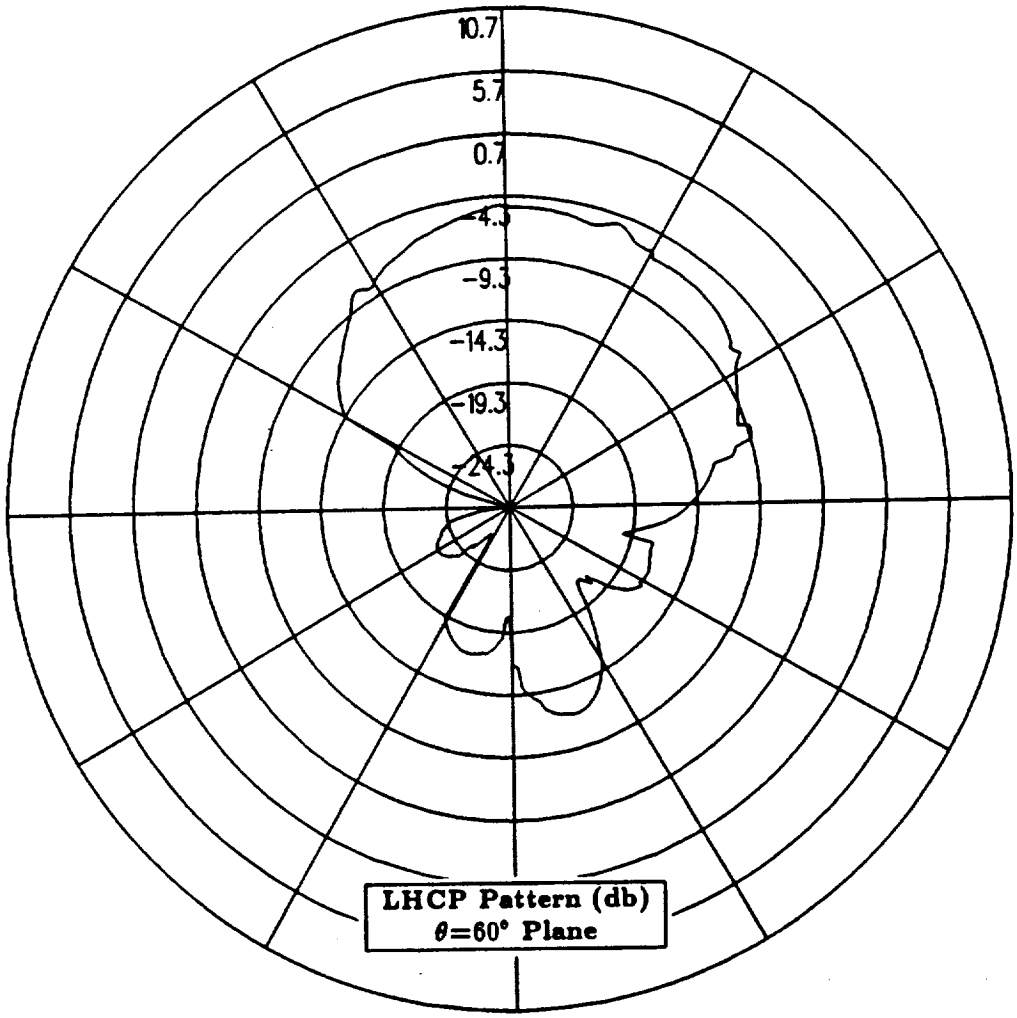

Figure 151: Conical plane pattern 30° above the horizon for DM C99-series antenna placed in radome located in the nose of the P-3C aircraft for left hand circular polarization at 244 MHz.

Chapter 3

Conclusions

The location study presented in Chapter 1 of this volume demonstrates that none of the ten test locations provides the necessary coverage in the horizon of the aircraft near the nose and the tail. Therefore, none of these test locations can be combined with the primary Boeing location to provide the desired pattern and polarization coverage throughout the complete pattern.

Chapter 2 of this volume demonstrates that placing a DM C99-2 antenna in the radome located in the nose of the P-3C aircraft does provide the necessary coverage in the horizon of the aircraft near the nose. Although this antenna configuration located in the nose of the aircraft does not provide the necessary coverage in the horizon near the tail, it can be combined with the primary Boeing location to provide the desired pattern and polarization coverage in all regions except in the horizon of the aircraft near the tail. To provide the necessary coverage in the horizon of the aircraft near the tail, an antenna would need to be placed in the tail of the aircraft. This is not physically realizable at this time due to the aerodynamics of the aircraft.

The study has demonstrated that the most extensive pattern and polarization coverage is achieved when a combination of antennas is used. The final antenna

Bibliography